

 $P_{i,j}$



HYDROCATALYSIS: A New Energy Paradigm

for the 21st Century

by Peter Mark Jansson, P.P., P.E.

A Thesis

Submitted in partial fulfillment of the requirements of the Master of Science in Engineering Degree in the Graduate Division of Rowan University

May 1997







HYDROCATALYSIS: A New Energy Paradigm

for the 21st Century

by Peter Mark Jansson, P.P., P.E.

A Thesis

Submitted in partial fulfillment of the requirements of the Master of Science in Engineering Degree in the Graduate Division of Rowan University

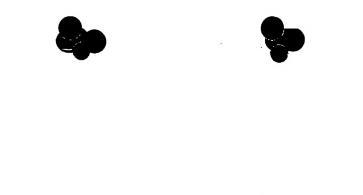
May 1997

Approved by Trupathi R. Chan Ingath Dr. Tirupathi R. Chandrupatha

Approved by _______
Dr. Anthony J. Marchese

External Advisors

Dr. Jonathan Phillips - Pennsylvania State University Dr. Randell L. Mills - BlackLight Power, Inc. William R. Good - BlackLight Power, Inc.



*<u>+</u>





Copyright © 1997 by Peter Mark Jansson

All rights reserved. No part of this publication may be reproduced or transmitted in any form or by any means, electronic or mechanical, including photocopy, recording, or any information storage and retrievel system now known or to be invented, without prior permission in writing from the author, except by a reviewer or other researcher who wish to quote brief passages in connection with a review written for inclusion in a magazine, newspaper, internet web page, broadcast or research for other scholarly purposes.

Library of Congress - Cataloguing in Progress

Published in the United States by Peter Mark Jansson, P.P.,P.E. Integrated Systems P.O. Box 4 Tuckerton, New Jersey, 08087-0004







to Joy,

who encouraged me to return to college ever since we left



*

.

مستوعي المرابعين والمنافض والمرابي والمرابع والمنافض والمعيوم والمنتفوني ويراب والمرابع والرابع والرابع





TABLE OF CONTENTS

					age
Table of Contents .		• • • • • •	• • • • • • •		:::
		• • • • • •	• • • • • • •		. 111
List of Figures		• • • • • • •	• • • • • • •	• • • • • •	. 1V
Abstract					
Mini Absract					
					1
Introduction and Thesis Overview			• • • • • •		•
					2
PART I - An Energy Technology Overvi	<u>ew</u>	• • • • • • •		••••	_
					. 4
Chapter I - Alternate Technolog	y Overview				. 5
1.1 Fossil Fuels					
1.2 Nuclear Energy -					. 11
Fission & Fusion					. 14
1.3 Solar Energy					
1.4 Geothermal Energy			• • • • • •		20
1.5 Tidal Energy		• • • • • •			. 20
	. 1 -1				. 21
Chapter 2 - Overview of Mills	echnology	• • • • • •	• • • • • •	• • • • •	
2.1 HydroCatalysis - A 1	heoretical				22
Overview		• • • • • •	• • • • • • •	• • • • • •	25
2.2 Astrophysical Corro	boration	• • • • • •		••••	22 28
2.3 Enigmas Solved		• • • • • •		• • • • •	20 20
2.4 Technological Embe	odiments	• • • • • •	••,••••	••••	27
					36
PART II - Analysis of Previous Experi	mental Resul	<u>ts</u>		• • • • •	
Chapter 3 - Summary Review	of Gas Phase	;			
O-11 Famorimen	tal Recilits				30
2 1 Disself inte Dower 1	cothermal C	ell			3
3.1 BlackLight Fower 1 3.2 Penn State Univers	ity Calvet				
3.2 Fenn State Officers					4
1 1 MINSON CAIVE					





TABLE OF CONTENTS [continued]

PART III - Mathematical Model	Page52
Chapter 4 - Analysis of Model Performance	
vs. Experimental Results	52
Chapter 5 - Key Learnings and Insights from Model	57
PART IV - Implications for the Future	63
Chapter 6 - Implications for the Future and	
Recommended Next Steps	64
PART V - Reference Materials	66
Footnotes	67
Description of Appendices	72
List of Appendices	
Appendix 1. BLP Research Partners - Catal	logue of Experimental Results
Appendix 2. An Overview of Mills Theory	delenations verifying RIP
Appendix 3. Jansson Astrophysical Data C Reported Results	•
Appendix 4. BLP/AEI Experiment 15.6 -	May 1996
Appendix 5. Analysis of BLP Isothermal (December 1996
Appendix 5. Analysis of Desired Results and Appendix 6. PSU Calvet Testing Protocol	Vehour - December 1990
Appendix 7. Jansson Calvet Testing Protoc Appendix 8. Jansson Calvet Test Results -	June 1997
Appendix 9 Jansson Heat Loss Model Ca	libration & Performance





LIST OF TABLES

	Page
TABLE 1.1 - 1995 Energy Use by Fuel Type	3
TABLE 12 - Energy Sources and Technologies	4
TADIE 13 - Energy Release Processes for Possii Fuels	5
TABLE 1.4 - Fossil Fuel Reserves and Resource Lifetimes	7
Decoarge for Nuclear Fuels	12
TABLE 1.5 - Energy Release Processes to Proceed to Half-lives TABLE 1.6 - Nuclear Fission By-Products Radioactive Half-lives	13
TABLE 2.1 - BlackLight Power Research Partners	
TABLE 2.2 - Energy Released From Lower Energy Hydrogen	23
TABLE 2.2 - Energy Released Trom TABLE 2.3 - Commonly Observed Wavelengths & Mills Theory	28
TABLE 2.4 - BLP Technologies	30
TABLE 2.4 - BLF Technologies TABLE 2.5 - The Search for Hydrinos	34
TABLE 2.5 - The Search for Hydrides TABLE 3.1 - Isothermal Cell Results Summary	39
TABLE 3.1 - Isothermal Cell Results Summary TABLE 3.2 - Penn State Calvet Cell Results Summary	40
TABLE 3.2 - Penn State Carvet Con Results States	41
TABLE 3.3 - Jansson Calvet Testing Objectives	42
TABLE 3.4 - Jansson Calvet Tests Completed Column Testing Protocol Summary - Control	42
TABLE 3.4 - Jansson Calvet Testing Protocol Summary - Control TABLE 3.5 - Jansson Calvet Testing Protocol Summary - Exps.	43
TABLE 3.6 - Jansson Calvet Testing Protocol Summary - Exps.	43
TABLE 3.7 - Jansson Calvet Testing - Calibration Curves	44
TABLE 3.8 - Jansson Calvet Cell Results Summary	52
TABLE 4.1 - Isothermal Cell Results - May 3-4, 1996	53
TABLE 4.2 - Isothermal Cell Heat Loss vs. Temperature TABLE 6.1 - Global Reports/Observations on BLP Technology	63
TARTE 61 - Global Reports/Observations on BLP recimology	

Appendix 2

TABLE A.1 - Mills' Theory Predictions
TABLE A.2 - The Electron Orbitsphere





LIST OF FIGURES

	Page
FIGURE 1.1 - Relationship Between Energy Consumption	•
and Economic Activity (1971)	9
FIGURE 1.2 - Per Capita GNP vs. Per Capita Energy	
Consumption (1987)	10
FIGURE 1.3 - Neutron Induced Fission of ²³⁵ U	
FIGURE 1.4 - PV Historical Costs 1958-1996	18
FIGURE 2.1 - Quantized Sizes of Hydrogen Atoms	24
FIGURE 2.2 - Astrophysical Observations and Mill's Theory	27
FIGURE 2.3 - Astrophysical Data vs. Mill's Theory Illustrated	27
FIGURE 2.4 - Dewar Experimental Vessel	
FIGURE 2.5 - Advanced Electrolytic Cell	
PROTECT 2.4 Non Electrolytic Gas Phase Cell	32
FIGURE 2.7 - Isothermal Calorimeter Gas Phase Cell	32
FIGURE 2.7 - Isodictimate of the FIGURE 2.8 - Calvet Calorimeter Gas Phase Cell	
FIGURE 2.9 - XPS Anomalous 55 eV Peaks	35
FIGURE 3.1 - Excess Power vs. Filament Length	45
FIGURE 3.1 - Excess 1 of 10 cm Experimental Results	46
THE 2.2 Calibration Curve 10 cm Control	
FIGURE 3.4 - Summary of 20 cm Experimental Results	48
FIGURE 3.5 - Calibration Curve 20 cm. Control	49
FIGURE 3.6 - Summary of 30 cm Experimental Results	50
FIGURE 3.7 - Calibration Curve 30 cm. Control	51
FIGURE 4.1 - Isothermal Cell Performance May 4, 1996	54
FIGURE 4.1 - Isothermal Model vs. Actual Performance	55
FIGURE 4.2 - Isothermal Cell Heat Loss vs. Temperature	56

Appendix 2

FIGURE A.1 - The Electron Orbitsphere FIGURE A.2 - The Electron Orbitsphere





Peter Mark Jansson, P.P.,P.E. Abstract

ABSTRACT

Peter Mark Jansson, P.P., P.E.

HYDROCATALYSIS: A NEW ENERGY PARADIGM FOR THE 21st CENTURY

May 1997

Dr. John L. Schmalzel, P.E. - Thesis Advisor Graduate Engineering Department

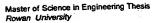
This thesis will review the problems of worldwide energy supply, describe the current technologies that meet the energy needs of our industrial societies, summarize the environmental impacts of those fuels and technologies and their increased use by a growing global and increasingly technical economy. This work will also describe and advance the technology being developed by BlackLight Power, Inc. [BLP], a scientific company located in Malvern, Pennsylvania. BLP's technology proports to offer commercially viable and useful heat generation via a previously unrecognized natural phenomenon - the catalytic reduction of the hydrogen atom to a lower energy state. A review of this experimenter's laboratory data conducted as part of this research as well as that of others is provided to substantiate the fact that replication of the experimental conditions which are favorable to initiating and sustaining the new energy release process will generate controllable, reproducible, sustainable and commercially meaningful heat. By the end of the thesis the reader will have substantial information to draw a conclusion for themselves as to the potential of BLP technology to achieve commercialization and become a new energy paradigm for the next century.





-







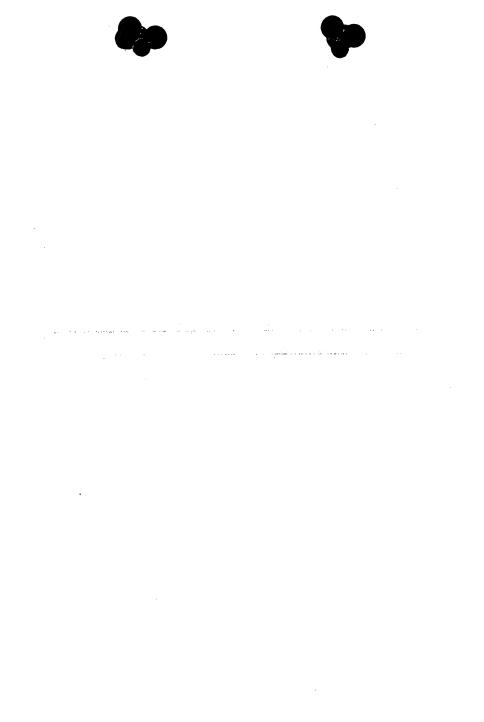
Peter Mark Jansson, P.P., P.E. Mini-Abstract

MINI-ABSTRACT

Peter Mark Jansson, P.P., P.E.
HYDROCATALYSIS: A NEW ENERGY PARADIGM FOR THE 21st CENTURY
May 1997

Dr. John L.Schmalzel, P.E. - Thesis Advisor Graduate Engineering Department

This thesis reviews the technologies used worldwide to meet the energy needs of our industrial societies. This work also describes a new technology being developed by BlackLight Power, Inc. [BLP] of Malvern, Pennsylvania. Laboratory data of the author as well as that of other scientists substantiates that the new BLP energy release process generates sustainable, commercially meaningful heat.







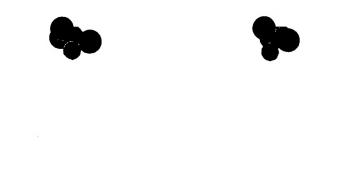
Peter Mark Jansson, P.P., P.E. Page 1 of 73

HYDROCATALYSIS: A New Energy Paradigm for the 21st Century

Introduction and Thesis Overview

This thesis will review the problems of worldwide energy supply, describe the current technologies that meet the energy needs of our industrial societies, summarize the environmental impacts of those fuels and technologies and their increased use by a growing global and increasingly technical economy. After reviewing both the renewable and non-renewable options we have as a society, this work will describe and advance the technology being developed by BlackLight Power, Inc. [BLP], a scientific company located in Malvern, Pennsylvania. BLP's technology proports to offer commercially viable and useful heat generation via a previously unrecognized natural phenomenon - the catalytic reduction of hydrogen to a lower energy state. This reduction of hydrogen to fractional quantum energy levels is based upon a radical modification to the theoretical hydrogen atom energy equation developed by E. Schrödinger and W. Heisenberg in 1926. Dr. Randell Mills of BLP has proposed that a new boundary condition, derived from Maxwell's equations, be applied to that fundamental hydrogen equation. Dr. Mills' model then would suggest a purely physical model of particles, atoms, molecules and overall cosmology. His mathematical solutions contain fundamental constants only and energy values predicted by his theoretical approach agree in a most compelling way with observations scientists have made of the universe and stars.

This source of energy is proported to comprise a significant portion of the radiant energy created by stars. The new form of hydrogen atoms with their electrons below the current "ground" state have been named "hydrinos" by their discoverer, Dr. Mills. BLP scientists believe it is this matter that comprises the significant part of the dark matter of space. It will not be the attempt of this engineering thesis to debate the merits of Dr. Mills' theory in this regard but rather to review and sometimes replicate the scientific calculations and supporting data which indicate the merits of the existence of hydrinos. This thesis will also review this experimenter's laboratory data as well as that of others that substantiates the fact that replication of the experimental conditions which are favorable to initiating and sustaining the new disproportionation process will generate controllable, reproducible, sustainable and commercially meaningful heat. It will describe the technologies currently used in the disproportionation reaction, report on the state-of-the-art for the BLP technology and state the author's opinion as to this technology's potential for successfully addressing [or solving] some of the global energy issues above. [environmental degradation from growing energy use, limits to energy supply at forecasted growth rates, etc.1







Peter Mark Jansson, P.P.,P.E. Page 3 of 73

use coal for heating as well as wind and water power for grinding grains [26,000 kcal daily per capita - 30.2 kWh]. During the Industrial age of the 19th century we added the steam engine as a source of mechanical energy and increased the use of fuel energy in homes for lighting and heating [77,000 kcal daily per capita - 89.3 kWh]. Modern technological society uses the internal combustion engine for transportation, electricity for appliances and comfort which find their energy source in fossil, hydro and nuclear fuels which power steam turbines, furnaces and generators [230,000 kcal daily per capita - 266.8 kWh daily per capita]. [2] This trend indicates that as we improve the quality of life for society a commensurate increase in direct and indirect energy use is requisite. World energy and economic statistics today also demonstrate that there is a direct correlation between a nation's gross national product [GNP] and its energy consumption. The countries of Ethiopia, Mali, Malawi and Niger all have GNPs less than \$250 per capita while energy use is less than 0.4 barrels of oil per capita per year [680 kWh/year]. In contrast, the U.S., Norway, Canada and Sweden are leading economic nations with over \$10,000 of GNP per capita. They use in excess of 40 barrels of oil per capita per year [68,000 kWh].[1] This one hundredfold increase in energy use is not a coincidence. It is characteristic of a steady evolution of society from a primitive [2.3 kWh] to technological [266.8 kWh] level of advancement and is illustrative of the critical role energy plays in increasing societal maturity, quality of life and productivity.

The sections which follow illustrate the fuels, technologies and methods used around the world to sustain this societal evolution and summarize limits on these elements which must be addressed in order to avoid major problems as the now developing nations [where over 3/4 of the world's population resides] strive to achieve western standards of living through industrialization. Table 1.1 below summarizes the current levels of energy use in the world and U.S. as of 1995.

TABLE 1.1 - 1995 Energy Use by Fuel Type (in trillions of kilowatthours)

Energy Sour	ce	World	u.s.	U.S. % of World
Fossil Fuels	Natural Gas	22.7	6.6	29.2 %
rossii rueis	Petroleum	39.5	10.1	25.5 %
		26.8	6.1	22.9 %
	Coal	7.1	2.2	30.3 %
Nuclear Solar	Fission HydroElectric	2.5	0.3	10.6 %
TOTAL		98.8	25.3	25.6 %





Peter Mark Jansson, P.P.,P.E. Page 4 of 73

It is important to note that only commercially traded fuels are included in the summary data. The overview provided in Chapter 1 of this thesis presents the energy sources in an order prioritized by the contributions these sources make to industrialized society today.

Chapter 1 - Alternate Technology Overview

Prior to the announcement of the hydrocatalysis process being put forth by BlackLight Power there were fundamentally only five known sources of energy. In addition to the most commonly exploited, fossil fuels, there are nuclear [both fission and fusion], solar [in its many forms], geothermal and tidal. Table 1.2 below briefly summarizes the major energy sources available in our society.

TABLE 1.2 - Energy Sources and Technologies

Energy Source	Fuel Type	Technologies in Use
Fossil Fuels	Natural Gas Petroleum Coal Shale Oil Tar Sands	Heaters, Furnaces, Boilers, etc. Heaters, Furnaces, Boilers, etc. Heaters, Furnaces, Boilers, etc. Processing facility yields petroleum Processing tacility yields petroleum
Nuclear [Fission]	Uranium	PWR creates steam / electricity BWR creates steam / electricity
	Plutonium	Breeder technology - LMFBR
Nuclear [Fusion]	Hydrogen	No Technology Exists as of Yet
Solar	Solar Thermal	Passive & Active Water Htg. Systems Passive & Active Space Htg. Systems Power Tower/Parabolic Dishes / Troughs
	Photovoltaic	Amorphous Cells Crystalline Cells [single, multi, etc.]
	Biomass Hydroelectric	Wood, Seaweed, algae, etc. Agricultural Crops [alcohol, waste, etc.] Municipal Solid Waste [paper primarily] Reservoirs, darms, water wheels, generators, pumped storage
	Wind Power Ocean Waves Ocean Thermal	Wind Mills, Sailing, Turbines [VAMA] Pilot Systems - Compressor/Generator OTEC Design [1930, 1975]
Geothermal .	Geopressured Hot Dry Rock formations Hot Water Res. Normal Grad. Res. Natural Steam Molten Magma	Heaters, Turbine/generators Heaters, Turbine/generators Water and Space Htg. Systems Heaters, Turbine/generators Heaters, Turbine/generators No Technology Exists as of Yet
Tidal	Potential Energy of Earth-Moon-Sun gravity	Reservoirs, dams, generators
Hydrocatalysis	Binding Energy of Hydrogen Atom [p* to e* relationship]	Disproportionation Furnace





Peter Mark Jansson, P.P.,P.E. Page 5 of 73

For each energy source the types of fuels used and the technologies in use today which convert those fuels into useful work and energy for humans is highlighted.

1.1 Fossil Fuels

In the United States fossil fuels provide 89.2% of the energy we consume. In 1995 this consisted of a combined consumption of coal equivalent to 787 million tons per year, natural gas of about 22 trillion cubic feet per year and petroleum product use of 5.9 billion barrels per year. ^[5] It is clear that an industrial society like ours could not continue without these resources. Globally in 1995 our societies consumed 3441 million tons per year of coal, 75 trillion cubic feet per year of natural gas and 23.3 billion barrels per year of petroleum. ^[5] The U.S. was the leader in the global use of fossil fuels [specifically petroleum] from the very beginning of its industrialization with the oil strike of Edwin L. Drake in Titusville, Pennsylvania in 1859. "By 1909, when the industry was just 50 years old, the United States was producing 500,000 barrels a day, which was more than was produced by all the other countries combined." We remained dominant in the petroleum production and manufacturing markets through 1950 when we still produced over 50% of the world's supply. The key reactions for each of the fundamental fossil fuel types are shown below in Table 1.3.

TABLE 1.3 - Energy Release Processes for Fossil Fuels

Fossil Fuel Type	Chemical Reaction[s]	By- Products
Natural Gas 85% Methane[CH ₄] 15% Ethane[C ₂ H ₆]	CH ₄ + 2O ₂ → CO ₂ + 2(H ₂ O)	CO ₂ , CO, water, hydrocarbons and heat [exothermic reaction]
Bottled Gas Propane [C ₃ H ₆] Butane [C ₄ H ₁₀]	$2C_3H_8 + 9O_2 \implies 4CO_2 + 2CO + 8(H_2O)$	CO ₂ ,CO, water, hydrocarbons and heat [exothermic reaction]
Petroleum Gasoline Pentane[C ₅ H ₁₂] Hexane [C ₆ H ₁₄] Heptane[C ₇ H ₁₆] Octane [C ₆ H ₁₆]	$C_8H_{18} + 12O_2 \longrightarrow 7CO_2 + CO + 9(H_2O)$	CO ₂ ,CO, water, hydrocarbons and heat [exothermic reaction]
Coal contains carbon plus impurities	$\begin{array}{l} C + O_2 \longrightarrow CO_2 + CO \\ S + O_2 \longrightarrow SO_2 \ [plus SO_x] \\ N + O_2 \longrightarrow NO_2 \ [plus NO, NO_3, NO_2] \end{array}$	CO ₂ , CO, SO ₂ , NO ₂ , water, hydrocarbons, SO _x , NO _x particulates, etc. and heat [exothermic reaction]





Peter Mark Jansson, P.P.,P.E. Page 6 of 73

It is important to note at this point that all fossil fuels release their energy to man through the chemical reduction process known as oxidation. In this reaction the energy that has been stored in carbon and hydrocarbon chains created during the early history of the earth [250-500 million years ago] is released. In this chemical reaction oxygen combines with the carbon fuel in the presence of heat to release additional heat and form water, carbon-dioxide as well as a host of other hydrocarbons and by-products.

The impact on the environment of the use of the stored chemical energy provided in fossil fuels is significant. "One example is the added burden of carbon dioxide in the earth's atmosphere, with its corresponding potential for modifying the world's climate. Other examples . . . include the acidification of the atmosphere and surface waters, . . . early deaths of thousands by sulfur dioxide in the air, ... ozone formation, ... problems of coal mining, ... acid drainage, ... carbon monoxide and other pollutants from auto traffic, ... thermal pollution of rivers and lakes". [7] We must add to those impacts the environmental degradation to the air, water and soil that is caused by the release of large quantities of these direct pollutants and the other heavy metals and radioactive elements stored by nature in these fuels [lead, mercury, etc.] It was not until the burning of fossil fuels during the 19th century that the element lead began being deposited in regions as remote as the arctic and continent of Antarctica. Many scientists believe that the acidification and resulting "deaths" of many high altitude lakes have been caused by the release of the pollutants generated by fossil fuel combustion [by industry, homes and in automobiles]. The increased sulfur dioxides and nitrogen oxides generated by industrialization are present in the atmosphere and lead to "the formation of acids, primarily H2SO4 and HNO3, from these pollutants and the resulting damage caused by the acidic rain formed is a story of growing importance."[8] Presently the latest environmental alarm sounded has been that of global warming, a proported warming crisis attributable to a significant increase in the presence of so-called greenhouse gases. The earth's surface radiates thermal energy in the infrared region [approximate wavelengths of 4 to 20 µm] which keeps the global environment cooling at a steady rate. Carbon dioxide [CO2], methane [CH4] and nitrous oxide [N2O] represent molecules formed by the use and manufacture of fossil fuels which trap heat at the above wavelengths, heat that would otherwise be radiated from the earth into space. "Carbon dioxide now accounts for about two-thirds of the greenhouse effect, methane about 25%." [9] These environmental impacts caused by growing fossil fuel use are forcing many nations to rethink the role these fuels will play in the future.

The limited amount of fossil fuel resources poses a second major risk to continued expansion of the global economy. At present rates of consumption these fuels only have a limited remaining supply, on the order of decades for a few of them to less than a century in the case of coal. [See Table 1.4] In order to meet the needs of our increasingly advancing and growing societies we must find alternatives. Additionally we must preserve some of these fuels since they also serve as key chemical stores in many critical manufacturing and medicine roles in industrial society. If we conservatively grow the current rates of fossil





Peter Mark Jansson, P.P. P.E. Page 7 of 73

fuel consumption for the energy sector to include the demands that will likely be placed on the finite supply by the developing nations as the globalization megatrend continues we find that the lifetimes are much shorter still.

TABLE 1.4 - Fossil Fuel Reserves and Resource Lifetimes

Fossil Fuel Type	Proven Reserves*	Est. Remaining Lifetime**
Giobal U.S.	999 x 10 ⁹ bbl 72 x 10 ⁹ bbl	40 years 16 years ***
Natural Gas Global U.S.	5185 x 10 ¹² ft ³ 600 x 10 ¹² ft ³	60 years 20 years
Coal Global U.S.	7.64 x 10 ¹² tonne 1.5 x 10 ¹² tonne	200 years 86 years, 66 years ****

Remaining as of 1990

As the limits to the fuel reserves in Table 1.4 are approached the price of energy will begin to climb steadily. It is important to note that one of the key drivers to economic expansion is the readily available supply of affordable energy. Already we see a migration of industry in this country moving from the high-energy cost areas [Northeast and California] to the more inexpensive energy cost areas of the Northwest and Southern states. Many industries which were energy intensive have left the service area of Atlantic Energy [southern New Jersey] to move south over the past decade to North Carolina or another lower energy cost state for primarily energy reasons. [NOTE: economics has played the major role in corporate decisions to relocate from Atlantic Energy's region including costs associated with energy, taxes, employment and environmental compliance] We can estimate that on a global scale the trend will be the same, manufacturing [and the associated benefits of its economic engine] will move to where energy, overall manufacturing and labor costs can keep the company competitive. As industry and manufacturing leave the U.S. for less developed nations the commensurate growth in energy demand and desire for a higher standard of living on the part of those nations' workforces will all press the global

At current consumption rates

Since 1948 the U.S. has imported more oil than it has exported. In 1984 the U.S. was importing 50% of its needs At current consumption rate increased by 5% per year, if coal fills all U.S. energy needs when other fuels deplete





Peter Mark Jansson, P.P.,P.E. Page 8 of 73

energy reserves via higher growth rates in consumption. Examples of this include the nations of Indonesia, Malaysia, Thailand and Vietnam where the annual growth in electricity demand has become double digit during the last 10 years. Were the nations of the developing world [China, India, Southeast Asia, Africa] to develop an energy appetite just a fraction as great as their technologically advanced sister countries [U.S., Canada, Japan, Norway, Sweden] the pressure on the limited global reserves and the strain on the atmosphere would become severe.

This researcher estimates that the values in Table 1.4 for the expected remaining lifetime of global fossil fuel reserves can be reduced by as much as a factor of 2 if the trend in third world energy development follows the forecasts outlined by the World Bank. As these pressures on conventional fuels drive price upward shale oil and tar sand reserves as well as many enhanced oil recovery technologies will become more economic.

An excellent illustration of the demands placed on energy by a developing. industrializing society is illustrated by the following two figures. Figure 1.1 demonstrates the relationship between energy consumption and economic activity based upon figures developed in a Scientific American article in 1971. Figure 1.2 develops similar data on per capita gross national product vs. annual energy consumption based upon World Bank data in 1987. [11] If one observes the nation of Japan on both figures and considers the position it had in the global economy in the early 1970s contrasting it with the economic powerhouse it was becoming by the late 1980s we can see the increase in energy demand that was placed upon the global energy market in order to sustain that one country's economic advancement. Japan's population in 1961 was 89.2 million^[12] and it grew to 119.5 million in 1983. [13] In 1971 Japan's populus consumed approximately 33 x 10⁶ Btus per capita [9,669 kWh] annually. In the short 16 years of their continued economic growth between 1971 and 1987 their energy use per capita grew to 22 barrels of oil [37,400 kWh] annually. This represents a 4 fold increase in per capita consumption and a 5 fold increase in overall national energy consumption [based upon a 1971 population of 103M and a 1987 population of 125M]. This energy growth correlates directly with their GNP growth from \$550 US [1971] to \$12,000 US [1987] and the extensive industrialization of their economy. Japan's energy consumption now is 43,285 kwh per capita [1995] and while it continues to grow, their population remains steady at 125M. Were a single, large developing nation such as India [population 936M in 1995] to undertake an economic expansion similar to Japan the impact on global fossil fuel markets would be substantial. India's per capita energy consumption in 1995 was 2,563 kWh annually, were they to reach Japan's per capita energy use it would represent a 17 fold increase in their energy use. By 2020 they would become a nation that consumes 5.7 x 10¹³ kWh annually [assumes continued current population growth rate and acheivement of Japan's level of industrialization and commensurate per capita energy usage]. India's one year energy use in that year would represent 64% of the entire World's energy consumption in 1995 [see Table 1.1]. At those usage rates that one nation alone could consume the entire world's remaining supply of oil



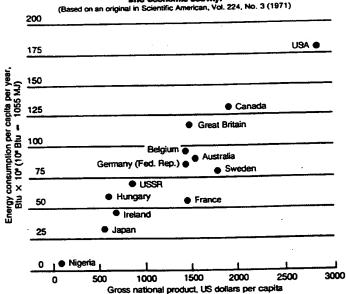


Peter Mark Jansson, P.P., P.E. Page 9 of 73

in less than 30 years. In aggregate, the developed nations' growing energy consumption rates combined with their continued population growth will substantially reduce the estimates of fossil fuels' expected remaining lifetimes from those shown in Table 1.4. "There is no escaping the reality... fossil fuels are formed over very long time periods, and although some new deposits will certainly be discovered, there will be no significant increases in the world inventory over human history... the era in which we live is extraordinarily specialized and is set off from all human history and future on this planet by our use of fossil fuels. These energy resources were laid down over hundreds of millions of years during the earth's evolution, and they are now being consumed in what is essentially an instant in our occupation of the planet." Without the discovery and development of an environmentally friendly, inexpensive energy source to significantly offset the consumption of these ancient energy reserves, we will enter the new millennium only to quickly find that the standard of living developed by western civilization is not a sustainable one.

FIGURE 1.1

Relationship between energy consumption and economic activity.







Peter Mark Jansson, P.P.,P.E. Page 10 of 73

FIGURE 1.2 Per Capita GNP vs. Per Capita Energy Consumption

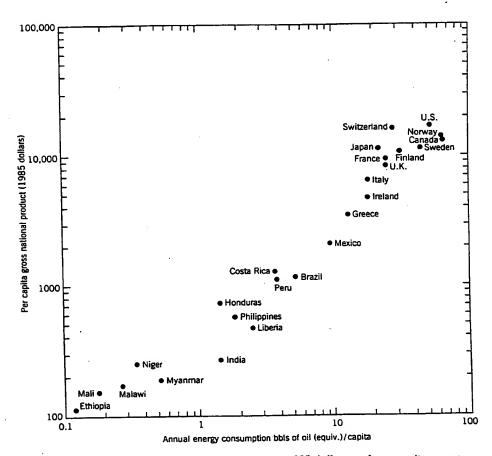


Figure 1.15 Per capita gross national product in 1985 dollars and per capita energy consumption per year in terms of the equivalent barrels of oil. (Source: World Bank [1987]. Adapted from E. S. Cassedy and P. Z. Grossman Introduction to Energy, resources technology and society Cambridge: Cambridge University Press [1990].)



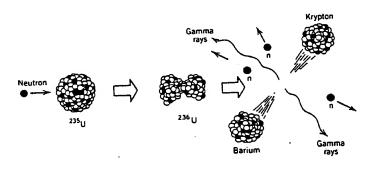


Peter Mark Jansson, P.P.,P.E. Page 11 of 73

1.2 Nuclear Energy - Fission and Fusion

While the fissionability of uranium was first discovered in 1938 it was not until Enrico Fermi constructed a sustainable nuclear reactor in 1942 that the usefulness of this technology for energy production was truly demonstrated. In a parallel way in which chemical [electronic] bonds between carbon atoms are broken down through chemical combustion with oxygen, the breaking of nuclear bonds via a fission reaction is caused by the bombardment of a radioactive uranium atom's nucleus with neutrons. This bombardment, upon successful collision, causes the nucleus of the uranium atom [235 U] to become a highly excited uranium atom [236 U], this atom rapidly separates [or fissions] into smaller pieces forming new nuclei as a result. This is more clearly illustrated in Figure 1.3 below. The energy released via this nuclear reaction is equal to Einstein's famous equation $E = mc^2$. To put this in perspective, the energy available within a ton of coal that is chemically released through combustion [ie; breaking down all of the carbon bonds] is 7056 kWh. Were that same ton of coal to be converted to energy via a nuclear reaction the energy available is 22.7 trillion kWh, this is 3.2 billion times more energy.

FIGURE 1.3 Neutron Induced Fission of ²³⁵U



This process of working on the nuclear bonds of the atom, rather than the chemical bonds of molecules releases a significant amount of the nuclear binding energy within the atom. What makes this a sustainable chain reaction is the creation of additional neutrons [see fission reaction in Table 1.5] from the fission reaction which can then go and impact additional uranium nuclei to keep the bombardment occurring without external neutron input. Control rods used in commercial nuclear power plants provide a moderating effect





Peter Mark Jansson, P.P.,P.E. Page 12 of 73

on the reaction by absorbing excess neutrons in order to slow or to bring the reaction to a stop. The process outlined above is used in both pressurized water reactors [PWR] used significantly in nuclear submarines and power plants as well as in boiling water reactors [BWR] used widely for commercial applications.

TABLE 1.5 - Energy Release Processes for Nuclear Fuels

Nuclear Process	Nuclear Chain Reaction[s]	Energy Release
Fission	$n + {}^{235}U_{143} \rightarrow {}^{236}U_{144} \rightarrow {}^{144}Ba_{88} + {}^{89}Kr_{53} + 3n$	+ 177 MeV
Breeder	$n + {}^{238}U \rightarrow {}^{239}U \rightarrow {}^{239}Pu + {}^{1}n$	+ 177 MeV
Fusion	${}^{1}H_{0} + {}^{1}H_{0} \implies {}^{2}H_{1} + \beta^{+} + \nu + \text{energy}$ (1) ${}^{1}H_{0} + {}^{2}H_{1} \implies {}^{3}He_{1} + \text{energy}$ (2) ${}^{3}He_{1} + {}^{3}He_{1} \implies {}^{4}He_{2} + 2{}^{1}H_{0} + \text{energy}$ (3) ${}^{4}H_{0} \implies {}^{4}He_{2} + 2\beta^{+} + 2\nu + \text{energy}$	

Detailed descriptions of the nuclear energy process is not within the scope of this research but rather an overview of these technologies and their associated economic and environmental risks are described below.

The breeder reactor is a concept not yet fully commercialized which takes advantage of the fact that free neutrons are not only capable of inducing fission via a conversion of ²³⁵U to ²³⁶U, but are also as equally capable of converting a ²³⁹U atom into ²³⁹Pu. This is very valuable since ²³⁹Pu is also a fissionable material capable of acting as a fuel in standard nuclear reactors. If the design of a breeder reactor could be optimized to create additional ²³⁹Pu while also creating uranium fission it would be a reactor that created its own fuel and would significantly increase the lifetime of nuclear fuel materials.

Fusion is a nuclear reaction that occurs commonly on the stars and in the case of our sun is likely the source of approximately 60% of the energy it provides. This estimate is based upon observed solar neutrino flux as measured by the Gallex solar neutrino detector in Italy. ^[15] As shown in Table 1.5 above according to the Standard Solar Model fusion begins with the combining of two hydrogen nuclei (protons) to form a deuterium nucleus. The process then continues to build a heavier helium nucleus all the while releasing large amounts of the nuclear binding forces within the atom. For a more complete explanation of this process the reader is referred to pages 108-111 of "Energy and Problems of a Technical Society" ^[16], which is an excellent summary of energy technology information





Peter Mark Jansson, P.P., P.E. Page 13 of 73

referred to often in this paper. Due to the very high temperatures involved, the limits of current materials and the fact that proof of the scientific feasibility of the essential reactions has not yet been established it is unlikely that significant additional funding will go into the development of fusion. The Tokamak Fusion Test Reactor [TFTR] located at the Princeton University Plasma Physics Lab was designed to answer some of these fundamental questions. It appears that after significant resources have been invested in this test those questions will still not be sufficiently addressed. The TFTR was shut down on April 3, 1997 "many say prematurely ... for lack of money". [17]

In the U.S. during the last decade no new nuclear power facilities have been opened, ordered or planned. This is due in large part to 4 primary developments during the past 15 years. These facilities have become very expensive to build and meet all Nuclear Regulatory Commission [NRC] standards, the issue of nuclear waste storage has yet to be resolved by the utilities and the Federal government, there was and continues to be significant public opposition to this technology and there have been key nuclear accidents which have increased the financial risks and liabilities to investors and owner / operators of such facilities. When nuclear advocates were espousing the virtues of this technology in the 1960's and 1970's it was believed that the energy would be so cheap that utilities would not need to meter customers any longer. As the technology was deployed, many safety features were required "along the way" by the emerging NRC which wanted to assure the safety of the technology. This often led to major cost overruns and units that were intended to come on line for \$1,000 - 1,500 per kilowatt escalated to often over \$4,000 per kilowatt. Many units in the Northeastern and Western regions of the U.S. were never finished due to these massive costs. This is clearly one of the key reasons utilities are not interested in the technology today. Another reason is the longevity of hazardous nuclear radioactive wastes. Table 1.6 below indicates the lifetimes of radioactive materials generated as by-products from the nuclear industry.

TABLE 1.6 - Nuclear Fission By-Products Radioactive Halflives⁽¹⁸⁾

Radionuclide	T _{1/2} [Halflife]	Decay Particle
²³³ U [uranium-232] ²³⁹ Pu [plutonium-239] ³ H ₂ [hydrogen-3, tritium] ⁹⁰ Sr [strontium-90] ¹³¹ I [iodine-131] ¹³⁷ Cs [cesium-137] ⁸⁵ Kr [krypton-85]	1.59 x 10 ⁹ years 2.41 x 10 ⁴ years 12.35 years 29 years 8.04 days 30.17 years 10.72 years	α β β β β β β β





Peter Mark Jansson, P.P.,P.E. Page 14 of 73

It is clear that wastes from the nuclear industry will need to kept away from the human population and environment for excessive lengths of time [often exceeding many generations]. Although this was known in the early years of this technology, as of today, after over 20 years as an active industry, the government and utilities have yet to find an acceptable long-term high level waste repository. It is unlikely that the nuclear industry in the U.S. will see any significant expansion during the next few decades. In Sweden recently the government ratified its 17 year old promise to remove all nuclear reactors from service in its country by 2010. The first two reactors will be officially removed from service in 1998 and 2001 "before their technical life expires". [19] This leaves only France, Japan and a few developing nations that will be expanding their commitments to nuclear fission as a viable energy source for the future.

1.3 Solar Energy

Without a doubt the most widespread form of energy in the universe is the energy radiated from the stars. Specifically in our solar system, the Sun is the source of nearly all forms of useful energy. From the fossil fuels first formed by carbon fixing organisms [plants and animals] in the presence of solar energy 250-500 million years ago to the hydroelectric plants operating on major rivers, the Sun is responsible for creating the potential energy each represents. This section will briefly summarize all of the primary forms of solar energy and prioritize their discussion from the most economical and technologically ready to the forms that are the least economical and require the most additional development. It is important to note that although significant attention is given to these sources of energy because of their potential for the future, at the present time solar energy in all of its forms represents less than 3% of the World's commercially traded forms of useful energy. Of that small fraction over 90% represents the use of solar energy in the form of hydropower.

The most developed form of solar energy is hydroelectricity. The hydrologic cycle driven by the sun evaporates over 5.5 quadrillion cubic feet of water from the earth every year. This same energy falls back to the earth in the form of rain and the potential energy of water at higher elevations. Of the more than 100 quadrillion kilowatthours of energy in the hydrologic cycle only a very small portion is harnessable. Most precipitation falls back into the oceans with only a fractional amount falling upon dry land at higher elevations where its potential energy becomes available for exploitation via rivers, dams, waterwheels and hydroelectric generating facilities. World energy usage statistics indicate that in 1995 we were providing approximately 2.3 trillion kilowatthours^[20] of our global society's energy needs through hydroelectric sources. This represents approximately 2.5% of all energy consumed. Man's use of falling water to displace human and animal energy dates back over 2000 years. Hydropower also played a major role in the industrialization of western





Peter Mark Jansson, P.P.,P.E. Page 15 of 73

Europe the 16th century when waterwheels served as the primary powerhouses. While many believe the potential for exploiting more hydropower is great there are environmental considerations and social concerns that make extensive expansion unlikely. Due to the need to create large dams and reservoirs to harness hydropower there is often substantial displacement of people as well as restriction of the normal ecology of the river. While it represents a significant capital investment, where it can be practically developed hydropower remains an economic source of electricity.

The most widely known and experienced form of solar energy is biomass. A significant majority of the World's now 5.8 billion people^[21] come in contact with this fuel on a daily basis. The biomass category represents fuelwood, charcoal, agricultural products and waste [alcohol, dung, mill residues, rice hulls, straw, etc.] as well as the less recognized biomass of industrial society - municipal solid waste [mostly paper and packaging materials]. Least recognized in the category of biomass is the harvesting of ocean biologic life [seaweed, algae, etc.] for fuel production. "Noncommercial biomass fuels ... already supply more than 10 percent of total global energy needs and a much higher percentage of the energy needs in developing nations, albeit with low levels of efficiency and service quality." This source does not appear in Table 1.1 since very little biomass is commercially traded on the global level. The sun plays the critical role in the creation all the biomass fuels either directly through photosynthesis or indirectly via man's or animal's use of a product the sun's energy created [ie; foodstuffs, paper, etc.]. Besides using biomass for meeting heating and other human energy needs probably the most common use is in the food we eat. Vegetables, fruits and other animals all received their energy from the solar source as well through the process of photosynthesis shown below:

$$6CO_2 + 6H_2O \xrightarrow{\text{LIGHT}} C_6H_{12}O_6 + 6O_2$$

The energy release processes for biomass are very similar to fossil fuels where the biomass is directly burned in the presence of oxygen to release the energy of carbon chains and form CO₂, H₂O, etc. Continued use of biomass is inevitable, expanded use of wood and woodwaste as a fuel in the U.S. is likely as well. Without specialized biomass growing and harvesting techniques and efficient fuel conversion systems it will be quite a few years into the future before these fuels will become economic on a large scale and find a major place in the growing global energy market. The energy densities of biomass fuels are relatively low, on the order of lignite to peat coal resources, and this also presents barriers to commercial development.

Another widely experienced form of solar energy is the direct heating of the sun known as solar thermal energy. From the highly technological systems we have created [passive and active solar space and water heating systems] to the primitive habit of laying out in the sun for a siesta or tan, the human race daily takes advantage of the direct warming





Peter Mark Jansson, P.P.,P.E. Page 16 of 73

available from the sun. Many societies still use the sun for drying grains [such as rice] as a critical step in their agricultural process. In the U.S. the most prevalent form of solar thermal energy use is in passive and active heating systems for homes as well as heating systems for hot water. During the late 1970s and early 1980s the Federal government provided significant tax incentives for renewable energy systems. This led to many domestic solar hot water heating systems being installed throughout the country. These systems typically consist of a solar collector device that traps incoming short wavelength incident solar radiation and upon collision with a dark, metallic 'absorber' plate the light energy is converted directly to heat [or mechanical molecular vibrational energy] in the absorber plate. This collector is typically called a flat-plate solar collector. The absorber plate typically has an antifreeze solution which runs through it [i.e. it acts as a heat exchanger to move the incoming solar energy it absorbs into the fluid] and this fluid is used to capture, move and store the solar energy for use either in a hot water system or for heating a home or building. Another example of solar thermal energy systems is the focusing collector which comes in various shapes, sizes and configurations. From the Solar One power tower demonstration in Barstow, California which had a commercial production of 10 megawatts, to modular, parabolic dish and trough systems that collect watts to kilowatts of power, directly focusing the sun's energy on a light-absorbing surface can create commercially meaningful heat. The drawbacks with all of these systems was that they were never economically attractive. Most solar thermal heating systems have between a 15 and 30 year simple economic payback. Without significant social policy change or government subsidy these types of heating and energy production systems will not be commercially significant.

Another solar resource is wind power. In 1995 it was estimated that geothermal, wind and solar of all types accounted for nearly 5% of the world's primary electricity generation [ie; 0.5% of the world's total energy resources]. This resource was used from the most ancient of times by mariners in their quest for increasing the speed of their then human powered vessels to the applications of water pumping and grain grinding by animals in Europe and America in the 19th and 20th centuries. Wind power is still used in many locations throughout the world for these purposes. As an electricity generating source wind power first began to find its way into the marketplace in the 1970s and 1980s in both Europe and the U.S. While we know that the mechanical motion of air is a direct consequence of solar heating of the planet it has always been a challenge to economically extract the energy in this air movement. Modern wind turbines are designed to remove the kinetic energy in the wind and use that energy to turn a generator to provide electricity. They do this by placing their aerodynamically efficient blades into the wind to enable the mechanical force of the wind to cause those blades to rotate and sweep over a large area. Present technologies include vertical axis wind turbines as well as horizontal axis wind turbines; manufacturing is dominated by the latter at the present. The energy that can be removed by a wind turbine is proportional to the area its blades sweep out as well as the cube of the wind velocity. For this reason most turbines are mounted on towers to place





Peter Mark Jansson, P.P.,P.E. Page 17 of 73

them more aloft where higher wind regimes are present. In areas of moderate to high annual wind speed, wind turbine generators are able to create electricity at approximately \$.05 per kWh assuming a 20 year equipment life. It is difficult to find areas where local citizens are willing to allow wind facilities to be located at the present time and it is also increasingly difficult to find investors willing to tie up their capital for a project that produces electricity at a higher cost than where the electricity market is at present [i.e. \$.02-03 per kWh].

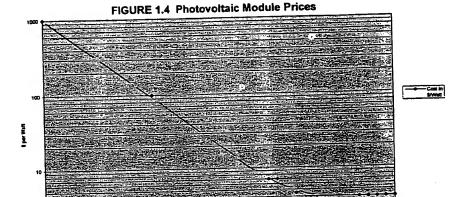
A widely acclaimed technology that showed promise in the 1980s of becoming a major player in the solution to the energy crisis is photovoltaics. These are semiconductor devices made of materials that are designed and oriented in such a way as to convert light energy [photons] directly into electrons at efficiencies of 5-30%. PV devices being developed commercially employ similar physics in their operation. The photovoltaic effect is created when incoming photons interact with electrons in a semiconductor material so as to create a charge carrier pair; an electron and a "hole". Each PV device is constructed with positively and negatively doped layers so as to maximize the cell's ability to separate the charge carriers and keep them separated so as to induce a voltage across the cell as long as the incoming light is present to induce this voltage. The photovoltaic effect was first discovered by 17 year old French physicist Edmund Becquerel in the 1850s when he was experimenting with batteries. He noticed that his batteries were able to provide significantly more energy in the presence of light than when shaded in the darkness. He noted this in his journal but it wasn't until Albert Einstein's work in 1905 that the principles behind the photoelectric effect were described scientifically. This technology's potential lay dormant for another 50 years until the space race began. After Russian scientists launched Sputnik in 1957 and the U.S. had fallen behind in the race they wanted to assure that their first satellite would 'last longer'. As a result in 1958 the Vanguard satelite was launched by the U.S. powered with not only a battery, but a battery recharged on-board by the world's first commercial application of photovoltaic cells. [Sputnik lost its battery energy and floated useless in space after only a few months] Those cells, costing over \$1000 per watt kept the Vanguard satelite's batteries charged for years of successful operation.

Since that time the cost of photovoltaic [called PV] cells continued to plummet driven by advances in technology, increased manufacturing volume and increasing demand for satellite applications, remote power applications as well as commercial electricity uses. Figure 1.4 shows the progressive decline in PV cell prices as advances in technology continued through the 1980s. By the late 1980s as Federal research monies for renewables decreased during the Republican Administration, the commensurate investment in and advancement of PV technology subsided. Current pricing for PV cells has not substantially changed from those present in 1989





Peter Mark Jansson, P.P.,P.E. Page 18 of 73



In addition to the photovoltaic modules that are made up of cells configured to provide adequate current and voltage, a PV system requires balance of system components. These components are module mounting and wiring peripherals, a DC to AC inverter for typical interface with home wiring and the installation [roof or ground mount, etc.] of the entire system. In 1996 these were estimated to cost \$2 per watt, \$1 per watt for the inverter and \$1 per watt for balance of system hardware and installation. This would bring a total PV system's cost to \$6-7 per watt installed. To put this in perspective, a typical home could use a 4kW system which cost \$24,000 to install. This system would provide approximately 6,000 kilowatthours of useful energy each year at present electricty rates this \$750 per year savings represents a simple payback of 32 years. Near term growth in economic expansion of the PV market for utility connected customers appears unlikely. Market research conducted by the author and his colleague indicate that until installed PV prices reach \$0.6-1.3 per watt, no major changes in the demand for PV by the grid-connected market is likely. [23] There are many different types of PV cells that have been attempted from single crystalline to multi crystalline to amorphous cells. In the last five years only minor additional improvements to the technologies have been made leading to a flattening of the price curve at \$4 per watt since 1990 [see Figure 1.4].

1600 - 16

Probably the forms of solar energy with the least potential for future development and expansion are ocean thermal and wave power. The ocean is a source and sink for energy of many types. It is probably the vast dihydrogen oxide resource of the ocean that





Peter Mark Jansson, P.P.,P.E. Page 19 of 73

keeps the temperature, environment and atmosphere of the planet moderated and suitable for human life. In that same environment thermal gradients and atmospheric disturbances cause currents, waves and temperature differences around the world. Ocean Thermal Energy Conversion [OTEC], is a technology that was conceived of in 1880 by d'Arsonval. OTEC takes advantage of the thermal gradient which exists in the sea and is especially pronounced around the tropical regions where surface water temperatures can get very high. This approach to energy generation uses ammonia as a working fluid. This fluid runs an evaporator-condensor cycle where cold water from deep in the ocean condenses the ammonia vapor while warm water on the ocean surface is used as a heat source to boil the ammonia to give it the vapor pressure needed to drive a gas turbine. The gas turbine in turn drives an electric generator. In 1930 the first demonstration plant was constructed in Cuba; since that time no additional plants or demonstrations have been constructed. The islands in the tropic zones may have potential for this technology at some point in the future but presently the technology is very expensive which has limited its development. Wave energy systems are not commercially available at the present, but it is believed that the difference in wave heights may be commercially exploited at some point in the future. Ocean currents may provide a significant potential source of energy as well but no commercial technologies currently exist to harness it effectively. Similarly to OTEC, ocean current systems will be further hindered by the fact that where the energy source is located is often far from where the demand for energy exists.

1.4 Geothermal Energy

If you have ever sat or swam in a natural hot spring you are familiar with one of the benefits of Nature's outpourings of geothermal heat. While less dramatic than the volcanos or geysers, low temperature geothermal sources make up a significant portion of the global geothermal resource. The most widely used type of geothermal resource for energy generation is the natural steam reservoirs. By 1990 the U.S. was generating "over 2800 MW_e at 4 to 6 cents per kWh^{n[24]} from these reservoirs in the western states. While the U.S. potential for geothermal is estimated at 22,675 QBtu [this compares with an annual U.S. energy use of 82 QBtul there has been little additional exploitation of these reserves since the removal of Federal tax subsidies in the 1980s. The most economical and expanding market for geothermal energy applications exist in the residential and commercial sectors. Geothermal heating and cooling systems use the earth as a heat source and sink with an electric heat pump to move heat into or out of the conditioned space. Geothermal heatpumps move 3-4 kWh of energy for every one kWh of energy they consume. This technology was perfected in Sweden and is seeing extensive application in the U.S. and other industrialized countries. In many applications it represents the least costly heating and cooling system on an annual energy as well as operation and maintenance cost basis. The use of geothermal energy in these applications is likely to expand.





Peter Mark Jansson, P.P.,P.E. Page 20 of 73

1.5 Tidal Energy

There are presently no commercial tidal facilities in the United States and only three tidal power systems in the world. These facilities operate on principles that are very similar to those of hydroelectric stations. They require a reservior, a dam and a series of turbine generators. In the case of tidal systems they are capturing the kinetic energy that exists in the movement of tidal waters into and out of an estuary or man-made reservior four times each day. The energy is being created by the gravitational interaction of the Sun, the Moon and the Earth which causes this motion in the seas daily. In the lower 48 continental U.S. the tidal variations range from 2 to 16 feet between mean high and mean low waters. In the U.S. the potential for tidal power represents less than 15,000 MW. The global potential for the most favorable tidal power sites is about 63,000 MW, or about 1/50th the world's potential for hydroelectric power. The three tidal facilities in operation worldwide are a 1-MW plant on the White Sea in Russia [1969], a 240-MW plant on the Rance River in France [1966], and most recently a 20-MW plant on the Bay of Fundy in Canada.





Peter Mark Jansson, P.P.,P.E. Page 21 of 73

Chapter 2 - An Overview of Mill's Technology

This chapter will focus specifically on the hydrocatalysis technology developed by Dr. Randell Mills of BlackLight Power, Inc.. After providing an overview of the theory behind the design of the various technologies I will move to a review of the astrophysical data which supports Dr. Mills' claim that fractional state hydrogen is common and abundant throughout the universe. I will highlight some key enigmas that Dr. Mills' theory solves and review the current technological devices that capture energy from this new found fuel source. Table 2.1 below summarizes the significant government, corporate and university research centers that have partnered to corroborate many of BLP's experimental findings.

TABLE 2.1 - BlackLight Power Research Partners

LABORATORY

Government

Idaho National Engineering Laboratory

SDIO-Wright Patterson AFB Chalk River National Lab [Canada] NASA - Lewis Brookhaven National Lab

University

Lehigh University - Zettlemoyer Center for Surface Studies M.I.T. Lincoln Laboratory Pennsylvania State University Ursinus College Moscow Power Engineering Institute Laboratory for Electrochemistry of Renewed Electrode-Solution Interfaces [LEPGER]

Corporate

Thermocore, Inc.
Air Products & Chemicals
Westinghouse Electric Corporation
Charles Evans & Associates Laboratories
Schrader Analytical & Consulting Laboratory
BlackLight Power Laboratories

WORK PERFORMED

Electrolytic Cell [850% VI]
X-ray Photoelectron Spectroscopy
Diffusion Cell
Electrolytic Cell [130% Vi DC]
Electrolytic Cell [170% Vi DC]
Electrolytic Cell

X-ray Photoelectron Spectroscopy

Electrolytic Cell [400% Vi DC]
Gas Cell [>2000% H₂ Energy]
Electrolytic Cell
Electrolytic Cell [250% Vi DC]
Electrolytic Cell

Electrolytic Cell [2100% Vi AC]
Mass Spectroscopy
Electrolytic Cell [150% Vi DC]
TOF-SIMS
Mass Spectroscopy
Electrolytic Cells [2100% Vi AC]
Gas Cells [2 - 50 waft Energy]
Mass Spectroscopy
Gas Chromatography





Peter Mark Jansson, P.P., P.E. Page 22 of 73

In the column entitled "Work Performed" I have summarized the types of devices tested or work performed in each laboratory. In all cases these labs provided data and results which were consistent with the results anticipated by the Mills theory [i.e. excess heat production, hydrino or dihydrino signatures, etc.]. The numbers in brackets, where provided, show the energy output to energy input ratio confirmed by the lab. I gathered this data by reading and summarizing the reports produced by the labs themselves. A detailed bibliography of the reports generated by these partnerships, plus others I was able to catalogue has been provided in Appendix 1. It is important to note that all of the work in Table 2.1 is very recent, having been completed during the last five years. The four subsections of Chapter 2 are as follows: Section 2.1 will briefly describe the theory Dr. Mills developed leading to the design of the various BLP technologies. Section 2.2 will summarize and analyze some of the astrophysical data which supports Dr. Mills' claims with that this new form of hydrogen is prolific throughout the universe, Section 2.3 will describe a few of the enigmas that Dr. Mills' theory solves, and Section 2.4 will provide a brief synopsis of the state of the art of current BLP technological devices that demonstrate energy production from the new found fuel source.

2.1 Hydrocatalysis - A Theoretical Overview

The catalytic reduction of atomic hydrogen below its ground state of n=1 has been postulated by Dr. Randell Mills of BlackLight Power, Inc. There is substantial data that has been gathered confirming an unexplainable amount of energy being released from hydrogen; these energy values are well in excess of any known chemical reaction with hydrogen and were observed by others when reproducing BLP experiments. In addition, new electronic signatures corresponding to the expected [ie; calculated] energy values for low energy hydrogen via mass spectroscopy, gas chromatography, x-ray photoelectron spectroscopy and extreme ultraviolet spectroscopy have been identified. A non-trivial number of independent laboratories and research centers have been involved in the confirmations described in the above findings. In addition, a sound theoretical basis for the phenomenon has been postulated by Dr. Mills which unifies field theory with a completely classical approach to physics. Mills theory holds at its foundations inviolate the classical laws of physics, including all of those listed below:

- 1] Conservation of mass-energy
- 2] Conservation of Linear and Angular Momentum
- 31 Maxwell's Equations
- 4] Newton's Laws of Mechanics
- 5] Einstein's Special Relativity
- 6] Einstein's General Relativity

The postulated reduction of hydrogen to fractional quantum energy levels represents a radical departure from currently held quantum theory. But when it comes to





Peter Mark Jansson, P.P.,P.E. Page 23 of 73

the classical laws of physics the Mills' theory rather than contradicting current models actually builds upon them. Dr. Mills' approach is fundamentally based upon the theoretical hydrogen atom energy equation developed by E. Schrödinger and W. Heisenberg in 1926 shown below.

$$E_n = -e^2 / n^2 8\pi \epsilon_0 a_H = -13.598 \text{eV} / n^2$$
 (1a)

$$n=1,2,3,\ldots \tag{1b}$$

Dr. Mills has proposed that a new boundary condition, derived from Maxwell's equations, be applied to Schrödinger's original equation. When it is applied to the fundamental hydrogen equation the Mills' model suggests a purely physical model which applies for all of known nature. This same model applies on the microscale [i.e. particles, atoms, molecules] and through the macroscale [i.e. planets, stars, galaxies and the overall universe]. A more detailed overview of Mills' theory for the interested reader was developed by this researcher and is provided in Appendix 2. The modification Dr. Mills' theory would make predicts that equation (1b) above be replaced with equation (1c) below which allows for lower than n=1 non-radiative valence states for the hydrogen atom.

$$n = 1, 2, 3, \ldots, \text{ and, } n = 1/2, 1/3, 1/4, \ldots$$
 (1c)

His mathematical solution uses fundamental constants only and the energy values predicted by his theoretical approach agree in a most compelling way with observations scientists have made of the universe and stars. The new form of fractional valence states of the hydrogen atoms [named "hydrinos" by their discoverer, Dr. Mills] are able to radiate meaningful amounts of energy as they undergo electron relaxation to lower energy states [see Table 2.2].

TABLE 2.2 - Energy Released From Lower Energy Hydrogen

_	R [radius]	Energy Released (eV)						
n	K [radios]	r=∞ tor=R	$\Delta E_{final} - \Delta E_{initial}$					
4	a _H	13.6	 .					
1	а _н /2	54.4	40.8 [1->1/2]					
1/2		122.4	68.0 [1/2 ->1/3]					
1/3	a _H /3	217.7	95.3 [1/3 -> 1/4]					
1/4	a _H /4	340.1	122.4 [1/4->1/5]					
1/5	a _H /5	1360	258.4 [1/9->1/10]					
1/10	a _H /10		2706.4 [1/99 -> 1/100					
1/100	a _H /100	136keV	2100.4 (1155 × 11100)					





Peter Mark Jansson, P.P.,P.E. Page 24 of 73

This source of energy likely represents more than 40% of the radiant energy created by stars. Figure 2.1 below is an illustration of the change in radii of the hydrogen atom taken from his text on his theory "The Grand Unified Theory of Classical Quantum Mechanics". [27] The well accepted model [i.e. when a hydrogen atom absorbs a photon and increases the radii between its electron and proton, n=2, n=3, n=4, etc.] is shown in the top half of the page.

FIGURE 2.1 Quantized Sizes of Hydrogen Atoms Effective Nuclear Charge +1/3x 27.21 eV; n = 1,23. Absorption οĒ Photon +1/n +1/2 Normal +1 Ground State +2 +3 Absorption +4 +n **Energy Hole** +5 O 0 +6





Peter Mark Jansson, P.P.,P.E. Page 25 of 73

The radical new model Dr. Mills has proposed [i.e. that there exist stable forms of hydrogen in fractional energy states below the accepted ground state, n=1] with its commensurate fractional radii between the electron and proton [i.e. n=1/2, n=1/3, n=1/4, etc.] are shown on the next page. The model being proposed will hereinafter be referred to as "Mills Theory".

It is important to emphasize at this point that the transistions described are not nuclear. This is a chemical reaction that only effects the binding energy of the hydrogen atom's electron. The fundamental energy release mechanisms in this process are hydrocatalysis and disproportionation. Hydrocatalysis occurs when a hydrogen atom with its electron at its normal ground state or a lower ground state [ie; $n \le 1$] reacts with a catalyst having a net enthalpy of 27 eV. Energy is released per equation (1d). Disproportionation occurs when a lower energy state hydrogen atom [ie; n < 1] collides with another lower energy state hydrogen atom [ie; n < 1] which results in the ionization of one atom [ionization energy is a multiple of 27 eV] and the transition of the electron of the other atom to a stable, lower energy level. Energy is released per equation (1e) when the atom which ionizes has its electron at its n = 1/2 state.

$$E = (1/n_f^2 - 1/n_i^2) \times 13.6 \text{ eV}$$
 (1d)

$$E = (1/n_f^2 - 1/n_i^2) \times 13.6 \text{ eV} - 54.4 \text{ eV}$$
 (1e)

The interested reader is referred to Appendix 2 for more detail on Mills theory.

2.2 Astrophysical Corroboration

The theoretical model proposed by Mills might remain an interesting approach to unifying physics but be written off as a theory of no import were it not for the fact that the laboratory of the universe provides a prodigious amount of data which appears to support his predictions. For example, his theory predicts that the electronic transition of atomic hydrogen below its ground state of n=1 is a widespread phenomena which provides a significant amount of the energy radiated by all stars. The theory also predicts this transition reaction occurs in the atmosphere of some of the larger planets [Jupiter and Saturn] as well as in the dark regions of space. Hydrogen is the most abundant element in the universe, and if it also is able to exist in a stable form in lower energy states it must be measurable and detectable. There is substantial observational data confirming that possibility. One source is the extreme ultraviolet spectrometer data collected and analyzed by Simon Labov and Stuart Bowyer of the Center for Extreme Ultraviolet [EUV]

Astrophysics at UC-Berkeley. They designed and had launched a diffuse, grazing





Peter Mark Jansson, P.P.,P.E. Page 26 of 73

incidence EUV spectrometer into space from White Sands Missile Range in the spring of 1986. They analyzed their data and published it in the Astrophysical Journal in the spring of 1991. Their data is remarkable in many ways; 1] it was not believed that such data could be collected, 2] they observed and validated significant emission features and signatures from the dark regions of space, 3] they acheived a very high statistical confidence that the data was real [in many cases >99% confidence] and 4] their explanations for what these emission signatures must be postulate that an unexplainably high temperature [million degree gases] must exist in what was otherwise believed to be a vastly cold region.

Upon review of this data the scientists of BLP, being chemists by background believed that "hot interstellar gas" view of dark space was not very plausible. They undertook to view this data in light of the fundamentals of the Mills' theory which predicts that lower energy hydrogen can collide with other lower energy hydrogen atoms and undergo an energy transition to a lower non-radiative energy state. These transitions radiate at specific energy levels and wavelengths as predicted by equations (1d) and (1e) as described above. While the Labov and Bowyer's interpretation of these signatures originating from hot interstellar gases [Fe_{XIX} , Fe_{XI} , O_V , etc.] is more widely accepted by astrophysicists, other scientists see the explanation as less plausible.

The BLP assignment of these and many other planetary, stellar and interstellar radiation signatures to a calculated amount of energy being released from hydrogen atoms undergoing collisional effected transitions to lower energy states appears to be much more plausible. When the data is analyzed and one views the assignments of the probable hydrogen transitions and sees the reasonableness of such a theoretical match it appears to be much more than a remarkable coincidence. The analysis provided by BLP in Table 1 [on page xiii of the Forward] as well as page 424 of the text on the theory 1271 shows a match between the background data and theoretical transitions for nearly all of the transitions that are probable to the n=1/8 state of hydrogen. I have reproduced these calculations in Appendix 3 and provide a summary of one of those spreadsheets on the page that follows as Figure 2.2.

Perhaps an even more compelling way to view this data is in the manner developed by Jim Kendall, P.E., a Ph.D. Nuclear Engineer from Technology Insights [a technology assessment firm from southern California]. He graphically stacked the Labov and Bowyer data side by side with Mills theory predictions as shown in Figure 2.3 to reveal a correlation which is most persuasive.





261.2

302.5

459.1

584.0

607.5

633.0

10

11

12

13

14

15

16

Peter Mark Jansson, P.P.,P.E. Page 27 of 73

40.8

13.6

27.2 2nd order Peak 9

21.2 Helium Resonance

20.4 2nd order Peak 11

19.6 He scattered

303.9

455.9

584.9

607.8

633.0

911.7

FIGURE 2.2 - Astrophysical Observations and Mills Theory

Raw Extreme UV Background Spectral Data * MILLS PREDICTED Fractional State **OBSERVED DATA** WaveInth Energy 1/ni 1/nf WaveInth Energy Calc e۷ eV eΥ Peak 149.6 7 82.9 146.2 8 146.2 84.8 122.4 101.3 6 122.2 7 122.2 101.5 2 108.8 2 114.0 106.2 4 106.2 116.8 3 95.2 130.2 5 95.7 95.6 129.6 87.6 He scattered 141.6 2 88.8 88.88 139.6 74.8 2nd order Peak 1 5 165.8 76.0 75.9 163.2 6 68.0 182.3 68.2 5 68.3 61.2 2nd order Peak 2 7 181.7 202.6 7 61.8 200.6 61.8 8 54.4 227.9 3 53.0 53.0 233.8 46.8 He scattered 9 265.0

47.5

27.0

21.2

20.4

19.6

·~41.0

47.5

41.0

27.0

21.2

20.4

19.7

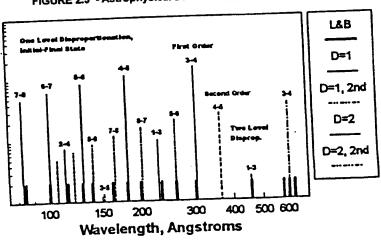
FIGURE 2.3 - Astrophysical Data vs. Mills Theory Illustrated

3

3

3

2







Peter Mark Jansson, P.P.,P.E. Page 28 of 73

The analysis completed by this researcher in Appendix 3 corroborates the findings of BLP in regard to the extreme ultraviolet data in the background of space [above] as well as from our star, the Sun, as well as from a stellar flare on AU Mic and star EQ Pegasi. Dr. Mills' text also provides many other sources of astrophysical data which produce information that regularly display the lower energy hydrogen transition energies that would be most likely from a probabilistic standpoint. Table 2.4 on the page that follows lists the most commonly occurring wavelengths and energies in all of the data described above [ie; data that appeared in at least 3 of the 4 sources cited] and the match I have calculated for that data by equation (1e) above.

TABLE 2.3 - Commonly Observed Wavelengths & Mills Theory Predictions

Wavelength	Mills Theo	# of sources	
A	A	of 4	
044.0	912.3	1/2 -> 1/3	1*
911.8	303.9	1/3 -> 1/4	3
302.8-304	265.0	1/4 -> 1/5 He scattered	3
261.2-265		1/4 -> 1/5	4
182-183	182.3	1/5 -> 1/6	4
129.1-130	130.2	1/6 -> 1/7 He scattered	3
122.2-123	122.6		4
101-101.3	101.3	1/6 -> 1/7	3
89-90	89.0	1/7 -> 1/8 H scattered	3
81-81.1	81.1	1/3 -> 1/5 H scattered	

^{*} NOTE: Only one source, the solar spectral data, included observations above the 600 Å wavelength

2.3 Enigmas Solved

Perhaps the two most compelling enigmas that the Mills theory resolves are solar problems. They are; an inadequate solar neutrino flux and a solar coronal temperature that is inexplicably too hot. For two decades we have known that the standard solar model predicts that the primary energy source of our star is the nuclear fusion of hydrogen atoms. The problem is that scientists have been unable to account for an appreciable amount of the solar neutrino flux that would be predicted by assuming all of the Sun's radiant energy is from fusion. The Gallex solar neutrino detector in Italy sees only 60% of the neutrinos that the standard solar model would predict. $^{[29]}$ The Homestake detector reports neutrino flux of 2.1 ± 0.03 SNU or only 27% of the standard solar model's 7.9 ± 2.6 SNU. $^{[30.32]}$ Where





Peter Mark Jansson, P.P.,P.E. Page 29 of 73

then, if not fusion, could the rest of the Sun's energy be coming from? A similar problem exists with the description of all of the Sun's energy coming from nuclear fusion when we consider the temperature gradient from the surface of the Sun into space. The photosphere [visible surface layers] of the Sun is 6000 K, "whereas the temperature of the corona [solar atmosphere] based upon the assignment of the emitted X-rays to highly ionized heavy metals is in excess of 1,000,000 K." [33] The Mills theory is able to explain both of these seeming mysteries by postulating the disproportionation of hydrogen atoms in the atmosphere of the Sun. This transition of hydrogen to lower energy states as previously discussed gives rise to significant non-nuclear radiant energy [ie; transitions of hydrogen to the n = 1/100 level yield energy densities (139 keV) on the order of nuclear reactions]. The disproportionation reaction takes place in the coronal region of the Sun giving rise to the much higher temperatures there. Together the Mills theory makes sense of what otherwise could only be explained by difficult-to-believe concepts. The standard solar model has no answers for this enigma but two theories attribute the higher coronal temperature to "the conversion to heat energy by the dissipation of the energy in electric currents or magnetohydrodynamic [MHD] waves." [34] If the corona consists of an "almost fully ionized plasma contained in closed magnetic field loops or of plasma expanding outwards along open magnetic field lines" [35] it is quite a stretch and additional complication to propose the electric currents or MHD.

Another key enigma solved is that of the total mass or matter in the universe. For years physicists have been wrestling with the fact that either "black holes" or an unidentified "dark matter" must exist out there in space in order to explain why our calculated mass of the universe can not be obtained by adding up all of the radiative and observable matter. We need more mass to explain the observation that galaxies rotate at a higher angular velocity than possible with only the observed [visible] matter providing the stabilizing gravitational attraction. [36] Is it too much a stretch for the logical mind to postulate that if over 95% of the known matter of the universe consists of hydrogen that the large amount of "missing matter" may also be some non-radiative form of hydrogen? Mills theory predicts that stars consume hydrogen and convert it into lower energy state hydrogen as the "ash" residue of the reaction. This ash is non-radiative, microscopically smaller than ground state hydrogen and is believed by Mills to be ubiquitous throughout the universe. It would appear to be an excellent candidate for the undiscovered, yet ubiquitous dark matter of the universe.

2.4 Technological Embodiments

This final section of Chapter 2 is devoted to devices and apparatus that have been designed and operated by BLP scientists in order to prove that the catalytic reduction of atomic hydrogen below its ground state of n=1 is not only acheivable but is repeatable,





Peter Mark Jansson, P.P.,P.E. Page 30 of 73

predictable and consistent. Table 2.4 below indicates the types of devices that have been designed and developed by BLP scientists to demonstrate the phenomenon.

TABLE 2.4 - BLP Technologies

Device	Туре	Other
Dewar Flask	Electrolytic Cell	
Electrolytic Cell	Electrolytic Cell	DC electricity
Electrolytic Cell	Electrolytic Cell	AC electricity
Non-Electrolytic Cell	Gas Phase	
Glass Lamp	Gas Phase	
Isothermal Calorimeter	Gas Phase	
Calvet Calorimeter	Gas Phase	Oven Moderated
Nickle Hydride Wire Cell	Gas Phase	Water Cooled
Quartz Firebrick Cell	Gas Phase	
Test Cell 1	Gas Phase	Steady State Flow

Furthermore, all of the devices in the above table exhibit the ability to generate anomolous heat that is inexplicable by any known chemical or nuclear reactions. These devices generate heat with no flux or radioactive materials, reduction or consumption of known chemical or molecular reactions or bonds and follow directly from the Mills theory. The specific devices are in essence the embodiment of his concepts for bringing hydrogen atoms into contact with a catalyst in order to begin the hydrocatalysis and subsequent disproportionation reactions. The devices developed by BLP are both test and demonstration units.

The two and one-half pages following below provide illustrations of some of the key BLP technological embodiments. Figure 2.4 illustrates the dewar experimental vessel. Figure 2.5 shows the typical arrangement for one of BLP's advanced electrolytic cells. Figure 2.6 illustrates the device developed by the BLP joint venture with Thermacore — a non-electrolytic first generation gas phase cell. Figure 2.7 illustrates the isothermal calorimeter and Figure 2.8 is a typical Calvet calorimeter arrangement. I am focusing on these few devices to keep the reader directed to the specific technological embodiments of the Mills theory that demonstrate that the production of excess and anomalous heat from each apparatus is conditional upon bringing all of the elements of Mills' theoretical requirements to the experiment. If any one of the key elements is





Peter Mark Jansson, P.P., P.E. Page 31 of 73

missing, the experiment functions as a typical control with no excess heat being produced.

FIGURE 2.4 - Dewar Experimental Cell

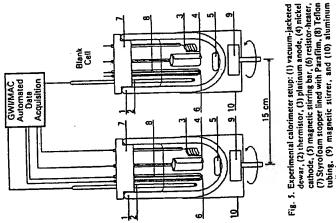
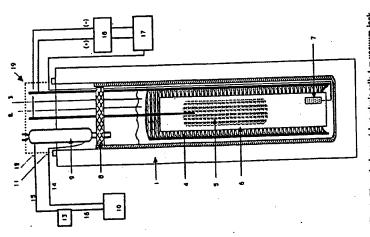


FIGURE 2.5 - Advanced Electrolytic Cell



6 = Tellon spacer, 7 = resistor heater, 8 = Tellon cap, 9 = condenser, 10 = peristaltic pump, 11 = inlet thermistor, 12 = outlet thermistor, 13 = water denser outlet tubing, 16 = reservoir to pump tubing, 17 = power supply, function generator, power meeted dewar, 2 = electrolyte thermistor, 3 = conduclivity sensor, 4 = nickel anode, 5 = nickel cathode. Fig. 1. The calorimeter/electrolysis cell: 1 = vacuum jacker, 18 = oscilloscope, 19 = insulated cap.





Peter Mark Jansson, P.P.,P.E. Page 32 of 73

FIGURE 2.6 - Non-Electrolytic Gas Phase Cell

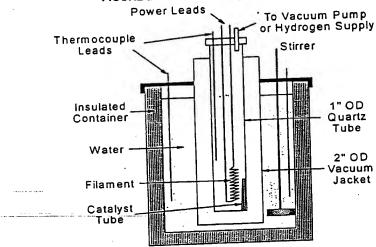
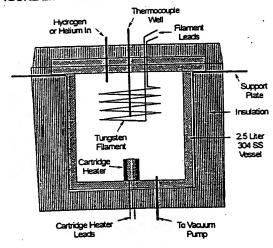


FIGURE 2.7 - Isothermal Calorimeter Gas Phase Cell





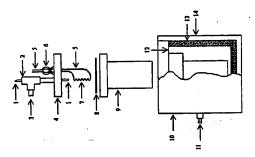


.....

Peter Mark Jansson, P.P.,P.E. Page 33 of 73

FIGURE 2.8 - Calvet Calorimeter Gas Phase Cell

Figure 1. Schematic of the Gas Cell for the Calvet Calorimeter and Cross Sectional View of the Calvet Calorimeter. 1 - (1/16)" OD stainless steel tube (to hydrogen supply), 2 - stainless steel tube (to vacuum marifield), 4 - cell id, 5 - filament leads, 6 - Conax-Buffato gland, 7 - precision resistor, 0.1 mm OD tungsten filament, or nickel hydride filament treated with catalyst, 8 - copper ring gasket, 9 - cell body, 10 - Calvet Calorimeter, 11 - thermopile signal output, 12 - thermal shunt, 13 - thermopile, 14 - insulated calorimeter base.



In the case of the electrolytic cells it is very important that the hydrogen atoms be formed on the cathode contact with the right concentration of the catalytic ions in order for the heat generation phenomenon to be replicated. In the case of the gas cells a small, partial atmosphere of hydrogen gas, a small partial pressure of the catalytic ions as well as a mechanism to cause hydrogen dissociation all need to be present for the reaction to commence and continue. The experiments and subsequent demonstration units were designed specifically to assure that the mean free path for the hydrogen atoms [once formed] to interact with and collide with the catalytic ions was appropriate to favor the collision and catalytic reaction prior to hydrogen atom recombination into H₂.

Each of the cells illustrated above were able to regularly, consistently and repeatedly generate heat in amounts that were far in excess of the any known chemical reaction for hydrogen and any other known elements. In the case of the vacuum gas cells this reaction was developed and maintained using only very small amounts of hydrogen gas, a filament to dissociate H₂ into its atomic form and a catalyst with the appropriate resonant enthalpy of 27 eV. Part II of this thesis will highlight the performance of BLP's isothermal cell, Penn State University's Calvet cell experiments as well as the experiments of this researcher in the Calvet cell at BLP laboratories.

To more fully document the BLP theory that lower energy hydrogen [hydrino formation] was the source of the heat in the reaction, the residue "ash" as it were from the reaction gases from both the electrolysis and vacuum cells was collected. According to Mills theory this "ash" should contain the lower energy form of hydrogen postulated by





Peter Mark Jansson, P.P.,P.E. Page 34 of 73

BLP. The difficulties of capture make this effort quite a challenge since the atoms being searched for will have significantly smaller diameters than the smallest of all atoms. BLP and four other scientific laboratories began this search a few years ago. They used the methods of mass spectroscopy, gas chromatography and X-ray photoelectron spectroscopy [XPS]. Table 2.5 below highlights the results of those investigations thus far.

TABLE 2.5 - The Search for Hydrinos

Device	Results/Observations	Investigating Laboratory
Mass Spectroscopy	Large signal with ionization energy in calculated range of dihydrino	BLP Laboratory Air Products & Chemicals Lab Schrader Analyt. & Cons. Lab
Gas Chromatography	Significant signal peaks which can be associated with n=1/2, 1/3 and 1/4 dihydrino molecules	BLP Laboratory
X-Ray Photoelectron Spectroscopy [XPS]	Signal Peaks associated with the binding energy of n=1/2, 1/3 and 1/4 hydrino molecules	Lehigh University - Zettlemoyer Center for Surface Studies Idaho National Engineering Lab Clark Evans & Associates

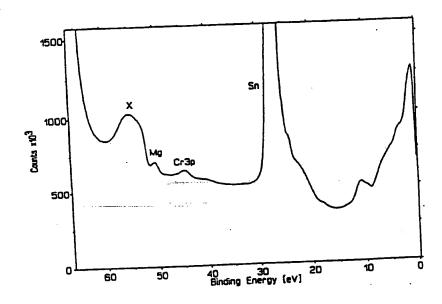
Figure 2.9 which follows on the final page of Part I illustrates the location of an anomalous peak near 55 eV binding energy which was detected by Zettlemoyer Center for Surface Studies at Lehigh University, Charles Evans & Associates and Idaho National Engineering Laboratories [INEL] in separate analyses of BLP and INEL samples. BLP asserts that the n=1/2 state of hydrogen, which has a calculated binding energy of 54.4 eV, is the source for the peaks in each independent study. At present all other potential known sources of a peak at that energy level [i.e. Fe_{3p}] have been ruled out as a source.





Peter Mark Jansson, P.P.,P.E. Page 35 of 73

FIGURE 2.9 - XPS Anomalous 55 eV Peaks







Peter Mark Jansson, P.P.,P.E. Page 36 of 73

PART II - Analysis of Previous Experimental Results

As noted in Chapter 2 [Table 2.1] there have been a substantial number of tests of BLP electrolytic cells. This researcher was not able to find any documented results from tests that had been performed on BLP cells which indicated that the cells did not operate in a manner to generate the anomalous heat predicted by BLP scientists. However, due to the controversial nature of electrolytic cell and the close association of the work with the continuing debate regarding cold fusion claims I have directed my research toward reviewing the test results which have been achieved in the gas phase cells. It is worthy of note at this point that there continue to be significant publications in Fusion Technology where well respected scientists are continuing to claim excess heat in so called "cold fusion" cell experiments. Of particular note is a recent technical paper in the March 1997 Fusion Technology journal. The authors [from Shell Research / CNAM Laboratoire des Sciences Nucléaires in Paris, France] describe how they have detected and verified that they are creating excess energy from hydrogen "7300 times higher than the most exothermic known reaction" at a high confidence level [99%]. They also detect missing hydrogen in their exhaust samples. Further, they present their postulate that the source of the additional energy is from "the formation of a tightly bound state of hydrogen...In such bound states, the electron is much closer to the proton than in normal hydrogen. This could explain both a high energy of formation and a greater than normal capacity to diffuse through any material" [37] All of these findings are consistent with the Mills theory. Part II of this thesis will focus on summarizing the results of two of the gas phase cell experimental results developed to date noting with special interest the experiments conducted by this researcher in section 3.3. In each case the gas phase cells produce a statistically significant [ie; beyond the error range and accuracy of the measuring device] amount of unexplainable heat. In the experiments the heat generated is well beyond the most energetic of chemical reactions known for hydrogen. I will attempt to explain, when possible potential reasonable alternative explanations for the repeatedly observed phenomenon. Often, however, there is no reasonable explanation other than the potential for a new energy source resulting from the interaction of hydrogen and the catalyst materials in the cells. After summarizing all of the gas phase cell experiments, the results of a singular isothermal cell test will be reviewed in detail [the experimental results from this cell formed the basis for the computer modeling work detailed in Chapter 4]. Results from the Penn State University cell will be reviewed and then the closing section will summarize the results of my work with Mr. William Good, the Chief Scientist and Director of Research & Development at BLP.

Chapter 3 - Summary Review of Gas Phase Cell Experimental Results

Table 2.4 illustrated seven gas phase cell experimental devices. I will provide a detailed explanation the operation of two of these devices in sections 3.1 through 3.3. I will place special focus [sections 3.2 and 3.3] on the Calvet device [see Figure 2.8] which is the most accurate in measuring the heat generated in a BLP reaction. Prior to the announcement of the hydrocatalysis process developed by BlackLight Power the





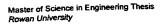
Peter Mark Jansson, P.P.,P.E. Page 37 of 73

paradigm for hydrogen as a fuel revolved around its energetic reaction with oxygen. In nature, water [H₂O] is a very abundant, stable and versatile molecule. Hydrogen is very energetically bound to oxygen, and requires significant energy to break these these stable bonds to yield H2. After they are broken, hydrogen in its molecular form [H2] is also stable, but reacts well and energetically with many other elements to form a plethora of molecules and compounds. The basic principle being tested with the gas phase cells of BLP is the ability of the hydrogen atom, once dissociated from its molecular form, to undergo electronic transition to lower energy levels [as described in Chapter 2] when it collides with a catalyst. All of the experiments therefore that will be described in the next three sections are configured to provide a reaction chamber [capable of operating at vacuum or near vacuum pressures], a means for hydrogen to be introduced to the chamber, a catalytic material to be introduced in the reaction chamber, a means for dissociating the hydrogen molecule into its atomic form, and a method for measuring heat generated by the reaction. Fundamentally the two cells reviewed in Chapter 3 are identical in nearly all respects except for the method for measuring or determining meaningful heat generation. The Calvet cell utilizes very accurate thermopiles to measure the heat flowing out of the vessel into the constant temperature oven. The isothermal cell uses the laboratory environment as the 'stable' external temperature and assumes the internal cell temperature represents a steady state heat loss previously measured by control runs to yield an 'estimate' of the additional power [anomalous heat] being provided by the reaction in a more indirect way. The Calvet cell experiments yield heat on the order of 6% to 12% more than energy being provided by the reaction than that used in the reaction zone [0.6 to 1.2 watts over a 10 watt filament power]. The isothermal cell experiments indicate heat gains of 52% to 171% over the energy being provided to the reaction zone [43 to 55 watts over a 32-86 watt input power]. It is the isothermal cell experiments that are of the greatest interest to this researcher since they portend the greatest potential for creating commercially significant heat. Section 3.1 focuses specifically on that BLP technological embodiment.

3.1 BlackLight Power Isothermal Cell

In the laboratory of BLP in Malvern, Pa. this researcher observed an experimental test on May 1, 1996 which was quite intriguing. A stainless steel vessel of 2 liters in volume was evacuated to a pressure of 1150 millitorr. [760 torr = 1 atm.]. This vessel was being maintained at a steady state temperature of 275° C by way of a cartridge heater consuming 97.1 watts located in the base of the vessel [see Figure 2.8]. The only materials inside this vessel were a 200 cm tungsten filament [0.01 cm. diameter] supported by 4 ceramic rods connected by 1/8th inch stainless steel tees and 3 grams of KNO₂ catalyst. Hydrogen was introduced into the system at a pressure of 1 atmosphere, the valve to the vacuum was opened and the pressure reduced to 2 torr minutes later. When the vacuum vessel comprised a closed system it had a steady state pressure of 1150 mtorr. When the power to the tungsten filament was turned on and raised to 15 watts the cartridge heater turned off and did not come back on for about one half hour. The temperature rose from







Peter Mark Jansson, P.P., P.E. Page 38 of 73

275° C to about 285° C during this period. When the cartridge heater did begin cycling again to maintain the vessel temperature at approximately 275° C it did so at a steady state energy consumption rate of 48.5 watts. [The details of this experiment are found in Appendix 4] The filament wattage was successively increased to 25 watts, 35 watts and 40 watts in three additional steps during which the cartridge heater energy decreased to 17.2 watts, 5.7 watts and 0 watts respectively. The vessel continued to maintain a temperature of 288-289° C without any energy being provided by the cartridge heater. The filament steady state power consumption was 40 watts indicating that something [presumably the Hydrocatalytic effect] occurring within the vessel appeared to be providing the additional 57 watts of heating that was necessary to keep the vessel at temperature. If one assumes that all the data being gathered on this closed system [i.e; energy in, temperature, pressure and chemicals involved] are accurate, then this appears to be a compelling illustration of this technology's capability. Table 3.1 illustrates a significant number of BLP experimental and control runs on their isothermal calorimeters.

I have summarized the results for each of the runs but the reader is encouraged to review the detailed data in Appendix 5. The Appendix includes all of the detailed experimental data as well as the analysis completed by this researcher. It is clear from the few control studies that the isothermal cell exhibits different behavior when it is operating on filament power versus cartridge heater power. As shown in experiments 15.5 and 15.8 the isothermal cell uses significantly less power with the filament than that required on the cartridge heater. This researcher believes that this apparent 25-54% savings may be due to four factors in the following order of significance; 1] The relative distances between the heating sources and the thermocouple [The filament was closer in proximity to the thermocouple and therefore had greater radiant coupling], 2] Radiant coupling of the filament with the thermocouple may have resulted in the thermocouple being at a higher temperature than actual temperature. [This condition would allow the cell to cool down and thus reduce to some degree its heat loss and associated energy requirements]. 3] Increased stratification may have occurred under filament power [i.e.; convective mixing of gases may not have occurred sufficiently allowing stratification. With the upper regions of the cell warmer than the lower regions of the cell heat loss would have decreased across the entire cell surface]. 4] In the case when the cartridge heater was the only source of power, heat loss through the bottom of the cell may have been higher, thus the thermocouple in the cell will need to see greater power from the cartridge heater in order to cycle off the power. It is important to note that another way of considering this last point is that the filament provided all of its heat interior to the cell most efficiently, while the cartridge heater entered through and was connected to the bottom surface of the calorimeter allowing a larger percentage of its heat energy to leave the cell without affecting thermocouple temperature.

Nonetheless, it is important to note that experiments 15.4, 15.6, 15.9 and 15.10 all create anomalous heat far beyond the cartridge/filament differential calculated by the control experiments. From the heat loss model developed on these cells in Part III of this





Peter Mark Jansson, P.P.,P.E. Page 39 of 73

thesis it appears that the isothermal cells are able to create at least tens of watts of useful power even in their very primitive development state.

TABLE 3.1 - isothermal Cell Results Summary

Experiment #	Temp	Pressure (Torr)		Watts [Filament]	Excess Heat [Watts]	Power Gain [%]
15.4	259	2.0	95.2	45.7	49.5	108.3%
15.5 control	273 273	low atm 2.0	94.3 94.3	61.3 75.7	33.0 18.6	53.8% 24.5%
15.6	271	1.4	92.0	43.6	48.4	111.0%
15.8 control	261	low atm	87.3	62.5	24.8	39.7%
15.9	280	1.7	103.5	41.7	61.8	48.2%
15.10	264	1.6	92.7	32.2	60.5	187.9%
15.12	284	0.02	106.0	97.8	8.2	8.3%
15.12	319		131.2	83.6	47.6	56.9%

It is recommended that the isothermal cells be outfitted with external temperature measurement thermistors and that a full set of controls and experiments be carried out on these cells. From this work we can develop heat loss calibration curves under various temperature and pressure regimes. In addition, each cell should be blanketed with a standard jacket to reduce heat loss variability from experiment to experiment. From a very high temperature the cell should be turned off and a heat loss decay model be fit to its heat loss rate over time. This empirical model could then be used as a second source of validation for the calculated excess energy created in the hydrocatalytic reaction within the vessel.

3.2 Penn State University Calvet

In late 1996 Dr. Jonathan Phillips, Professor of Chemical Engineering at the Pennsylvania State University, and Julian Smith, his graduate research assistant undertook significant control experiments and tests on the heat generation of gas phase Hydrocatalysis. A complete copy of their report and findings is provided in Appendix 6. The Calvet cell





Rowan University



Peter Mark Jansson, P.P., P.E. Page 40 of 73

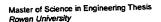
that they used is shown in Figure 2.9. The Calvet calorimeter cell is configured much like the isothermal cell described above but it includes much more accurate direct measurement of heat flux out of the reaction vessel. This measurement device is accurate to within 0.5% in recording energy flow. Unfortunately, in order to gain this extremely high accuracy one must place this vessel into a very controlled environment and into a thermopile base. This makes a large device very costly. The size of the Calvet cells used by Penn State are 20 cubic centimeters. The tests were conducted during the period of October - December 1996 in Penn State Chemical Engineering Department laboratories. The following excerpt from the report summarizes their key work and findings; "In three separate trials between 10 and 20 K Joules were generated at a rate of 0.5 Watts, upon the admission of approximately 10⁻³ moles of hydrogen to the 20 cm3 Calvet cell containing a heated platinum filament and KNO₃ powder. This is equivalent to the generation of 1x10⁷ J/mole of hydrogen as compared to 2.5x10⁵ J/mole of hydrogen anticipated from standard hydrogen combustion. Thus, the total heats generated appear to be two orders of magnitude too large to be explained by conventional chemistry, but the results are completely consistent with the Mills' model." [38]

It is noteworthy that in all cases the Penn State tests [summarized in Table 3.2] were terminated by removing the hydrogen from the reaction vessel by opening the valve to the vacuum and pumping the gas from the vessel. It is not clear how long these reactions would have continued if the vessel was not emptied of the hydrogen gas. The method used by PSU included bringing their Calvet reactor cell to steady state in a controlled environment oven with only a platinum filament and small vessel of KNO₃ present within the reactor vessel. They would zero out the Calvet output at this point and then admit hydrogen to observe the reaction that this precipitated. There experiments showed a significant exothermic reaction upon the admission of hydrogen which could not be replicated upon the admission of helium [which they used as a control gas for their experiments]. In all cases this exothermic reaction was curtailed by the researchers once the total energy that had been produced was significantly greater than that available in known chemical reactions of hydrogen.

TABLE 3.2 - Penn State Calvet Cell Results Summary

Experiment #	Temperature (°C)	Pressure (Torr)	Total Time (minutes)	Total Energy (Joules)	Excess Heat (milliWatts)
BL1218CD	250	170	612	21,560	586.8
BL1220BC	250	180	364	13,003	595.9
BL1221AB	250	120	284	10,293	604.7







Peter Mark Jansson, P.P.,P.E. Page 41 of 73

3.3 Jansson Calvet

In early 1997, this researcher approached Mr. William R. Good, Research Director of BLP to discuss the possibility of replicating the isothermal cell work at BLP to determine more conclusively the primary parameters of the gas phase reaction. It was this researchers intent to determine the effect of filament surface area on excess heat formation as well as begin parameterizations of other key variables such as reaction zone volumes, gas partial pressures, temperature, and other variables. BLP was most gracious in offering their Calvet cells for any experiments I would choose to run. The isothermal cells could be used as a follow-up in the event that the data from the Calvet work indicated a significant isothermal cell demonstration was feasible. In as much as it is believed that the formation of excess energy is caused by hydrogen atoms colliding with catalyst ions or hydrinos, I undertook to prove that increasing filament surface area would increase atom generation rate and thus increase power output from the Calvet cell. The protocol for my experiments is included as Appendix 7. A copy of my control and experimental results are included as Appendix 8. My original intent was to reproduce the Penn State experimental results and then go on to vary only the filament length in two subsequent experiments. If this could be done successfully, I believe it would demonstrate that specific parameters of the reaction could be controlled and engineered. We followed the PSU protocol in all aspects except reaction vessel pressure; this was because it appeared we were unable to demonstrate the excess heat effect at the 150-1000 torr range where the PSU reaction had operated successfully. We were successfully able to replicate numerous times the anomalous heat gain results in the 50-200 mtorr pressure regime. When we completed many of our post-experimental calibrations without the KNO3 catalyst we believe we were able to identify excess heat that was being generated from the small amount of hydrogen that was off gasing from the platinum filament. This is my present interpretation of the results I obtained. Presently I can not offer an alternative expalantion for the consistent excess heat activity when only the filaments and KNO₃ catalyst are present in the experiments. Table 4.3 below summarizes my testing objectives.

TABLE 3.3 - Jansson Calvet Testing Objectives

- Replication of PSU Results
- * Vary Filament Length [10cm , 20 cm , 30 cm]
- * Analyze Results for Consistency and Patterns
- Determine if Effect Appears Engineerable
- * Develop New Technical Skills and Knowledge





Peter Mark Jansson, P.P.,P.E. Page 42 of 73

Table 3.4 below summarizes the 9 experiments and controls that I performed during the period of February 27 through May 5 1997. Each was conducted according to the primary protocol summarized in Appendix 7.

TABLE 3.4 - Jansson Calvet Tests Completed

- * 20 cm Experiments 1 control 2 experiments February 27 - March 21, 1997
- * 10 cm Experiments 1 experiment / post control-calibration run March 25 - April 13, 1997
- 30 cm Experiments
 1 control
 4 experiments
 March 22 25, 1997
 April 13 May 5, 1997

The following tables [3.5 & 3.6] summarize the testing protocol which was followed for each of the controls and experiments conducted in the BLP laboratories:

TABLE 3.5 - Jansson Calvet Testing Protocol Summary - Control

- Prepare Calvet Reactor Vessel
- ♦Install Filament and Vacuum Test
- Place Calvet in Thermopile Cup
- ◆Vacuum test, connect leads, insulate
- Bring Oven & Calvet to Steady State
- +250° C, vacuum cell to remove all H₂O, etc.
- Start DAS, Turn On Power, Close Vac.
- ◆0,1,5,6,10,11,15,16, etc. watts to steady state
- Wait Until Steady State is Acheived
- Observe Changes in V_C



Peter Mark Jansson, P.P., P.E. Page 43 of 73

TABLE 3.6 - Jansson Calvet Testing Protocol Summary - Experiments

- Prepare Calvet Reactor Vessel
- ◆Install Filament, KNO₃, Vacuum Test
- Place Calvet in Thermopile Cup
- ♦Vacuum test, connect leads, insulate
- Bring Oven & Calvet to Steady State
- +2500 C, vacuum cell to remove all H2O, etc.
- start DAS, Turn On Power, Close Vac.
- +0,1,5,6,10,11,15,16, etc. watts to steady state
- Wait Until Steady State is Acheived
- ◆Stable V_C , W_{in} , V_f , KNO₃ vapor pressure
- Observe Changes in V_c
- Inlet H₂ to Double Current Pressure*
- Wait 5 min. and Vacuum Down to < 0.1 T
- Observe Changes in V_c

NOTE: V_c is the Calvet calorimeter voltage indicative of heat output, W_h is the total energy being consumed by the filament within the Calvet, V_i is the Voltage associated with the energy being dissipated by the filament [allows us to know I'R losses], and vapor pressure is measured in mTorr.

 $^{\bullet}$ in all cases it was not necessary to add additional $\mathrm{H_2}$ in order to observe an elevated $\mathrm{V_c}$

Table 3.7 below illustrates the calibration curves and linear regression analysis fits which I obtained for each of the control runs used in calculating the excess heat from each experiment.

TABLE 3.7 - Jansson Calvet Testing - Calibration Curves

■ 10 cm
•
$$V_c = 0.2016$$
 (W_{in}) - 0.0806 $R^2 = 0.9966$

= 20 cm

$$\bullet$$
 V_C = 0.2333 (W_{in}) - 0.0605 R^2 = 0.9996

■ 30 cm
•
$$V_c = 0.2297 (W_{in}) + 0.5188$$
 $R^2 = 1.0000$





Peter Mark Jansson, P.P.,P.E. Page 44 of 73

Pages 45-51 graphically and tabularly depict the results of the many days [over 555 hours] of analyzed Calvet cell experiments and controls. The results begin with a summary slide and then summarize the data by 10 cm., 20 cm. and 30 cm. experimental and control runs. These are labeled Figures 3.1, 3.2, 3.3, 3.4, 3.5, 3.6 and 3.7. Table 3.8 below is a numerical summary of the results obtained for all KNO₃ experiments as well as KNO₃ plus hydrogen experiments. All excess heat calculations for the experiments is based upon the difference between the Calvet output power anticipated via the control runs contrasted with the actual input power used to generate that Calvet voltage output during the experimentals. All controls and experimentals were completed in a closed system in an oven with temperature of 250 °C. In all cases the vacuum integrity of the reaction vessel was maintained throughout the entire run of the experiments.

Table 3.8 Jansson Calvet Cell Results Summary

Filament Length [cm]	Excess Po Mean	wer Genera Max	ted [Watts] Min	Hours of Operation	Total Energy Produced [W-hrs]	% Over * Chemical
10	0.581	0.635	0.523	297.97	173.013	234,387
20	0.818	1.231	0.337	125.22	102.464	138,090
30	1.572	2.092	0.635	131.95	207.467	278,151

^{* - %} Over Chemical - is the amount of energy generated by the reaction divided by the energy that would have been created had all of the hydrogen available at anytime in the experimental apparatus been consumed in the most energetic chemical reaction calculated [ie; hydrogen combining with oxygen to form water - H₂O] expressed in percent.

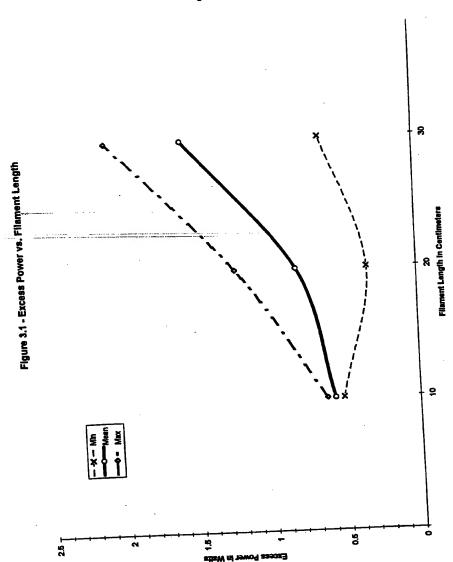
The energy produced by these experiments significantly exceeds that which could be released by any known or potential chemical reaction by several orders of magnitude. The value shown in the table above is extremely conservative in that it was determined assuming the following; 1] all potential hydrogen in the system was converted with perfect efficiency into water, 2] all of the impurities in the platinum wire [99.99% pure] were hydrogen, 3] all hydrogen admitted at any time into the reraction chamber reacted within the vessel, even though it was rapidly brought under vacuum pressure and drawn out early in each experiment. Even when these conservative assumptions are applied, there remains a significant and large amount of energy that is unaccounted for. This ranges from about 1,400 to 2,800 times the amount of energy that was available at any time to the system assuming it was able to be perfectly released in a chemical reaction. These results would appear to be entirely consistent with Mills theory.





Peter Mark Jansson, P.P.,P.E. Page 45 of 73

Figure 3.1



Peter Mark Jansson, P.P.,P.E. Page 46 of 73

Figure 3.2

14.940 24.349 10.572 14.883 13.356 14.788 11.485 14.347 173.013 Energy Produced Yes Yes Yes Yes Yes Additional H27 Yes Yes Yes 0.12T 0.14T 0.13T 0.12T 0.12T Minimum Madmum 8td. Devletton % 0.14T 0.14T 0.13T Sid. Devlation Pressure 0.14-104T Figure 3.2 - Summary of 10 cm Experimental Results 0.635 0.042 0.523 0.539 0.597 0.598 0.591 0.538 0.628 0.581 0.523 7.30% Excess Power [watts] 23.438 23.514 23.514 25.018 25.018 45.618 23.556 23.5684 17.872 297.970 8.053 Hours [88] tours of Operation 27-Mar 30-Mar 1-Apr 1-Apr 2-Apr 4-Apr 6-Apr 7-Apr Dateisl of Run

Figure 3.2 - Summary of 10cm

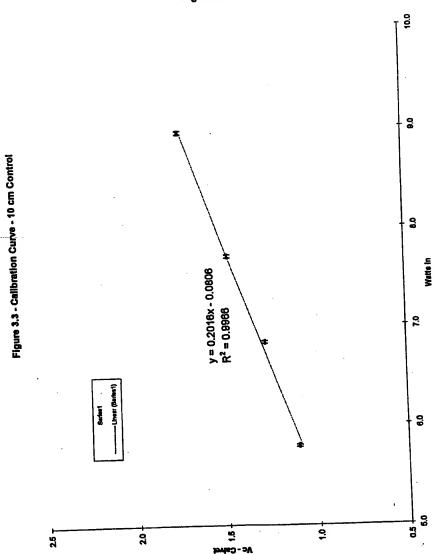


132



Peter Mark Jansson, P.P.,P.E. Page 47 of 73

Figure 3.3



Master of Science in Engineering Thesis Rowan University

Figure 3.4

			Watt-hrs	-	3.358	1.879						16.807	38,400	12.992				6.555				102.464	Energy Produced				+		
			Pressure Additional H22		Š	Yes	No	2	TBS	Yes	Yes	Yes	Yes	Yes	Vac	3	163	Yes											
		1	Pressure A		253.7	COT 40main	Audot-100	253	0.15T-1.7stm	253-265T	0.1-576T	0.0757	D DOG O MYST	Topog	0.0001	- 1	0.0875-0.069T	0.08757		1	Ave. Power (Watts)	Minimum	Минфин	è		2 100			
	Strongwortel Besufts	Figure 3.4 - Summary of 20 cm Experimental results	Event Down [watter	EAVES I WILL IN THE	777		0.337		0.568	0.607			100.0				0.404				0,818	0.337		0.288	74 020	0.4.02.10			
	40.	mary of 20		Honus Issu	000	3.62U	5.575	4.272	2 899	49 838	13,033	404	14.438	31.194	14.781	3.578			14.080			49E 997	140.44	Hours of Operation					
		Figure 3.4 - Sum		Date s of Kun Hours 1881		12-Mar	13-Mar	15-Mar	48 Mar	- Calaida	IBM-OL	17-Mar	17-Mar	18-Mar	19-Mar	19-Mar	201100	IBM-07	20-Mar										
										•																			

Figure 3.4 - Summary of 20 cm.

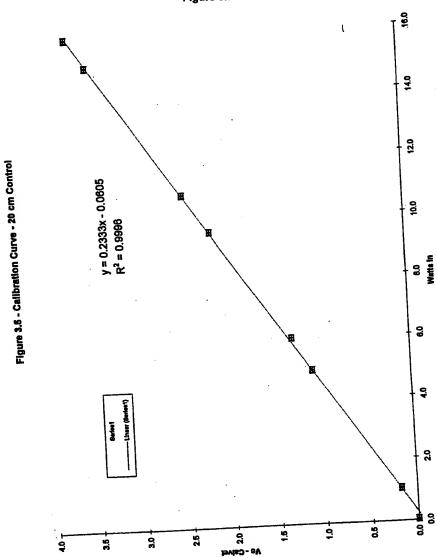


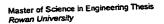
Master of Science in Engineering Thesis Rowen University



Peter Mark Jansson, P.P.,P.E. Page 49 of 73

Figure 3.5







Peter Mark Jansson, P.P.,P.E. Page 50 of 73

Figure 3.6

22.612 49.080 27.919 7.884 12.888 5.154 207.467 ours of Operation 22.118 20.369 28.399 4.392 6.651 Watt-hra Pressure Additional H22 Minimum 6td. Deviation % Std. Devisition <1.312T 0.335-0.443T Ave. Power [Wells] 0.352-0.5827 0.453-0.6797 0,447-0,5967 0.386-0.591T 0,385-0.683T 0.349-0.5767 0,425-0.5827 132,5-178,27 0.38-5497 1.572 29.32% 2.082 Floure 3.6 - Summary of 30 cm Experimental Results 1.459 1.889 1.335 0.835 1.954 2.092 2.067 1.284 1.135 1.079 0.461 1.181 Excess Power [watts] 5.632 15.160 12.080 21.273 6.016 11.572 13.507 13.507 4.777 131.950 tours of Operation Date(s) of Run Hours [ss] 25-Apr 3-May 14-Apr 15-Apr 16-Apr 17-Apr 18-Apr 23-Apr 24-Apr 4-May 5-May

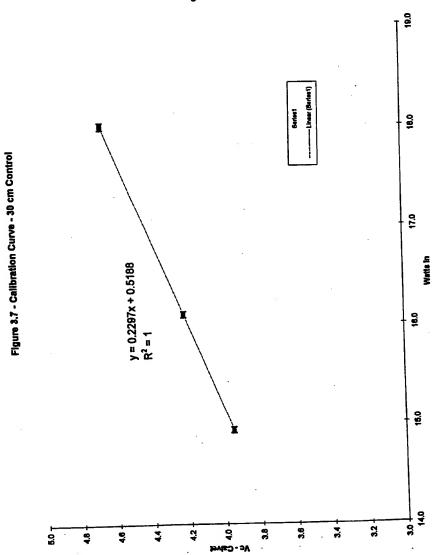
Figure 3.6 - Summary of 30cm.





Peter Mark Jansson, P.P. P.E. Page 51 of 73

Figure 3.7







Peter Mark Jansson, P.P.,P.E. Page 52 of 73

PART III - Mathematical Simulation Model

In order to assess the commercial potential of the BlackLight Power technology I performed some mathematical simulation modeling on one of their most promising devices. The isothermal cell described in Section 3.1 produced meaningful excess power on the order of 50-60 watts and at meaningful temperatures 250-320 °C. The simulation model I developed attempts to recreate the heat loss profile of the isothermal cell in order to assess how much energy theoretically would be required to maintain the cell at any temperature level. I developed this method as a theoretical modeling method to cross-check the calibrations and excess energy results acheived by the experiments on the isothermal cell. Chapters 4 and 5 below provide the results of the simulation model as well as my insights and lessons learned from the exercise. In addition, I developed a comprehensive testing protocol which, if implemented, could conclusively prove the energy gain of the isothermal cell and provide additional documentation for its performance.

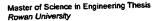
Chapter 4 - Analysis of Model Performance vs. Experimental Results

In order to model thermally the heatloss for the BLP Isothermal Calorimeter I used the data provided from the BLP Experiment 15.6 witnessed by AEI employees on May 3,1996. The method of operation of the Isothermal Cell is provided in Section 3.1. The experiment which we observed operated according to BLP's predictions, previous experiments and protocol. We were able to observe the results detailed in Appendix 9. A summary of that test has been provided on Table 4.1 below.

TABLE 4.1 - Isothermal Cell Results: May 3-4, 1996

TIME	CRITICA CELL	L TEMPERA ROOM	TURES - oC	PRESS. MILLTORR	FILAMENT WATTS	HEATER WATTS	EXCESS WATTS
10:45 AM	279.50	28.42	251.08	1150	0	96.99	0.01
10.40 /101	2,0.00				0	97.07	-0.07
		•			0	97.32	-0.32
11:10 AM							
11:15 AM				4400	15	48.54	33.46
11:45 AM	285.09	28.04	257.05	1400			33.06
					15	48.94	
					15	49.26	32.74
11:50 AM							
12:05 PM							
12:15 PM	288.86	27.88	260.98	1400	25	16.23	55.77
12.10					25	17.75	54.25
					25	17.78	54.22
12:20 PM							
2:10 PM							
2:15 PM	289.24	27.45	261.79	1700	35	5.73	56.27
2:25 PM					42	0.00	55.00
2.25 FW							







Peter Mark Jansson, P.P.,P.E. Page 53 of 73

At approximately 2 A.M. on the morning of May 4, 1996 the filament inside the Isothermal Cell which we were testing burnt out. This caused a significant and dramatic fall in cell temperature. The Isothermal Cell at that point in the experiment was receiving all of its input power and cell heating from the tungsten filament and the associated heat of reaction from the believed Hydrocatalytic reduction of the hydrogen gas at the near vacuum pressure [1.2-1.7 torr] within the cell. Figure 4.1 on the following page illustrates the dramatic drop in cell temperaure which was observed when the filament ceased to operate. The intent of my simulation model was to develop mathematical formulae that could match the heat loss profile of the cell while it underwent this steady state cooling toward room temperature and also match in to the calibration tests conducted at the 260-320 °C temperature levels. I pursued this approach assuming simplistically that all significant heat loss was acheived via conduction [U*A*\DT] and that radiative and convective heat losses from the Isothermal Cell were minimal. With this approach I was able to get an excellent correlation at the lower temperature regime of operation [≤160 °C - see Figure 4.2] with a good fit at the higher temperature profile [≥ 260-320 °C - see Figure 4.3].

From those two pieces of the model I was able to develop an estimate of the heat loss of the Isothermal Cell at its entire range of operation in the tests conducted by BLP. This data is summarized below on Table 4.2.

TABLE 4.2 - Isothermal Cell Heat Loss vs. Temperature*

Cell Temperature [°C]	Calculated Heat Loss [watts]
27	0.0
50	9.3
75	19.3
100	29.4
125	39.5
150	49.6
175	59.6
200	69.8
225	79.8
250	89.9
250 275	100.0
300	110.1
300 325	120.2

^{* -} assumes ambient temperature is 27 °C

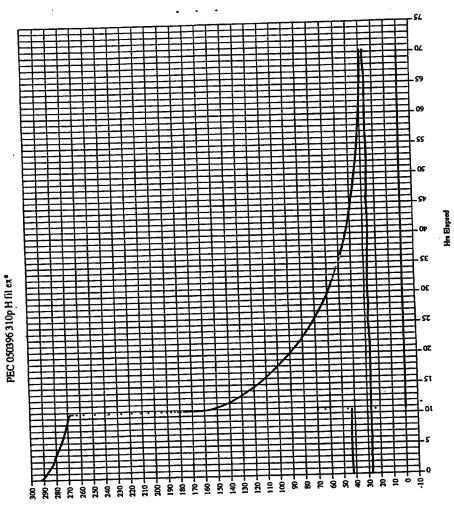




Peter Mark Jansson, P.P.,P.E. Page 54 of 73

FIGURE 4.1 - Isothermal Cell Performance - May 4, 1996

Room Temp Temp(*C) N. Cutt.



Temp(*C) & Watts

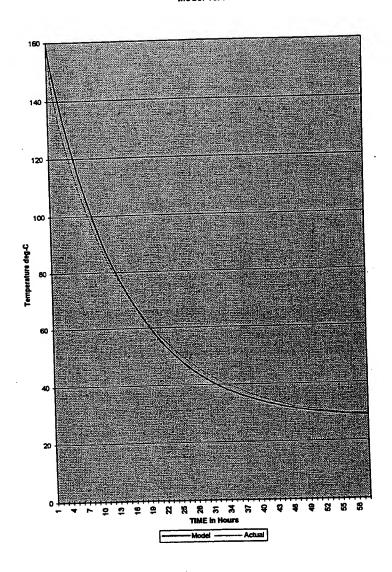




Peter Mark Jansson, P.P.,P.E. Page 55 of 73

FIGURE 4.2 - Isothermal Cell Model vs. Actual Heat Loss

Model vs. Actual Data



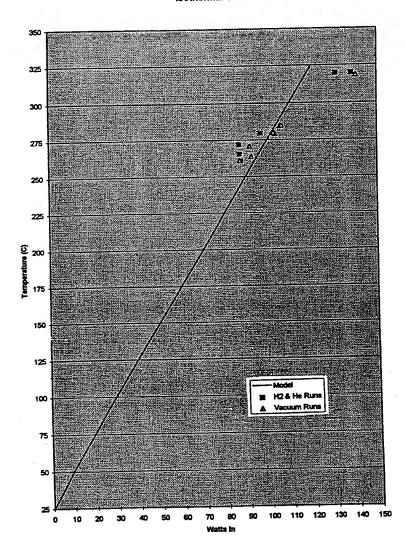




Peter Mark Jansson, P.P.,P.E. Page 56 of 73

FIGURE 4.3 - Isothermal Cell Heat Loss vs. Temperature

Isothermal Cell - Heat Loss







Peter Mark Jansson, P.P.,P.E. Page 57 of 73

Chapter 5 - Key Learnings and Insights From Simulation and Model

What does all this modeling tell us? The specific experiment that we reviewed in order to develop the model can now be looked at with a greater degree of detail and understanding. We know that the Isothermal Cell was able to maintain a temperature measured by the thermocouple at between 280-290 °C. While under cartridge heater power it took 97-103 watts to maintain this temperature [our model says it should have taken approximately 102-106 watts]. When the hydrogen gas was exposed to the filament the thermocouple reading said that the temperature was maintained at approximately the same level. However, in this case the filament was using only 42 watts at steady state. If we were to estimate from the simulation model what the Isothermal Cell temperature would have to be in order for its steady state heat loss to be satisfied with only 42 watts of input power we would see that the equivalent temperature was 132 °C. It is hard to believe the cell was operating at this low of a temperature during the experiment since our heat loss model was well able to accurately track the heat loss of the cell from when the filament burnt out all the way up to 160 °C with an extremely high degree of accuracy. While these learnings indicate that the cell was in fact producing anomalous heat, it must be pointed out that due to cell variability observed between experimental runs and control runs and also between similar experiments the accuracy of heat measurement in the Isothermal Cell is not fully quantified and known. Due to the significant number of BLP experimental and control runs on their isothermal calorimeters the summary results highlighted in Table 3.1 it is most probable that the cell in fact produces heat consistently. Due to the variability of the few control studies that were run by BLP demonstrating that the Isothermal cell exhibits different behavior when it is operating on filament power versus cartridge heater power, more control studies are needed. As discussed in section 3.1 this researcher believes that some of the variability between cell heating source performance may be due to the four factors described in Section 3.1 [i.e.; the relative distances between the heating sources and the thermocouple, etc.] Nonetheless, it is important to note that this experiment does appear to create anomalous heat far beyond the cartridge/filament differential calculated by the control experiments. From the heat loss model described above it appears that this isothermal cells was able to create at least 10-30 watts of useful power even in its early development state.

Included on the pages that follow I have outlined a proposed testing protocol for the Isothermal Cells which I believe will conclusively demonstrate their performance or lack of performance. In that protocol I recommend that the isothermal cells be outfitted with external temperature measurement thermistors and that a full set of controls and experiments be carried out on these cells. From this work we can develop heat loss calibration curves under various temperature and pressure regimes. In addition, each cell should be blanketed with a standard jacket to reduce heat loss variability from experiment to experiment. From a very high temperature the cell should be turned off and a heat loss decay model be fit to its heat loss rate over time. This empirical model can then be used as a second source of validation for the calculated excess energy created in the hydrocatalytic reaction within the vessel.





Peter Mark Jansson, P.P., P.E. Page 58 of 73

<u>ISOTHERMAL CALORIMETER</u> Definitive and Conclusive Testing Protocol

SETUP:

Develop and Install Standard Insulation Jacket [2-4" min. thickness]
Install 2 Internal [Top and Bottom] Thermocouples and/or Thermistors
Install 6 External Thermistors top, bottom, each 90 degrees alternate up down 1/3
Measure total weight, and total volume of isothermal vessel
Develop computer controlled program to initiate steps 1-3 of each protocol

Control Run #1 - He at 1 atmosphere

1. Measure all relevant temperature, pressure parameters and time for following protocol:

USING ONLY CARTRIDGE HEATER

10 watts in for 1-4 hours or until steady state is achieved up power to 20 watts in for another 1-4 hours or until steady state temperatures are reached

up power to 30 watts in [until steady state temps] up power to 40 watts in [until steady state temps] continue..... in 10 watt increments noting all temps and time up to 200 watts in or until cell temps are over 400 °C Shut off all power and monitor temperature decline vs. time

2. Measure all relevant temperature parameters and time for following protocol:

USING ONLY 200 CM. FILAMENT

10 watts in for 1-4 hours or until steady state is achieved up power to 20 watts in for another 1-4 hours or until steady state temperatures are reached

up power to 30 watts in [until steady state temps] up power to 40 watts in [until steady state temps] continue..... in 10 watt increments noting all temps and time up to 200 watts in or until cell temps are over 400 °C Shut off all power and monitor temperature decline vs. time

3. Measure all relevant temperature parameters and time for following protocol:

USING FIRST CARTRIDGE HEATER FOR 10 WATTS THEN FILAMENT FOR NEXT 10 WATTS

10 watts in for 1-4 hours or until steady state is achieved up power to 20 watts in for another 1-4 hours or until steady state temperatures are reached

up power to 30 watts in [until steady state temps]





Peter Mark Jansson, P.P., P.E. Page 59 of 73

up power to 40 watts in [until steady state temps] continue..... in 10 watt increments noting all temps and time up to 200 watts in or until cell temps are over $400\,^{\circ}\text{C}$

Control Run #2 - H2 at 1 atmosphere

1. Measure all relevant temperature parameters and time for following protocol:

USING ONLY CARTRIDGE HEATER

10 watts in for 1-4 hours or until steady state is achieved up power to 20 watts in for another 1-4 hours or until steady state temperatures are reached

up power to 30 watts in [until steady state temps] up power to 40 watts in [until steady state temps] continue..... in 10 watt increments noting all temps and time up to 200 watts in or until cell temps are over 400 °C Shut off all power and monitor temperature decline vs. time

2. Measure all relevant temperature parameters and time for following protocol:

USING ONLY 200 CM. FILAMENT

10 watts in for 1-4 hours or until steady state is achieved up power to 20 watts in for another 1-4 hours or until steady state temperatures are reached

up power to 30 watts in [until steady state temps] up power to 40 watts in [until steady state temps] continue..... in 10 watt increments noting all temps and time up to 200 watts in or until cell temps are over 400 °C Shut off all power and monitor temperature decline vs. time

3. Measure all relevant temperature parameters and time for following protocol:

USING FIRST CARTRIDGE HEATER FOR 10 WATTS THEN FILAMENT FOR NEXT 10 WATTS

10 watts in for 1-4 hours or until steady state is achieved up power to 20 watts in for another 1-4 hours or until steady state temperatures are reached

up power to 30 watts in [until steady state temps] up power to 40 watts in [until steady state temps] continue..... in 10 watt increments noting all temps and time up to 200 watts in or until cell temps are over 400 °C

Control Run #3 - He at 2 Torr

1. Measure all relevant temperature parameters and time for following protocol:



-

Master of Science in Engineering Thesis Rowan University Peter Mark Jansson, P.P., P.E. Page 60 of 73

USING ONLY CARTRIDGE HEATER

10 watts in for 1-4 hours or until steady state is achieved up power to 20 watts in for another 1-4 hours or until steady state temperatures are reached

up power to 30 watts in [until steady state temps] up power to 40 watts in [until steady state temps] continue..... in 10 watt increments noting all temps and time up to 200 watts in or until cell temps are over 400 °C Shut off all power and monitor temperature decline vs. time

Measure all relevant temperature parameters and time for following protocol:

USING ONLY 200 CM. FILAMENT

10 watts in for 1-4 hours or until steady state is achieved up power to 20 watts in for another 1-4 hours or until steady state temperatures are reached

up power to 30 watts in [until steady state temps] up power to 40 watts in [until steady state temps] continue..... in 10 watt increments noting all temps and time up to 200 watts in or until cell temps are over 400 °C Shut off all power and monitor temperature decline vs. time

3. Measure all relevant temperature parameters and time for following protocol:

USING FIRST CARTRIDGE HEATER FOR 10 WATTS THEN FILAMENT FOR NEXT 10 WATTS

10 watts in for 1-4 hours or until steady state is achieved up power to 20 watts in for another 1-4 hours or until steady state temperatures are reached

up power to 30 watts in [until steady state temps] up power to 40 watts in [until steady state temps] continue..... in 10 watt increments noting all temps and time up to 200 watts in or until cell temps are over 400 °C

Control Run #4 - H₂ at 2 Torr

1. Measure all relevant temperature parameters and time for following protocol:

USING ONLY CARTRIDGE HEATER

10 watts in for 1-4 hours or until steady state is achieved up power to 20 watts in for another 1-4 hours or until steady state temperatures are reached

up power to 30 watts in [until steady state temps] up power to 40 watts in [until steady state temps]





Peter Mark Jansson, P.P., P.E. Page 61 of 73

continue..... in 10 watt increments noting all temps and time up to 200 watts in or until cell temps are over 400 °C Shut off all power and monitor temperature decline vs. time

2. Measure all relevant temperature parameters and time for following protocol:

USING ONLY 200 CM, FILAMENT

10 watts in for 1-4 hours or until steady state is achieved up power to 20 watts in for another 1-4 hours or until steady state temperatures are reached

up power to 30 watts in [until steady state temps] up power to 40 watts in [until steady state temps] continue..... in 10 watt increments noting all temps and time up to 200 watts in or until cell temps are over 400 °C Shut off all power and monitor temperature decline vs. time

3. Measure all relevant temperature parameters and time for following protocol:

USING FIRST CARTRIDGE HEATER FOR 10 WATTS THEN FILAMENT FOR NEXT 10 WATTS

10 watts in for 1-4 hours or until steady state is achieved up power to 20 watts in for another 1-4 hours or until steady state temperatures are reached

up power to 30 watts in [until steady state temps] up power to 40 watts in [until steady state temps] continue..... in 10 watt increments noting all temps and time up to 200 watts in or until cell temps are over 400 °C

Control Run #5 - Near Vacuum [<25 mTorr]

1. Measure all relevant temperature parameters and time for following protocol:

USING ONLY CARTRIDGE HEATER

10 watts in for 1-4 hours or until steady state is achieved up power to 20 watts in for another 1-4 hours or until steady state temperatures are reached

up power to 30 watts in [until steady state temps] up power to 40 watts in [until steady state temps] continue..... in 10 watt increments noting all temps and time up to 200 watts in or until cell temps are over 400 °C Shut off all power and monitor temperature decline vs. time

2. Measure all relevant temperature parameters and time for following protocol:

USING ONLY 200 CM. FILAMENT





Peter Mark Jansson, P.P.,P.E. Page 62 of 73

10 watts in for 1-4 hours or until steady state is achieved up power to 20 watts in for another 1-4 hours or until steady state temperatures are reached

up power to 30 watts in [until steady state temps] up power to 40 watts in [until steady state temps] continue..... in 10 watt increments noting all temps and time up to 200 watts in or until cell temps are over 400 °C Shut off all power and monitor temperature decline vs. time

3. Measure all relevant temperature parameters and time for following protocol:

USING FIRST CARTRIDGE HEATER FOR 10 WATTS THEN FILAMENT FOR NEXT 10 WATTS

10 watts in for 1-4 hours or until steady state is achieved up power to 20 watts in for another 1-4 hours or until steady state temperatures are reached

up power to 30 watts in [until steady state temps] up power to 40 watts in [until steady state temps] continue..... in 10 watt increments noting all temps and time up to 200 watts in or until cell temps are over 400 °C

Conduct Full Experiment Series

Repeat Series of Experiments [ie; 15.6, 15.9, 15.10, etc.] w/ 200 cm. filament to isolate optimal zones of operation for maximizing excess heat generation effect. Track power dissipation per surface area on filament.

Replace filament with tungsten of greater surface area. First increase diameters, then increase roughness. Assure 100% and 200-500% changes in area.

Increase total areas of tungsten filament in reactor vessel by 1000% via curled filament etc.

Use parameters above to design meaningful 1-5 kW water heater design and 1-20 kW space heater design



Peter Mark Jansson, P.P.,P.E. Page 63 of 73

PART IV - Implications for the Future

The world energy market represents over 100 trillion kilowatthours of equivalent energy consumed each year and traded for well in excess of \$1 trillion. It is clear that the BLP process is in a very early stage of development and is not likely to impact this market in any significant way before the turn of the century. However, the experimental evidence reviewed and the data developed by this thesis indicates that there is an extremely high probability that the effect predicted by Dr. Mills' work in his unified field theory and the laboratory devices developed by William R. Good and his BLP associates in the laboratory may play a major role in the future of the energy industry. Gas and electrolytic phase cells and devices currently capable of releasing heat on the order of 1-20 times energy input show promise for significant technical expansion as more focus and scientific and engineering resources are brought to bear on the task. BlackLight Power currently raised over \$10M in additional investment through its final private placement offering which will make it possible for them to hire additional scientists and engineers for this very purpose. Across the world others are beginning to note with interest the reproducible and predictable production of anomalous heat via test cells that incorporate hydrogen and appropriate catalytic materials [see Table 6.1] While the "cold fusion scandal" has created a stigma which has made it difficult for the academic community to perform a complete and unbiased analysis of the claims the many researchers have made over the past few years, it appears clear that the dike holding this information back is about to burst. Table 6.1 is a brief snapshot of but a few claims that have been documented by credible scientists in industry and academia in the last few years.

TABLE 6.1 - Global Reports/Observations on BLP Technology

Journal	Observed Data / Reported Results*	Researcher(s) & Affiliation
FUSION TECHNOLOGY March 1997	2,500 times energy out of hydrogen, hydrogen is lost in reaction, new form of tightly bound hydrogen is the model proposed to explain energy and loss results	DuFour, Foos, Millot and DuFour of Shell Research/CHAM Laboratoire des Sciences Nucleaires, Paris, France
JOURNAL of ELECTRO- ANALYTICAL CHEMISTRY (1993) and (1991)	Significant heat production from electrolytic cells and the observation of a dideutrino molecule with a higher ionization energy similar to the Mills energy predictions	Miles, Bush, Lagowald , Ostrom and Miles of China Lake Naval Air Warfare Center Weapons Division, US
3rd Conference on Cold Fusion - October 1992	Significant excess heat production from cell with mass spec data indicating a diduction molecule (i.e.; lower energy deuterium molecule via Mills)	Yamaguchi and Nishioka of the NTT Basic Research Laboratories and BMRA Europe S.A.

· - see footnotes 39 - 43





Peter Mark Jansson, P.P.,P.E. Page 64 of 73

Within the next five years there will be a significant increase in awareness of the factual information surrounding the experiments conducted by many on hydrogen technologies which are taking advantage of the natural effect first observed by Dr. Mills. The data provided in this thesis is but a brief summary of the wealth of work that has already been performed in this area of science. Most academicians I have spoken with regarding the work of Dr. Mills and Mr. William Good are annoyingly critical and pessimistic before even asking to hear the details of their experiments or supporting data. It does not surprise this researcher that it has taken at least five years for Dr. Mills work to begin to gain the recognition that it needs to have for appropriate peer review and true academic critique. It is hoped that this thesis work will draw attention to the need for a balanced and open debate on the legitimacy of the BLP claims, which though they seem extensive are also grounded in excellent technical and theoretical research.

Chapter 6 - Implications for the Future and Recommended Next Steps

A new energy paradigm will not be quickly embraced by those currently in decision-making positions in the energy industry. Literally trillions of dollars have been invested over the past fifty years in the current energy infrastructure and its early retirement could cause major economic disruption. However, the deregulation of the gas industry over the past decade combined with the current efforts to deregulate the electric industry have positioned at least the U.S. and much of the U.K. energy industry for the major competitive forces and shifts that the introduction of a new technology like BLP would cause. Cogeneration and independent power producer competition have already ushered in the pre-competitive era for most in the electric industry while the gas, oil and other traded energy commodities have been fiercely competitive for some time. Nonetheless, there is little to gain for the established energy providers to accelerate the adoption of a new energy technology based upon hydrogen. Adopting a 'wait and see' strategy not only minimizes the risk of embarrassment should the technology prove to have little commercial potential, but also could stall or delay the day when the technology is ready and able to compete directly with the energy providers for their customers. History has shown that only a few in business adopt the Peter F. Drucker strategy of creating their future. [Drucker quote; "The only way to control the future is to create it"] Most are content to watch it being created around them and then getting involved once it is clear what the winning technologies are likely to be. In the case of a paradigm shift as radical as the one proposed by Dr. Mills and BLP, waiting could be a devastating business strategy. This researcher has advised his energy company to become involved from the beginning and other companies should also follow this advice. Knowing how quickly the technology may develop and emerge best positions the energy company to plan for the timely deployment, divestiture and or disposition of its assets that may be most at risk should commercialization move on a fast or slower track. This closing section of my thesis however, is not dedicated to what the energy industry should do as next steps but rather to what BLP should do in the near future to solidify their position with this technology and maximize the benefits for their shareholders for the investment





Peter Mark Jansson, P.P.,P.E. Page 65 of 73

they have made in developing this technology. The following list of recommended next steps is brief and succinct, but should assure BLP success in their endeavors if completed in a timely manner.

Recommended Next Steps

- Clarify the Vision, Mission and Purpose of BlackLight Power, Inc. and communicate it clearly to all employees, contractors and owners. Align all corporate and employee goals and compensation strategies with the attainment of these. Identify the corporate competencies needed to execute the goals and mission of organization.
- 2. Focus on maximizing the intellectual property developed, owned and applied by BLP employees [individually and as a group]. Maximize new patent filings for all supportive device technologies and innovations. [If overarching patents fail, supporting patents will still protect the embodiments of the BLP effect in most apparata] Maximize the technical and journal papers published and defended during years 1-5.
- Focus on Communicating the BLP Vision, Mission and Purpose to all appropriate audiences and keep an adequate supply of current, accurate and appropriate information flowing to the media and necessary constituents.
- 4. Focus on Identifying and Quantifying the Key Parameters controlling the Hydrocatalysis and Disproportionation effects including the isolated optimization of each as well as their interactions with each other. [ie; dissociation surface area, partial pressures -catalyst vs. hydrogen atoms, mean free paths, temperature regimes, volumetric proportionalities, time dependence, etc.] This should be completed for all key embodiments gas phase, electrolytic phase, etc.
- 5. Develop a self-contained, self-sustaining "Hot Black Box" which irrefutably demonstrates the ability that BLP has to control all key parameters and engineer the optimization of the effect for commercial application and manufacturing. This must not be left to others to develop, it should be the work and competence of BLP at the end of the day in order to maintain a competitive advantage in this field.
- Develop the BLP management model and compensation strategy. Hire sufficient numbers of management and staff with the necessary competencies to successfully execute items 1- 5 during the first 18 months after sufficient funding is achieved.





Peter Mark Jansson, P.P.,P.E. Page 66 of 73

PART V - Reference Materials

The data reviewed in this thesis was substantial and unfortunately only a brief overview was able to be provided in the limited space. Many items referenced can be easily obtained from the author or from a librarian. This section is devoted to making that exercise more simple. The reference materials have been divided into two sections. First, a straightforward list of all Footnotes cited in the text grouped by their section or subsection number is available on the next three pages. Second, where key information was substantial and of primary relevance to the thesis but could not be afforded adequate coverage in the text, Appendices were developed to provide the needed reference support. Placing them at the end of this thesis allowed the continuity of idea flow without distracting the reader from the key points being made. The full list of relevant supporting appendices is shown on the page before they begin as the final page in Part V.

References Provided in this Thesis

Footnotes

Pages 67-71

Description of Appendices

Pages 72-73

Full Appendices Follow





Peter Mark Jansson, P.P.,P.E. Page 68 of 73

THESIS FOOTNOTES [continued]

PART I. Chapter 1. Section 1.1 - Fossil Fuels [continued]

- Nesbit, William, "World Energy- Will There Be Enough in 2020?", Decisionmakers Bookshelf, Vol. 6, Edison Electric Institute, © 1979, ISBN 0-931032-06-7
- 11 Kraushaar, Jack J., Ristinen, Robert A., "Energy and Problems of a Technical Society", 2nd Edition, John J. Wiley & Sons, Inc., © 1984, 1993, ISBN 0-471-57310-8, Figure 1.15, p. 21
- "World Book Encyclopedia J-K", Field Enterprises Educational Corporation, © 1961, Library of Congress Cat. No. 61-5169, p. 32a
- Weinfeld, Steven G., "Funk & Wagnalls New Encyclopedia Volume 14", Funk & Wagnalls, ©1986, Library of Congress Cat. No. 72-170933, ISBN 0-8343-0072-9, p. 402
- 14 Kraushaar, Jack J., Ristinen, Robert A., "Energy and Problems of a Technical Society", 2nd Edition, John J. Wiley & Sons, Inc., © 1984, 1993, ISBN 0-471-57310-8, pp. 2-3

PART I. Chapter 1. Section 1.2 - Nuclear Energy - Fission & Fusion

- 15 Schwarzchild, B., Physics Today, October 1990, pp. 17-20
- 16 Kraushaar, Jack J., Ristinen, Robert A., "Energy and Problems of a Technical Society", 2nd Edition, John J. Wiley & Sons, Inc., © 1984, 1993, ISBN 0-471-57310-8, pp. 108-111
- 17 Associated Press, "Princeton reactor's closure casts doubt on fusion prospects", The Press of Atlantic City, March 30, 1997
- 18 Kraushaar, Jack J., Ristinen, Robert A., "Energy and Problems of a Technical Society", 2nd Edition, John J. Wiley & Sons, Inc., © 1984, 1993, ISBN 0-471-57310-8, Table 4.1, p. 95
- 19 "Barsebick to Close Down by 2001", The Swedish Press, March 1997, p. 9





.





Peter Mark Jansson, P.P.,P.E. Page 69 of 73

THESIS FOOTNOTES [continued]

PART I. Chapter 1. Section 1.3 - Solar Energy

- Energy Info Home Page, http://www.energyinfo.co.uk:80/wstats.html, World Fuel Consumption by Country, pp. 1-2, ©1996 by EnergyInfo, last modified April 26, 1996
- 21 U.S. Census Bureau World POPClock Web Page, http://www.census.gov/cgi-bin/ipc/popclockw, International Programs Center, World Population projected to 2/24/97 at 7:09:44 PM EST
- Energy Info Home Page, http://www.energyinfo.co.uk:80/wstats.html, World Fuel Consumption by Country, pp. 1-2, ©1996 by EnergyInfo, last modified April 26, 1996
- P.M. Jansson and R.A. Michelfelder, "Market-Driven Photovoltaic System Economics for Grid-Connected Residential and Commercial Customers", 14th European Photovoltaic Solar Energy Conference, Barcelona, Spain, June 30 - July 4, 1997

PART I. Chapter 1. Section 1.4 - Geothermal Energy

24 Kraushaar, Jack J., Ristinen, Robert A., "Energy and Problems of a Technical Society", 2nd Edition, John J. Wiley & Sons, Inc., © 1984, 1993, ISBN 0-471-57310-8, p. 204

PART I. Chapter 1. Section 1.5 - Tidal Energy

25 Kraushaar, Jack J., Ristinen, Robert A., "Energy and Problems of a Technical Society", 2nd Edition, John J. Wiley & Sons, Inc., © 1984, 1993, ISBN 0-471-57310-8, p. 210, Table 7.8

PART I. Chapter 2. Section 2.1 - Theoretical Description

- 26 Mills, Randell L., "The Grand Unified Theory of Classical Quantum Mechanics", Black Light Power, © September 1996, Library of Congress Cat. No. 96-70686, ISBN 0-9635171-2-0, p. x
- 27 Mills, Randell L., "The Grand Unified Theory of Classical Quantum Mechanics", Black Light Power, © September 1996, Library of Congress Cat. No. 96-70686, ISBN 0-9635171-2-0, p. 138





Peter Mark Jansson, P.P.,P.E. Page 70 of 73

THESIS FOOTNOTES [continued]

PART I. Chapter 2. Section 2.2 - Astrophysical Corroboration

- 28 Labov, S.E., Bowyer, S., "Spectral Observations of the Extreme Ultraviolet Background", The Astrophysical Journal, 371:810-819 © 20 April 1991, The American Astronomical Society
- 29 Schwarzchild, B., Physics Today, October 1990, pp. 17-20
- Bahcall, J., et. al., "Solar neutrinos: a field in transition", Nature, 334, 11 1988, pp. 487-493
- 31 Taubes, G., Science, 256, 1992, pp. 1512-1513
- 32 Taubes, G. Science, 256, 1992, pp. 731-733

PART I. Chapter 2. Section 2.3 - Enigmas Solved

- Mills, Randell L., "The Grand Unified Theory of Classical Quantum Mechanics", Black Light Power, © September 1996, Library of Congress Cat. No. 96-70686, ISBN 0-9635171-2-0, p. 426
- Phillips, Kenneth J.H., "Guide to the Sun", Cambridge University Press, © 1992, ISBN 0-521-39483, p. 166
- Phillips, Kenneth J.H., "Guide to the Sun", Cambridge University Press, © 1992, ISBN 0-521-39483, p. 367
- 36 Chown, Marcus, "Dark matter is still the only game in town", New Scientist, January 7, 1995, p. 15

PART II. Chapter 4

37 DuFour, J., Foos, J., Millot, J.P., DuFour, X., "Interaction of Palladium/ Hydrogen and Palladium/Deuterium to Measure the Excess Energy Per Atom for Each Isotope", Fusion Technology, Volume 31, March 1997, pp 198-209

PART II. Chapter 4. Section 4.2 - Penn State University Calvet

38 Phillips, Jonathan, "Report on Calorimetric Investigations of Gas-Phase Catalyzed Hydrino Formation", Department of Chemical Engineering, Penn State University, Final Report for period of October - December 1996, p. 1





Peter Mark Jansson, P.P.,P.E. Page 71 of 73

THESIS FOOTNOTES [continued]

PART IV

- 39 DuFour, J., Foos, J., Millot, J.P., DuFour, X., "Interaction of Palladium/ Hydrogen and Palladium/Deuterium to Measure the Excess Energy Per Atom for Each Isotope", Fusion Technology, Volume 31, March 1997, pp 198-209
- Miles, M.H., Bush B.F., Ostrom, G.S., Lagowski, J.J., "Helium Production During the Electrolysis of D₂O in Cold Fusion Experiments", Journal of Electroanalytical Chemistry, 301, p. 271 (1991)
- Miles, M.H., Hollins, R.A., Bush B.F., Lagowski, J.J., Miles, R.E.J., "Correlation of Excess Power and Helium Production During D₂O and H₂O Electrolysis using Palladium Cathodes", Journal of Electroanalytical Chemistry, 346, p. 99 (1993)
- Notoya, R. and M. Enyo, "Proceedings of the Third Annual Conference on Cold Fusion, Nagoya, Japan" October 21-25, 1992, H. Ikegami, Editor, Universal Academy Press, Inc., Tokyo, ©1992, pp. 421-426
- 43 Yamaguchi, E. and Nishioka, T., "Direct Evidence for Nuclear Fusion Reactions in Deuterated Palladium", Proceedings of the Third Annual Conference on Cold Fusion, Nagoya, Japan, October 21-25, 1992, p. 179



Peter Mark Jansson, P.P.,P.E. Page 72 of 73

DESCRIPTION OF APPENDICES

Appendix 1. BLP Research Partners - Catalogue of Experimental Results
This researcher compiled a log of numerous experiments and studies that had been
performed on BLP technologies over the past 5 years. These are summarized by title,
author, report name, date of work and subject matter in this appendix.

Appendix 2. An Overview of Mills Theory

The theory of Dr Mills is rather complex in that it unifies all of the aspects of a new classical quantum mechanics, Maxwell's Equations, Einstein's Special and General Relativity as well as the fundamental classical theories and models of physics. A more full description of his theory is provided in this appendix.

Appendix 3. Jansson Astrophysical Data Calculations Verifying BLP Reported Results

Specific calculations provided by Dr. Mills in his text as part of demonstrating that data being collected from space is able to validate that the theoretical results of his model are sound have been made by this author. The Excel spreadsheet has produced the tables found in this appendix.

Appendix 4. BLP/AEI Experiment 15.6 - May 1996

Atlantic Energy witnessed testing of the Isothermal Cell at the BLP Laboratories in Malvern, Pa. On May 4-6, 1997. The actual lab notes from that experiment and associated calculations done by Atlantic Energy staff to verify the results observed are provided in this appendix

Appendix 5, Analysis of BLP Isothermal Calorimetry Data

Analysis of the Isothermal cell experiments was conducted by this researcher to see if the results that were being observed were consistent with heat loss modeling estimates. The actual data provided by the BLP data logger was reviewed to see if excess heat of formation was actually occurring. This appendix summarizes these results.

Appendix 6. PSU Calvet Test Results and Report - December 1996

This appendix contains the full research report completed by Pennsylvania State University on their tests of the BlackLight technology via a Calvet calorimeter.

Appendix 7. Jansson Calvet Testing Protocol

This appendix describes the protocol that was used in the control and experimental runs performed in BlackLight Power's laboratory facility during February through May 1997 by Peter Mark Jansson., P.P.,P.E.





Peter Mark Jansson, P.P., P.E. Page 73 of 73

DESCRIPTION OF APPENDICES [continued]

Appendix 8. Jansson Calvet Test Results June 1997

The results of the experimental and control runs are provided in more detail in this appendix. While the Lab Note Book has not been included each day of experiments that were analyzed in the summary data provided in the thesis are shown explicitly. Each data set name is listed as well.

Appendix 9. Jansson Heat Loss Model Calibration & Performance

Specific mathematical modeling of the Isothermal cell was developed by this researcher to see if the results that were being observed were consistent with those that a heat loss model could predict. The calibration of the model was made via actual data provided by the BLP data logger and produced results which indicated excess heat of formation was actually occurring. This appendix summarizes these results.







.

arrivered)

New York

decisions.

protote ...

THESIS APPENDIX ONE



٠.







Peter Mark Jansson, P.P.,P.E. Appendix 1

Appendix 1 - Catalogue of Relevant Publications and Experimental Results

This appendix provides a brief overview of relevant publications and printed experimental results that this researcher was able to acquire, review and summarize. I have not made an exhaustive search for electrolytic cell experimental data since it is extremely lengthy. The catalogue begins on the page which follows and forms the essence of this appendix.









Appendix 1 - Catalogue of Relevant Publications and Experimental Results

hor
eport - Auf
Paper/R

HydroCatalysis Technical Assessment TECHNOLOGY INSIGHTS San Diego, CA 619-455-9500 The Grand Unified Theory of Classical Quantum Mechanics R.L. Mills BLACKLIGHT POWER CORP Malvem, PA 610-651-4938

The Grand Uniffed Theory
R.L. Mills and J.J. Farrell
HYDROCATALYSIS POWER CORP
Makem, PA 610-651-4938

Excess Heat Production by the Electrolysis of an Aqueous Potassium Carbonate Electrolyte and the Implications for Cold Fusion R.L. Mills and S.P. Kneizys HYDROCATALYSIS POWER CORP Maken, PA 610-631-4938

Dillydrino Molecule Identification
R.L. Mills, W.R. Good and R.M. Schaubach
HYDROCATALYSIS POWER CORP
HYDROCATALYSIS POWER CORP
-- of THERMACORE, INC.

Fractional Quantum Energy Levels of Hydrogen R.L. Mills and W.R. Good HYDROCATALYSIS POWER CORP.
MANER, PA 610-651-4938

Publication Status

PC - Confidential presented to Pacificorp printed 30 August 1996 BlackLight Power published September 1996

Science Press published 1989 Fusion Technology Vol 20., 65-81 published 1991 Fusion Technology Vol 25., 103 published 1994 Fusion Technology Vol 28., 1697-1719 published 1995

Purpose/Results/Conclusions

Independent Technology Assessment

Presentation and Defense of Theory w/ Experiments

Presentation and Defense of Theory

Experimental Electrolytc Cell Results

Experimental Electrolytic Cell Results Ditydrino Identification Experimental Electrolytc Cell Results Hydrino and Dihydrino Identification





Appendix 1 - Catalogue of Relevant Publications and Experimental Results

Paper/Report - Author	Publication Status	Purpose/Results/Conclusions
Nascent Hydrogen an Energy Source N.J. Gemhart, R.M. Schaubach WRIGHT PATTERSON - AFB Mahem, PA 610-651-4938	SBIR Phase I Project Report 11-1124 published March 1994	Experimental Permeation Cell Results
Report on Catortmetric Investigations of Gas- Phase Catalyzed Hydrino Formation S. Kurtz, J. Phillips and J. Smith Pem State Uriv., PA 814-883-4808	PSU -Confidential presented to BLP prepared December 1996	Penn State Gas Phase Calvet Calorimetry
A Calorimetric investigation of the Reaction of Hydrogen with Sample PSU #1 M.C. Bradford and J. Phillips Pern State Univ., PA 814-863-4809	PSU -Confidential presented to BLP prepared 1994	Penn State Solid Oxide Catalyst Calvet Calorimetry
Additional Calorimetric Examples of Anomalous Heat from Mixture of K/Carbon and Pd/Carbon J. Phillips and Shim, H. Pern State Univ., PA 614-863-4809	PSU - Corfidential presented to BLP prepared 1998	Penn State Spillover Catalyst Calvet Calorimetry
Additional Examples of Anomalous Heat: Hydrogen . Mass Balance J. Phillips Pern State Urb., PA 814-863-4809	PSU - Confidential presented to BLP prepared 1996	Penn State Spillover Catalyst Calvet Calorimetry
Replication of the Apparent Excess Heat Effect in a Light Water – Potassium Carbonate – Nickel Electrolytic Cell J. M. Niedra and I.T. Myers	NASA - Lewis Technical Memorandum 107167 prepared 1996	NASA Investigation & Experiments - Electrolydic Cell





Appendix 1 - Catalogue of Relevant Publications and Experimental Results

a B
اء
힐
Ħ
4
of
Repol
Ē
aber/
2

Evaluation of Heat Production from Light Water

Electrolysis Cells of HydroCatalysis Power Corp.

S. Deboord

Electrolysis Cells of HydroCatalysis Power I S.H. Peterson Excess Energy Cell Final Report C. Haldeman, et. al. Cambidge, MA Calorimetry for a NIIK,CO, Cell
M.T. Craw-Ivanco, R.P. Tremblay, H.A. Boniface
and J. Hilborn
CHALK RIVER LABORATORIES
CHAIK River, ON

Publication Status
Westinghouse
STC Report

Westinghouse Investigation of Electrolytic Cells

Purpose/Results/Conclusions

prepared 25 February 1994
M.I.T. Lincoln Lebs
Meeting Viewgraphs
prt.ted / reviewed 1995

M.I.T. Lincoln Labs Experimental Electrolytc Cell Results

Proprietary/EPRI
AECL Research
Chemical Engineering Branch
printed June 1994

Experimental Electrolytc Cell Results

as of: 31 May 1997

Bo

\$

.

a property of the second of

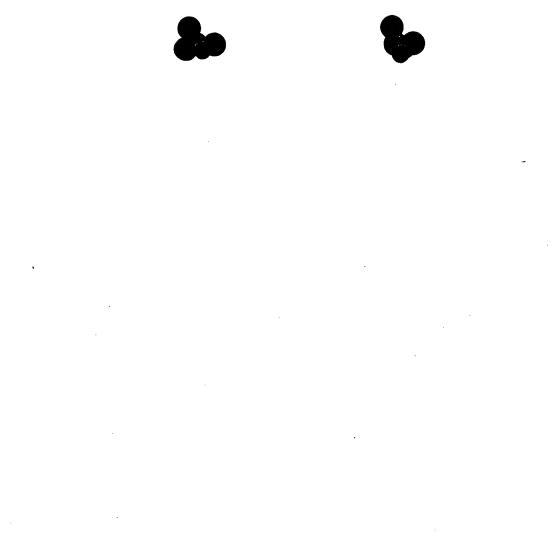




THESIS - APPENDIX TWO

escreto) Same

A



:





Peter Mark Jansson, P.P., P.E. Appendix 2

Appendix 2 - An Overview of Mills Theory

The section which follows is but a brief description of a theory that has clearly been years of development work on the part of Dr. Randell Mills. I refer the reader to his complete text on "The Grand Unified Theory of Classical Quantum Mechanics". Dr. Randell Mills received his BA in Chemistry from Franklin & Marshall College in 1982 where he graduated summa cum laude. He went on to graduate from Harvard Medical School receiving his MD in 1986 while simultaneously developing his theoretical model for unification while taking electrical engineering courses at M.I.T. He is the creator and owner of many medical patents and the recipient of many academic awards. He has published many technical papers and presented his Grand Unified Theory in 1989. The following year [1990] he went on to form the HydroCatalysis Power Corporation [now BlackLight Power]. Since that time he has been demonstrating the proof of his theory by using it to design devices that use proprietary catalysts to reduce hydrogen to the lower energy states predicted by his model of the hydrogen atom. This he has done successfully in many types of apparata. Concurrently he has filed patents in the U.S. and 23 foreign countries. A patent was awarded in Australia in 1996.

Dr. Mills is President of BlackLight Power [BLP]. presently a small, high technology firm and laboratory located in Malvern, Pennsylvania. It is a privately held company with numerous entrepreneunal investors but has at least two major utility owners [Pacificorp from the western U.S. and Atlantic Energy from the eastern U.S.] BLP is currently being courted by additional U.S. utilities and major U.S. energy equipment manufacturers. While significant data and experiments conducted by BLP and others appear to demonstrate conclusively the reproducibility of their new heat generation effects it would seem that the timing of their discovery was not conducive to its being objectively reviewed and granted widespread academic review for authenticity. The 1990-1991 debunking of "cold fusion" and the sharp criticism that still comes to scientists and academicians who research these claims has placed a cold, wet blanket on the hot findings that continue to be generated by the scientific team from BLP. This researcher believes that the *Pons and Fleischmann experience" has increased resistance in the academic community to objective investigation of the BLP findings and claims.

Table 2.1 in the thesis text summarizes the significant government, corporate and university research centers that have corroborated BLP's findings. At the present time the company's Board has voted to allow only one more private offering before an independent public offering planned sometime in the next 1 to 2 years. To date it is important to note that the work developed by BLP has been primarily funded by its investors with limited government research funding. The total effort to bring the company to its current state of technological development has cost its private owners less than a few million dollars over the past seven years. This needs to be contrasted with the billion dollar expenditures over the past few decades for particle accelerators, nuclear research and investigations into the claims of cold fusion.





Peter Mark Jansson, P.P., P.E. Appendix 2

To Dr. Mills' credit his theory holds at its foundations inviolate the classical laws of physics, including all of those listed below:

- 1) Conservation of mass-energy
- 2) Conservation of Linear and Angular Momentum
- 31 Maxwell's Equations on Electromagnetics
- 4) Newton's Laws of Mechanics
- 5] Einstein's General Relativity
- Einstein's Special Relativity

His theory produces the same equation for the principle energy levels of the hydrogen atom as both Bohr and Schrodinger but only Mills theory gets there through a derivation from first principles. Bohr's model [1913] represented the electron as a point particle whose circular orbit around the nucleus of the hydrogen atom was mainatained by a perfect balancing of the coulombic force of attraction [positive proton nucleus (e*) and negative electron (e*) satelite] between the two particles and the cetrifugal force of the electron. However, the non-radiation of the electron charge at such an orbit velocity led to this postulation being in defiance of Maxwell's Equations on electromagnetics. While "his model was in agreement with the observed hydrogen spectrum it failed for the helium spectrum and could not account for chemical bonds in molecules.**A1 Schrodinger's model [1926] was a totally mathematical view of the electron which he developed based upon de Broglie's wave postulate for electron motion. His famous wave equation has an infinite number of ways in which it can be solved. In order to create a solution for the electron he applied a boundary condition which in essence stated that as the radius of the electron's orbit approaches infinity [r $\rightarrow \infty$] his wave function approaches zero $[\Psi \Rightarrow 0]$. The problems of creating a classical or physical interpretation of Schrodinger's wave equation have been significant over the years and so, as a result, physicists have drifted more and more to a purely mathematical view of the interaction of physics at the atomic level, with no adequate physical description of particle behavior. This has set up a duality in the application of the laws of physics. The classical laws are used at the macro level but at the micro level probability and statistics reign. "According to the Copenhagen interpretation, every observable state exists in a state of superposition of possible states and observation or the potential for knowledge causes the wavefunction corresponding to the possibilities to collapse into a definite state^{-A2} It was these difficulties in the accepted physics of quantum mechanics that led Dr. Mills to seek an alternative. Through his theory, he sought physical laws which were exact on all spatial scales. Dr. Mills did not give the electron the wave nature adopted by Schrodinger and suggested by de Broglie and the Davisson-Germer experiment but developed closed-form calculations that use only the fundamental constants of physics already accepted and understood that predict these aspects of the electron.

Table A.1 below outlines the aspects of physics which Dr. Mills' theory can directly calculate with its closed form equations.





theory of alpha decay

Peter Mark Jansson, P.P., P.E. Appendix 2

TABLE A.1 - Mills' Theory Predictions

one electron atom w/ 4 quantum numbers
the Rydberg constant
the ionization energies of 1,2 & 3 electron atoms
equation of the electron in free space
electron g factor
excited states of the electron
parameters of pair production
bond energies, vibrational energies, rotational
energies and bond distances of hydrogen
-type molecules and molecular ions
equation of the expansion of the universe
the masses of atomic particles [leptons,
quarks and nucleons]
beta decay energy of the neutron

spin/nuclear hyperfine structure
the stability of atoms
equation of the photon
results of Stern-Gerlach experiment
spin angular momentum energies
results of the Davisson-Germer experiment
hyperfine structure interval of positronium
Quantum Hall effects
the Aharonov-Bohm effect
equations of gravitation
the gravitational constant
the basis for the antigravitational force
magnetic moments of nucleons
the binding energy of deuterium
the chemical bond energies of molecules

Mills theory begins with the classical, fundamental laws of physics [see 1-6 above] and then applies a boundary condition on the electron significantly different than Schrdinger. His boundary condition is that a bound electron can not radiate energy at 13.6 eV. "The mathematical formulation for zero radiation is that the function that describes the motion of the electron must not possess spacetime Fourier components that are synchronous with waves traveling at the speed of light. The permissible solutions for the electron function are derived as a boundary value problem with the application of the nonradiative boundary condition.**A3 By using only the classical laws of physics, mathematics and this one new boundary condition [NOTE: this boundary condition is essentially required to satisfy Maxwell's equations] a totally new view of the electron emerges. The result of this theory by Dr. Mills also leads to the unification of all of the standard classical laws of physics. These can be solved mathematically, discretely and without the need to resort to the arbitrary gauging constants developed by presently accepted quantum theory in order to "get the theory to fit" observed data. Dr. Mills calls this new electron perspective and new classical view an electron orbitsphere. The orbitsphere solution to the electron's mathematical function produces many interesting features some of which are highlighted in Table 2.3 below. For a complete summary of the features described by Mills' theory the reader is referred to pages 22-26 of Dr. Mills' text.





Peter Mark Jansson, P.P.,P.E. Appendix 2

TABLE A.2 - The Electron Orbitsphere

bound electron orbitspheres are described completely by a charge-density [mass-density] function that can exist only at specified distances from the nucleus

the function which totally describes an electron orbitsphere's motion is composed of two functions 1] a spin function and 2] a modulation function

electron orbitsphere radii are calculated by setting its centripetal force equal to the electric and magnetic forces of the orbitsphere

the electron orbitsphere behaves like a resonator cavity capable of absorbing photons of discrete frequencies [solutions to Maxwell's equations for excitation modes in this cavity give rise to four quantum numbers]

excited electron orbitsphere states are unstable because the incoming photon disturbs the chargedensity function creating a doublet function that has spacetime Fourier components synchronous with waves travelling at the speed of light, thus it is radiative

the photon is an orbitsphere with electric and magnetic field lines along orthogonal great circles

when an electron orbitsphere is ionized its radius goes to infinity and it becomes a plane wave

atom's energy is stored in their electric and magnetic fields, chemical bonding occurs when the total energy of the atoms can be lowered by forming equipotential orbitals with geodesic motion and the nonradiative boundary condition can be met

lower electronic states exist below *conventional* [n = 1] ground state, hydrogen atoms can react with a catalyst having a net enthalpy of 27 eV inducing them to electronically relax and decrease their radii with the emission of electromagnetic energy consistent with each of their change in total energy state [ie; electric and magnetic field energies]

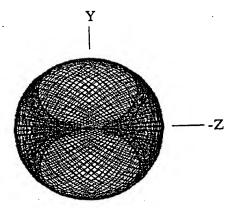
This thesis will not review the many mathematical formulations and proof calculations of Mills theory which is fully elaborated in his text. However the following illustrations may help the reader grasp more succinctly the new orbitsphere model proposed by Mills. Figures A.1 and A.2 below represents a physical view of Mills' model of the electron orbitsphere a spinning, two-dimensional spherical surface.



Peter Mark Jansson, P.P.,P.E. Appendix 2

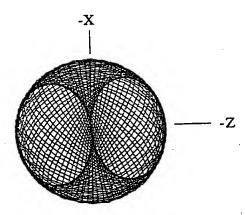
FIGURE A.1

Figure 1.4 B. The current pattern of the orbitsphere shown with 8.49 degree increments of the infinitesimal angular variable $\Delta\alpha(\Delta\alpha)$ from the perspective of looking along the x axis.



VIEW ALONG THE +X AXIS

Figure 1.4 C. The current pattern of the orbitsphere shown with 8.49 degree increments of the infinitesimal angular variable $\Delta\alpha(\Delta\alpha')$ from perspective of looking along the y axis.



VIEW ALONG THE Y AXIS

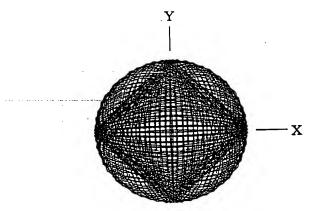




Peter Mark Jansson, P.P.,P.E. Appendix 2

FIGURE A.2

Figure 1.4 A. The current pattern of the orbitsphere shown with 8.49 degree increments of the infinitesimal angular variable $\Delta\alpha(\Delta\alpha')$ from the perspective of looking along the z axis.



VIEW ALONG THE Z AXIS





Peter Mark Jansson, P.P.,P.E. Appendix 2

In closing this overview of Mills' theory it is important to note that while the scientific community has been searching for a more classical unified field theory that could stand up to rigorous mathematical scrutiny for some time, there has not yet been a widepread review of his work by academia. The few academic reviews that have ben made on the merits, potential flaws or criticisms of Mills' work have come out glowingly in favor of his findings. This researcher believes that because Dr. Mills' is an outsider and not considered an expert in these fields that it will take much longer for his work to be widely discussed in academic circles. Mills theory is compelling and may offer just what Albert Einstein was looking for when he uttered his famous words denouncing the then emerging quantum theory "God does not play dice with the universe".

APPENDIX 2 FOOTNOTES

- [A1] Mills, Randell L., "The Grand Unified Theory of Classical Quantum Mechanics", BlackLight Power, © September 1996, Library of Congress Cat. No. 96-70686, ISBN 0-9635171-2-0, p. 7
- [A2] Mills, Randell L., "The Grand Unified Theory of Classical Quantum Mechanics", BlackLight Power, © September 1996, Library of Congress Cat. No. 96-70686, ISBN 0-9635171-2-0, p. 9
- [A3] Mills, Randell L., "The Grand Unified Theory of Classical Quantum Mechanics", BlackLight Power, © September 1996, Library of Congress Cat. No. 96-70686, ISBN 0-9635171-2-0, p. 22







Mary and Mary

wycara i Yad

Vacanta

i yanan da

THESIS - APPENDIX THREE



٠..





Mills Prediction vs. Data

		Raw Extrem	e IIV Back	oround St	ectral Dat	a ·			
			E OA Back	ractional	State	MILLS PRE	DICTED		
	OBSERVE			nf	ni	WaveInth	Energy		-
	WaveInth		Calc			A	eV		
eak	Α	eV	eV			82.9	149.6		-
1	84.8	146.2	146.2	8	7	101.3	122.4		
2	101.5	122.2	122.2	7	6		108.8		
$-\frac{1}{3}$	116.8	106.2	106.2	4	2	114.0			
4	129.6	95.6	95.7	6	5	130.2	95.2		
		88.8	88.8	4	2	141.6		He scattered	
		75.9	76.0	8	7	165.8		2nd order Pea	K1
		68.3	68.2	5	4	182.3	68.0		
7		61.8	61.8	7	6	202.6	61.2	2nd order Pea	k2
8	1	53.0	53.0	3	1	227.9	54.4	<u> </u>	
9			47.5	-5	4	265.0	46.8	He scattered	
10		47.5		4	3	303.9	40.8		
11		41.0	41.0	3		455.9	27.2	2nd order Pea	k9
12	459.1		27.0		<u>'</u>	584.9		Helium Resor	
13	584.0	21.2	21.2			607.8		2nd order Pea	
14	607.5	20.4	20.4	4	3	633.0		He scattered	1
15		19.7	19.6	4	3		13.6		
10				3	2	911.7	13.0	-	
·					l	L			
	+			1.60E-19	6.63E-34	3.00E+08			<u> </u>
				eV	<u>h</u>	C	L		
	+	 				1		ļ	
├		Raw Extre	me UV So	ar Spectra	Data **			1	
├ ─	OBSERV		MILLS PR	EDICTED			<u> </u>		<u> </u>
├	WaveInth		WaveInth						ļ
		delta	A	nf	ni	A	eV		J
<u> </u>	A 4045			2	1	911.74	13.0	<u> </u>	
<u> </u>	1215.			2	1	-911.74	-13.0	3	
<u> </u>	911.		911.74		2	911.74	13.0	5	
<u></u>	911.		811.74	1	1	-227.93		4	
	584.		070.00		1	373.60		2 CS-He	
L	373.				3	303.91			
	303.78				1 1	280.54		2 cs-H	1
	280.				1 1	280.54		2 CS-H	+
	280.					265.0		8 CS-He	+
	264.				4				+
	22	8 0.03%			1	227.93		8 CS-H	+
	215.1	6 0.29%			4	214.5			+
	182.1		182.3	5 5	4	182.3			
\vdash	167.		167.59	6	5	167.5		OCS-He	
-	152.1				1	82.8			., . —
-	145				5	145.8		.0 сs-н	
\vdash	143				2	141.5	6 87	.6 C S - He	
	129.8				5	130.2	5 95	.2	
 					2	125.7		.6 CS-H	
1	125			<u> </u>	6	122.5		2 CS-He	
_	122				2	113.9			
			6 113.9	7 4	1 4				
	1					4405	41 447	2146 1	•
	110		6 110.5	1 7	6	110.5		.2 CS-H	
E		.5 -0.019	6 110.5	1 7 0 7	6 6 7	110.5 101.3 96.5	0 122		





Mills Prediction vs. Data

							400.4		
	88.8	-0.17%	88.95	8	7	88.95	139.4		ļ
	87	-0.38%	87.33	5	3	87.33	142.0	He	<u> </u>
	82.9	0.02%	82.89	8	7	82.89	149.6		
	81.1	0.07%	81.04	5	3	81.04	153.0	н	
	79.58	-0.14%	79.69	9	8	79.69	155.6	He	l
	79.36	0.03%	75.98	5	3	75.98	163.2		-
		-0.05%	70.13	9	8	70.13	176.8		
	70.1	-0.50%	67.84	10	9	67.84	182.8	He	
	67.5		63.14	6	4	63.14	196.4	He	
	63.12	-0.03%	60.78	10	9	60.78	204.0		
	61	0.36%		6	4	59.79	207.4	Н	
	59.7	-0.14%	59.79						
				D1 6	L Doto ###				i
		Other Raw	Extreme L	V Spectra	I Data				1
	OBSERVE		MILLS PR	FUICTED		 			1
	SF Au Mic	EQ Pegasi				 			1
			WaveInth			A	eV		1
	Α	Α	Α	nf	ni		EA		
					 	303.91	40.8		
		304			3			U.	+
		265			4	265.01	68.0	ne	
	183	182			4	182.35			+
	168		167.6		5	167.59	74.0 95.2	He	+
	130	130			5	130.25	98.6		+
	126		125.8		2	125.76	101.2		+
	123	122.5			6	122.54	108.8		
	114		114.0		2	113.97			
	111		110.5		6	110.51	112.2		+
	101	101.3	101.3		6	101.30	122.4		
	97		96.6		7	96.58	128.4		-
	90	89	89.0		7	88.95	139.4		
	87		87.3		3	87.33	142.0		
	83	83			7	82.89	149.6		
	81	81	81.0	5	3	81.04	153.0		
	79.5		79.7	9	8	79.69			
	76		76.0	5	3	75.98	163.2		
	1							<u> </u>	
<u> </u>									
	1				1		<u> </u>		
	- Raw E	rtreme UV	Backgrour	nd Spectral	Data	1		<u> </u>	
—	SOURCE: L	abov. S., Bowy	er, S., "Spectra	el observations	of the extreme	ultraviolet back	ground",	<u> </u>	
	The Astrophy	sical Journal,	371, (1991), pp	. 8710-819				 	
	Pe Daw E	verama IN	/ Solar Sne	ctral Data		<u> </u>	1.04.4:22.2	1 464 465	
	SOURCES:	Thomas,R.J.,	Neupert, W.M.,	Astrophysical	Journal Supple	ment Series, V	ol. 91, (1994),	pp. 401-462	
	Malinasky &	4 Hemin I	Astronhysical -	Journal, Vol. 18	31. (1973). pp. 1	1009-1030 - Fig	ures 12-0		
	Noyes, R., TI	ne Sun, Our S	ar, Harvard Un	iversity Press,	Cambridge, M/	A, (1982), p. 17	4-18ure /.5	R-110	
			iun, Cambridge	University Pre	ss, cambridge	, Great Britain,	1 <i>332)</i> , pp. 11	J 10,	-
	120-121, 144	-145 - Danie Teatr		o eten! Dete	<u> </u>	+	 	+	
	- Othe	r Kaw Extr	eme UV Sp	CUAL DATE	5 50 Encel D	C.M.,et.al., Astr	ophysical Jour	nal. Vol. 449.	
 	SOURCES:	powyer, S., Sc	aerice, voi. 203	, (1854), pp. 5	, FUSSI, D.I	Carrietan, Aso	1	T	+
1	(1995), pp. 3	10-202		1					





THESIS - APPENDIX FOUR

and the second

westered speeded

property programs

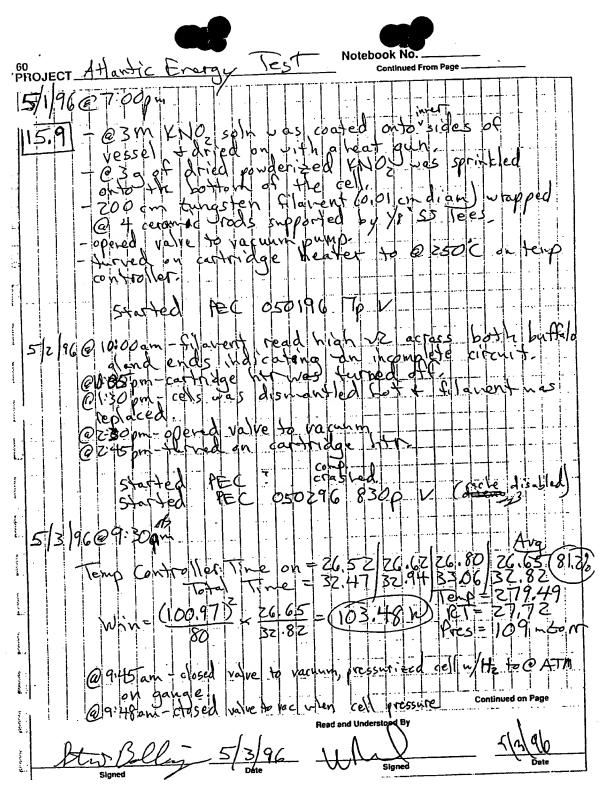


8

.

. . ______.

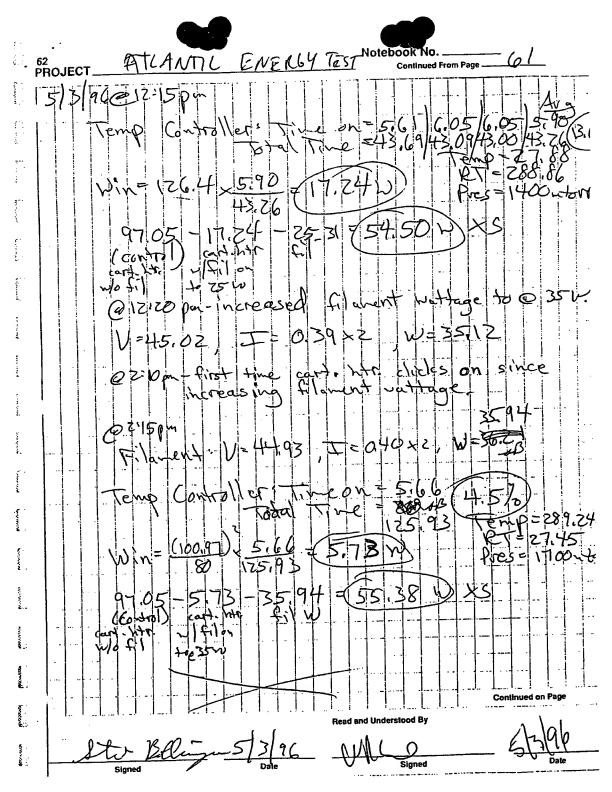
·







PROJECT ATLANGE ENELGYTEST Notebook No. 60 Continued From Page @10:45 an @10:10 an J since @11:450 rolle 127.8 250 0 251,31 since 88 - Beli 5/3/96 WK







Notebook No. 62 F. TEST Continued From Page PROJECT_ 06401 VIDEO Continued on Page Read and Understood By At Belin





10:45 AM my 15.2 -Witurosed: Mats Custa Auto mes

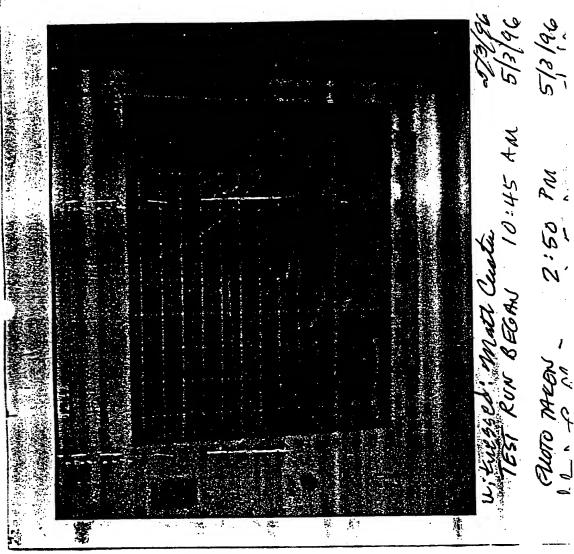
No. of the last

Total Services

a abstract

ried w

Khock



3:04 my 3 " זינדר

The second second

を からない なる しゅう

京 新華書 お TO SAND WINEST

2.60 PM

大学のでは、これには、これは大学を発展している。 これにはないないないないない

305

3

CABVIE

752

inservered exclanifier







The following is a list of the column headings and their meanings for the PEC data spreadsheet:

Column 1, Time(sec)-the time in seconds for each data point from the initial time (To) when the data acquisition system was started

Column 2, Room Temperature-room temperature measured on the data acquisition board

Column 3, Temperature(°C)-cell temperature in °C measured from the type K thermocouple which is positioned in a thermocouple well in the top flange of the vessel

Column 4, Watts-wattage going into either the cartridge heater or filament (depending on which it is connected to) at each of the data points

Column 5, Hours Elapsed-the time in hours elapsed from the initial time (To) when the data acquisition system was started; this number is calculated by dividing the corresponding-seconds in column 1 by 3600 in order to convert from seconds to hours.

Ex. $50 \sec (x) 1 \min / 60 \sec (x) 1 hr / 60 \min = 50 / 3600 (hr) = 0.014 hours$

Data = Excel Graphics = Pic





!PEC0503

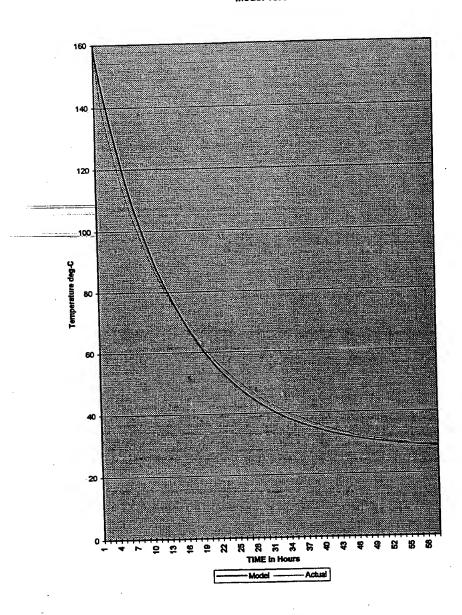
36887	27.082	268.98		10.24639	
36907	27.082	269.07	42.635	10.25194	
36927	27.082	268.99	42.655	10.2575	
36948	27,081	268.88	42.544	10.26333	
36968	27.08	268.9	42.546	10.26889	
36988	27.081	268.92	42.614	10.27444	
37008	27.083	268.87	42.626	10.28	
37028	27.08	268.9	42.551	10.28556	
37048	27.082	268.86	42.634	10.29111	
37068	27.083	268.91	42.552	10.29667	
37088	27.081	268.85	42.641	10.30222	
37108	27.082	268,91	42.635	10.30778	
37128	27.082	268.93	42.561	10.31333	
37148	27.08	268.78	42.543	10.31889	
37168	27.08	268.81	42.527	10.32444	
	27.079	268.93	42.528	10.33	
37188 37208	27.079	268.78	42.565	10.33556	
37228	27.079	268.82	42.609	10.33330	
		268.72	42.651	10.34667	
37248	27.078	268.91	42.596	10.35222	
37268	27.079		42.542	10.35778	
37288	27.078	268.84		10.36333	
37308	27.076	268.6		10.36889	
37328	27.077	268.74	42.566	10.37472	
37349	27.078	268.82		10.38028	
37369	27.077	268.73	42.58	10.38583	
37389	27.078	268.84	42.523		
37409	27.077	268.77	42.593	10.39139	
37429	27.08	268.76	42.61	10.4025	
37449	27.078	268.71	42.51	10.40806	
37469	27.076	268.64	42.537	10.41361	
37489	27.076	268.73	42.619		
37509	27.078	268.7	42.565	10.41917	
37529	27.079	268.69	42.507	10.42472	
37549	27.078	268.66	42.54	10.43028	
37569	27.078	268.59	42.62	10.43583	
37589	27.077	268.59	42.532	10.44139	
37609	27.078	268.63	42.543	10.44694	
37629	27.078	268.67	42.624	10.4525	
37649	27.078	268.51	42.53	10.45806	
37669	27.079	268.59	42.493	10.46361	
37689	27.079	268.47	42.503	10.46917	
37709	27.078	268.56	42.528	10.47472	
37729	27.08	268.51	42.577		
37750	27.077	268.41	42.613	10.48611	
37770	27.079	268.52	42.493		
37790	27.077	268.46	42.493		
37810	27.078	268.5	42.539		
37830	27.078	268.46	42.592		
37850		268.43	42.586	10.51389	
37870	27.076	268.36	42.479	10.51944	
37890		268.48	42.478	10.525	





Heat Loss Model - Vers 1.1 Chart 2

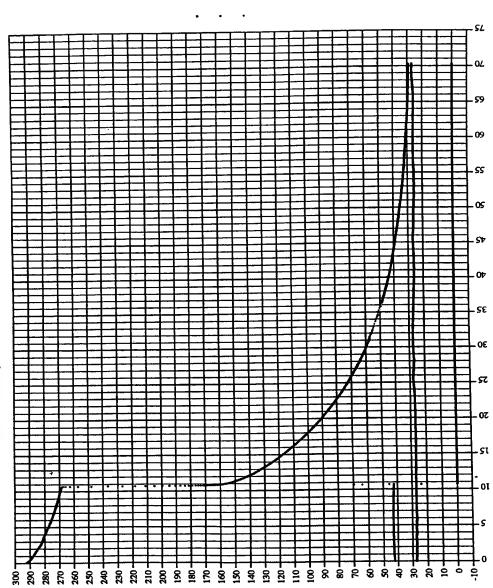
Model vs. Actual Data



Page 1

PEC 050396 310p H fil ex*

brown)



Room Temp Temp(°C) Watts



M. Custa.

Hrs Elapsed

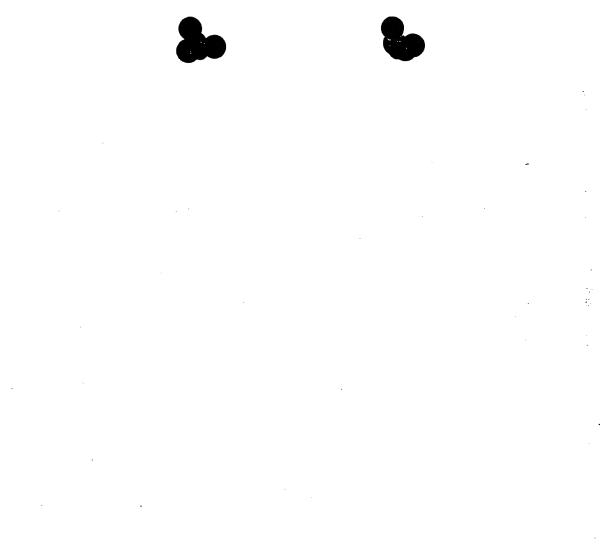






*......

THESIS- APPENDIX FIVE



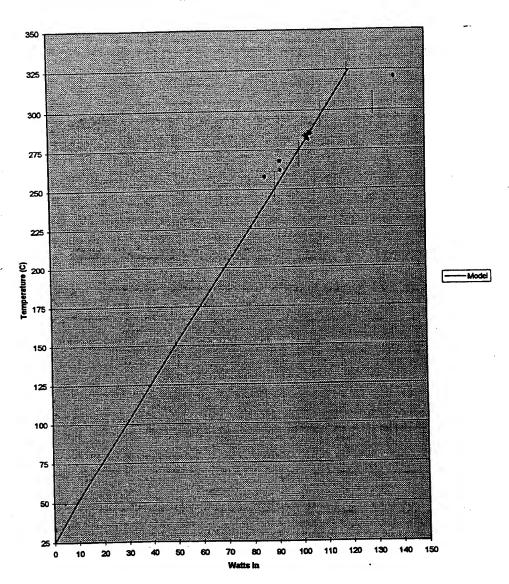
:





BLP Isothermal Cell Model Chart 3

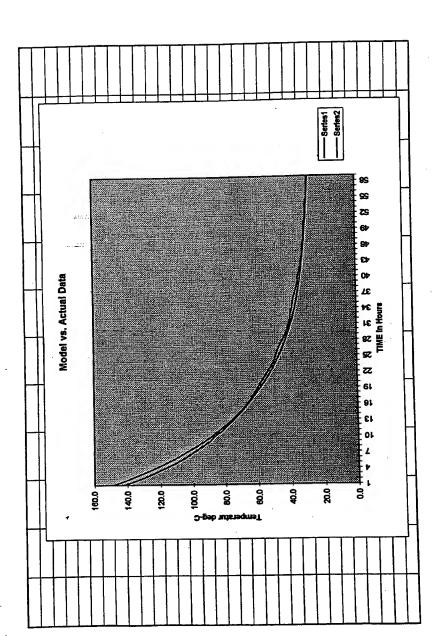
Isothermal Cell - Heat Loss



Page 1







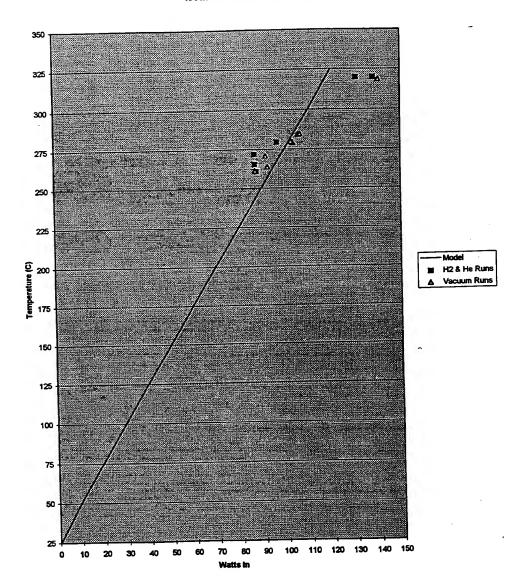
808





BLP Isothermal Cell Model Chart 3

Isothermal Cell - Heat Loss



Page 1





BLP Isothermal Cell Model

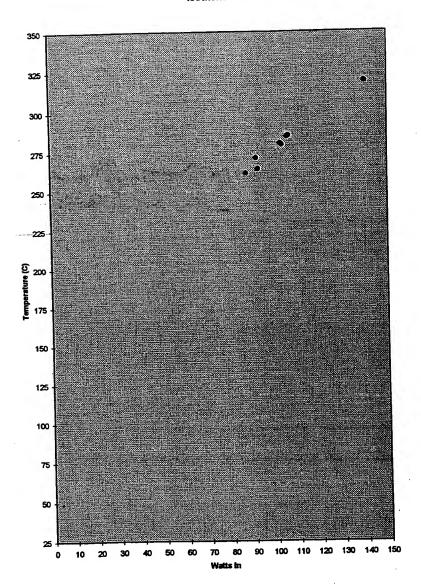
	ALL RUNS WITH ISO	HERMAL CALORIN		
	- 1- T	Temperature (C)	Steady State Watts	\vdash
perimental Run	Cell Pressure (mtorr)	Temperature (O)	Cartridge Heater Only	Gas
		270.73	91.95	V
15.6	38	271.79	87.07	H2
	1800	261.07	87.29	V
15.8	48	260.82	87.85	H2
	1350	279.49	103.48	V
15.9	109	279.5	97.05	H2
	1150	263.72	92.71	TV
15.10	56	265.41	87.16	H2
	1600	284.33	106.02	V
15.12	21		106.71	Tv
	20	284.72	138,29	He
15.13	2000	319.91	140.45	TV.
	35.5	318.45	131,22	H2
	1900	319.83 279.01	103.7	 v
16.2	22.3		102.96	ار
	22	279.97	102.50	+-
	VACUUM RUNS ONL			-
Cell Pressure (mtorr)	Temperature (C)	Steady State Wat		+-
		Cartridge Heater Only	V	+-
38	270.73	91.95	-V	+-
48	261.07	87.29	lv .	\top
109	279.49	103.48	V	\top
56	263.72	106.02	v	_
21	284.33	106.02	V	_
20	284.72		V	
35.5	318.45	140.45 103.7	V	\neg
22.3	279.01	103.7	v	\neg
22	279.97	102.50		\neg
				\dashv
		THE PARTY	CALORIMTER	\dashv
	GAS RUNS ONLY W	NITH ISO I HEKMAL	Unit Unit Later	
	<u> </u>	Standy State Ma	He .	\dashv
Cell Pressure (mtorr	Temperature (C)	Steady State Wa		$\neg \vdash$
		Cartridge Heater On	7	_
		67.07	H2	-+
1800	271.79	87.07	H2	_
1350	260.82	87.85	H2	-+
1150	279.5	97.05	H2	-+
1600	265.41	87.16	He .	
2000	319.91	138.29	H2	
1900	319.83	131.22	JF12	





BLP Isothermal Cell Model Chart 1

Isothermal Cell - Vacuum



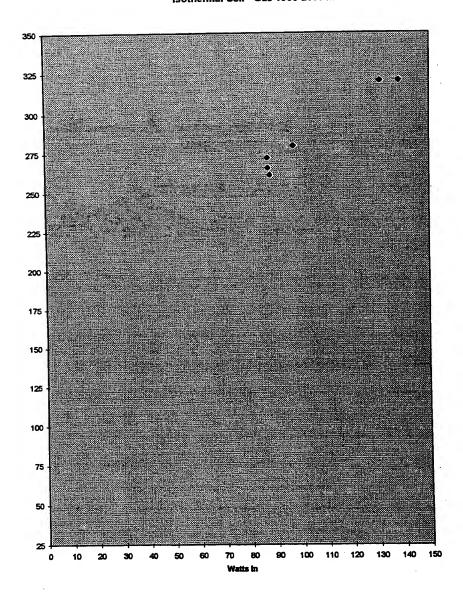
Page 1





BLP isothermal Cell Model Chart 2

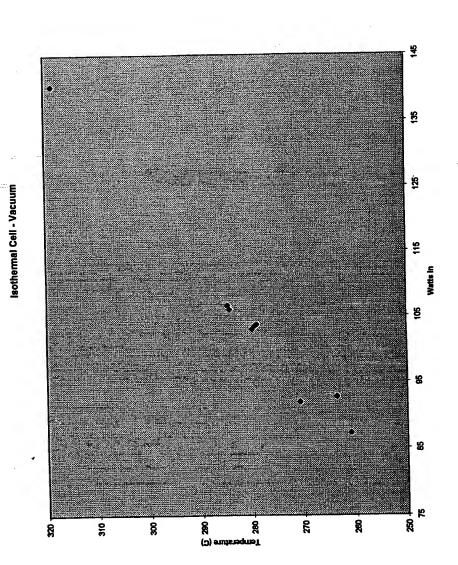
Isothermal Cell - Gas 1500-2000 mtorr







BLP Isothermal Cell Model Chart 1







Dear Peter,

Here is the data for the isothermal calorimeter which you requested. I tried to give you the most complete and representative data for our work on the isothermal calorimeter. The data includes one control and one experiment for a short (66 cm) tungsten filament, and also one control and five experiments for a longer (200 cm) tungsten filament. Varying diameters of tungsten filament were used for the 200 cm experiments and these diameters are noted. Other variables and data are listed under each experiment number (15.x) and description.

If you have any questions about the data, give me a call.

Sincerely,

Stev Bollinger

											•	Ç	_		_		7			1	7	_			3		Т						- 1	_	7	
_				-	EHCW																0							ļ							_	l
		+	1	furatte	MH =	1				E	an B	73.49			па	BL	25.39		E	na	65.38		ПВ	ВU	54.98			Bu	8.779	ยน	8.9		па		-	
		1	1	1110	TOTA		0	0		91.95	87.07	43.58			87.29	87.85	62.48		103.48	97.05	41.67 85.38		92.71	87.18	32.18	0	0	106.02	35.09 97.241	108.71	97.81		138.29	107.9		
-			1				\dagger		-	6	0	43.58			о	0	50.4		0	0	35.94				30.38			0	35.09	0	42.85		0	47.19		
-			+	offering of the control of the contr	wer impu	1 112	+	\dagger	\dagger	91 95	87.07	0			87.29	87.85	12.08		03.48	97.05	5.73		92.71	87.18	1.82			108.02	82.15	108.71	54.98		138.29	60.71	_	
-	+	H		-	7	- 1	+	+	+	27.070	1_	279.27						\mid	279.49 103.48	279.5	289.24		283.72	285.41	275.7		-	284.33 108.02	288.49	84.72	288.54		18.91	328.24		
	Cells	X				emperarue	11			7.6	27	27			82	28	87		27	-	2		2	×				7	2	2	2		8	က		
	Phase	RI P & Major US University			포니	- 1	+		1	90	1800	1350			48	1350	ow atm		100	4150	1700		58	1600	1600			21	6	20	20.8		2000	2000		
	_ Š	lor US			Chara	Pressure		4	-		1	1	0	0	-	-	F		1	-	+	٤	1	+	+	8	2000	-	-	L	\vdash	2000	ŀ	L	2000	
	wht Do	P&M			as Cell	Volume				2000			200	2000				0000	100			2000	3			20	20					20				Ì
	1300	DISCRI		-	9		1	1		6.2831853		1	6 2831853	6 2831853				01010	6.2831853		T	0 2024062	2000			15 70798325	15 70798325					15,70798325			15 70798325	
	Phase Cells	alysis or			[cm-cm2]	Diameter Surface Area				6.28			8.78	8.28					9.28			900	0.60			15.707	15.70					15.70			15.70	2
	H	₹	+	-	ristics	eter Sı	2	۲	2	0.0	\dagger	\dagger	5	5 6	3	\dagger	\dagger		5	\dagger	†	1	5	1	1	0.005	200	7,767	1		1	0 025	2,000	1	3000	0.020
					naracte	Diam			1		1	1				1	1			1	4	1	0	4	$\frac{1}{1}$	2	200	2	+	+	-	200	2	-	15	200
					Filament Characteristics [cm-cm2]	Length		86.04	98.0	200			000	200	2				200				200			5	3 6	3				1				7
						Type	H2 Run?	H2 Run?	Control	H2 Run	20147	KN	K Nuz	HZ Kunc	Control	YAC	24 .	1 to	H2 Run	KNO	KNDZ	KUCE	H2 Run	KN0;	A 02	1 No.2	Contract	Contra	Š	746	AAC.	Vac	Comito	£	Dr.	12 Run
		onfidential	+	+		T Oi tse	-15.3		1	BLP-15.6				BLP-13.7	BLP-15.8				BLP-15.9				BLP-15.10				BLP-13.11	BLP-15.12				9, 9,	BLP-15.13	1		BLP-15.13

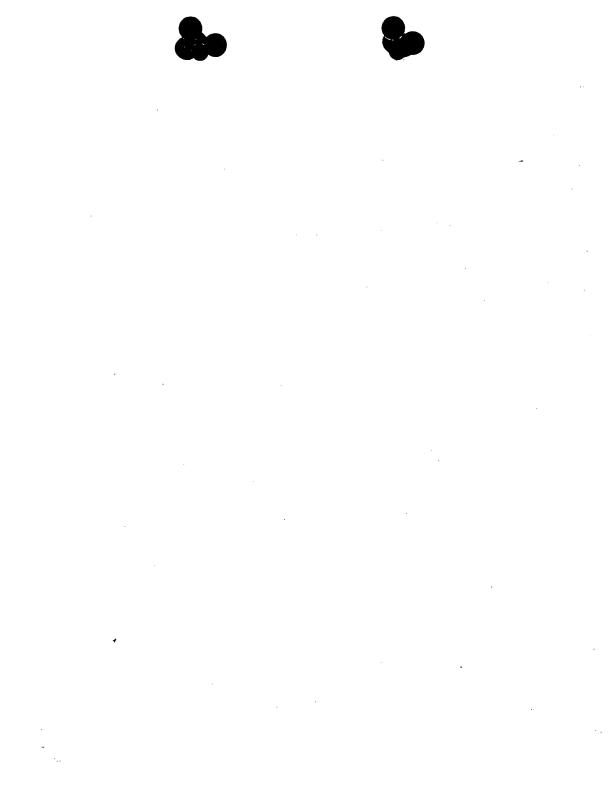


Analysis of Raw Lab Data vac HZ Control 20 35.5 318.45 140.45 0 140.45 na 100 140.45 102.21 102 100 319.63 131.22 132 100 319.63 131.22 132 100 319.63 131.22 132 100 319.63 131.22 132 100 319.63 131.22 132 100 319.63 131.22 132 100 319.63 131.22 132 100 319.63 131.22 132 100 319.63 131.22 132 100 319.63 131.22 132 100 319.63 131.22 132 100 319.63 131.22 132 100 100 100 100 100 100 100 1	emotro 1	¥										•			•								•	
Analysis of Raw Lab Data vac Vac H2 H2 H2 H2 H2 Control Control Vac	3	Γ	Ţ	1			<u>√</u>		_		T			ĺ	T				T		Γ	1	٦	
Analysis of Raw Lab Data vac Vac H2 H2 H2 H2 H2 H2 H2 Vac Control Control Vac		٩	2	77	B	3	() (2)		na na	90	3	2		+			_	_	1	_				
Analysis of Raw Lab Data vac Vac Control Control Vac Vac Vac Vac Vac Vac Vac Va		1		9.23 11.	1.22	8.27, 44.	.588 47.	-	l_	1 838 24	3	2.98	6	•	2	0			$\frac{1}{1}$		+			
Analysis of Raw Lab Data vac Vac Control Control Vac Vac Vac Vac Vac Vac Vac Va		1	-	46.64 12	0 13	47.77 8	74.8 83	-	L_	00 00	39.99	0 10		1			-							
Analysis of Raw Lab Data vac Vac Control Control Vac Vac Vac Vac Vac Vac Vac Va		3, 3,	140.45	82.59	131.22	38.5	8.79		403.7	200	42.00	102.98												
Analysis of Raw Lab Dativacy vac 35			318.45	323,36	319.83	328.48	331.03		270.04	10.072	281.62	279.97												
Analysis of Raw Lab E vac Vac Control Vac vac vac vac vac vac vac vac	ata		35.5	2	S	200	200	3	- 6	6.2	-	22					1	1				_	-	
V8C V8C V8C H2 H2 Control V8C	kaw Lab D				-	+					_			20	20	2 2	3		_				-	
V8C V8C V8C H2 H2 Control V8C	alysis of F							-				-									_	-	$\frac{1}{1}$	
V8C V8C V8C H2 H2 Control V8C V8C V8C V8C V8C V8C V8C V8	¥								7079832					57079632	C7070832	20001010	57079832							
Vac Vac Vac H2 H2 H2 H2 Control 200 Vac Vac Vac Vac Vac Vac Vac Vac			-	1	$\frac{1}{1}$	-	-					-		l	l			_			-			
V8C			-							_										_				_
S 및 및 및 및 및									2					6	"	7	2							
				VBC	Vac	H2	Н2	HZ	Control	CBX	2	V8C	VAC	0.0	על אמווי	H2 Run	H2 Run		+					
					_				RI P.18.2	L				7 1 101	MUSC-I	MUSU-2	MUSU-3			 -	1			+





Confidential	sothermal Calonmeter Data	alonmeter	Data		15.9-KNO2. 200 cm(0.01 cm dia) tungsten filament	cm(0.01 cr	n dia) tung	sten filamer	بو
			- Glomon		status	Temp(°C)	Temp(°C) Wcart htr Wfil	Wfil	Wtotal
102, 66 cl	m(U.Q.I cm	dia) tungst	ייפון וומווונפון	Mitatal	109 torr	279.49	103.48	0	103.48
╗	Temp("C) Weart htr Will	Wcart ntr	(WIOLE	U2 1 15 torr	2795	97.05	0	97.05
vac 0.075 torr	258.7	95.2	5	33.6	100 611 711	70 000		25 94	41.67
H2 1.6 torr	255.45	65.4	6.95	72.35	HZ 1.7 torr	47.697	3.73	10.00	
H2 2.0 torr	256.91	55.03	8.16	63.19					
H2 2.0 torr	257.87	43.62	10.36	53.98				5	1
112 < 2 0 torr	259.05	28.76	16.96	45.72	15.10-KN02, 200 cm(0.01 cm dia) tungsten filament	0.0m(0.01	cm dia) tui	gsten filam	enc
72.7.0 (0)	2000				status	Temp(°C)	Temp(°C) Wcart htr Wfil		Wtotal
					vac 0.056 torr	263.72			92.71
15 E (control) ampty 66 cm(0.01 cm dia) tungsten filament	monty 66 cm	n(0.01 cm (dia) tungst	ten filament	H2 1.6 torr	265.41	8		
ביבים	Tomn(°C)	Tomn(°C) Weart htr Wfil	Wfil	Wtotal	H2 1.6 torr	275.7	1.82	30.36	32.18
var 0 086 torr	272.88	94.33	0	94.33					
H2 22 0 torr	272 55	83.31	5.05	88.36					
U2 > 2 0 tor	273 68	81.12	8.23	89.35	15.12-KNO2, 200 cm(0.025 cm dia) tungsten filament	0 cm(0.02	5 cm dia) t	ungsten fila	ment
112 2 2 421	272 67		10.21	75.66	status	Temp(°C)	Wcart htr Wfil	Wfil	Wtotal
H2 2.0 TOIT	275 64		16 93		vac 0.021 torr	284.33	106.02	0	
HZ IOW A I M	27.3.04	25.7	200		vac 0,019 torr	288.49	62.15	35.091	97.24
					vac 0.020 torr	284.72	106.71	0	
1 C CNO 200 cm/O 01 cm dia) tringsten filament	0 0 0/00	m dia) time	icten filam	ent	vac 0.0208 torr	288.54	54.96	42.85	97.81
13.6-KINUZ, ZUL	Tomp/°C)	Tomp(°C) (Weart htr Wfil	Wfil	Wtotal					
Status	270 73	9195	0						
Vac 0.030 tor	271 70				15.13-KNO2, 200 cm(0.025 cm dia) tungsten filament	0.00 cm	5 cm dia)	tungsten file	ament
HZ 1.0 tor	270 27	L	43.5		status	Temp(°C)	Temp(°C) Wcart htr Wfil	Wfil	Wtotal
HC 1.33 toll	213:51				vac 0.0355 torr	318.45	140.45	0	
	_				vac 0.020 torr	323.36	5 82.59	9 46.638	
		100	m dia) tum	neten filament	H2 1.9 torr	319.83	3 131.22	0	-
15.8-(control), empty 200 cm(0.01 cm dia) tungsten manage	empty 200	משונטים ב	14/61	Mitotal	H2 1.6 torr	328.48	38.5	5 47.77	86.27
status	lemp(c)	S C			H2 1.9 torr	331.03	3 8.79	9 74.798	83.59
vac 0.048 torr	70.192	07.70			He 2.0 torr	318.91	138.29	0	
H2 1.35 torr	200.02			-	He 2.0 torr	326.24	4 60.71	1 47.194	107.90
H2 low ATM	269.38	12.06	30.4	١	211				





(Property

THESIS - APPENDIX SIX









Final report for period October-December 1996 In fulfillment of Service Contract with HydroCatalysis Power Corp. (now BlackLight Power, Inc.)

REPORT ON CALORIMETRIC INVESTIGATIONS OF GAS-PHASE CATALYZED HYDRINO FORMATION

Submitted by Prof. Jonathan Phillips* and Julian Smith Department of Chemical Engineering Penn State University University Park, PA 16802

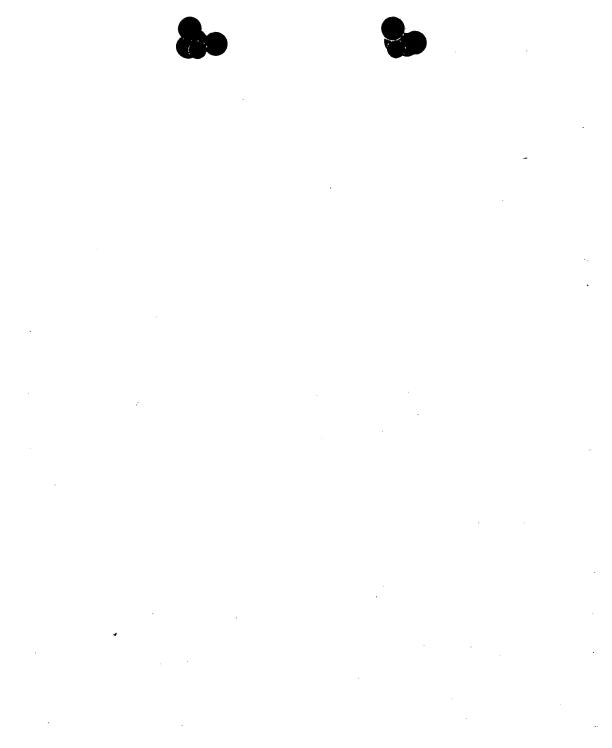
Ph: (814) 863-4809 Fax: (814) 865-7846 Professor Stewart Kurtz Department of Electrical Engineering Penn State University University Park, PA 16802

Ph: (814) 863-8407 Fax: (814) 863-8561

Istian Smith

Stewart Kurtz

*Corresponding Author







SUMMARY

Tests for heat production associated with hydrino formation were carried out with two types of calorimeters during the period October-December 1996. Experiments carried out in a modified Calvet system yielded extremely exciting results. Specifically, initial results are apparently completely consistent with the Mill's Hydrino formation hypothesis. In three separate rials between 10 and 20 K Joules were generated at a rate of 0.5 Watts, upon the admission of approximately 10-3 moles of hydrogen to the 20 cm 3 Calvet cell containing a heated platinum filament and KNO3 powder. This is equivalent to the generation of 1*10⁷ J/mole of hydrogen, as compared to 2.5 *10⁵ J/mole of hydrogen anticipated from standard hydrogen combustion. Thus, the total heats generated appear to be two orders of magnitude too large to be explained by conventional chemistry, but the results are completely consistent with the Mill's model. It must be noted that although the results presented in this report are very exciting, they require further verification. Moreover, it should be noted that some control studies are not yet complete.

Also included is a brief report on an attempt to replicate the Calvet cell results on a larger scale using the water bath calorimeter (described in some detail in an earlier report). Unfortunately, no evidence of 'excess heat production' was found. This can be linked to a failure to maintain the catalyst ions (K+) in the vapor phase. Specifically, it is hypothesized that the KNO3 catalyst evaporated from the containing pot at the reactor center, where the temperature is high, and deposited on the reactor walls, which are cold due to immediate contact with the calorimeter water bath. (That is, the catalytic material is 'cryo-pumped' by the cold walls.) Indeed, at the conclusion of the experiment, when the reactor was removed from the water bath, the walls of the quartz reactor were observed to be white in the general vicinity of the pot which contained the KNO3.





INTRODUCTION

Experiments were conducted to test the hypothesis that in the gas phase potassium ions will catalyze the conversion of hydrogen atoms to hydrino atoms. These experiments were initially carried out in a Calvet cell as this type of calorimeter is highly sensitive and accurate. Moreover, the conditions of the calorimeter are controlled.

RM's theory of hydrino formation requires that both K+ ions and H-atoms are present in the gas phase. In order to generate gaseous K+ ions, KNO3 is placed in a small (2cc) quartz 'boat' inside the calorimeter cell. The boat is heated, to increase the vapor concentration of KNO3, with a platinum filament, which is wound around the boat. A second function of the platinum filament is to generate H-atoms. It is well known that hydrogen molecules in contact with a heated filament will decompose, yielding a relatively high H-atom concentration in the boundary layer around the filament. Thus, according to RM's model, in a cell containing KNO3 in the boat and vapor phase hydrogen, there is a small region in the boundary layer around the heated metal filament which should contain sufficient concentrations of both H-atoms and K+ ions for hydrino formation to occur.

Calorimetric considerations require that a stable baseline exists before the heat generating process is initiated. Thus, signal change away from the baseline can be correlated to the onset of the process under investigation. In the present experiments the cell was run with KNO3 in the boat and the filament fully 'powered'. The calorimeter was allowed to equilibrate until a steady baseline existed. The 'hydrino formation' process was initiated by then adding gaseous hydrogen. Good calorimetric practice also requires that adequate control studies be carried out. Also required are repeated electric calibrations.

In the present work, data is presented which indicates that significant heat evolved upon the introduction of hydrogen to the Calvet calorimeter cell. In contrast, no heat was evolved upon the admission of helium. Repeated calibrations were also conducted. Thus, it appears that The RM





hypothesis is supported by the present results. A more definitive statement must await repeats of these experiments, and the results of a few additional control experiments.

An attempt was also made to employ the water bath calorimeter (see previous report to HPC) to detect excess heat. Indeed, the positive results of the Calvet study present a staggering challenge to conventional physics. Challenges of this magnitude require enormous experimental support. Thus, evidence of excess heat production from a second type of calorimeter would be useful. Unfortunately, the experiment failed to yield any evidence of excess heat. However, there is reason to believe that catalyst concentration was low and thus the failure to observe excess heat does not disprove the Mill's hypothesis.

EXPERIMENTAL SYSTEM

<u>Calvet Calorimeter</u>. The Calvet-type calorimeter employed in this study is similar to one described in the literature (attached) and is also described in earlier reports to HPC (now BLP). In essence a stainless steel cup of almost exactly 20 cm³ volume is placed in a calorimeter well such that the cup is surrounded by thermopiles on its sides and bottom. The cup and calorimeter are surrounded by a thick layer of insulation, and the entire device is placed inside a commercial convection oven. In all cases experiments were conducted with the oven temperature set to 250 C.

Reaction cell. For these experiments the top of the calorimeter cup/reactor cell was fitted with a Conflat knife edge flange. The top element of the flange is connected to a gas supply system outside the convection oven with a 0.5 cm OD ss tube, and with two welded vacuum high current copper feedthroughs. The feedthroughs were connected on the cup side of the flange to a coiled section of 0.25 mm platinum wire approximately 18 cm in length. Fitted inside the coiled platinum was a small quartz boat into which 200 mg of powdered KNO3 were placed.

Plumbing. On the outside of the oven the gas feed through is connected to a line leading to hydrogen and helium tanks, a pressure gauge, and a standard vacuum roughing pump. It is notable that the gas lines were all well insulated, both inside the oven, and for about 50 cm outside the oven.





The plumbing system was so arranged that the cell could be evacuated, and then isolated from the pump in such a way that hydrogen or helium could be added directly from high purity gas tanks. Great care was taken before the experiments were initiated to evacuate and flush the gas lines several times. It was also determined that the lines held gas pressure, with no loss in pressure, for several days. That is, there were no leaks.

Water Bath Calorimeter. This instrument is described in detail in the previous report to HPC. Two minor modifications were made for the present experiment. First, to facilitate the decomposition of hydrogen, the center section of the mandrel was wrapped with a 60 cm length (about 8 cm of mandrel) of 0.25 mm diameter platinum wire. Second, in the center of this section the same quartz boat (again filled with about 200 mg of catalyst) used in the Calvet system, wrapped with the same coil of platinum wire, was inserted into the circuit. (The experiment described was carried out after the completion of the Calvet system experiments.)

RESULTS

<u>Calvet Calorimeter</u>. The Calvet studies suggest large amounts of heat are generated upon the admission of hydrogen to the cell. In contrast, virtually no heat is observed upon admission of helium to the cell.

Calibration. The first tests performed on the Calvet system were electrical calibration experiments. The system was set-up for full experimentation: KNO3 was in the boat, the system was evacuated, and 10 watts of steady power were supplied to the platinum coil. After a steady baseline was achieved (approximately 10 hours after the oven was adjusted to 250 C), the cell was isolated from the pump and the pressure allowed to equilibrate (approximately 100 Torr). This did not appear to impact the baseline in any fashion. The power supply was then adjusted to deliver an additional 1 watt (11 watt rather than 10) for a specified time period. The power was then returned to the original 10 watt setting. A typical response curve is shown in Figure 1. The area under the response curve can be used to obtain a calibration constant which relates signal area increase to the number of extra Joules delivered. This was done in four cases (Table I). As can be seen, there is some error (+/- 15%) in the calculated calibration constant.





Control Studies. Helium was admitted, approximately 10 psig, to the cell to test the impact of a change in pressure, and heat transfer characteristics on the response of the cell. The helium was admitted after the cell had been isolated from the pump for a considerable time and a steady pressure (approximately 100 Torr) achieved. As can be seen in Figure 2a, the response was a short-lived small increase in output signal, followed by a relatively short time period during which the signal gradually returns to the original baseline. Within an hour the signal returned to the original baseline, with some drift evident.

The response of the system is expected. The helium increases the rate of heat transfer away from the platinum filament, and heated boat. Thus, the initial addition of helium to the system results in a temporary increase in the amount of heat reaching the thermopiles. That is, the boat and the filament cool off, until such time as the boat and filament have reached their new steady state temperatures. The steady state temperature of boat and filament are a function of heat transfer mechanism. After the admission of helium most heat transfer is occurring by convection to the walls. Before the admission of helium a considerable fraction is by radiation. Radiative transfer of 10 watts requires a higher filament/boat temperature than does convective heat transfer.

Figure 2b illustrates again the impact of adding pressure, or removing gas, from the system. Upon the addition of helium there is a very short lived increase in heat reaching the thermopiles. Upon pumping there is a period of time, perhaps an hour, during which the heat signal goes below the baseline. This is consistent with the model in that pumping makes convective and diffusive heat transfer minimal. Virtually all heat transfer is by radiation, which requires that the filament/boat temperature increase. It takes some time for this new steady-state temperature to be reached.

Hydrogen Admission. Hydrogen admission was carried out in much the same fashion as helium admission. The cell reached an equilibrium pressure, approximately 100 Torr, and then hydrogen at 10 psig was admitted to the cell. The valve to the hydrogen source, which was a steel line 4 meters by 0.6 cm OD, was closed off by a valve in front of the regulator during admission. Moreover, it was open for only a couple of seconds in each case. This was done on three separate





occasions, and the signal that evolved in response to these three processes is recorded in Figures 3, 4 and 5. One other observation recorded was that the pressure decreased gradually over time, such that after about an hour the pressure returned to the original equilibrium pressure of the cell. It must also be noted that the heat production was ended deliberately in all three cases by pumping the system to 5*10⁻³ Torr. It is clear 'excess heat' evolution would have continued in all cases if the system had not been evacuated.

It is expected that in the absence of reaction that the response of the cell to the addition of hydrogen would be similar to that observed for helium. Indeed, given that pressure measurements suggest that most hydrogen is adsorbed, or in some other fashion removed from the cell after an hour, even heat transfer effects should be totally transitory. Even in the event of reaction no more than a small heat signal is expected. Indeed, a high end estimate is that 25 cm³ of hydrogen at a temperature of 300 K and a pressure of 2 atmospheres entered the cell. This is equivalent to 2*10⁻³ moles of hydrogen. If all of that hydrogen interacted with oxygen to form water only 510 J would be generated. It is possible to imagine that the hydrogen could interact with nitrogen in KNO3 to form ammonia. Even less energy would evolve from this process. Thus, the largest heat peak might be expected to be 0.5 watts for 1000 seconds (approx. 17 minutes). A block of this size is marked on Figure 3.

It is clear from figures 3, 4 and 5 that hydrogen admission to the cell apparently leads to far more energy evolution than can be explained by any conventional chemical process. It is interesting in this regard to graphically contrast the response of the system to helium admission to the response to that for hydrogen admission. This is done on Figure 6 in which Figure 3 and Figure 2a are superimposed.

Water Bath Calorimeter. Studies conducted with the water bath calorimeter do not indicate the evolution of any excess heat. As shown in Figure 7 the increase in temperature almost exactly parallels the increase predicted on the basis of the amount of energy added to the system and the known heat capacity of water.





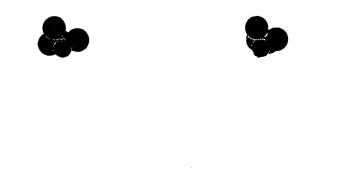
Do the results of the experiment refute the RM hypothesis? No. At the conclusion of the experiment the large cell was removed from the water bath and a white coating was seen on the walls in the vicinity of the pot which contained the KNO3. This suggests that the KNO3 was rapidly cryopumped by the walls, and that the gas phase concentration of catalyst was too low to be effective.

DISCUSSION

The evidence presented in this report clearly suggests that an extraordinary phenomenon takes place upon the admission of hydrogen to a cell containing a heated platinum filament and KNO3. This phenomenon appears to generate a tremendous amount of 'excess' heat. Still, the author of this report urges that a cautious approach be taken at present. Additional experimental work is required. A partial list of proposed additional experiments is given below:

- A control experiment consisting of admission of hydrogen to a cell in which 10 watts of power is applied to a platinum filament, but no KNO3 is present.
- 2) Hydrogen is admitted to a cell containing a platinum filament and KNO3 in a boat, but no power is applied to the filament.
- 3) The experiments are run as described in the present report, but the boat containing KNO3 is at the bottom of the cell, rather than in the center of the platinum coil.
- 4) The hydrogen admission experiments described above are repeated BUT continued for times sufficient to return the signal to the original baseline.

In addition, modifications in the apparatus should be made. First, insulation should be added to improve the stability of the baseline. Second, a quality pressure gauge should be attached to a known volume outside the oven such that all uncertainty regarding the number of moles of hydrogen admitted to the cell can be eliminated. Third, the plumbing should be re-arranged to facilitate 'capture' of gas for analysis using gas chromatography. Fourth, provision should be made to permit pressure to be recorded as a function of time.



.



Typical Calibration Experiment: 1 W Input, 20 Mins

report of carotimeure inv gations or nydrifte communication

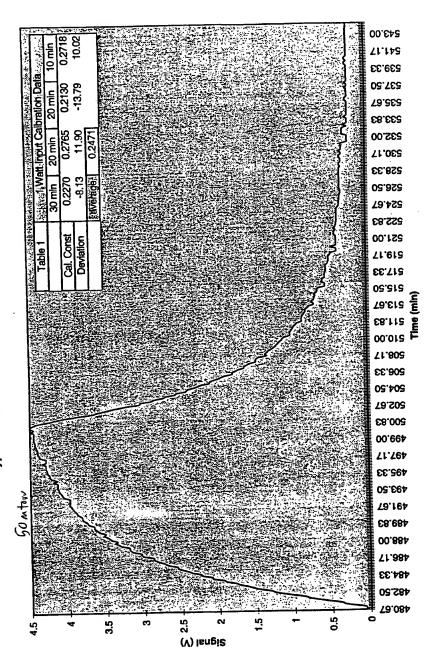
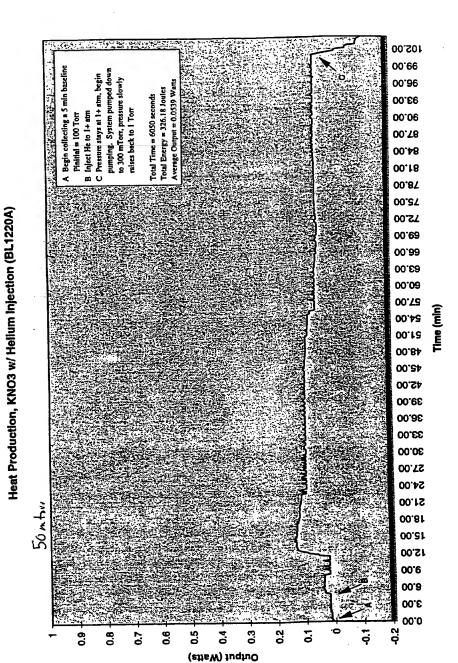


Figure 1









Heat Production, KNO3 w/ Hellum Injection (BL1219B)

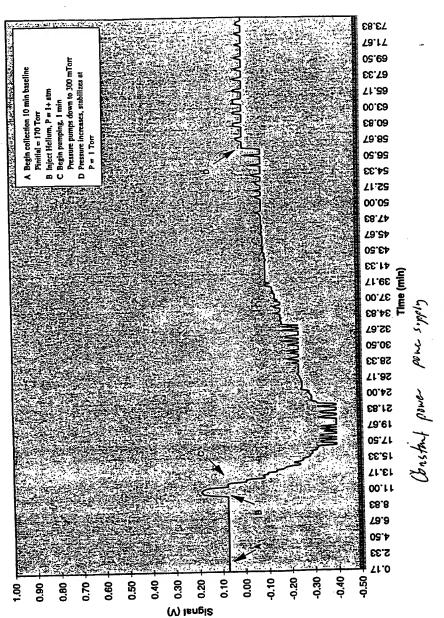
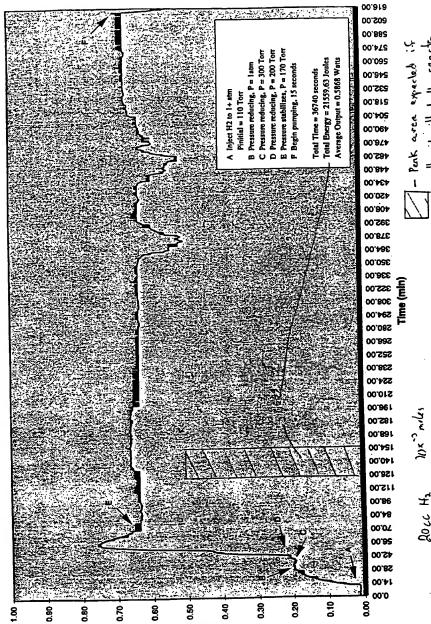


Figure 2B

Heat Production, KNO3 w/ H2 Injection (BL1218CD)







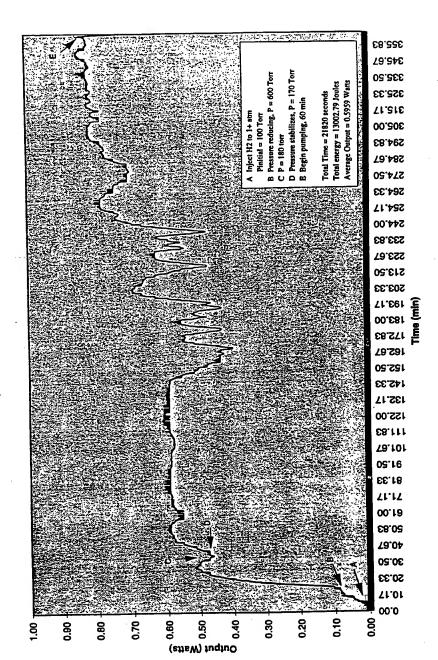
Output (Watts)

all ait without 112 ranchs ₹ 3





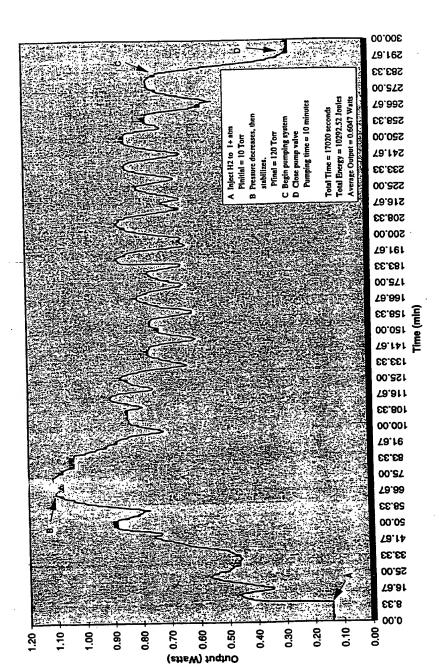
Heat Production, KNO3 w/ H2 Injection (BL1220BC)







E∋at Production, KNO3 w/ H2 Injection (BL1221AB)

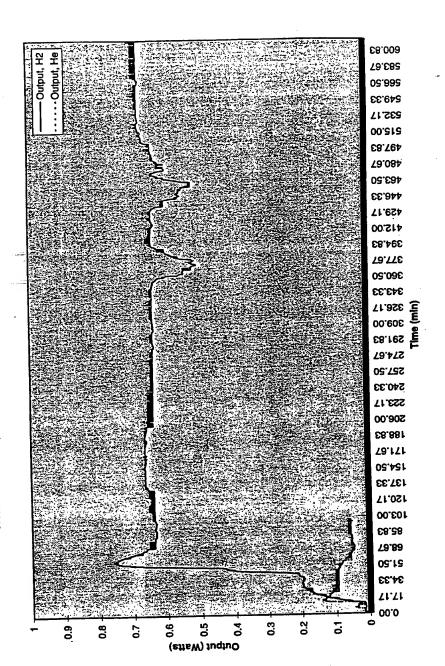


igure 5

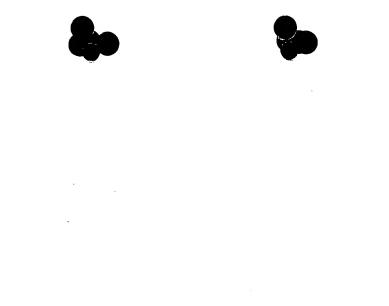




Heat Production, KNO3 w/ H2 and He Injection (BL1218CD,BL1219B)

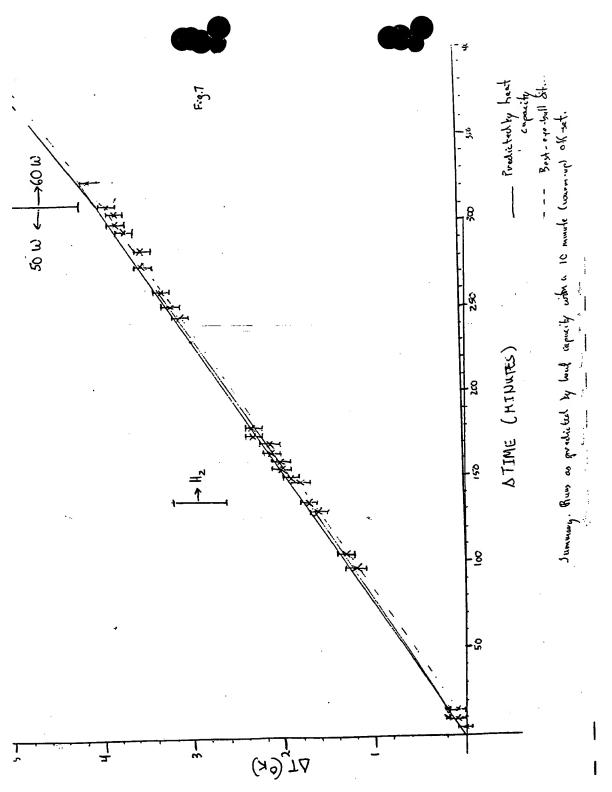


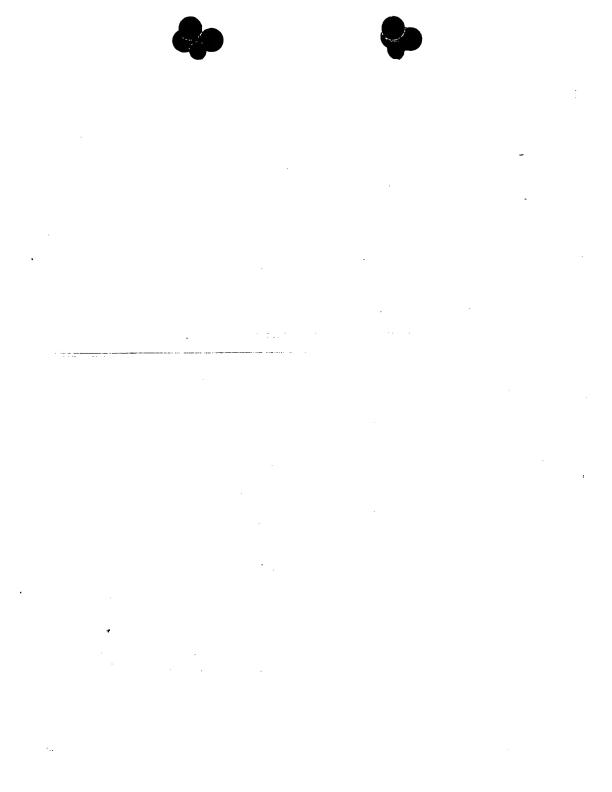
igure 6

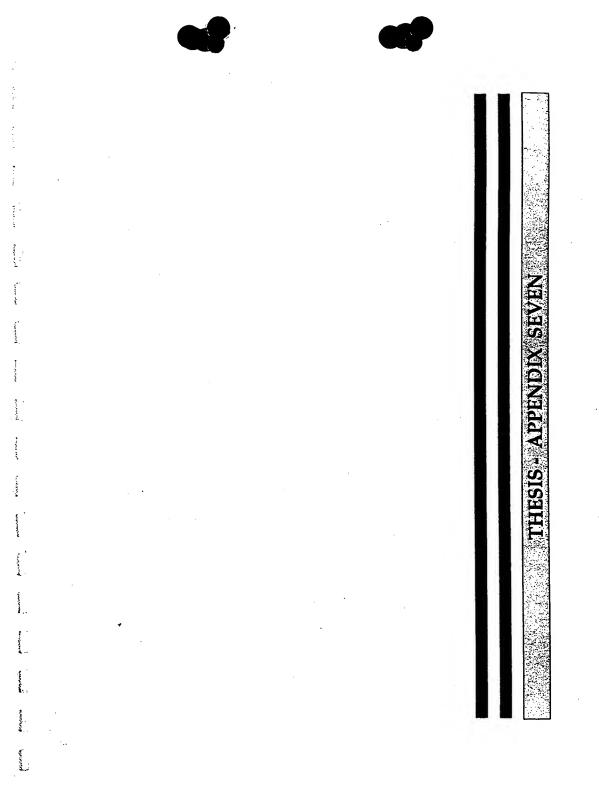


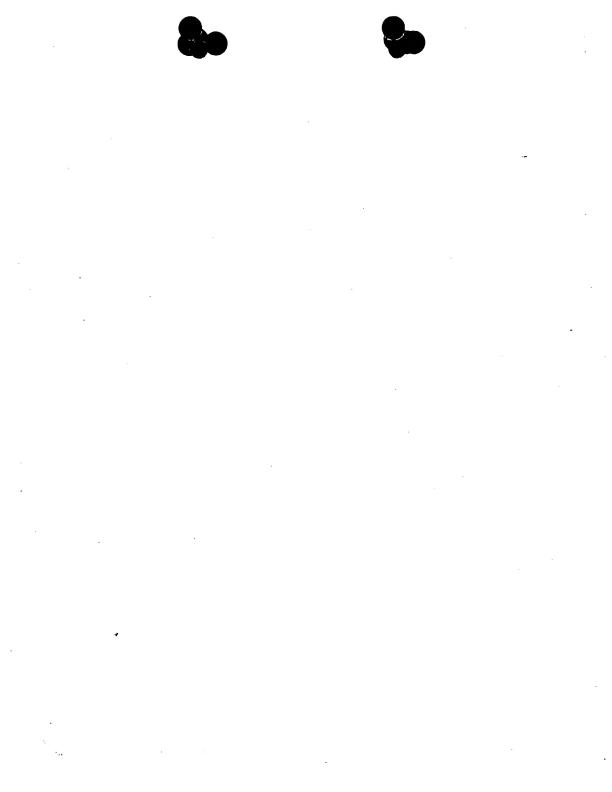
•

.













FINAL REVISED 12 APRIL 1997



BLACKLIGHT POWER CORPORATION

EXPERIMENTAL PROTOCOL FOR CALVET HEAT MEASUREMENTS

CALVET HEAT MEASUREMENT OF A HIGH TEMPERATURE VAPOR PHASE CELL

EXPERIMENTS BY P.M. JANSSON, P.P., P.E.

B.S.C.E. MASSACHUSETTS INSTITUTE OF TRICENOLOGY '78
FOR M.S.E. THESIS AT ROWAN UNIVERSITY '97

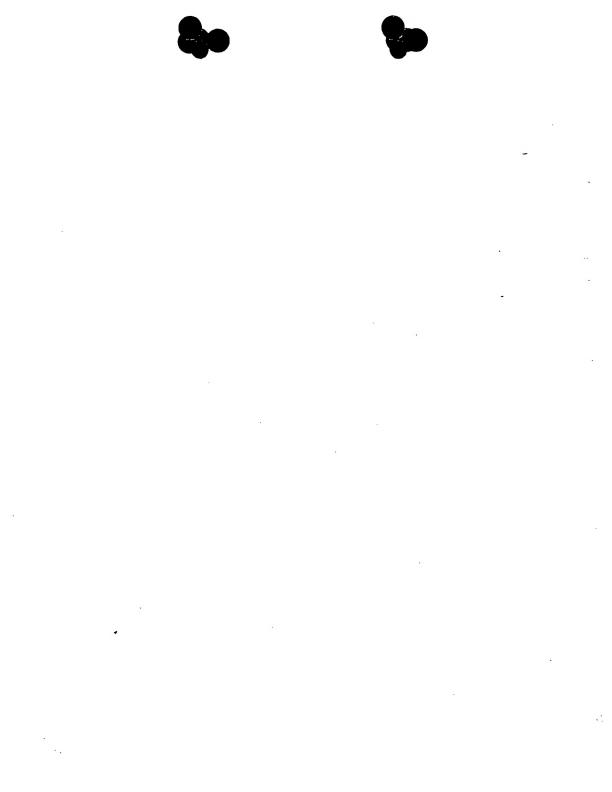
TO DETERMINE FILAMENT SURFACE AREA EFFECTS ON HEAT GENERATION

3 March 1997 - 20 April 1997

Experiments Conducted in Laboratory of:

BLACK LIGHT P O W E R inc.

Great Valley Corporate Center 41 Great Valley Parkway Malvern, PA 19355







CALVET HEAT MEASUREMENTS OF THE HIGH TEMPERATURE VAPOR PHASE CELL

Objective

A number of experimental observations from BlackLight Power and Pennsylvania State University lead to the conclusion that atomic hydrogen can acheive fractional quantum states that are at lower energies than the traditional "ground" (n =) state which form the basis of a new hydrogen energy source. Certain inorganic ions which are proprietary to the BlackLight Power serve as transition catalysts which resonantly accept energy from hydrogen atoms and release the energy to the surroundings. The reaction of hydrogen to lower-energy states is referred to as a transition reaction. The transition catalyst should not be consumed in the reaction. It accepts energy from hydrogen and releases the energy to the surroundings. Thus, the transition catalyst returns to the original state. And, the energy released from hydrogen atoms is very large compared to conventional chemical reactions including the combustion of hydrogen. Multiple cycles of catalysis are possible with increasing amounts of energy with successive cycles of transitions.

The goal of this project is to perform precise Calvet calorimetric measurements of a hydrogen gas energy reactor wherein the predicted exothermic reaction of electronic transitions of hydrogen to lower energy states could be measured. This new reaction occurs in the gas phase of atomic hydrogen. If successful, the experiments should produce statistically significant excess heat much greater than any known chemical reactions for hydrogen. The experiment will also vary the size [length] of the platinum filament used in the reactor to dissociate the hydrogen molecules to make hydrogen atoms available for the anticipated catalytic transition to reduced energy states. The intent will be to demonstrate that heat generation from this reaction will be directly related to available hydrogen atoms, which should be generated at different rates by varying filament size while keeping all other controllable parameters constant [ie, filament temperature, partial pressure of the catalyst, partial pressure of the H2 gas, vessel temperature and pressure, etc.]

Vapor Phase Energy Cell

The hydrogen gas energy reactor wherein the exothermic reaction of hydrogen occurs in the gas phase comprises a vacuum vessel; a source of hydrogen; a means to control the pressure and flow of hydrogen into the vessel; a material to dissociate the molecular hydrogen into atomic hydrogen, and a transition catalyst. The hydrogen transitions occur by contact of the hydrogen with the transition catalyst such that the resonant energy transfer occurs. catalytic reaction rate is maximized in the gas phase. The gaseous transition catalyst includes ions that sublime, boil, and/or are volatile at the elevated operating temperature of some regions of the gas energy reactor. In this project, the source of hydrogen atoms in the gas phase comprises an external tank of pressurized hydrogen gas at room temperature conditions.

Volatilized Transition Catalyst, K* /K*, in a Gas Cell for a Calvet Calorimeter

The transition reaction occurs in the gas phase. Gas phase hydrogen atoms are generated with a high purity platinum filament. The general cell schematic is shown in Figure 1. The cell comprises a 20 cc stainless steel vessel capable of containing a vacuum or a pressure





above atmospheric. The cell is maintained at an elevated isothermal temperature by a forced convection oven. The operating temperature of the convection oven [and gas cell when no filaments are energized] is 250°C. The cell is used in the vertical position and is inserted into a thermopile [13]. The flange [4] is sealed with a copper gasket [8] that has had its surface oxidized and softened by direct heating with a propane torch or oven. The flange has a two hole Conax-Buffalo gland [6] for the leads [5] of the filament that is present during the calibration of the cell and varied in length for the experiments 1-3 of the reaction vessel. The flange [4] also has a 1/4" vacuum port through which the hydrogen is passed. The vaccum port connects to a Tee [3], a OE bellows valve, a pressure gauge, and then the hydrogen supply. The elbow port of the Tee [3] is attached to vacuum gauges, a bellows valve, and then a vacuum pump. The filament is platinum wire [0.25 mm. diameter] of 99.99% purity. The lengths of the filament [and resulting surface areas] are varied 20cm, 10cm and 30cm for experiments 1 through 3 respectively.

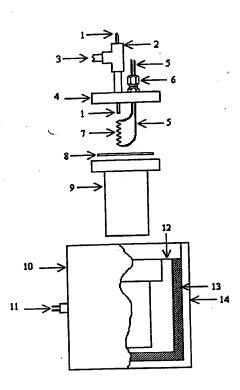
A small ceramic vessel is secured at the base of the Calvet cell [by a nickle wire stand] which contains the catalyst potassium nitrate (KNO3). A vacuum is pulled on the cell while the oven is brought to operating temperature. The appropriate power is dissipated in the filament at an established rate calculated to keep the filament surface temperature constant [10watts for 20cm., 5 watts for 10cm., 15 watts for 30cm.] The oven maintains the surrounding ambient temperature at 250°C. The catalyst's vapor pressure is observed as a function of temperature, and once Calvet cell reaches its steady state output at the supplied input energy, the vacuum pump is stopped and the catalyst pressure within the outlet tube [3] is observed to be constant in the range of about one-hundred to two-hundred torr. Hydrogen gas is then added to the cell to bring its overall total static pressure including the hydrogen pressure measured in the outlet tube [3] by the vacuum gauge to be 3 times the stable pressure of the catalyst (KNO3). The data is recorded with a Macintosh based computer data acquisition system (Apple Quadra 800) and the following National Instruments, Inc. hardware: Lab-NB Data Acquisition Board; Back-Plane with amplifiers: (2) 10 mV to 5 V and (2) 50 mV to 5 V.

NOTE: Minor Edits to Figure 1 below need to be made.





Figure 1. Schematic of the Gas Cell for the Calvet Calorimeter and Cross Sectional View of the Calvet Calorimeter. 1 - (1/16)" OD stainless steel tube (to hydrogen supply), 2 - stainless steel tee union, 3 - (1/4)" OD stainless steel tube (to vacuum manifold), 4 - cell lid, 5 - filament leads, 6 - Conax-Buffalo gland, 7 - precision resistor, 0.1 mm OD tungsten filament, or nickel hydride filament treated with catalyst, 8 - copper ring gasket, 9 - cell body, 10 - Calvet Calorimeter, 11 - thermopile signal output, 12 - thermal shunt, 13 - thermopile, 14 - insulated calorimeter base.







Sequence of Controls and Experiments

Control #1

Install 20 cm Platinum [Alfa] filament, 0.25mm diameter in Reaction Vessel Warm up oven Temperature 250°C.

Filament input wattage = 0

Vacuum down pressure in Reaction Vessel below 10 mtorr to remove moisture.

Stabilize Oven and Vessel Temperature to 250°C.

Close all valves and vacuum pump.

Inlet H2 gas to 650 torr pressure.

Run Calibration #1 through full sequence allowing Calvet Cell to reach steady state output [Vc] for each power level shown below:

0 watts, 10 watts, 11 watts, 5 watts, 6 watts, 15 watts, 16 watts, 0 watts, 1 watt.

Develop 'BEFORE' Calibration Curve.

Experiment #1

Install New 20 cm Platinum [Aldrich] Filament [99.99% purity], 0.25 mm diameter Weigh approx. 0.25 grams of KNO3 and place in ceramic boat

Support boat via nickle wire support legs

Reassemble reaction vessel

Pressure check Calvet and all gas & vacuum lines

Insulate Calvet Calorimeter close oven

Warm up oven Temperature 250°C.

Filament input wattage = 0

Vacuum down pressure in Reaction Vessel below 10 mtort to remove moisture.

Close all valves and vacuum pump.

Stabilize Oven and Vessel Temperature to 250°C.

Observe catalyst vapor pressure steady state [100-200 torr]

Begin Experiment #1 by Increasing Filament Power Level to that shown below:

10 watts

Inlet H2 gas to bring vessel to 3 times overall catalyst steady state pressure. [Ie; if catalyst pressure is 200 torr add 400 torr of H2 gas to bring Calvet to 600 torr.

Wait 5 minutes for mixing to occur.

Slowly vacuum down Vessel to 30-70 mtorr level until excess heat formation commences.

Keep Vessel under vacuum to maintain 'active' pressure regime [ie; 38 mtorr, 70 mtorr, etc.]

Stabilize Readings and Develop Experimental Data Curves.

Save Data Acquisition System [DAS] file daily, using the same standard naming

convention: tpdate[mmddyy] time[930a] watt[7w] id[h]

Take 1 or 2 new data points [controls] to develop specific curve after reaction ceases.

OPTION 1: Close valve to Vacuum to quench reaction if required.

OPTION 2: Repeat experiment if it is believed that catalyst pressure is inadequate or hydrogen atom generation is compromised





Experiment #2

Install New 10 cm Platinum [Aldrich] Filament [99.99% purity], 0.25 mm diameter

Weigh approx. 0.25 grams of KNO3 and place in ceramic boat

Support boat via nickle wire support legs

Reassemble reaction vessel

Pressure check Calvet and all gas & vacuum lines

Insulate Calvet Calorimeter close oven

Warm up oven Temperature 250°C.

Filament input wattage = 0

Vacuum down pressure in Reaction Vessel below 10 mtorr to remove moisture.

Close all valves and vacuum pump.

Stabilize Oven and Vessel Temperature to 250°C.

Observe catalyst vapor pressure steady state [100-200 torr]

Begin Experiment #1 by Increasing Filament Power Level to that shown below:

5 watts...

Inlet H2 gas to bring vessel to 3 times overall catalyst steady state pressure. [Ie; if catalyst pressure is 200 torr add 400 torr of H2 gas to bring Calvet to 600 torr.

Wait 5 minutes for mixing to occur.

Slowly vacuum down Vessel to 30-70 mtorr level until excess heat formation commences.

Keep Vessel under vacuum to maintain 'active' pressure regime [ie; 38 mtorr, 70 mtorr, etc.]

Stabilize Readings and Develop Experimental Data Curves.

Save Data Acquisition System [DAS] file daily, using the same standard naming

convention: tpdate[mmddyy] time[930a] watt[7w] id[h]

Take 1 or 2 new data points [controls] to develop specific curve after reaction ceases.

OPTION 1: Close valve to Vacuum to quench reaction if required.

OPTION 2: Repeat experiment if it is believed that catalyst pressure is inadequate or hydrogen atom generation is compromised

Experiment #3

Install New 30 cm Platinum [Aldrich] Filament [99.99% purity], 0.25 mm diameter

Weigh approx. 0.25 grams of KNO3 and place in ceramic boat

Support boat via nickle wire support legs

Reassemble reaction vessel

Pressure check Calvet and all gas & vacuum lines

Insulate Calvet Calorimeter close oven

Warin up oven Temperature 250°C.

Filament input wattage = 0

Vacuum down pressure in Reaction Vessel below 10 mtorr to remove moisture.

Close all valves and vacuum pump.

Stabilize Oven and Vessel Temperature to 250°C.

Observe catalyst vapor pressure steady state [100-200 torr]





Begin Experiment #1 by Increasing Filament Power Level to that shown below:

15 watts

Inlet H2 gas to bring vessel to 3 times overall catalyst steady state pressure. [Ie, if catalyst pressure is 200 torr add 400 torr of H2 gas to bring Calvet to 600 torr.

Wait 5 minutes for mixing to occur.

Slowly vacuum down Vessel to 30-70 mtorr level until excess heat formation commences.

Keep Vessel under vacuum to maintain 'active' pressure regime [ie; 38 mtorr, 70 mtorr, etc.]

Stabilize Readings and Develop Experimental Data Curves.

Save Data Acquisition System [DAS] file daily, using the same standard naming

convention: tpdate[mmddyy] time[930a] watt[7w] id[h]

Take 1 or 2 new data points [controls] to develop specific curve after reaction ceases.

OPTION 1: Close valve to Vacuum to quench reaction if required.

OPTION 2: Repeat experiment if it is believed that catalyst pressure is inadequate or hydrogen atom generation is compromised

Control #2

Install New3 20 cm Platinum [Aldrich] filament [99.99% purity], 0.25mm diameter in Vessel Warm up oven Temperature 250°C.

Filament input wattage = 0

Vacuum down pressure in Reaction Vessel below 10 mtorr to remove moisture.

Stabilize Oven and Vessel Temperature to 250°C.

Close all valves and vacuum pump.

Inlet H2 gas to 650 torr pressure.

Vacuum down to 40-100 mtorr range.

Run Calibration #2 through full sequence to steady state at each power level shown below:

0 watts, 10 watts, 11 watts, 5 watts, 6 watts, 15 watts, 16 watts, 0 watts, 1 watt. [add any new points determined via Experiments 1-3 then repeat sequence above]

Develop 'AFTER' Calibration Curve.

Compare Calibration Curves 'Before' and 'After' Analyze and Report on Results Based upon above

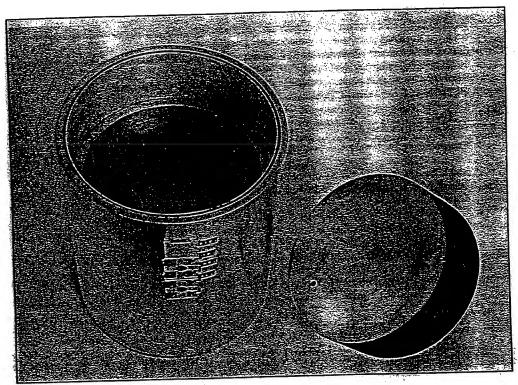
final revised 12 April 1997

developed by: William Good - BlackLight Power
Peter Jansson - Atlantic Energy





RADIGISOTOPE MICROCALORIMETERS



CR-100 7" Thermoelectric Enclosure

The series CR-100 Microcalorimeters provide an accurate measurement of radioisotope heat release rates.







PRINCIPLE

The thermal gradient calorimeter transfers all the heat developed in a reaction to its surrounding heat sink at a constant temperature. The calorimeter walls thermoelectrically transduce sample heat release into an electrical signal which is directly proportional to the energy release of the source. Transient as well as steady state energy releases may be measured.

FEATURES

- · Whole body heat release measurements
- · Microwatt to kilowatt sample output
- · High sensitivities and repeatability
- Linear output
- · Transient and steady state response
- Wide temperature range
- · Simple "In-situ" recalibration
- No excitation required

SPECIFICATIONS

Sample chamber solume range: 1in³ to 3000 in³

Secsitivities:

to 15 milliwatts per millivolt

Temperature range:

Cryogenic to 600°F

Besponse times:

10 sec. to 10 min.

. Vəranar

to 10° torr.

Sutput impedance range: 10Ω to 7500Ω

Accuracies

to 0.5%

Repeatability: 0.01%

Power supply:

not required

Materials:

Aluminum, stainless steels, copper, composites

CONSTRUCTION

The calorimeter walls are composed of a thin, high temperature thermopile structure containing thousands of junctions. One set of junctions is in

thermal contact with one wall surface, and the other set is in contact with the opposite surface. As heat flows through the walls, (Fig. 1) a temperature difference is established between both sets of thermopile junctions, thus generating a voltage which is directly proportional to the heat flow. The large number of thermopile in the set flow.

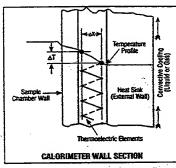


Figure 1

mopiles develop extreme sensitivity to minute heat flows. Calorimeters are constructed in a range of designs incorporating large sample chambers for high heat fluxes (cover) or small sample chambers capable of measuring low heat releases (Figure 2).

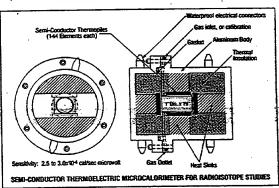


Figure 2

CALIBRATION

Each calorimeter is calibrated at a base temperature of 70° F by a known, electrical heat source in thermal equilibrium with the system.

The calibration constant is expressed in terms of wattage input versus millivolt output. A temperature correction curve is also supplied for use at elevated temperatures.





APPLICATIONS

The CR-100 Series calorimeters are designed to measure both microcaloric and macrocaloric heat release from pure or mixed radioisotopes. The magnitude of the generated signal is strictly proportional to the mean intensity of the sample.

Other applications include: physical, chemical and biological thermogenesis, specific heats, heats of fusion and reaction.

EXAMPLE OF OPERATION

Reactive materials are placed in a suitable container within the calorimeter sample chamber and permitted to reach equilibrium. To decrease the equilibrium time, it is desirable to heat sink the container to the sample chamber wall. The calorimeter should be situated in a constant temperature environment cooled either by gas or liquids. The time required for the calorimeter assembly to attain thermal equilibrium is a function of the conductivity and size of the sample, the thermal contact at the sample chamber wall, calorimeter wall characteristics, and the external cooling rate.

At thermal equilibrium, the output signal will reach a mean steady state value which is proportional to the total heat release from the sample. With the known calibration constant (milliwatts/millivolt), the total heat liberation rate is accurately determined. For radioisotopes with mean decay rates greater than calorimeter response time, the signal is proportional to radioisotope sample decay (Figure 3).

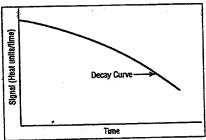


Figure 3

MICROWATT DETERMINATIONS

To measure microwatt heat flow accurately, it is necessary to provide a stable, cooling environment.

However, most constant temperature cooling teths exhibit small fluctuations which may generate signals the same order of magnitude as those produced by the sample. To avoid this large noise to signal ratio, a temperature compensated enclosure has been developed (Figure 4). This double

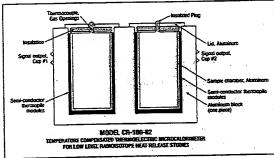


Figure 4

cup system contains both an active and passive chamber having matched sensitivities in opposition. Thus, spurious, external temperature fluctuations are compensated for, and only the heat release from the sample source is detected.

COMPENSATED MICROCALORIMETER SPECIFICATIONS

	raucher series: 5° Dia. x 1°-12° Depth
Sensitivit To 1	j. 5 milliwatis/millivoti.
Materials Alun	: ninum, composites, semi-conductor elements
Calibratio	
	hamber matching: hin 1/2%
	resistance: -7500Ω
Beadout Mail	required: ivalt patentiameter/Recorder
Engirons	nental requirements: bient temperature operation/Constant

temperature bath





STANDARD MODELS, SINGLE CHAMBER

Model	Internal Dimensions		External Dimensions		Accuracy	Sensitivity,		Temperature		
Number	Diameter, in.	Depth, in.	Diameters, in.	Length, In.	%	Milliwatts per Millivolt	Output Resistence	F° (Note 1)	Response Time, Min.	
CA-100-1	1	1	3	3	1%	15	4	250*	1	
CA-100-2	2	4	4	6	1%	15	10	250*	1	
CA-100-4	4	8	5	12	1%	250	2000	600	3	
CA-100-8	8	16, 32	9	21	1%	250	4000	600	3	
CA-100-C	Custom	Custom	Custom	Custom	1%	250	Varies	600	Varies	

^{*} Models CR-100-1 and CA-100-2 are also available for 600°F operating temperature at reduced sensitivities.

READOUT INSTRUMENTATION

Suitable readouts for all CR-100 models include: millivolt potentiometers/recorders, data loggers, or conventional D.C. millivolt meters.

ORDERING INFORMATION

Delivery :	6-8 weeks, ARO
	5 to 200 lbs
	net 30 days to established customers
ene .	Del Mar, California

OTHER ITI THERMAL

Thermal Conductivity Apparatus, Heat Flux Meters, HEAT-PROBE™ Accelerator target Calorimeters, Radiometers, Thermal Flux Standards.



INTERNATIONAL

THERMAL

INSTRUMENT

COMPANY



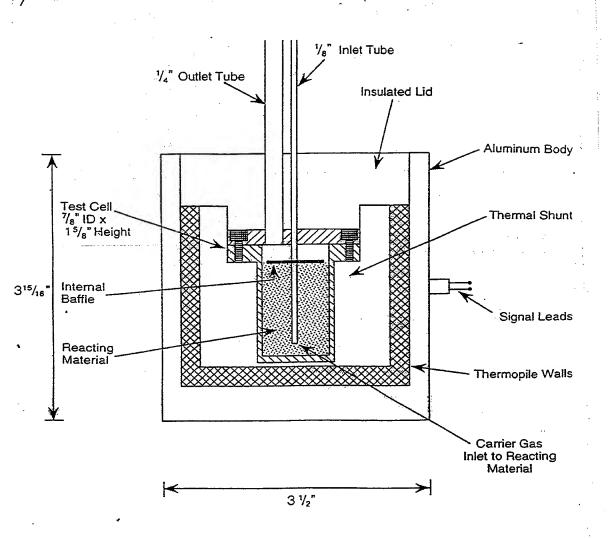
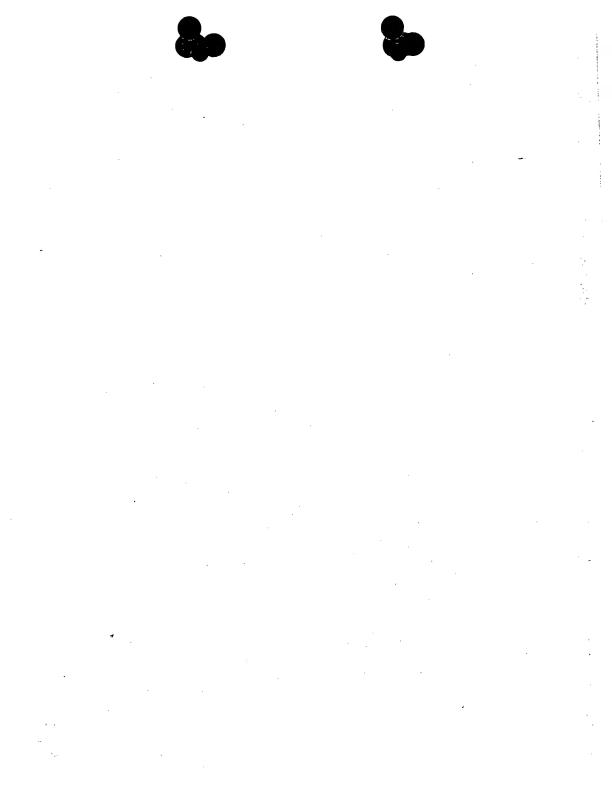


Figure 1. Scale Drawing of Calorimeter Assembly

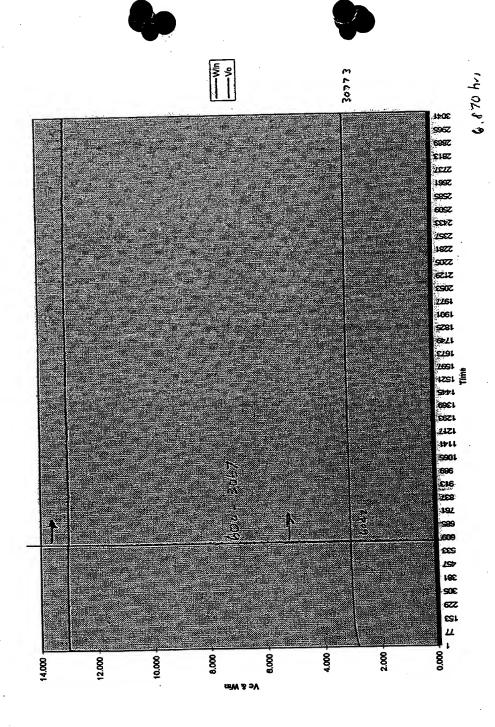






March 5 - March 10, 1997

 	m 12 - 27 - 24 - 24 2	-	 				
Win	Predicted 1	<u>/c</u>	1	0.070			
0	-0:0605		Given Vc=	3.076			
 1	0.1728		Estimated				
 2	0.4061		Watts Out		watts of pow		
 3			Actual =		watts of inpu		
 4	1			0.404	excess watts		1
 5	1		 				
 6			 		13.1		
			+			1.	
7			 				
8							-
 9	2.0392						┼──
 10	2.2725		1		L		
 11	2.5058						1
 12					L		<u> </u>
 13							
 14					1		<u> </u>
 15			1			·	
 16			1				
 10	3.0723		1				
 			1				
	<u> </u>						1
 1	l				 		+



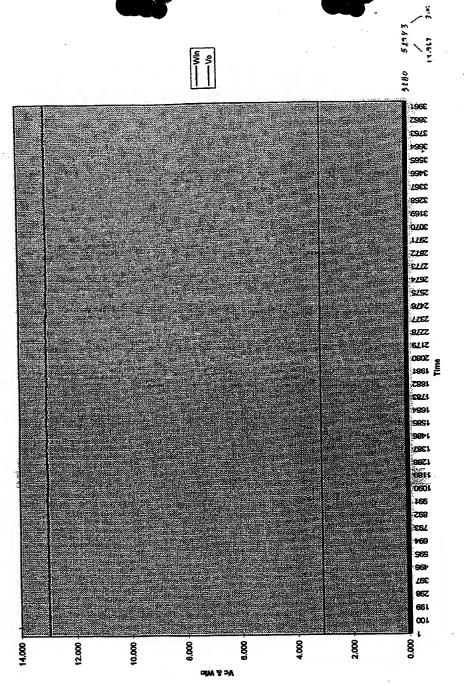


													-		_							
			0	3 1	/		_	-			_											4
		Max		1	13.077		_															
	hrs	Min	9 004	3,041	12.777																	
	280 [14.698	Day Day	9,44	0.018	0.034														,			
	3 083 Statistics from 2 to 5280 [14.698 hrs]	Assessed	PAGION	3,078	13.007 0.034 1.											-						
	Statistics		;	S	Win																	
200	1	1	3.063	3.083	3.083	3.083		3.083	3,084	3.084	۱	١	3.084	3.084		1		3,083	3.083	200	200,0	3,083
2	42.003	2007	12,996	12,996	12 99R	12 082	2	13,015	13.017	12 973		12.983	12.979	12 074		13,015	13.008	13.013	ľ	Ŧ	14.804	13.010
	0000	0.200	0.260	0.260	0 280	Dac o	0.400	0.280	0.280	0.050		0.260	0.260	0.260	0,400	0,260	0.280	0.280	0.360	0.400	0.260	0,260
Va.	J	-	0.617	0.817	7190	1,100	2.01.0	0.617	0.817	0.047	3	0.617	0.847	7.047	210.0	0.617	0.617	0.817	0 047	70.0	0.617	0.617
	400	3.063	3,083	2 083	2000	0000	3,053	3.083	2 0R4	700 0	0,004	3.084	2 084	1000	3.004	3,083	3.083	2 083	000	3.003	3,083	3.083
W Fand	IIIII IBBUI	32	42	63	70	70	7/	82	6	70	102	112	422	77.	400	143	163	183	3	1/3	183	183





	1				T
Win	Predicted \				+
	0 -0.0605		3.078		
	1 0.1728	Estimated		1	
	2 0.4061	Watts Out		watts of power	
	3 0:6394	Actual =		watts of input power	
	4 0.8727		0.446	excess watts	1
	5 1.106				
	6 1.3393				
	7 1.5726				
	8 1.8059				
	9 2.0392				4
	10 2.2725				
	11 2.5058				
	12 2.7391				-
	13 2.9724				
	14 3.2057				+-
	15 3.439			}	-
	16 3.6723				
				1	1



14.69.8 hr

Dana 1





		1					T		1											1			T		1
																					Ŧ				
		Wax	2.844	12.932					ğ		13.188				Max	3.075	13,087								
	2 hrs]	u <u>R</u>	2.792	12,601				98 hrs	틀		13,091			616 hrs]	Min	3.071	12.38		hrs]						
	3 400 [0.7 <i>6</i> ;	Std Dev	0.011	0.097				0 1120 [1.1	Std Dev		0.021			to 1735 [0.	Std Dev	0,001	0.052		1736 [4.838	Std Dev	0.109973	13,01482 0,115441			
	3.03 Statistics from 130 to 400 [0.752 hrs]	Average	2.802	12.779				3.029 Statistics from 690 to 1120 [1,198 hrs]	Average	3.1	13.151			3.03 Statistics from 1550 to 1735 [0.515 hrs]	Average	3.073	13.02		3,029 Statistics from 2 to 1735 [4.836 hrs]	Average Std Dev					
	Statistics		ş	WIN				Statistics		ş	NIX.			Statistics		No.	3.029 Win		Statistics	1	<u>۷</u>	3 Win	-	6	9
Λc	1	3.03	3.03 Vc	3 029 WIn					3.029	3,029 Vc	3.029 Win	3.029			3,029		L			3,029	3,028	3.028			3.028
WIN	12.851		L	ľ	1		13:008	12,992	12.99	12,983		١.	1	12:855	Γ	1				12,936		12.912			3 12,975
,	0.257	0.258	A 258	0.25R	007.0	0.28	0.26	0.28	0.28	0.28			0.258		L					0.259			_	0.26	0.28
1/5/	0.807	0.807	OACA	9000	0000	0,606	0.608	0.608	0.606	0.808	0.608	0.808	0.807	0.808	O ROR	١								0.608	1_
	202	303	200	000	3.028	3,029	3.029	3.029	3.029	3 029	3 020	3.029	3.03	20.8	3 030	0,020	2000	2020	3 029	2 020	2008	3.028	3.028	3.028	2 02R
Who food We	200 0111	47	12	200	/0	77	87	26	101	417	127	137	147	13	100	2 2	9	90	208	248	228	238	248	258	288





Win		Predicted Vc		- 046			
	0	-0.0605	Given Vc=	3.016			
	1	0.1728	Estimated		28.00	1	
	2	0.4061	Watts Out	13.187	watts of por	wei	
	3		Actual =	13.015	watts of inp	un power	
	4			0.172	excess wat	ES ·	
	5						
	6	1.3393			10.7		
+	7	1.5726					
	8	1.8059					
	9	2.0392					
	10	2.2725					
	11	2.5058			ļ		
	12	2.7391					
	13						
	14				 		
	15				 	 	
	16	3.6723			 		
-					 		
			1		ļ	 	





		Max	2 844	10.9	12.932				Max	3.113	13,188					Max	3,075	10 007	10,007		
	2 hrs]		200	7017	12.601			98 hrs]	Min	3.067	13.091				616 hrs]	Min	3.071		14.300		
	3 030 Statistics from 130 to 400 [0.752 hrs]	Str Dav	1	١	0.097			3,029 Statistics from 690 to 1120 [1.198 hrs]	Std Dev	0.012		1			3.030 Statistics from 1550 to 1735 [0.515 hrs]	Average Std Dev Min	2000		790'0		
	from 130 to	Althrono	PROTONU		12.779			from 690 to	Average	3.100					from 1550	Average		ľ	13.020		
	Statistics			٥ ۲	Win			Statistics		Λ	3				Statistics		7		Win	6	•
2				3.030	3.029	3,029							3.029								3,029
MIN	12.85	1		12,882	12.893			12.992		ŀ	-		12.928	12,880	12.855		1	12,953	12.972	12.884	12,92
×	0.257	1		0.258	l							ACZ'0	0.259	0,258	0.257			0.259	0.259	3 0,258	0.259
Ve.	2000		0.607	0.808								0.608	0,608	0.607				0.606	0.608	0.608	0.608
Ne.	000	3.030	3.030	3 030	2000	4 020			0.00			3.028	3.029					3.029	3.029		
me foor		3/	47	77	7.8	12	67	00	107	/0L	117	127	137	147	10.7	/61	168	178	188	198	208





1					
Win	Predicted V	C			
0		Given Vc=	2:802		
1	0.1728	Estimated	والمتحراء الأ		
- 1 2	0.4061	Watts Out	12.270	watts of power	
	0.6394	Actual =		watts of input power	-
4	0.8727		-0.509	excess watts	
	1.106				
	1.3393				
	1.5726				+
	1.8059				_
	2.0392			<u> </u>	
10					-
11	2.5058			 	
1:					
1:					
1-				 	-
1:				 	
10	8 3.6723			 	
	1			 	-





, probjekt	end by	100,000			1
	The Substantian .				
Win	Predicted Vo				
0	-0:0605	Given Vc=	3.1		
1	0.1728	Estimated			
2	0.4061	Watts Out	13.547	watts of power	
3	0.6394	Actual =	13.151	watts of input power	<u> </u>
4	0.8727		0.396	excess watts	
5	1.106				
6	1.3393				
7	1.5726				
8	1.8059				
9	2.0392				<u> </u>
10	2.2725				
11	2.5058				
12	2.7391				
13	2.9724				
14	3.2057				ļ
15	3.439				
16	3.6723				ļ
					<u> </u>
				<u> </u>	





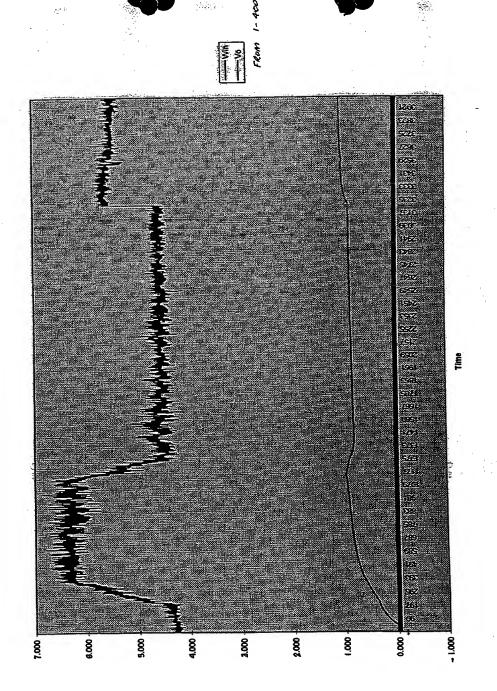
		Marie Same V.		De dia			A Section of Land	
		The second secon	. 1				24.6	
						<u> </u>		
	in	Predicted V	c	The Charles				
	0	4.0	: :	Given Vc=	3.073			
	1	0.1728		Estimated		2	V 200	
	2			Watts Out	13.432	watts of po	ower	
	3			Actual =	13:020	watts of in	put power	
	4				0.412	excess wa	nts	
	5						 	
	6	1.3393					1	
	7	1.5726				- 3	 	
	8	1.8059					 	
	9	2.0392					1	
	10			<u> </u>		<u> </u>	+	
	11			1		ļ		
	12	2.7391			<u> </u>			
	13				<u> </u>	 		
· ·	14				 	 	+	
	15							
	16	3.6723		<u> </u>	 	 	- 	
					 	 		+
				1				

Page 1

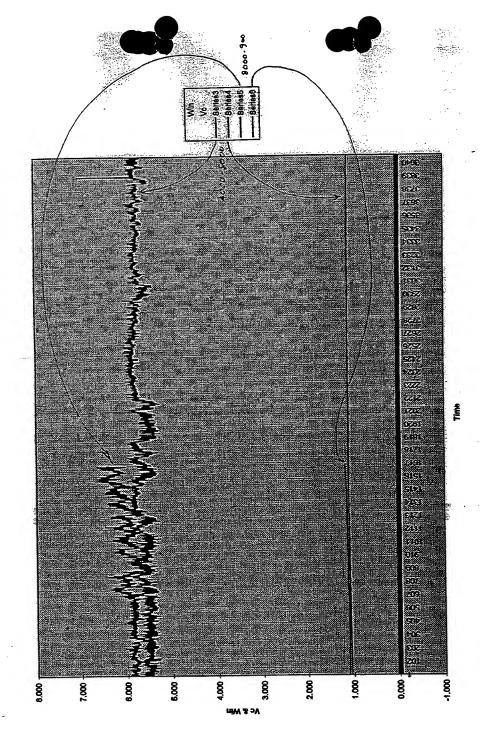


							3.52		·					نب	<u>.</u>
1								3						Serie Control	S. Carried S. Carried
	Max	1.121	7,004												
	S	1.089	1												
hrs	8td Dev	0.004	0.122												
3700 [7.616 hrs]	Average	1,102	in 5.791 0.122												
rom 6000±		ΛC	Win				,						-		
Statistics from 6000-870															
Ve	0,000	000'0	0,000	0,000	0.000	0.000	0.000	0.000	0.000	0.000	0.000	0.000	0.000	0.00	0,000
VIII)	2.923		1.180			4.278					7	,	4.325		4.290
	0.058	000	0.024	0.082	0.087	0.086	0.085	0.085	0.085	0.085	0.085	0.085	0.088	0.088	0.088
×	0000	0000	0.000	0.000	0000	0,000	0.00	0000	0.000	0.000	0.000	0000	0000	0.000	000
νς. Λς,	000	000	0.00	0,000	0000	0.00	0.000	0000	0000	0.00	0000	0.000	000'0	0.00	0.000
Fime [sec] Vc		70	88	66	110	120	130	140	150	160	170	180	180	200	210

No Hydraggan



⊅809 1



TP032697 Chart 1

في دوه دو





30 Centimeter Calibration Run

	. 246						
		호[And			-	
 GRAPHIN	G of 30 CM	Control E	xperimenta	l Points			
 Jan	1782	· · · · · · · · · · · · · · · · · · ·					
 	7.3						
 Vc	Win	Vc-SD	Win-SD			%-Win-SD	Hours
 3.951	14.943	0.004	0.013	29-Apr	0.10%	0.09%	2:539
 3.951			0.010			0.07%	
 4.221	16.123		0.008	30-Apr	0.02%	0.05%	0.590
 4.663		0.002				0.04%	0:808
 4.000	10.011			-			
 	 						
 	<u> </u>		 	-			
 			 	1	-	<u> </u>	
	ļ	ļ		1			
I .	ı	}	1	1	1	1	



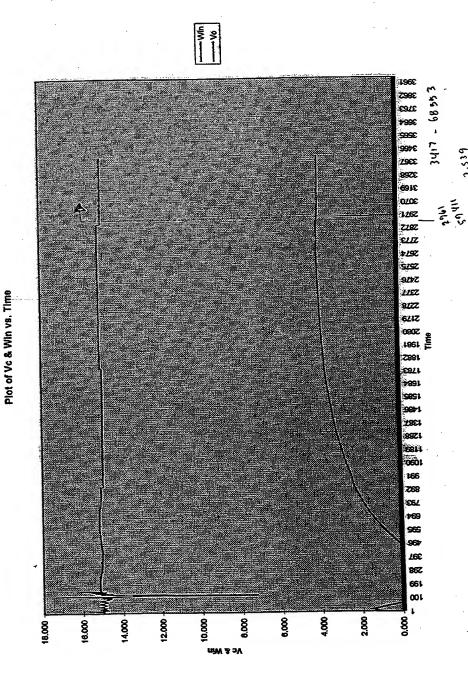


[2,639 hrs]	Std Dev	0,004	0,013												
Statistics for 2961 - 3417 [2,639 hrs	Average 8td	Vc 3.951	Win 14.943					1							_
	0.838	0,908	0.971 W	1.029	1.084	1.139	1.190	1.241	1.284	1.343	1.388	1.431	1.478	1.514	1 548
Win	15,044	14,983	14,999	15,019	15:003		14,977	14/997	14,971	141972		14,990	14,969		4K 005
	0.00	0.00	00.0	00.0	0.01	0.03	0.04	0.08	0.09	0.11	0.14	0.17	0.21		76.0
PILI	0.179		1.				0.164					0.188	0.164		744
DIE	0 549											L			
Г	3	: 5	श्र	18	8	2	1	6	1	2	1	18	8	8	1

TP042997

30 cm Carbo!

Ve = 3.951



TP043097

											7			- 11					
						-						Ì							
	Std Dev	200700	- 1	0.010438															
Statistics from Points	Average Std Dev	1	3.931	14,940															
Statistics f			ΛC	Win															
Ve	3.040		3.950	3.950	0200	OCA'S	3.951	3.951	3,951	3.951	7.00	3,801	3.951		3,951	3.951	3,951	1906	0.001
Vin	000 77	14,000	14,932	11 05A	2012	14,852	14,948	14,930	14.914	14 913		14.934	14.936	14.932	14,935	14,934	14.921	ľ	14.821
10/	0 0 0	2.000	2,352	0 280	2000	2,352	2,353	2.353	2.353	2 262	2000	2.352	2.353	2,353	2,353	2.353	2.353	4.00	2.353
V LIIG	_!*	0.131	0.158	677.5	, <u>.</u>	0,152	0.152	0,159	0.185	0 194		0.157	0.150		ľ	0.158	0.141		0.152
DIMI	4	0,5(0	0.375		01334	0,355	0.382	0.398	0.418	17.0	0 40	0.374	0.358	0.343	0.38	0 380	71217	2	0.388
di Alli		14,930	44 032	1	14.955	14,952	14.948	14 930	14 014	47.0	14,913	14.934	14 938	14 932	14 035	14 024	14.024	17014	14 927
401	- 1	0.780	0 700	1	0.790	0.790	0 700	0 790	0.700	0.700	0.780	082.0	0 790	0 700	700	200	00,700	0,180	U 704
		3.949	0 000	0.600	3,950	3.950	2 054	2 084	0.00	0.80	3,851	3 951	2 064	2 054	0.00	0.00	0,00	3,901	2 0.64
	18 SBC VC	00	6	8	9	120	1	707	3 5	2	<u>700</u>	220	070	200	200	200	36	320	116

30 cm control Vc = 3.951 Win = 14.940

Page 1

April 30, 1997 - 1.7 hours



Æ 20,000

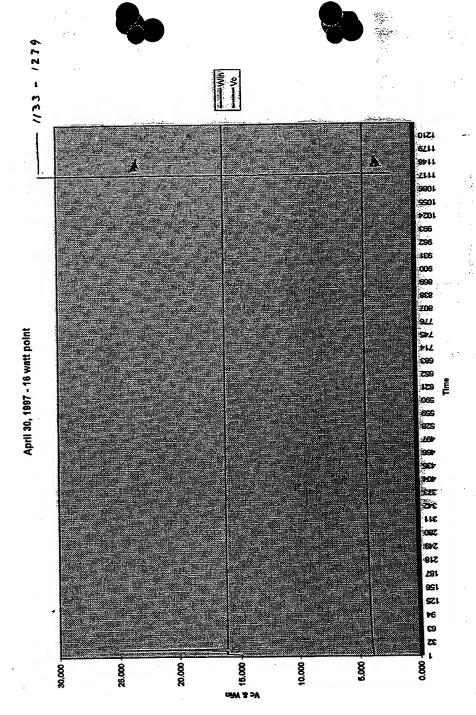
age 1

veja:		



			Ī	T	1	T			1	T						1	T		Ī			
80 hrs					1	1	1	1	1	1	-	-			-	1	1		1	-		
0 1239 (0.8	8td Dev	000	900	3																		
olnte 1133	Average	1-	1000	10,123																		
Statistics from Points 1133 to 1239 (0.690 hrs.)	Ā	3	2	E E			-	-	1						1	1						4
Staff	2 048	200	3,840	3.948	3.948	3.948	3,948	3.950	3,955	3,982	3,969	3,975	3.984	900	2,800	3,997	099.5	000	4.004	4,009	4.012	111212
Ş.															1					9.705	14 1-18	١
Win	20.77	14,004	14.931	14,949	14,952	14,942	15,487	16,131	18.147		16.170	16,163	18 115	1		1	-		25,080		1	١
	1000	7,301	2,350	2,350	2.350	2.350	2.350	2,351	2,355	2,362	2.367	2.373	9746	6,010	2.382	2,386	2,390	2,394	2,398	2.401	A 40E	41.70
N	1	0.134	0.157	0,158	0,149	0.153	0,153	0,152	0.154	0.158	0.152	0 154	307.0	2	0,153	0.152	0,152	0.155	0.152	0 482		0.102
L HOI	1	0.375	0,379	0.378	0:362	0.375	0,376	0,385	0.381	0,399	0.378	N.387	188	0,381	0,393	0,378	0.381	0,388	0.373	1440	1	0.378
11111	=										***		1					100			1	
	MIN.	14.934	14,931	14.949	14.952	14.942	15.487	18.13	18.147	16.159	18.170	10 102	21.	18.145	16,154	18,151	16,42	20,443	2R ORC	105.01		16,115
		0.790	0.790	0 790	0 790	0 790	0 790	0 700	791	0.793	D 794	0 70E	20.7	0.788	0.797	0.798	0.799	0 800	2 80		0.00	0.803
	Vc.	3.948	3 948	3 048	4 04B	2 048	2 048	2 050	206	2 0A2	2000	2500	0,8/0	3.981	3.986	3.991	3 998	4 000	2007	4.004	4.009	4.012
	- 1	123 3									l			343		L	L		.,,	444	484	484
	Ime [sec] Vc	12	۲	- =		- 6	10	4 6	۲۱۶	16	46	3		6	6	6				4	•	4

30 cm Control Vc = 4.221 Win - 16.123



age 1

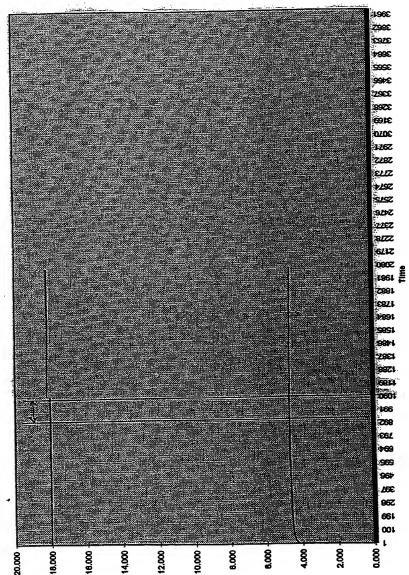


0.439 0.154 2.587 0.394 0.148 2.588 0.448 0.148 2.588 0.435 0.151 2.586 0.437 0.163 2.805 0.443 2.615 2.695 0.441 0.149 2.623 0.445 0.161 2.637 0.420 0.161 2.649 0.446 0.161 2.649 0.146 0.151 2.649 0.146 0.151 2.649 0.148 0.161 2.695 0.148 0.161 2.695 0.148 2.676 0.148 2.676 0.148 2.677 0.148 2.674 0.148 2.674 0.148 2.674		12	ľ	thing.	1 110	Vell	Win	Vc	Stallstics from	n Points 966	Statistics from Points 966 - 1100 [0.808 hrs]	
0.143 2.586 17.170 4.222 VC 4.663 0.148 2.586 17.170 4.224 WIn 18.041 0.151 2.586 18.035 4.224 WIn 18.041 0.153 2.605 18.035 4.245 0.149 2.623 18.035 4.256 0.149 2.637 18.032 4.274 0.149 2.637 18.036 4.286 0.149 2.637 18.036 4.296 0.151 2.654 18.036 4.296 0.151 2.654 18.036 4.316 0.152 2.654 18.033 4.319 0.162 2.654 18.033 4.316 0.163 2.654 18.033 4.336 0.163 2.654 18.033 4.336			1	רותו	1		40 100	L		Average	Std Dev	
0.143 2.566 17.170 4.222 Win 18.041 0.146 2.566 16.035 4.224 Win 18.041 0.151 2.566 16.035 4.233 0.143 2.615 16.036 4.265 0.149 2.633 18.031 4.265 0.149 2.637 18.022 4.274 0.149 2.637 18.038 4.281 0.149 2.637 18.038 4.286 0.149 2.637 18.038 4.308 0.151 2.659 18.023 4.319 0.160 2.656 18.023 4.319 0.162 2.656 18.025 4.314 0.148 2.679 18.039 4.325	0.845 16.129		23		0,134				7,0	1 000		
0.146 2.588 18.035 4.224 WIN 78.041 0.151 2.586 18.040 4.233 18.045 4.245 0.143 2.615 18.045 4.245 18.045 4.245 0.149 2.623 18.031 4.255 4.274 18.022 4.274 0.149 2.637 18.022 4.274 4.286 6.046 4.286 0.149 2.643 18.036 4.286 6.314 6.326 4.306 0.151 2.649 18.036 4.306 6.314 6.314 6.314 0.151 2.665 18.026 4.316 6.314 6.326 6.314 0.152 2.670 18.036 4.325 6.314 6.432 0.148 2.670 18.036 4.325 6.4314 6.432	0.845 17.170	17.1	2	0394	0.143		,	4.222		2003		
0.151 2.596 18.040 0.153 2.605 18.045 0.143 2.615 18.031 0.149 2.633 18.022 0.149 2.633 18.022 0.161 2.643 18.028 0.146 2.643 18.036 0.149 2.654 18.036 0.151 2.654 18.035 0.151 2.654 18.035 0.152 2.654 18.035 0.153 2.654 18.035 0.154 2.654 18.035 0.155 2.654 18.035 0.156 2.654 18.035 0.157 2.654 18.035	0.845 18.035	18.0	5		0.148		•	4.224		18,041	7000	
0.153 2.605 18.045 0.143 2.615 18.036 0.149 2.623 18.031 0.149 2.637 18.022 0.149 2.637 18.028 0.149 2.654 18.036 0.149 2.654 18.036 0.151 2.659 18.025 0.150 2.654 18.035 0.151 2.655 18.025 0.152 2.674 18.039 0.152 2.674 18.039	L	18.04	0		0.151	L		4.233				
0.145 2.615 18.038 0.146 2.623 18.031 0.149 2.637 18.022 0.149 2.637 18.036 0.146 2.654 18.036 0.146 2.654 18.036 0.150 2.654 18.036 0.150 2.654 18.038 0.150 2.654 18.038 0.162 2.670 18.039 0.162 2.670 18.039 0.148 2.670 18.039		18.04	180	1	0.152							
0.149 2.623 18.031 0.149 2.630 18.022 0.149 2.637 18.028 0.161 2.643 18.036 0.146 2.654 18.033 0.151 2.654 18.033 0.151 2.659 18.019 0.162 2.655 18.025 0.162 2.679 18.039 0.163 2.679 18.039		18.03	1	Ĺ			`					
0.149 2.630 18.022 0.149 2.637 18.028 0.161 2.643 18.036 0.146 2.654 18.036 0.151 2.654 18.033 0.150 2.655 18.023 0.148 2.670 18.033 0.162 2.674 18.039 0.148 2.679 18.039	L	18.031										
0.149 2.637 18.028 0.151 2.643 18.036 0.146 2.644 18.036 0.149 2.654 18.023 0.151 2.655 18.019 0.152 2.655 18.039 0.162 2.675 18.039 0.148 2.679 18.039	0.855 18,022	ľ		0,415								
0.161 2.643 18.036 0.146 2.849 18.036 0.149 2.854 18.023 0.151 2.859 18.019 0.150 2.855 18.025 0.148 2.879 18.039 0.148 2.879 18.039	0.858 18.028			0,420		·						
0.146 2.849 18.036 0.149 2.854 18.023 0.151 2.859 18.019 0.150 2.865 18.025 0.148 2.874 18.039 0.148 2.874 18.039 0.148 2.879 18.031	0.858 18.038	_		0,424	0.15		•					
0,149 2,654 18,023 0,151 2,859 18,019 0,150 2,665 18,025 0,148 2,670 18,039 0,162 2,674 18,039 0,148 2,679 18,041				0,409								
0,151 2,859 18,019 0,150 2,865 18,025 0,148 2,874 18,039 0,162 2,874 18,039 0,148 2,879 18,041												
0,160 2,665 18,025 0,148 2,670 18,033 0,162 2,674 18,039 0,148 2,679 18,041	Ĺ	Ĺ		0.416								
0.148 2.670 18,033 0,162 2.674 18,039 0.148 2.679 18.041	0.863 18.025	Ĺ	MO		-							
0,162 2,674 18,039 0,148 2,679 18,041	Ľ	ľ	100	1								
0.148 2.679 18.041	Ĺ	Ĺ	18	1								
	0.888 18.041	L	F	3		2						

TP043097

30 cm Control Ve = 4.663 Win = 18,041 April 30, 1997 18 watt point

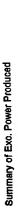




Ve & Wen

100





	Additional H22	No	Yes	Yés	Yes	Yes	S N	Š	S Z	S	Yes	Y68						
	Pressure	132.6-178.2T	0.38-549T	0.388-0.591T	0,385-0,883T	0.349-0.576T	0.425-0.582T	0.352-0.582T	<1.312T	0.335-0.443T	0.453-0.879T	0.447-0.598T	Average of Points	Minimum	Medmum	8td. Devlation	Std. Deviation %	
entel Results	Excess Power Iwatts1	1.181	1,459	1.689			1,954	2,092	2.087	1,284	1,135	1.079	1,445	0,635	2.092	0.481	31.91%	
em Experim	Hours [88]	5.632	15.160	12.080	21.273	6.918	11.572	23.461	13.507	6,237	11,355	4.77.7						
Summary of 30 cm Experimental Results	Date[s] of Run Hours Iss	14-Anr	15-Apr	18-Apr	17-Apr	18-Apr	23-Apr	24-Aor	25-Apr	3-Mav	4-Mav	6-Mav						





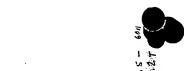
Statistics of 5011 - 5033(5)32-1115. Average. Std.Dev. Min Max Vc 4,288 0,015 4,240 Win 15,141 0,081 14,970 1
0,015
Average Std: Dev 4,268 0,0 15,141 0,0
Win
0000
0.674 2.634 0.150
0,000
0 0 0
1.007 0.997 1.035
0.150 0.150
0.000
0.000
100 100





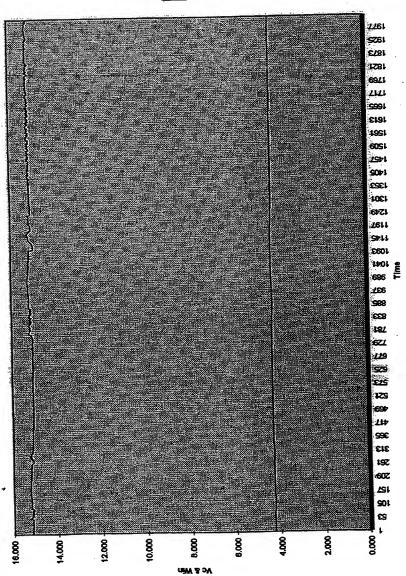
	eran taken			200	
					·
Win	Predicted Vc				
14.5		Given Vc=	4.268		
15.0	3.964	Estimated			
15:5		Watts Out	16.322	watts of power	
16:0		Actual =	15.141	watts of input power	
16.5			1.181	excess watts	
17.0					
17.5					
18.0					
18.5					
	1 1			1	<u> </u>

April 14, 1997 - 16 watt warmup









Page 1





								4.	330			_	·	_	_		رواند. د ادمور	<u></u>		el i	-3	
	Max	000	4.300	15,269		14.07.7	25.5													1	1	
	Min	200		14.954		1100	01,260															
Statistics for 2 - 5445 [15.160hrs]	At Dav		_	0.083																		
or 2 - 5445	Assessed Bath Day	Aveiago	4,331	15.137			2.42															
Statistics f			Š	MiN			P.															
\sqrt{\sq}\}}}}}}}} \end{\sqrt{\sq}}}}}}}}}}}} \end{\sqrt{\sqrt{\sqrt{\sqrt{\sqrt{\sqrt{\sqrt{\sq}}}}}}}}}} \end{\sqrt{\sqrt{\sqrt{\sqrt{\sqrt{\sqrt{\sqrt{\sqrt{\sqrt{\sqrt{\sqrt{\sqrt{\sqrt{\sqrt{\sq}}}}}}}}}} \end{\sqrt{\sq}}}}}}} \end{\sqrt{\sqrt{\sqrt{\sq}}}}}}}} \end{\sqrt{\sqrt{\sq}}}}}}} \end{\sqrt{\sqrt{\sqrt{\sq}}}}}}} \sqrt{\sqrt{\sqrt{\		4,282	4,292				4.291	4.291	4.290		4.290	4,290	7 200		4.290	4.280	4.290	A 200			4,290	
Min	Ç, Ç . ,	15,242	15.244	ľ	0,400	15,248	15.251	15,258			15.258	15.284			15.255	15,255	15.248	T		15.250	15.252	
×	:1	2.658	2.848	1		2.645	2.845	2.845			2.045	2,645	1	2.645	2,644	2.845				3 2,845	3 2.644	
I WILL	-	0 89.976	A 00 07		-	98.978	0 99.978	0 99 978	te	_1	0 99,978	45 984 944 NOT 99 978		0 99,976	96,976	0 99:976	le	d	5	70 99:976	01 99 976	
MILLI	FLUE	15.242 243.980	45 244 243 ORD	20 77 20	15,239 244,000	15.248 244.00	15 251 244.04	15 958 344 N3	20.64	15.248 244.040	16,258 244,070	AA DAA NO		15,257 244,110	16 255 244 130	15 255 244 17	4 5 AB 244 10	200	5,251 244,22	50 244.27	52 244 3	
Min		•	ľ						ľ		ľ	ľ		•	ľ	ľ		١		39 15,250	18.	121
19/4	2	0.859	1	1	2 0.859	1 0.859	L	L	┸	ACR'O IO	0.859	1	- 1	0 0.859	1	ı	1	- 1	0.859	0.859	O ARO	- 3
	C	292 P	7 202	4.40	4.282	4.291	100 F	200	4.20	4.290	A 200		4.480	4.290	A 200	000 V	4,46	1	4.280	4.290		•
100	Time [sec] VC	8	3	76	102	112	133	770	36	142	183	3 5	701	172	Car	100	700	707	212	223	000	1007





	- SWielland				2000
	38				
Win	Predicted Vc				4
14.5		Given Vc=	4.331		1
15.0		Estimated			
15.5		Watts Out	16:596	watts of power	
16:0		Actual =	15.137	watts of input power	
16.5	4.309		1.459	excess watts	
17.0	4.424	1			
17.5	4.539				
18.0	4.653				
18.5	4.768				
· ·					





						3						į.			, . ·					4		_
	Max	5.135	1000	18,203		0.591	C					No. of the last	200 m					•				والمستنسا
		6.040		18,058		0.386									alian salah	4						
40 [12:060	Std Day	0.007		0,039		0.029																
Statistics for 4192-8540 [12:060 hrs]	Average	A STORE		18.146		0.486																
Statistics			2	Win		IHJa																1
Ş	1.000	4,000	4:338	4,339	4.339	0 K F	1	4,338		4,338	4,338	1 220			4.338	4,339	4.340			4.30		4.368
Min	047 2	10.1/0	15.179	15,184	15.178	ľ				15.199	15,198	46 406	۱	•	16.540	17.450	18.087	1				18,093
	7000		2.680	2.879	2 879	1			2.679	2.679	2.678			2.679	2.679	2.879	2 880		١			3 2,704
1 1 1	HA	0.154	0.154	1_	L		1		0.158	3 0.163	0 150	1	1	5 0.133	5 0.133	Γ				- 1	7 0.130	2 0.133
100	PLO	8 0.446	0.445	L	1_	1	1	0 0.452	6 0,434	9 0.448	0.450	1		0.495	0.508	L	L	1		se 0.608	990 06	19 0.61
2000	3	15.178	15 179	ľ				15,180	15.178	_	ľ	1	16.195	15.200	1	ľ				18,138	18.1	18,093
1	.o	9989	O AAA	1	_	-1	5 0.868	\$ 0.868	4 0.868	1	1	1	4 0.868	4 0.868	1	1	I	1	0 0.869	7 0.870	5 0.872	4 0.874
	Š	4.335	1 225	4.000	1.00	4.335	4,335	4,334	788 P	A 23.4			4.334	4.334						4.347		
	me [8ec] Vc	125	100	000	143	155	165	175	185	104	200	202	215	225	2000	200	647	255	265	275	286	205





48.00	Acres 6	- 17664 have 2			, dia	2 - a m	diam'r de
1999						-3	ic.
Win	Predicted	Vc	444			- 955 	
14.5	3:849		Given Vc=	5.075			
15.0			Estimated				
15.5			Watts Out	19.835	watts of power		*
16.0			Actual =	18.146	watts of input	рожег	
16.5				1.689	excess watts		
17:0	4.424						
17.5							
18.0	4:653						
18.5	4.768						
			1				
			1				
				<u> </u>			<u> </u>





	Max	5.051	48 22R	2012		0,603										1	35.5					
$\overline{}$	MIN	4.864	17.766	2011		0.385		1					***************************************		-		A Control of the Cont			-		
21.2		0.058	7900	100in		0.035																
Statistics for 2 - 7640	Average, 8td Dev	1 001	1	18.135		0.492		***************************************														
Statistics		5		Win		HJa							_			_			_		0	00
Ve	5.050	0,00		5,050	5,049	E 040			5,049	5.049			5.050	A DED		5.050	6.050				6,050	
MIN	18 141	100	18,139	18,143	18.139	10.447		18,151	18.149	18.153		10,130	18,150			18,153	18 149		18.148		18,142	
IM	2000	1	3.285	3,294	3.294	1		3,294	3,294	4 204	1	3,284	3,294		3.285	3.295	2 20K	1	5 3,295			8 3,295 A 3,295
S OF LI		1	7 0,155	7 0,160	0 152	1		0.158	13 0.146	Γ	T	[8] 0,150	0 158	ľ	32 0.149	10 0.152			81 0,155		Ī	0.543 0.146
HIM	-	1	19 0.517	13 0.487		1		51 0.48	49 0 643	L	1	50 0.518	EA 0.407		53 0,532	R2 0:810	1		48 0148		L	
Win			18.139	Ľ				18,151	18 149	1		18.150	10 150		18.153	18 183		10.149	18,148		_	18,142
1/0,	51	1.010	1.010	ľ	ľ		1.09	1.010	ľ	ľ	טוט.ר	1.010	4 040	-	1.010		-1	1.010	1010		ľ	1.010
	- 1	4.999	4 999	000	1,000	4.99	4.999	4 999	4 000	4.000	4.989	4.999	1	4.999	4 999	1	4.888	4.888	4 000	,	1	4.999
Victory IV	me 1890, VC	92	BB	3	OB.	108	118	128	2007	2	148	158	100	00	178	200	001	188	anc.		200	216

ige 1





		ANTES COL			Library Sugar
X				1	
Win	Predicted Vc		7 1		
1	4.5 3.849	Given Vc=	4.991		1.0
	5.0 3.964	Estimated			
1	5.5 4.079	Watts Out	19.470	watts of power	x]
1	6.0 4.194	Actual =		watts of input	
1	6.5 4.309	1	1.335	excess watt	5
1	7.0 4.424				
1	7.5 4:539				
1	8.0 4.653		,		
1	8.5 4.768				
		1			
	1.	1 1			17

•	
\$	

			<u>`</u> '					200						. ,			
	Max	4.816	18,105	0.578		•	ľ			Transaction of the last				Section 4	***************************************		
	3		17.888	0.349			·		1								
Statistics for 2-2485 (6.9/640)	Std Dev	0.009	0,048	0:030													
for 2-24	Average	4.791	17.984														
Statistics		2				5	0.7	2	2			0	0	0	0	8	8
No.	4.801		ŀ			4.802	,	,		0 4.801				4			1 4.798
WIR	17.938	ľ			1			,		17,900	17,908	4 17.899	17.910	17.907	4 17,910	3 17.921	2 17.931
<u>*</u>	3.093	3.088	L	ļ	1_	1_	3,088		3,086	L	30 3.085		29 3.084		30 3,084	32 3.083	30 3,082
L IV	10 13	0	0 122					0.128	99 0.132	0.130	08 0.130	92 0.13	10 0.129	91 0.132	0,508 0,130	00 0.1	0,502 0,130
MIM	A 0 504	1	1	1		L	L	6 0.505	5 0.489	0.508	99 0.508	99 0.492	0.5	37 0.491		21 0,500	
Milin				1			Ĺ	Ĺ	Ĺ	L	L	Ĺ		Ĺ	Ĺ	17.921	ľ_
177	0 084	1		. 1	0.981	2 0.981		ı	0.981	1	1	1	1	1	1	1	0.980
	1 804	١		4.601		1	4.802				1						
First Page 1	A CAR AULI	20	2	0	8 8	105	115	125	135	145	185	185	175	188	195	205	215





	. AMA	The second second			
Win	Predicted Vc			4	<u> </u>
14.5		Given Vc=	4.791		1
15.0		Estimated			1
15.5		Watts Out	18.599	watts of power	
16:0		Actual =	17:964	watts of input power	1
16.5			0.635	excess watts	
17.0					1
17.5					1
18.0	4.653				1
18.5	4.768				<u> </u>
				<u> </u>	
					1
					
					-
				l	





0.005 0.064 0.000 Average 8td Dev Min 0.000 0.063 0.000 Vc 4.431 0.040 4.318 0.000 0.070 0.000 Win 15.078 0.015 15.018 0.000 0.070 0.000 PHI 0.508 0.021 0.425 0.000 0.089 0.000 PHI 0.508 0.021 0.425 0.000 0.070 0.000 0.000 0.000 0.000 0.000 0.000 14.910 0.096 0.0177 0.000 0.000 0.498 0.000 14.982 0.317 0.000 0.498 0.317 0.000 0.000 14.992 0.317	W. Win	Wiln	Γ	۲	17	3	1110	*	Win	2	Statistics	Statistics for 2437 - 4515 [11.572 hrs]	615 [11.67	2 hrs]	
0.000 0.063 0.000 Vc 4.31 0.040 4.318 0.000 0.070 0.000 Win 15.078 0.015 15.018 1 0.000 0.070 0.000 PIH 0.506 0.021 0.425 0.000 0.082 0.000 PIH 0.506 0.021 0.425 0.000 0.081 0.000 0.000 0.000 0.000 0.000 0.000 0.000 0.000 0.000 0.000 0.000 0.000 0.000 14.940 0.177 0.000 0.000 0.361 0.000 0.000 14.982 0.317 0.000 0.000 14.982 0.317 0.000 15.026 0.317 0.000 0.000 14.982 0.317	0 000 0 000 0 507	0 000 0 000 0 507	0 00 0 CO7	0 507	70.	je	0 138	0 005	0.084	0.00	_			Min	ğ
0.000 0.070 0.000 Win 15.078 0.015 15.018 1 0.000 0.062 0.000 plrjj 0.506 0.021 0.425 0.000 0.089 0.000 0.000 0.000 0.000 0.000 0.001 0.000 0.000 0.000 0.000 15.024 0.000 0.015 0.000 0.000 14.910 0.017 0.000 0.000 0.000 14.980 0.250 0.317 0.000 0.000 14.992 0.317 0.000 14.992 0.000 15.029 0.361 0.000 0.000 14.992	0.00	0.00	0.004	803.0	1	13	, _	000	0 083				0.040		
0.000 0.082 0.000 p[H] 0.506 0.021 0.425 0.000 0.089 0.000 0.000 0.000 0.000 0.000 0.001 0.000 0.000 0.000 0.000 0.083 0.000 0.000 0.000 15.024 0.000 0.015 0.000 14.940 0.177 0.000 0.000 14.940 0.250 0.317 0.000 14.982 0.317 0.000 0.000 14.982 0.317 0.000 0.000 14.982 0.317 0.000 0.000 14.982 0.317 0.000	0.000	0.000	0.000	0.500		14	10	0000	0.070					•	
0.000 0.089 0.000	0.000 0.000	0.000 0.000	0.0.0	200			o la	200	OND						İ
0.000 0.	0.000 0.062 0.530	0.000 0.062 0.530	0.062 0.530	0.530	1	2 5	D 0	000	0.02						
0.000 0.001 0.001 0.000	0.069 0.531	0.000 0.089 0.531	0.069 0.531	1.531	_	2	٥to	١							
0.000 0.070 0.008 0.000 0.000 0.008 0.000	0.000 0.000 0.061 0.531 0.148	0.000 0.081 0.531	0.061 0.531	0.531		0.1	<u>ত্</u>	١							
0.000 0.068 0.000 0.000 8.831 0.000 15.024 0.000 14.926 0.000 14.940 0.000 14.980 0.000 14.980 0.000 14.980 0.000 14.980 0.000 15.028	0,000 0,000 0.070 0.522 0.278	0.000 0.070 0.522	0.070 0.522	0.522		0.27	9	1							
0.000 8.831 0.000 15.024 0.000 14.926 0.000 14.940 0.000 14.969 0.000 14.969 0.000 14.969	1	0.000 0.068 0.534	0.068 0.534	0.534		0.28	1	0.00							
0.000 15.024 0.000 15.086 0.000 14.926 0.000 14.940 0.000 14.989 0.000 14.989	0.00	0.000 8.831 0.523	8.831 0.523	0.523	1	1	2	İ		0.00					
0.000 15.086 0.000 14.926 0.000 14.910 0.000 14.940 0.000 14.989 0.000 15.028	0.000	0.000 15.024 0.577	15.024 0.577	0.577	L	0.35	Ξ	0.000							
0.000 14.926 0.000 14.910 0.000 14.940 0.000 14.989 0.000 15.028	0.000	0.000 15.086 0.653	15.086 0.653	0.653			2								
0.000 14.910 0.000 14.940 0.000 14.969 0.000 14.992	1	0.003 14.928 0.708	14,928 0.708	0.708	1	1	3				2				
0.000 14.940 0.000 14.999 0.000 14.992 0.000 15.029	0.098 0.019 14.910 0.741 0.595	0.019 14.910 0.741	14.910 0.741	0.741		0.59	2								
0,000 14,992 0,000 15,029	1	0.035 14,940 0.750	14,940 0.750	0.750	١	١	$\overline{}$				_				
0.000 14.992 0.000 15.029	0.050	0.050 14.969 0.755	14.989 0.755	0.755	l	l									
0.000 15.029	1_	0.083 14.992 0.842	14,992 0.842	0.842	1	1	-	0.000			_				
	\mathbf{I}_{-}	0.076 15.029 0.767	15,029 0,787	0.787	l	l	-		`						

TP042397

Page 1





Win	Predicted	Vc	+				
14.5			Given Vc=	4.431			
15.0			Estimated			ــــــــــــــــــــــــــــــــــــــ	
15.5			Watts Out		watts of p		
16.0	4.194		Actual =			put power	
16.5	4.309			1.954	excess w	atts	↓
17.0							
17.5							
18.0					<u> </u>		
18.5	4.768						+
		<u> </u>					╂
			- 				+
		 	 			+	+
		ļ	 		 		+
	L	↓				+	+-







	X	AARA		15.114	0.582														
	Min	0777	2	14.937	0.352		-		+			+							
Statistics for 2 -4215 (23.441 hvs	Std Dev	242	0.012	0.035	0.038														
for 2 -421	Average	-		15.053	0.459	5													
Statistics 1			ΛC	Win	P.L.	7.14		٠											
Vc	A 470	21.1	4.470	4.470	A A74	1	4.4/1	4.471	4.471	4.471	4,471	4.471	4.471	4.471	4.471	4.471	4.471	4.472	4.472
Win	46.004	13,031	15.094	15.083	45.084	100.01	15.077	15.082	15.075	15.078	15.073	15.077	15.071	15.080			15.078	15.079	15.086
Λί	200	1	2.801	2.801	1		2.801	2.801	2.801	2.801	2.801	2.801	2.801	1	ì				2 802
L IJu	1	0.134	0.132	١.	1	_	0.137	0.138	0.134	0.137	0.130	0.138	L	L	!			<u> </u>	134
DEP.		0.500	0.508	L	1	4	0.552	0.528	0.513	0.539	0.503	0.528	L	1	1	1		1_	\mathbf{L}
Miles	1110	15.091	15.094		1	15.081	15.077	15.082	ľ	ľ	ľ	ľ	Ĺ				Ţ		
11/0.	اد	0.894	7 89 T	1	4	0.894	0.894	0.894	ļ.,	丄	┸	Ļ	1	4		1	┸	丄	1
		4.470	A 470	27.7	4.4/0	4.471	4.471	4 471	4 471	A 473	A 471	1474	17.		4.471	4.471	4.47	4.472	100
1000	me [sec] vc	58	ar ar	2 8	8	118	138	158	178	90	248	2000	300	62	8/2	240	200	350	3 8





 Win	Predicted	Vc				
 14.5			Given Vc=	4.457		
 15.0			Estimated			
 15.5			Watts Out	17.145	watts of power	
 16.0	4.194		Actual =		watts of input power	
 16.5	4.309			2.092	excess watts	
 17.0	4.424					
 17.5						
18.0						
18.5	4.768					+
	Ĺ					
		<u> </u>				
					ļ	
		<u> </u>			 	+-
	i	<u> </u>			ļ	



	Ĵ







- 	Predicted Vo	:			
		- 100 - Mar	4,442		1
14.5		Given Vc=	4.442		+
15.0	3.964	Estimated			
15.5	4.079	Watts Out	17.080	watts of power	
16.0	4.194	Actual =		watts of input power	<u> </u>
16.5	4.309		2.067	excess watts	
17.0	4.424				
17.5	4.539				┵
18.0	4.653				4_
18.5	4.768				4
					-
_					
					1
					







2.491 0.488 15.08 0.448 0.152 3.620 15.086 2.491 Average Std Door Min 2.504 0.502 15.089 0.448 0.160 3.621 15.089 2.508 Vc 4.262 0.006 1 2.524 0.505 15.084 0.392 0.148 3.619 15.084 2.524 Win 15.032 0.006 1 2.524 0.505 15.084 0.392 0.148 3.619 15.084 2.524 Win 15.032 0.006 1 2.544 0.508 15.087 0.148 3.620 15.077 2.524 Win 15.032 0.005 2.557 0.512 16.077 0.348 0.145 3.618 15.067 2.574 Win 15.032 0.015 2.557 0.518 1.5065 0.389 0.147 3.618 15.065 2.891 0.015 15.081 2.622 0.891 0.015 0.005 0.381 0.				Win	17.0	L III	V#12	Win	٥	Statistics	for 3085 - 4	Statistics for 3085 - 4205 [6.237 hrs]	hrs]	
2.591 0.502 15.084 0.160 3.621 15.089 2.508 Vc 4.282 0.006 1 2.524 0.505 15.084 0.392 0.148 3.620 15.084 2.524 Win 15.032 0.009 1 2.524 0.505 15.084 0.392 0.148 3.619 15.084 2.524 Win 15.032 0.009 1 2.557 0.512 15.077 0.397 0.148 3.619 15.077 2.557 PPH 0.038 0.015 2.557 0.515 15.072 0.379 0.146 3.618 15.072 2.574 PPH 0.383 0.015 2.591 0.518 15.087 0.146 3.618 15.085 2.591 0.015 0.015 2.607 0.521 15.085 0.381 0.145 3.621 15.085 2.622 0.521 0.015 2.622 0.521 15.084 0.48 0.145 3.621 15.083	2002	2 404	7000	15 ABB	0.408	0 152	3.620	15.086			ł		Min	Max
2.524, 0.505 15.032 0.1405 15.032 0.100 1 2.524, 0.505 15.004 0.392 0.146 3.670 15.084 2.524 Win 15.032 0.009 1 2.547 0.506 15.004 0.392 0.146 3.619 15.087 2.557 PlHJ 0.303 0.015 2.557 0.512 15.072 0.379 0.146 3.618 15.072 2.574 PlHJ 0.393 0.016 2.574 0.516 15.072 0.379 0.146 3.618 15.062 2.574 PlHJ 0.393 0.016 2.574 0.516 15.065 0.389 0.146 3.618 15.065 2.574 PlHJ 0.393 0.016 2.574 0.516 15.065 0.389 0.146 3.619 15.065 2.574 PlHJ 0.393 0.015 2.622 0.521 15.065 0.381 0.146 3.621 15.065 2.687 PlHJ 0.393	5 6		1		L		ļ		2.508				4.250	4.273
2.524, 0.30 15.08 15.08 0.146 3.619 15.083 2.541 VVI2 3.624 0.003 2.544 0.518 15.083 0.410 0.148 3.620 15.077 2.557 plhj 0.393 0.016 2.557 0.515 15.072 0.379 0.146 3.618 15.072 2.574 plhj 0.393 0.016 2.591 0.518 15.072 0.374 0.518 0.146 3.618 15.065 2.591 0.016 2.591 0.518 15.064 0.386 0.147 3.618 15.065 2.591 0.016 2.697 0.521 15.064 0.386 0.147 3.619 15.065 2.627 0.016 2.697 0.528 15.065 0.381 0.145 3.621 15.067 2.657 0.016 2.627 0.528 15.065 0.381 0.150 3.621 15.067 2.657 0.016 2.627 0.528 15.063	5				0.302	1	1		2.524			_	15.011	15.057
2.557 0.512 15.072 0.557 p[H] 0.393 0.016 2.557 0.512 15.072 0.379 0.145 3.610 15.072 2.574 p[H] 0.393 0.016 2.591 0.516 15.072 0.379 0.146 3.618 15.065 2.591 0.016 2.591 0.518 15.065 0.383 0.146 3.618 15.065 2.591 0.016 2.607 0.521 15.065 0.381 0.145 3.620 15.065 2.637 0.522 2.622 0.525 15.065 0.381 0.145 3.621 15.065 2.637 0.622 2.637 0.528 15.065 0.414 0.150 3.621 15.067 2.687 0.672 2.687 0.534 15.061 0.414 0.150 3.621 15.067 2.687 0.672 2.712 0.534 15.060 0.386 0.146 3.621 15.060 2.687 0.672	2 5		4		0.410		1	Ľ	2.541		_		3.619	
2.574 0.515 15.072 0.379 0.145 3.618 15.072 2.591 0.518 15.065 0.393 0.146 3.618 15.065 2.607 0.521 15.064 0.386 0.147 3.619 15.064 2.622 0.525 15.065 0.381 0.145 3.620 15.065 2.637 0.528 15.065 0.381 0.145 3.621 15.063 2.657 0.531 15.061 0.421 0.153 3.621 15.061 2.687 0.534 15.063 0.420 0.150 3.621 15.063 2.687 0.540 15.063 0.420 0.150 3.621 15.063 2.726 0.537 15.063 0.386 0.146 3.619 15.059 2.726 0.545 15.069 0.418 0.153 3.621 15.059 2.738 0.548 15.060 0.396 0.146 3.619 15.060	144		┸		0.397		1	1	2.557				0.335	0.443
2.591 0.518 15.085 0.383 0.146 3.818 15.085 2.607 0.521 15.084 0.386 0.147 3.619 15.084 2.622 0.525 15.085 0.381 0.145 3.620 15.085 2.637 0.528 15.085 0.381 0.151 3.621 15.083 2.652 0.531 15.083 0.420 0.151 3.621 15.083 2.657 0.534 15.087 0.444 0.150 3.621 15.061 2.687 0.540 15.083 0.420 0.150 3.821 15.057 2.787 0.540 15.083 0.440 0.165 3.621 15.060 2.776 0.545 15.059 0.348 0.146 3.619 15.059 2.738 0.548 15.060 0.396 0.146 3.619 15.060	184				上	l	<u> </u>							
2.607 0.521 15.084 0.386 0.147 3.619 15.084 2.622 0.525 15.065 0.381 0.145 3.620 15.065 2.637 0.528 15.063 0.420 0.151 3.621 15.063 2.652 0.531 15.061 0.421 0.153 3.621 15.063 2.667 0.534 15.067 0.444 0.150 3.621 15.063 2.687 0.537 15.063 0.420 0.150 3.621 15.063 2.7897 0.540 15.063 0.386 0.146 3.623 15.059 2.778 0.545 15.059 0.386 0.146 3.613 15.059 2.738 0.548 15.060 0.396 0.146 3.619 15.060	185		1_		L	_		1						
2.622 0.525 15.065 0.381 0.145 3.620 15.065 2.637 0.528 15.063 0.420 0.151 3.621 15.063 2.652 0.531 15.061 0.421 0.153 3.621 15.061 2.667 0.534 15.067 0.444 0.150 3.621 15.061 2.687 0.537 15.063 0.420 0.150 3.621 15.063 2.697 0.540 15.063 0.386 0.146 3.620 15.060 2.776 0.545 15.059 0.418 0.148 3.619 15.059 2.738 0.548 15.060 0.396 0.146 3.619 15.060	204				L.	l			2.607					
2.637 0.526 15.063 0.420 0.151 3.621 15.063 2.652 0.531 15.061 0.421 0.153 3.621 15.061 2.667 0.534 15.067 0.414 0.150 3.621 15.067 2.682 0.537 15.063 0.420 0.150 3.621 15.063 2.697 0.540 15.060 0.385 0.146 3.621 15.060 2.712 0.543 15.059 0.386 0.146 3.621 15.059 2.726 0.545 15.059 0.418 0.145 3.619 15.059 2.738 0.548 15.060 0.396 0.146 3.619 15.060	224	L			1	0.145								
2.652 0.531 15.061 0.421 0.153 3.621 15.081 2.667 0.534 15.057 0.414 0.150 3.621 15.057 2.682 0.537 15.063 0.420 0.150 3.621 15.063 2.697 0.540 15.080 0.385 0.146 3.620 15.080 2.712 0.543 15.059 0.386 0.145 3.619 15.059 2.728 0.545 15.059 0.418 0.153 3.621 15.059 2.738 0.548 15.080 0.396 0.146 3.619 15.060	244		1	L	١	L	3.621	_						
2.667 0.534 15.057 0.414 0.150 3.621 15.057 2.682 0.537 15.083 0.420 0.150 3.621 15.063 2.697 0.540 15.080 0.385 0.146 3.620 15.080 2.712 0.543 15.059 0.386 0.145 3.619 15.059 2.728 0.545 15.059 0.418 0.153 3.621 15.059 2.738 0.548 15.080 0.396 0.146 3.619 15.060	284		L		١.	0.153	l		2.85%	6:				
2.682 0.537 15.083 0.420 0.150 3.621 15.083 2.697 0.540 15.080 0.385 0.146 3.620 15.080 2.712 0.543 15.059 0.386 0.145 3.819 15.059 2.726 0.545 15.059 0.418 0.153 3.621 15.059 2.738 0.548 15.080 0.396 0.146 3.619 15.080	284		١.		_	_		15.057	2.667					
2.697 0.540 15.080 0.385 0.146 3.620 15.080 2.712 0.543 15.059 0.386 0.145 3.619 15.059 2.726 0.545 15.059 0.418 0.153 3.621 15.059 2.738 0.548 15.080 0.396 0.146 3.619 15.080	304		<u>l_</u>		1				2.687					
2.712 0.543 15.059 0.386 0.145 3.619 15.059 2.726 0.545 15.059 0.418 0.153 3.621 15.059 2.738 0.548 15.080 0.396 0.146 3.619 15.060	324		1		1	1	l		2.69					
2.728 0.545 15.059 0.418 0.153 3.621 15.059 2.738 0.548 15.080 0.398 0.148 3.619 15.080	344		1		1					2				
2 738 0 548 15,060 0,396 0,148 3,619 15,060	364		1		l					9				
	384		1	ľ	1					31				





				+				i
	Win	Predicted	Vc					
	14.5	3.849		Given Vc≃	4.262			↓
	15.0			Estimated				
	15.5			Watts Out	16.296	watts of por	wer	↓
	16.0			Actual =		watts of inp		<u> </u>
	16.5				1.264	excess wa	tts	ļ
	17.0							↓ —
	17.5							┼
	18.0	4.653						┼
	18.5	4.768						┼
-						<u> </u>		+
						<u></u>		+
								┼
							ļ	
	T		L				 	+-
			l					+
						ļ		 -
								_





	3.620 15 3.620 15 3.618 15	0.370 0.253	
15.090 4.310		1	253
15.096 4.312 Vc		3.620	0.256 3.620
15.089 4.313 Win		3.618	0.259 3.618
15.090 4.314 p[H]	Ŀ	3.619	
15.094 4.315 Vf/2	۲	3.619	
15.089 4.315	Ŧ	3.619	0.258 3.619
15.094 4.315	+	3.619	0.267 3.619
	=	3.619	0.255 3.619
15.095 4.314	ť	3.618	0.256 3.618
15.113 4.314	Ŧ	3.619	0.269 3.619
15.109 4.315	F	3.619	0.267 3.619
15.113 4.315	٦	3.619	0.268 3.619
15.112 4.315	÷	3.619	0.270 3.619
15.108 4.315	Ť	3.619	0.270 3.619
15.111 4.315	٦	3.620	0.273 3.620
15,118 4.314		3.619	0.272 3.619
15.114 4.314		3.619	0.273 3.619

.

Page 1





					+
Win	Predicted Vo				—
14.5	3.849	Given Vc=	4.200		4
15.0	3.964	Estimated			 _
15.5	4.079	Watts Out		watts of power	
16.0	4.194	Actual =		watts of input power	
16.5	4.309		1.135	excess watts	
17.0					
17.5	4.539				
18.0	4.653				丄
18.5					
	 				
	 				
	 				
					\neg





l	Г	Vc.	Win	HJa	off.1	Vf/2	Win	Vc	Statistics for	or 2-8\$7	1	(4.737 hvs)	
4 190		838	14.879	35	0.136	3.528	14.879	4.190		Average	Std Dev	Min	Max
180	10	0.838		0.574	1	3.528	14.878	4.189	S V	4.187	0.005	4.175	4.199
4 189	10	L		0.559	1	1	14.877	4.189	Win	14.891	0.028		
4 188	No.	1_	ľ	0.587	1	١	14.872	4.188	Vf/2	3.522	0.003	3.505	
4.188	100		ľ	1	0.141	3.527	14.876	4.188	CHI)	0.538	0.024	0.447	0.596
4.188	l m	1		0.592	0.142	3.527	14.883	4.188	,				
4.188	100	0.838	14.881	0.598	0.144	3.527	14.881	4.188					
4.189	6	1		0.514	0.134	3.528	14.888						
4.189	6	0.838	14.895	0.571	0.142	3.529	14.895	4.189					
4.190	0	0.838		0.550	0.139	3.530	14.897	4.190					
4.190	10		14.892	0.558	0.140	3.530	14.892	4.190					
4 191	1	ļ.,	14.885	0.552	0.139	3.530	14.885	4.191					
4.192	2	0.838	14.888	0.567	0.143	3.531	14.886	4.192	ì				
4.192	2	0.838	14.901	0.581	0.142	3.531	14.901	4.192	Ž.				
4.193	10	0.839	14.907	0.583	0.141	3.532	14.907						
4.194	14	0.839	14.908	0.558	0.141	3.534	14.908				_		
4 195	12	0.839	14.902	0.589	0.139	3.533	14.902	4.195	5				
	i		ļ										

Property Secured Secured Party Property Secured Party





					1
					+-
Win	Predicted Vc				+
14.5	3.849	Given Vc≃	4.187		
15.0	3.964	Estimated			—
15.5	4.079	Watts Out		watts of power	
16.0		Actual =		watts of input power	
16.5			1.079	excess watts	
17.0	4.424			<u> </u>	4—
17.5	4.539				
18.0	4.653				
18.5	4.768				+-
			···	 	+
	 				
	 				i i





THESIS - APPENDIX NINE

The second seconds

mercial approved

100000000

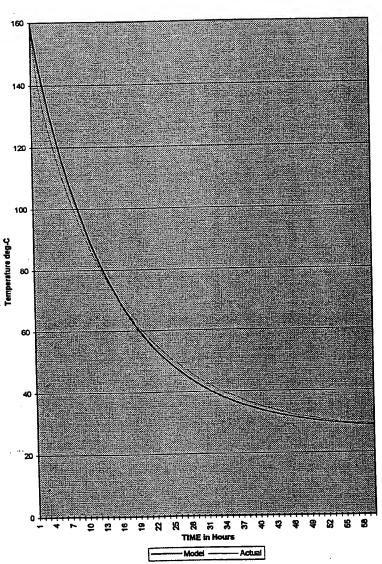
VIOLUTIAN.







Model vs. Actual Data



Page 1









aut Loss Model for HPC Test 15.9 - May 34, 1996 Kc- 40850 Best Loss Model for HPC Test 15.9 - May 34, 1996 Rodel Fit Test Model Fit Test 288.1 Amblent Delta - T Nerdicided Prediction Actual %. Error Terror 288.1 27.1 240.8 280.9 0.00% 286.0 27.1 240.8 280.9 0.00% 286.0 27.1 240.8 280.9 0.00% 286.0 27.1 240.8 280.0 0.00% 286.0 27.1 240.8 248.0 0.00% 286.0 27.1 240.8 248.0 0.00% 286.0 27.1 240.8 248.0 0.00% 286.0 27.1 191.2 218.3 217.8 21.62% 187.0 27.1 142.1 217.8 217.8 21.62% 188.2 27.1 142.1 217.3 216.2 22.42% 188.2 27.1 142.1 217.1 217.3 216.2 22.42%			•								
Temperature Cele Armblent Delta - T Next Pers Best Vis. Error Cele Armblent Delta - T Next Pers Best Vis. Error Cele Armblent Delta - T Next Pers Best Vis. Error Cele Armblent Delta - T Next Pers Best Vis. Error Cele Armblent Delta - T Next Pers Best Vis. Error Cele Armblent Delta - T Next Pers Best Vis. Error Cele Armblent Delta - T Next Pers Best Vis. Error Cele Armblent Delta - T Sele Cele Cele Cele Cele Armblent Delta - T Cele Cele Cele Cele Cele Armblent Delta - T Cele Cele Cele Cele Cele Armblent Delta - T Cele			Madel for 1	UDC Test	5.9 - May	3-4, 1996	₩ E	40850	-W	0.85	
Temperature Celi	=	981 LOSS	MOUEL IOI								
Temperature \ degrees of the first boundary of the first b		-		Ī	Heat 055	Prediction		Model Fit			
Cel. Amblent Delta - 1 Naxt = 11, Dest. Dest.	Ē	emperatu	ire - degret	,	1000	Doct			Temp.		
Second Prediction Predictio			٦,	Т	_	Desdiction			Error - C		
8211 268.1 27.1 241 200.0 8331 286.0 27.1 240.8 287.9 0.0 8331 287.0 27.1 240.8 287.9 0.0 8331 287.0 27.1 240.8 287.9 0.0 8331 286.6 27.1 240.8 28.6 0.0 851 248.0 27.1 191.2 218.3 217.8 217.8 851 218.3 27.1 140.2 217.8 217.8 16.4 8632 178.9 27.1 146.2 217.3 217.3 217.3 8632 178.9 27.1 146.2 217.3 217.3 215.4 8632 178.9 27.1 146.2 217.3 217.3 215.4 8632 178.1 27.1 137.4 216.9 216.9 30.2 18872 164.5 27.1 134.4 216.9 216.9 31.6 1893 164.5	(S)					ionoinoi L					
268.1 27.1 240.8 268.0 27.1 240.8 267.9 267.0 27.1 240.8 267.9 267.0 27.1 240.8 267.9 267.0 27.1 220.9 248.0 0.0 268.0 27.1 191.2 218.3 Start Model 0.0 27.1 191.2 218.3 Start Model 0.0 0.0 189.5 27.1 191.2 218.3 217.8 217.8 16.4 189.5 27.1 148.2 217.8					7,007						#VALUE!
268,0 27.1 240.8 267.9 0.0 267.9 27.1 240.8 267.9 0.0 267.9 27.1 220.9 248.0 0.0 248.0 27.1 191.2 218.3 Start Model 0.0 248.0 27.1 191.2 218.3 217.8 9.3 199.5 27.1 159.8 217.8 217.8 16.4 173.3 27.1 146.2 217.8 217.8 217.8 166.5 27.1 142.1 217.1 217.3 217.3 166.5 27.1 139.4 216.8 216.9 33.4 166.5 27.1 137.1 216.2 216.8 33.4 166.5 27.1 137.4 216.8 216.9 33.4 166.5 27.1 137.4 216.8 216.9 33.4 166.5 27.1 131.3 158.6 158.6 158.6 0.6 158.4 27.1 130.5 </td <td>38211</td> <td>268.1</td> <td>27.1</td> <td></td> <td></td> <td></td> <td></td> <td></td> <td></td> <td></td> <td></td>	38211	268.1	27.1								
267.0 27.1 240.8 267.9 0.00 265.6 27.1 238.5 265.6 0.00 265.6 27.1 220.9 248.0 0.00 248.0 27.1 191.2 218.3 Start Model 0.00 218.3 27.1 191.2 218.3 217.8 9.3 187.0 27.1 159.9 217.8 217.8 217.8 187.0 27.1 146.2 217.1 217.1 217.1 166.5 27.1 138.4 216.9 216.9 30.2 166.5 27.1 137.1 216.2 216.9 30.2 166.5 27.1 137.1 216.2 216.9 31.0 166.5 27.1 137.4 216.9 216.9 31.0 166.5 27.1 137.0 215.7 216.9 31.0 166.5 27.1 137.0 216.2 216.9 31.0 158.8 27.1 130.5 15	38271	288.0						7000		I hable to Replicate	
265.6 27.1 238.5 265.6 248.0 27.1 220.9 248.0 0.0 248.0 27.1 191.2 218.3 218.1 0.0 218.3 27.1 191.2 218.1 217.8 0.0 199.5 27.1 172.4 218.1 217.8 0.1 178.9 27.1 149.2 217.3 217.8 217.1 178.9 27.1 142.1 217.1 217.1 28.3 166.5 27.1 139.4 216.9 216.9 216.9 30.3 166.5 27.1 139.4 216.9 216.9 30.3 30.3 166.5 27.1 134.4 216.9 216.9 30.3 30.3 166.5 27.1 134.4 216.2 216.9 30.3 30.3 160.5 27.1 134.4 216.2 216.9 30.3 30.3 158.7 27.1 130.5 158.5 158.6 158.6 <td>28234</td> <td>287.9</td> <td></td> <td></td> <td></td> <td></td> <td></td> <td>0.00%</td> <td></td> <td>Dracinitous Dron In</td> <td></td>	28234	287.9						0.00%		Dracinitous Dron In	
248.0 27.1 220.9 248.0 218.3 27.1 191.2 218.3 Start Model 0.0 218.3 27.1 191.2 218.1 217.8 217.8 9.3 198.5 27.1 159.9 217.8 217.8 217.8 216.4 173.3 27.1 148.2 217.1 217.1 228.2 169.5 27.1 136.4 216.9 216.9 216.9 30.3 161.5 27.1 137.1 216.6 216.6 31. 36.4 31. 161.5 27.1 134.4 216.2 216.4 216.6 33.4 161.5 27.1 134.4 216.2 216.4 33.4 160.5 27.1 134.4 216.2 216.6 33.4 160.5 27.1 134.4 216.6 216.6 33.4 160.5 27.1 134.4 216.6 216.6 33.4 160.6 27.1 130.1	2020	285.8		L				0.00%		Interpitous City III	
218.3 27.1 191.2 218.3 Start Model 0.0 199.5 27.1 172.4 218.1 218.1 218.1 9.3 199.5 27.1 159.9 217.8 217.8 217.8 21.8 178.9 27.1 151.8 217.6 217.8 217.8 21.2 178.9 27.1 142.1 217.1 217.3 217.3 217.3 22.6 168.5 27.1 135.6 216.8 216.9 30.1 28.3 168.5 27.1 135.6 216.4 216.3 33.1 168.6 27.1 132.6 215.7 216.7 33.4 168.8 27.1 132.6 215.7 215.9 33.1 158.8 27.1 132.6 215.7 215.9 33.1 158.8 27.1 130.5 158.5 158.6 158.4 0 158.4 27.1 120.1 157.7 157.2 157.2 1	20081	248.0						0.00%		Illelia i calibalana	
196.5 27.1 172.4 218.1 218.1 198.3 187.0 27.1 159.9 217.8 217.8 217.8 17.8 16.4 178.9 27.1 151.8 217.3 217.3 217.3 217.3 225.4 178.2 27.1 142.1 217.1 217.1 28.3 25.4 28.3 27.1 130.4 216.8 216.9 30.5 30.5 31.4 216.2 31.4 216.2 31.4 31.4 216.2 31.4 31.4 216.2 31.4 31.4 216.2 31.4 31.4 31.4 216.2 31.4 31.4 216.2 31.4 31.4 216.2 216.2 31.4 31.4 31.4 216.2 216.2 31.4	30431	218.3		L		Start Mode	_	0.00%			
187.0 27.1 159.9 217.8 217.8 217.8 16.4 178.3 27.1 151.8 217.6 217.3 217.3 217.3 217.3 217.3 217.3 217.3 217.3 217.3 217.3 217.3 217.3 217.3 28.3 217.3 218.9 218.9 218.9 30.3 <td< td=""><td>30311</td><td>400 5</td><td></td><td>L</td><td></td><td>218.1</td><td></td><td>9.30%</td><td>ŀ</td><td></td><td></td></td<>	30311	400 5		L		218.1		9.30%	ŀ		
18.0 27.1 151.8 217.6 217.3 217.3 217.3 217.3 217.3 217.3 217.3 217.3 217.3 217.3 217.3 217.3 217.3 217.3 217.3 217.3 217.3 217.3 218.3 217.3 218.3 217.3 218.4	1000	407.0		L				16.48%			
1 0.8 27.1 146.2 217.3 217.3 217.1 25.4 1 06.5 27.1 139.4 216.8 216.8 30.2 1 06.5 27.1 136.4 216.8 216.8 31.2 1 06.5 27.1 137.1 216.8 216.8 31.3 1 06.5 27.1 135.5 216.4 216.8 33.1 1 06.5 27.1 134.4 216.2 215.9 34.1 1 06.5 27.1 134.2 215.7 215.9 34.1 1 58.6 27.1 131.7 215.5 158.8 Match Pt. 0. 35.1 1 58.4 27.1 130.5 158.6 158.8 158.0 0. 157.0 0. 1 56.6 27.1 130.5 158.5 158.6 157.0 0. 157.2 0. 1 56.6 27.1 120.5 158.1 158.6 158.6 157.6 0. 1 55.3 27.1 120.5 157.2	38032	2.00					-	21.62%			
1 (8.5) 27.1 142.1 217.1 217.1 217.1 218.9 216.9 216.9 30.7 30.7 30.7 31.3 216.8 216.9 31.3	38692	2007		L	L		-	25.42%			
168.2 27.1 138.4 216.9 216.9 30.7 166.5 27.1 137.1 216.6 216.6 316.6 316.6 164.2 27.1 135.5 216.4 216.2 31.6 162.6 27.1 134.4 216.2 216.2 33.1 160.5 27.1 134.4 216.2 216.2 33.1 160.5 27.1 132.6 215.7 215.7 33.1 158.4 27.1 131.3 158.6 158.4 0 158.4 27.1 131.3 158.6 158.4 0 157.6 27.1 130.5 158.3 157.2 0 157.6 27.1 130.5 158.3 157.2 0 158.6 27.1 129.5 158.1 157.6 0 156.2 27.1 129.3 157.7 155.5 1 155.3 27.1 128.4 157.2 157.2 154.6 1	38/97	1/3.3						28.32%			1
166.5 27.1 138.4 216.6 216.6 31.5 164.2 27.1 135.5 216.4 216.4 216.4 33.1 162.6 27.1 134.4 216.2 216.2 33.1 160.5 27.1 134.4 216.2 216.2 33.1 150.7 27.1 132.6 215.7 215.7 35.1 158.4 27.1 131.3 158.6 158.8 Match Pt. 0 157.6 27.1 131.3 158.6 158.4 0 0 157.2 27.1 130.5 158.5 158.6 157.6 0 157.2 27.1 130.1 158.3 157.2 0 0 156.8 27.1 129.5 158.1 156.0 156.2 1 156.8 27.1 129.3 157.2 157.2 1 1 155.5 27.1 128.4 157.2 157.2 154.6 1 154.8 <td>38812</td> <td>169.2</td> <td></td> <td></td> <td></td> <td></td> <td></td> <td>30.25%</td> <td></td> <td></td> <td></td>	38812	169.2						30.25%			
164.2 27.1 137.1 210.2 216.2 33.1 162.6 27.1 135.5 216.2 216.2 33.1 161.5 27.1 133.4 216.2 216.2 33.1 150.5 27.1 131.7 215.7 215.7 35.3 158.8 27.1 131.7 215.5 158.8 158.4 0 158.4 27.1 131.3 158.6 158.6 158.4 0 157.2 27.1 130.5 158.5 158.6 157.2 0 157.2 27.1 130.1 158.3 158.3 157.2 0 156.6 27.1 120.5 158.1 158.0 158.4 1 156.8 27.1 120.5 158.1 157.2 1 1 156.8 27.1 120.3 157.3 157.2 1 1 155.3 27.1 120.3 157.2 157.2 154.6 1 154.8	38872	166.5						31.93%	52.4		
162.6 27.1 135.5 2.10.4 2.10.4 2.10.4 2.10.4 2.10.4 2.10.4 2.10.2 2.10.2 3.3.1 3.4.1 2.10.4 2.10.2 2.10.2 3.4.1 3.4.1 3.4.2 3.6.2	38932	164.2						33.09%			
161.5 27.1 134.4 215.0 215.0 34. 160.5 27.1 133.4 215.7 215.8 158.6 158.4 0 0 158.4 0 0 158.4 1 0 158.2 157.8 158.6 0 0 158.4 1	38993	162.6						33.85%	54.7		
160.5 27.1 133.4 215.9 215.7 215.7 215.7 215.7 215.8 215.7 215.8 215.7 35.1 35.1 35.1 35.1 35.1 35.1 35.1 35.1 35.1 35.1 35.1 35.1 35.1 35.1 35.1 35.1 35.1 35.2	39053	161.5						34 53%	55.4		
158.7 27.1 132.6 213.7 215.5 158.8 Match Pt. 0. 158.8 27.1 131.7 215.5 158.8 Match Pt. 0. 158.4 27.1 131.3 158.6 158.6 158.6 158.4 0. 157.2 27.1 130.5 158.3 158.3 157.2 0. 157.2 27.1 129.5 158.3 158.0 158.0 158.6 27.1 129.5 158.1 158.0 158.0 158.4 1. 158.4 27.1 128.3 158.0 158.0 158.0 158.4 1. 158.2 27.1 128.3 157.7 157.7 157.7 155.5 1. 155.5 1. 155.5 1. 158.8 27.1 128.2 157.5 157.5 155.5 1. 158.8 27.1 127.5 157.2 157.2 154.8 1. 154.8 1. 157.8 157.8 158.8 1. 155.8 1. 157.8 158.8 1. 158.7 1. 15	39113	180.5						35.08%			
158.8 27.1 131.7 215.5 158.0 (Minucial I. C.) 458.4 27.1 131.3 158.6 158.6 158.6 158.4 0. 157.2 27.1 130.5 158.3 157.2 0. 157.2 27.1 129.5 158.1 158.3 157.2 0. 156.6 27.1 129.5 158.1 158.0 158.6 0. 158.4 27.1 129.3 158.0 158.4 1 1 158.2 27.1 129.1 157.8 158.4 1 1 158.2 27.1 128.1 157.8 158.4 1 1 156.2 27.1 128.2 157.8 158.2 1 1 155.3 27.1 128.2 157.5 157.7 155.5 1 154.8 27.1 127.5 157.2 154.8 1 1 154.8 27.1 127.1 157.0 157.0 154.2 1<	39173	159.						0000			
158.4 27.1 131.3 158.6 158.6 158.7 157.6 27.1 130.5 158.5 158.5 157.2 0 157.2 27.1 129.5 158.1 158.3 157.2 0 156.6 27.1 129.5 158.1 158.0 158.6 0 156.7 27.1 129.3 158.0 158.0 158.4 1 156.2 27.1 129.1 157.8 158.2 1 155.5 27.1 128.4 157.7 157.8 158.2 1 155.6 27.1 128.2 157.7 157.3 158.2 1 154.8 27.1 127.7 157.3 157.3 154.8 1 154.8 27.1 127.7 157.2 157.2 154.6 1 154.2 27.1 128.7 156.8 156.8 153.8 1 153.7 150.7 156.8 156.8 153.7 1	39233	158.8									
157.6 27.1 130.5 158.5 158.5 158.0 157.0 157.0 157.2 157.1 158.3 158.3 157.2 0.0 157.2 0.0 157.2 0.0 <th< td=""><td>39293</td><td>158.4</td><td></td><td></td><td></td><td></td><td></td><td></td><td></td><td></td><td></td></th<>	39293	158.4									
157.2 27.1 130.1 158.3 158.3 157.2 157.2 157.1 158.3 157.2 158.3 157.2 158.6 157.2 158.6 157.2 158.6 157.2 158.6 157.2 158.6 157.2 158.4 157.2 158.2 158.2 157.2 158.2 157.3 157.2 158.2 157.3 157.3 157.3 157.3 157.3 157.3 157.3 154.8 1 154.8 1 1 154.8 1 2 1 1 2 1 1 2 1 <t< td=""><td>39353</td><td>157.6</td><td></td><td></td><td></td><td></td><td></td><td>1</td><td></td><td></td><td></td></t<>	39353	157.6						1			
158.6 27.1 129.5 158.1 158.1 158.1 158.2 27.1 158.4 27.1 129.3 158.0 157.8 158.4 1 158.2 27.1 129.1 157.8 157.8 156.2 1 155.3 27.1 128.4 157.5 157.5 155.3 1 154.8 27.1 127.7 157.2 157.2 154.8 1 154.8 27.1 127.7 157.0 157.0 154.6 1 154.2 27.1 127.7 156.8 156.8 153.8 1 153.7 17.7 156.8 156.8 153.8 1 155.7 27.1 128.7 156.7 153.7 1	39414	157.									-
156.4 27.1 129.3 158.0 158.0 150.4 15.1 150.2 1	39474	158.				-					
156.2 27.1 129.1 157.8 157.8 158.2 158.2 158.2 158.2 158.2 157.7 157.7 155.3 155.3 155.3 155.3 155.3 155.3 155.3 157.3 158.3 158.3 158.3 158.3 158.3 158.3 158.3 158.3 158.3 158.3 158.3 158.3 158.2 158.3	39534	158.									
155.5 27.1 128.4 157.7 157.7 157.7 155.3 155.3 27.1 128.2 157.5 157.5 155.3 1 154.8 27.1 127.7 157.2 157.2 154.8 1 154.0 27.1 127.5 157.2 157.2 154.6 1 154.2 27.1 127.1 157.0 157.0 154.2 1 153.8 27.1 126.7 156.8 153.8 1 1 45.7 27.1 126.6 156.7 153.7 1 1	39594	158.				-	1	-			
155.3 27.1 128.2 157.5 157.5 155.3 155.3 154.8 27.1 127.7 157.3 154.8 1 154.0 27.1 127.5 157.2 157.2 154.6 1 154.2 27.1 127.1 157.0 154.2 1 154.2 1 153.8 27.1 126.7 156.8 158.8 153.8 1 153.7 17.1 126.6 156.7 153.7 1	20854	155								3 6	
154.8 27.1 127.7 157.3 157.3 154.8 1 154.6 27.1 127.5 157.2 157.2 154.6 1 154.2 27.1 127.1 157.0 157.0 154.2 1 153.8 27.1 126.7 156.8 153.8 1 153.8 27.1 126.6 156.7 153.7 1	20744	155		L				-		7	-
154.6 27.1 127.5 157.2 157.2 154.6 1 154.2 154.2 27.1 127.1 157.0 157.0 154.2 1 154.2 1 153.8 1 153.8 1 153.8 1 153.8 1 153.8 1 153.8 1 153.8 1 153.8 1 153.8 1 153.8 1 153.8 1 153.8 1 153.8 1 153.8 1 153.7 1 158.7 158.7 153.7 1 158.7	20774	154				·				6.2	
153.8 27.1 128.7 158.8 158.8 153.8 1 153.8 1 153.8 1 153.8 1 153.8 1 153.8 1 159.8 159.8 1 159.7	39835	154								2.0	
153.8 27.1 128.7 158.8 156.8 153.0 153.7 1 159.7	39895	154								3.0	-
158.7 158.7 158.7 158.7 158.7	10055	153						- `		200	
1	40045						١			- In	





	T																																			
3.3	3.6	3.7	3.8	4.0	3.8	4.1	4.1	4.3	4.3	4.4	4.8	4.6	4.7	4.8	4.9	2.0	5.0	5.1	5.3	5.3	5.4	5.4	5.6	5.6	5.5	5.8	20.00	5.8	6.0	5.8	6.1		6.9	7.5	7.1	6.5
				.9 2.62%		.5 2.87%	_		.8 2.83%		_												147.3 3.77%		\perp					1	145.5 4.20%					118.0 5.49%
			158.0 152.2	155.9 151.9	155.7 151.9	155.6 151.5	155.4 151.3				154.8 150.2	154.8 150.0		154.3 149.5						153.3 148.0	153.2 147.8			152.7 147.1							151.8 14	Model Actual			۱ ا	124.0 11
158.5	156.4	156.2												154.3								L				152.4				151.8	151.8	151.8	148.3			123.7
	125.7	L							1			122.9				L				L	L					1 119.5	1 119.3	1 119.2		118.8	1 118.4	0	114.5			8 90.7
								27.1							27.1								27.1												1.4 26.8	
L											450.5	1		L							T				ŀ			1				+	12 141.5		1	
40075	40135	40108	40104	40200	40310	403	40430	40496	40000	40616	4007	40707	40857	40017	40977	41038	41008	41158	44248	44278	41238	41300	41000	41470	41570	41839	41899	41759	41819	41879	41040	1 4 4 1				





																				_	_		_		_	_	_		T	_		_	_				_	
	+		+		+	1	1																															
L	$\frac{1}{1}$		+		-	-							-	1	-																							
	0.0	5.0	4.3	3.7	3.1	2.4	1.9	1.4	9.0	0.3	-0.3	-0.4	-0.7	-0.9	-1.3	-1.5	-1.8	4.9	-2.0	-1.9	-2.0	-2.0	-2.0	-19	6.1-	1.9	6.1-	-1.8	1.8	6.1.	1.9	-1.7	14	-	1.	1.3	-1.2	
	5.07%	4.78%	4.30%	3.89%	3.43%	2.76%	32%	1.75%	1.11%	%66.0	-0.45%	-0.57%	-1.12%	-1.39%	-2.19%	-2.58%	-2.85%	-3.59%	3.74%	3.83%	-4.07%	4.29%	4.31%	4.31%	4 34%	-4 39%	4 49%	-4.41%	3 92%	4 73%	4 92%	4 47%	2 84%	A 48%	2 R1%	3.61%	-3.59%	
	111.0 5.	105.0	100.0			L		78.0	1	1	890	1	1	1	1		1	l		1	1	1	į.	l	1	ļ	1	40.0		L	L	20.00	1	\perp	\perp		L	1
											77.0 80 5										47.4		2 2	43.4	- -	D 0	200	0.00	20.00	30.0	3.70	000	0.00	30.6	0,40	23.5	23.53	35.1
	116.9	1104			l		ŀ		1	١				١														39.8									33.5	
	1187	440.2	404.2	5 8	80.0		\				72.6			1	١	1	1	1		1			\														8.7	
	8 / B	5 6	9	13.4	١	-		55.5	١	1	45.5	- {	١	-	-	32.8	1	- [-		١		1	1	١				13.7				-					
	15.00	7.07	28.7	28.7	28.7	26.8	26.8	56.9	27.0	27.0	27.0	27.0	27.0	27.0	27.0	27.0	27.0	27.0	27.0	27.0	27.0	27.0	27.0	27.0	27.0	27.0	27.0	27.0	27.0	27.0	27.0	27.0	27.0	27.0	27.0	27.0	27.0	27.0
		111.3	105.4	1001	95.1	90.5	86.4	82.4	78.8	75.5	72.5	89.8	8.8	64.3	61.8	59.8	57.7	55.7	54.1	52.3	50.6	49.1	47.7	46.3	45.0	43.8	42.7	41.7	40.7	38.6	39.1	38.4	37.5	38.6	38.1	35.4	34.8	34.3
		16	17	18	18	20	21	22	23	77	25	92	27	28	58	30	31	32	33	34	35	38	37	. 38	39	40	14	42	43	44	45	48	47	48	48	20	51	52
				1	1	1.	1		1	1	1	1	1	1	1	1			1	1	1	١	1	-	1	1	1	1	١		1		1	1	1	1	1	

Heat Loss Model - Vers 1.1

															-						_
	-	2 *******	80	9	æ			9	8,	က	4	21.	4	4.	3	-	2	6:	.5	-0.5	uc.
							١					1					١			-1.71% -0	
1										İ										28.7 29.0	ļ
		ł				1	ļ			l					١	1				28.7	l
	8.7																			200	
				١														١		27.0 27.0	
		-						١		1										89	

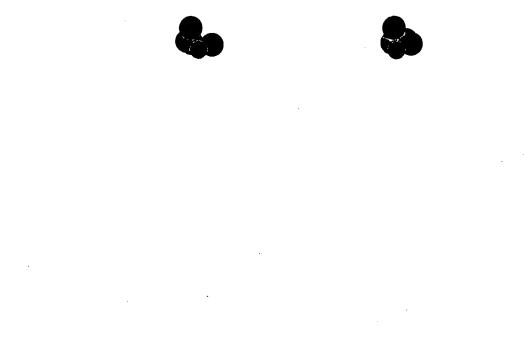




101 CA

Forders

THESIS - APPENDIX EIGHT







Wr. Win	Win				Ş	Statistics	Statistics for Analysis are	s are			
A 424 B 740	A 424 B 740	D 740	D 740	1	1 274		for 1000 - 3892 [8,053 hrs]	1892 78.053	hrsl		
0.710	0.735 0.134 0.710	0.710	0.710	1	:						
1 274 0 255 0 134 6.698 1.	0.255 0.134 6.698	6.698	6.698	÷	1.274		Average	Std. Dev.	E E	Max	
0 255 0 134 6.708	0 255 0 134 6.708	0 134 6.708	8.708	-	1.274	OA I		0.013	1.422	1.477	
0.252 0.131 6.563	0.252 0.131 6.563	0.131 6.583	6.583	-	1.271	Win	<u> </u>	7.084 0.057 8.	8.755	7.405	
0.126 6.317	0.247 0.128 6.317	0.126 6.317	6.317	-	1.268						
1.274 0.255 0.134 6.681	0.255 0.134 6.681	0.134 6.681	6.681	7	1.274						
0.255 0.134 6.715	0.255 0.134 6.715	0.134 8.715	8.715	-	1.274	•	·				
0.255 0.134 6.703	0.255 0.134 6.703	0.134 6.703	6.703	-	.274	-					
0.255 0.134 8.718	0.255 0.134 8.718	0.134 6.718	6.718	,	1.274	1					
1.274 0.255 0.134 6.708	0.255 0.134 6.708	0.134 6.708	6.708		1.274	4	-				
1 274 0.255 0.134 6.699	0.255 0.134 6.699	0.134 6.699	6.699		.274	*				_	
					۱						





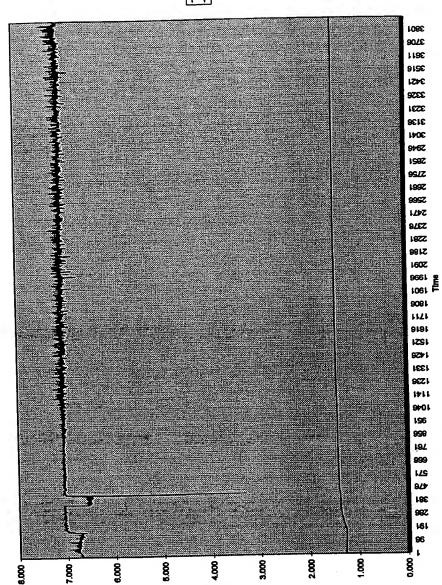
3	, JA			Wiln	Λc	Statistics	Statistics for Analysis are	are			
2 6	1 274	1.	0.134				for 2 - 3892 [10.832 hrs]	[10.832 h	rs]		
87	1 274	0.255	0.134	8.698	ľ		Average	Std. Dev.	Min	Max	
12	1 274	0.255	0.134				1.432	0.048	1.282	1.477	
87	1.271	0.252	0.131		1.271	S	7.051	0.129	3.307		
26	1.288	0.247	0.128								
20	1.274	0.255	0.134		1.274						
11	1 274	0.255	0.134		1.274						
127	1.274	0.255	0.134								
37	1 274	0.255	0.134	8.718	1.274						



TP032797 Chart 1







Page 1





- 1	0 142	Win 7 112	Vc 1.475	Statistics	Statistics for Analysis are for 2 - 16384 [45]	for Analysis are for 2 - 16384 [45.175 hrs]	hrs.		
	0 144	7.208	1.475		Average	Average Std. Dev. Min	Min	Max	
	0 143	7.131	1.475	Λc	1.452	0.001			
٦	0.143	7.150	1.475	Win	7.083	0.021	7.009	7.250	
0	0.143	7.140	1.475						
6	0.143	7.188	1.475						
0	0.142	7.078							
o	0.142	7,093	1.475						
P	0.142	7.118	1.474						
٥	0.141	7.088							
o	0.142	7.089							
0	0.142	7.115	1.474						
P	0.142	7.084	1.474						
	0.141	7.068	1.473						
	0.141	7.061	1.473						







- 1				140	1	Statistics	Statistics for Analysis are	s are			
ime [sec] Vc	ς Σ				١	Commo	000	1 0000 F47 708 hrel	la.		
T.	445	0.289	0.140	6.997	7 1.445	2	TOF 2 - 030	200			
	146	0 280	0.140	6.989	1.445	2	Average	Std. Dev. Min		MBX	
		200	0 440		5 1 445	VC	1,453	0.005	1.445		
	Ç .	0.408	0 44	١		Win	7.010	0.015	6.958	7.055	
96	.440	0.208	2								
105	1.445	0.289	0.140	6.988		2					
	445	0.289	0.140	6.982	1.445	2					
125	445	0.289	0.139	6.968	1.445	5					
	445	0 280	0.139	8.988	1,445	5					
	446	080	0 140	6.984	1.445	20					
2	2 7	2000	0 141	7 029	1.445	5	_				
	4445	0.209	0.140		ľ	5					
	1 445	0 289	0.140		1.445	5					
	1.445	0.289	0.140	7.010	1.445	5					
	1.445	0.289	0.140			55					
205	1 445	0.289	0.140	7.011	1.445	5					

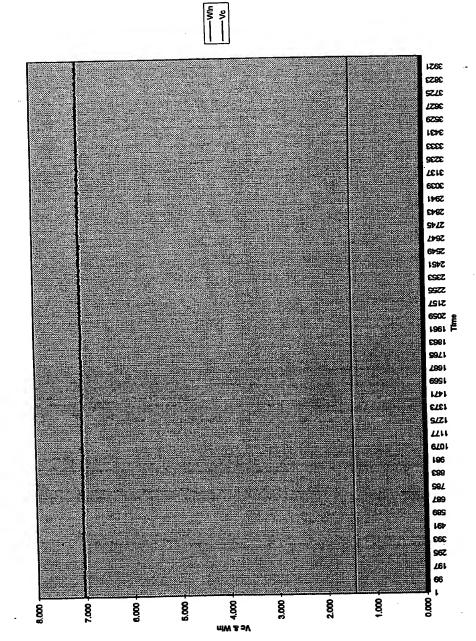




ime [sec]	<u>\</u>	, o	J	Win	Vc	Statistics for Analysis are	or Analysi	s are			
34	1.461	0.293	0.141	7.039	1.461		or 2 - 841	for 2 - 8419 [23.438 hrs]	S)		
44	1.481		0.141	7.050	1.481		Average	Average Std. Dev. Min	Min	Max	
54	ľ	L	0.141	7.030	1.481	×	1.489	0.00	1.460		
8			0.141	7.040	1.461	Win	7.047	0.012	7.004	7.093	
74	1.461	0.293	0.141	7.043	1.481						
84	1.461	0.293	0.141	7.044	1.461						
98	1.481	0.293	0.141	7.057	1.461						
104	1.481	0.293	0.141	7.049	1.461						
114	1.481	0.293	0.141	7.047	1.461						
124	1.481	0.283	0.141	7.045	1.481						
134	1,461	0.293	0.141	7.027	1.481						
144	1.481	0.293	0.141	7.062	1.461						
154	1,461	0.293	0.141	7.040	1.481						
164	1.461	0.293	0.141	7.044	1.481						
174	1.461	0.293	0.141	7.060	1.461						
184	1.461	0.293	0.141	7.050	1.461						











		n Max	1.457 1.472	6.985 7.287				•							
lysis are	for 2 - 8446 [23.514 hrs]	Average Std. Dev. Min	1.452 0.003	7.034 0.018											
Statistics for Analysis are	for 2 -	Averag	χ	Win											
۸c	1.471	1.471	1.472	1.472	1.472	1.471	1.471	1.471	1.471	1.471	1.471	1.471	1.471	1.471	727 7
Win	7.027	7.018			7.017	7.043	7.037	7.025	7.039	7.018	7.020	7.035	660.7	7.037	
×	0.141	0.140	0 140	0.141	0.140	0.141	0.141	0.140	0.141	0.140	0.140	0.141	0.141	0.141	•
Vc.	0.294	70 U				ļ	0.294	0.294	0.294	0.294	0.294	0.294	0.294	0.294	
	1.471	4 471	1 472	1 472	1.472	1.471	1.471	1.471	ľ		1.471	1.471	ľ		
me [sec] Vc	2	4	7	= =	6	10	111	121	132	141	151	181	172	182	





_	T		Τ		Γ	Ţ	_	Γ	1	_	Γ	7	_	Τ	7	_	1	Τ	_	<u> </u>	1
_	1		1																		
_	1		1	_	1	1.445	7 024		-	_	+		L	+		-	$\frac{1}{1}$	4		-	$\frac{1}{1}$
				Max		4.	7.0	!													
				Ī		1,395	COD	0.004		Ī											
-		107	I & Drs.	Act.		0.008	000	0.03B				_				+			-		$\frac{1}{1}$
	als are		86 [Z5.t	170	010		l	١	_	-	4		1		_	+	4	_	L	1	-
	or Analys		for 2 - 8986 [25.018 nrs]		Average oto. Dav. IVIIII	1 440		6.952													
	Statistics for Analysis are	201101101				5	2	Min													
			1 438	2	1.438	4 430	1.430	1.438	4 430	22	1.438	7 730	000	1.438	4 430	1.430	1.438	1 438		1.438	1.438
	N.	ر د	A 027	200	6.931		0.831	6.942	990	0.800	6.952	4,4	0.840	6.930	250	0.920	6.932	A 050		6.935	6.940
	141		١							ļ		١	ļ			-					
			04.00	0.138	0 139		0.138	0.139		0.138	0.139		0.139	0.139		0.138	0.139	0 130	2	0.139	0.139
		×	900	0.720	A 288	0.200	0.288	0 288		0.288	0.288		0.288	0.288		0.288	0.288	900	0.200	0.288	0.288
	-	د. خ		438			438		١	438	438	3	1.438	1 A2B	2	1.438	1438	2 5	1.436	1.438	438
		۳	ľ	4.	*	7.	7	-	-	7	-		-	-		÷	-	-	-	-	
		Time feec Vc	200	4	1	D.	82	1			8	70	102	445	711	122	122	3	142	152	182
		Time														L					L





		Max		6.708 7.079									
is are	for 2 - 7697 [21.428 hrs]	Std.	0.006	0.034									
Statistics for Analysis are	for 2 - 769	Average	Vc 1.432	Win 6.967						•			
Vc	1.445	1.446	1.448	1.448	1.448	1.448	1.445	1.445	1.445	1.445	1.445	1.445	10777
Win	6.973	6.981	6.958	6.975	6.971	6.960	6.972	6.953	6.974	8.974	6.955	6.975	
	0.139	0.139	0.139	0.140	0.139	0.139	0.139	0.139	0.139	0.139	0.139	0.140	1
vc.	0.289	0.289	0.289	0.289	0.289	0.289	0.289	0.289	0.289	0.289	0.289	0.289	
	1,445	1.446	1.448	1.448	1.448	1.448	1.445	1.445	1,445	1.445	1.445	1.445	
ime [sec] Vc	38	48	58	88	78	88	86	108	118	128	138	148	







Firms food	3	۸۶.	×	Win	<u>د</u>	Statistics	Statistics for Analysis are	s are			
	2	2000	0 430	A 050	4 432		for 2 - 163	for 2 - 16384 [45,618 hrs]	hrs		
CS.	7.432									-	
45	•	0 287	0.139	6.843	1.432		Average	Average Std. Dev. Min		MAX	
2	ľ				1.432	VC	1.428	0.008			
93	ľ	0.287				Win		0.039	6.703	7.065	
6	1007										
2	1	1									
82											
95	1.432	2 0.287	7 0.139								
105		1									
115			l.		1.432	C:					
125	1.432					6					
135			7 0.139								
145		2 0.287	7 0.139	6.938	1.432	~					





me feer! We		×,	2	Win	Vc	Statistics	Statistics for Analysis are	s are			
70	1 428	0 288	0.139	6.929	1.428		for 2 - 846	for 2 - 8462 [23.558 hrs]	's]		
2	4 42R		0.139	6.930	1.428		Average	Std. Dev.	Min	Max	
8 8	1 428		0.138	6.923	1.428	2	1.427		1.385		
2	1.428	ļ	0.138	6.910	1.428	Win	6.869	0.038	6.688	6.956	
88	1.428	0.286	0.139	6.944	1.428						
66	1.428	0.286	0.139	6.933	1,428						
109	1.428	0.286	0.139	6.934	1.428		,				
119	1.428	0.288	0.138	8.908	1.428						
129	1.428	0.288	0.139	6.930	1.428						
139	1.428	0.286	0.139	6.926	1.428						
149	1.427	0.286	0.138	6.919	1.427						
159	1.428	0.288	0.138	6.918	Ì						
169	1.428	0.286	0.139	6.928							
179	1.428	0.286	0.139	6.952	1.428	1					





										-	
ime [sec] Vc	Vc.	×	Win	Ş	Statistics for Analysis are	or Analysi	Sare		1		
45 1 4BD	10 0 292	0.141	7.028	1.460		for 2 - 814	for 2 - 8148 [22.684 hrs]	6			
ľ	١			1 459		Average	Std. Dev. Min	al L	Max		
		l		4 450	Š	1 483	0.001	1.459	1.464		
65 1.458			T	27.	2	l.		6.982	7.087		
5 1.459	59 0.292		1.027	1.43W							
85 1.459	59 0.292	0.141	7.028	Ì							
95 1.459	59 0.292	0.140									
	59 0.292	0.141	7.025								
5 1.459	59 0.292	0.141	7.027	1.459							
125 1.480		0.141	7.035	1.460							
ľ	80 0.292	0.141	7.042	1.460							
	80 0.292	0.141	7.033	1.460							
	80 0.292	0.140		•							
	.460 0.292	0.140		1.460							
175 1 46	1 ARD 0.292	0.141	7,031	1.460	,						
							İ				





1,462 0,263 0,140 7,011 1,462 40r2 - 868e [23,304 hrs] Max 1,462 0,263 0,140 7,016 1,462 0,001 1,460 1,462 0,293 0,141 7,034 1,462 0,001 1,460 1,462 0,293 0,141 7,023 1,462 0,001 1,462 0,293 0,141 7,023 1,462 0,293 0,141 7,023 1,462 0,293 0,141 7,028 1,462 0,293 0,141 7,028 1,462 0,293 0,140 7,015 1,462 0,293 0,140 7,014 1,462 0,293 0,140 7,014 1,462 0,293 0,140 7,014 1,462 0,293 0,140 7,014 1,462 0,293 0,140 7,014 1,462 0,293 0,140 7,014 1,462 0,293 0,140 7,024 1,462 0,293 0,140 7,024 1,462 0,293 0,140 7,016 1,462 0,293 0,140 1,462 0,293 0,140 1,462 0,293 0,140 1,462 0,293 0,140 1,462 0,293 0,140 1,462 0,293 0,140 1,462 0,293 0,140 1,462 0,293 0,140 1,462 0,293 0,140 1,462 0,293 0,140 1,462 0,293 0,140 1,462 0,293 0,140 1,462 0,293 0,140 1,462 0,293 0,140 1,462 0,293 0,140 1,462 0,293 0,140 1,462 0,293 0,140 1,462 0,293 0,140 1,462 0,293 0,140 1,462 0,2	The Page 1	9	1,00	,	Win	۶	Statistics	Statistics for Analysis are	s are			
1462 0.293 0.140 7.011 1.462 Average 864. Dev. Min Max 1.462 0.293 0.140 7.034 1.462 Vc 1.462 0.001 1.460 1.462 0.293 0.141 7.023 1.462 Win 7.027 0.012 6.978 1.462 0.293 0.140 7.023 1.462 Win 7.027 0.012 6.978 1.462 0.293 0.141 7.028 1.462 8.978 8.978 1.462 0.293 0.141 7.027 1.462 8.978 1.462 0.293 0.140 7.015 1.462 8.978 1.462 0.293 0.140 7.014 1.462 8.978 1.462 0.293 0.140 7.024 1.462 8.978 1.462 0.293 0.141 7.024 1.462 8.978 1.462 0.293 0.140 7.016 1.462 8.978	I IIII BEC	ı	اد	١	7011	ľ		for 9 - RERE	1 123 904 h	12		
1,462 0.293 0.140 7.016 1,462 Vc 1,462 0.001 1,460 1,462 0.293 0.141 7,034 1,462 Vc 1,462 0.001 1,460 1,462 0.293 0.141 7,023 1,462 Win 7,027 0,012 6,976 1,462 0.293 0.141 7,028 1,462 C 0.012 6,976 1,462 0.293 0.141 7,028 1,462 C 0.012 6,976 1,462 0.293 0.140 7,015 1,462 C 0.012	-	7.46Z				704.		2				
1462 0.293 0.141 7.034 1.482 Vc 1.462 0.001 1.480 1,462 0.293 0.141 7.035 1.482 Win 7.027 0.012 6.978 1,462 0.293 0.140 7.023 1.462 Win 7.027 6.978 1,462 0.293 0.141 7.023 1.462 Control 0.014 7.015 1.462 Control Control Control 0.014 7.015 1.462 Control Control Control 0.014 7.015 1.462 Control Control Control 0.014 7.014 1.462 Control Control Control 0.014 7.024 1.462 Control Control Control 0.014 7.024 1.462 Control Control Control 0.014 7.016 1.462 Control Control Control 1.462 Control Control Control 1.462 Control Control Control Control 1.462 </th <th>54</th> <th>1 482</th> <th>L</th> <th></th> <th></th> <th>1.462</th> <th></th> <th>Average</th> <th>Std. Dev.</th> <th>MID</th> <th>- 1</th> <th></th>	54	1 482	L			1.462		Average	Std. Dev.	MID	- 1	
1,462 0.293 0.141 7.035 1,462 Win 7.027 0.012 6.878 1,462 0.293 0.140 7.023 1,462 0.012 6.878 1,462 0.293 0.141 7.028 1,462 0.000 0.000 0.000 1,462 0.293 0.140 7.015 1,462 0.000	2	1 482				1.462	>	1.482	0.001	1.480		
1,462 0.293 0.140 7.023 1,462 0.293 0.141 7.028 1,462 0.293 0.141 7.037 1,462 0.293 0.140 7.015 1,482 0.293 0.140 7.011 1,482 0.293 0.140 7.024 1,482 0.293 0.140 7.024 1,482 0.293 0.141 7.027 1,482 0.293 0.140 7.018 1,482 0.293 0.140 7.018	17	1.482									7.085	
1,462 0.293 0.141 7.028 1,462 0.293 0.141 7.037 1,482 0.293 0.140 7.015 1,482 0.283 0.140 7.011 1,482 0.283 0.140 7.024 1,482 0.283 0.141 7.024 1,482 0.283 0.141 7.027 1,482 0.283 0.140 7.018 1,482 0.283 0.140 7.018	84	1.482										
1,462 0,283 0,141 7,037 1,462 0,283 0,140 7,015 1,482 0,283 0,140 7,011 1,482 0,283 0,140 7,024 1,482 0,283 0,141 7,027 1,482 0,283 0,140 7,016 4,482 0,283 0,140 7,016 4,482 0,283 0,140 7,016	91	1.482		ļ		ľ						
1,462 0,283 0,140 7,015 1,462 0,283 0,140 7,011 1,462 0,283 0,140 7,024 1,462 0,283 0,140 7,016 1,482 0,283 0,140 7,016 1,482 0,283 0,140 7,018	102	1.462				1.482						
1,482 0,283 0,140 7,011 1,482 0,283 0,140 7,024 1,482 0,283 0,141 7,027 1,482 0,283 0,140 7,016	111	1.482			ľ							
1.462 0.283 0.140 7.024 1.462 0.283 0.141 7.027 1.482 0.283 0.140 7.016	121	1.482		_		1.462						
1,462 0,283 0,141 7,027 1,462 0,283 0,140 7,016 1,482 0,283 0,140 7,018	132											
1.462 0.293 0.140 7.016	142					•						
4 AR2 0 293 0.140 7.018	152					Ì						
2010	162	1.462	0.293									



			_									_			_			_		
					19	7 187	5													-
			7.00	MAX	1.467							L			L					
		<u> </u>	1	E	1.458		۱													
920	010	117.872 h		Std. Dev.	0 003		0.014													i
Andread	Statistics for Analysis are	for 2 - 6420 [17.872 hrs]		Average Std. Dev. Min	1 484	ľ	7.020													
0.414-41-0	Statistics I				1		Win													
	<u>ح</u>	4 ASB	2	1.458	4 450	1.430	1.457	1.457	137,	1.45/	1 458		1.458	1 458		1.458	1 458			1.458
		7 005	3	7.019	900	6.996	7.012	7.017		7.010	7.010	0.0.	7.025	7 013	200	7.022	7 01R	210.1	7.018	7.020
	_	0770	5	0 140	3	0.140	0.140	0 140		0.140	9770	3	0.140	0770	2	0.140	0770	2.5	0.140	0.140
	*	ı	0.292	0000	7.77	0.292	0.292	0 202	7,7,7	0.292	500	0.282	0.292	000	D.282	0.292	500	0.682	0.292	0 202
	Λ		1.458	920	1.430	1.458	1 457	1 457	1.4.7	1.457		1.430	1 458		1.456	4 45B		1.455	1.458	4 AER
	We look! We	ונוום ואפר ו	43		25	63	72	2 6	60	မ	3	<u>2</u>	442	2	123	122	3	143	153	cat

TP040997

appropriate transported to

a my constraint





Sheet1

	GRAPHIN	G of 20 CM	Control E	rperimenta	I Points		
	Vc	Win	Vc-SD	Win-SD	Date	%-Vc-SD	%-Win-SD
<u> </u>	2.102		0.005	0.034	5-Mar	0.24%	0.34%
├ ──	2.355			0.013	6-Mar	0.51%	
<u></u>	2.353			0.012		0.19%	
<u> </u>	2.453		0.006			0.24%	
1 ——	1.084	4.932				0.88%	1.00%
<u> </u>				0.008		0.08%	0.13%
<u></u>	1,299						0.12%
ļ	3.451						0.08%
<u></u>	3.664			0.007			0.66%
L	0.174						2.00%
1	0.000	0.050	0.000	0.001	1 .0 ,0,0	1 319 - 11	

prior L Added Insulation

		_	_				_	,			_	_			_		_	_	_	_	7
1			1				İ	1	1		-					1	Ì		1		
			XBM	2.117	666 6																
	-		MIN	2.097	EPB O	2															
	4 60 40 kg	74/ 10,14.11	td Dev	0.005	7200	5															
-		0.000 Statistics from 2589-404/ 10.14 IIISI	Average Std Dev	2 102	2000	9.92/															
	֓֟֓֓֓֓֓֟֟֓֓֓֓֓֓֓֓֓֓֟֓֓֓֓֓֓֓֓֓֓֓֓֓֓֓֓֓	Statistics f		-	2	Win															
37	- 1	0.000	0000	270000	0.000	0.000 Win	0.000	0.000	0.011	0.084	0.129	0 189	1	0.241	0.287	0.329	0.368	0.408	0.442	0.477	0.510
	VVIII	0.053	0.050		0.061	0.083	0.181	8.095	9.947	9.950	9.928	0 014	200	9.903	9.922	9.928	9.942	9.938	9.952	9.952	9.925
	^	0.001	000	20.5	0.001	0.001	0.003	0.162	0.199	0.199	0.199	400	0.180	0.198	0.198	0.199	0.199	0.189	0.199	0.199	0.188
	×	0.00	000	200.0	0.000	0.00	0000	0.000	0.00	0.013	0.028	000	6.05	0.048	0.057	0.086	0.073	0.081	0.088	0 095	0.102
	<u> </u>	0000	000	0.000	0000	0000	0.000	000	0.011	0.084	0 1 20	3	0.189	0.241	0.287	0.329	0.388	0 408	0.442	0.477	0.510
	Time [sec] [Vc	¥	3 3	COL	125	145	185	188	205	228	276	7	286	288	308	328	AAR	200	286	808	428

20 cm Control 10-wall prount

X Th

Ve 2.102 0.005

Whis 9.527 0.034

Pure to Additional muchi





1966 2966 6976 医鼠蚤虫虫属 医马耳氏系统 医马马克氏病 医克克克氏病 医医克克氏氏病 医克克氏病 医克克氏病

Page 1

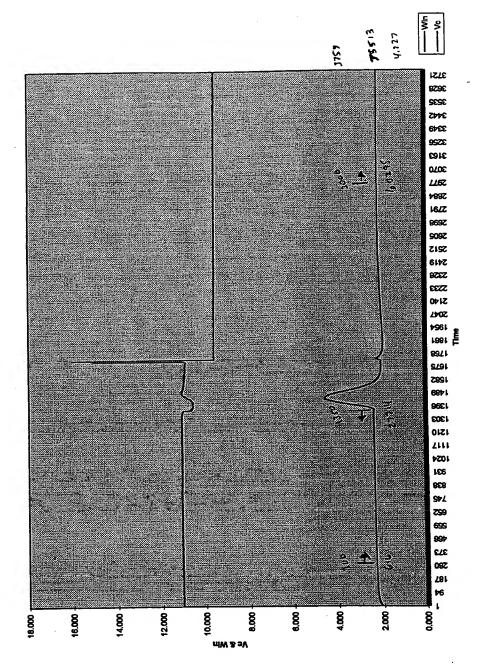




Т	7	_	Т	7	_	Γ	Т	7	_	Ţ	٦	_	Т	Т	_		T	٦
		7,7																
	5.84 hr	nel (1.2%	- 1		2.369	44 428	11.120		2 188		9.607							
_		40 west no.	I Wall BO	Average Std Dev Min Max	2.326	ľ	11.040		2 140		9.543							
	350 [11 wat	1000 2769 P	0000	Std Dev	0.012		บ.บาร		7000		0.012							
	2 096 Statistics from 300-1350 [11 watt point]	The state of the s	NIOII OUR	Average	2355		11.085		2 400	Z. 100	9.573							
	Statistics			2.096 11-watt		2	Min.	2 099 10 watt		Ç	Win							_
ş	2.098		2.096			Z.040	2.096 Win	2.089	١	2.103 VC	2 109 Win			2.120	2 425			2.135
Win	O RAA		9.860	9 859	40.049	10.213	11.031	11 045	2001	11.050	11 050	3	11.045	11.052	44 AE4	150.11	11.048	11.073
	0 407	6.10	0.197	0 197		0.204	0.221	0 224	0.221	0.221	1000	0.22	0.221	0.221	400	0.221	0.221	0.221
رة.	0,140	9.419	0.419	0110	0.110	0.419	0.419	0070	0.420	0.421	677	0.422	0.423	0.424		0.425	0.428	0.427
N	9000	7.080	2.096	1000	7.080	2.096	2 naa	200	4.08B	2 103	100	7. JOB	2.114	2 120	2	2.125	2.130	
Time feed	-12	\ <u>8</u>	207	200	177	247	787	100	/87	202	200	35/	347	787	3	387	407	101







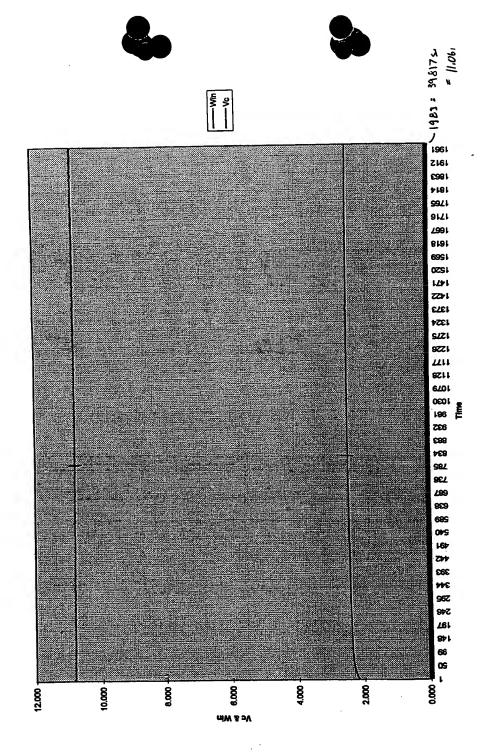
1 000





	T																7
1696 848 12 6,36 hours			Max	2.464	-												
54. 17. 12.			Min	2 439		1											
10001		983	Average Std Dev	O OOKE1	- [901100											
		2 168 Statistics from 834-1983	Average	SA C	2.433	10.808											
TP030797		Statistics			2	2.179 Win							-	6	2	8	0
	200							2.190	2.195	2.201	2.208	2.210	2.214	3 2.219	2.222	3 2.228	3 2.230
	Win	10 557				10.840	10.838	10.851	10.833	10.824	1	١	10.830	10.816	10.807	10.828	10.818
	,	0 244	1		0.217	0.217	0.217	0.217	0.217	0.216			0.217	0.216	0.218	0.217	0.218
	/	3	-	0.434	0.435	0.438	0.437	0,438	0.439				l			0.445	0.448
	3	200	Ì	2.170	2.174	2.179					1			Ì			١
	- 1	IIIII Seci	66	119	139	159	179	199	210	220	250	279	300	320	340	380	280

0.0055 0.0055 20cm control 2,453 10.60E





TP03797P

340005

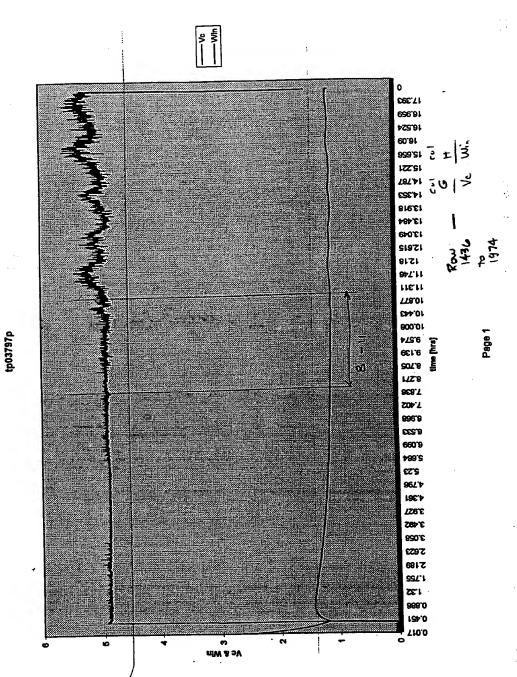
_	_	_	1	<u>~ 1</u>	_	_	_	_	-			_	7	_	_	Т	_	٦		г	ī	7
		1	YRIM	1.105	5.179																	
			ZiiZi	1.067	4.79																	
		Т		1.084258	1888		1	+				1	_						-	t	1	1
\ -	44		Average.	43 1.08	0 040137 4 931686			-	_	-	+	-		-	1	+		_	-	1	+	
	Low House	OL HOL	Std. Dev.	0.009543	0 0401	2.5							_									
	And Market	3.637 Statistics from Dougle-11		ş	Alle	AAIII																
uj.M		3.637	0,113	0.094 Vc	0 00 V	0.00	0.066	0.083	0 071	200	0.0/3	0.079	0.077	-	١	0.074	0.073	0.071				0.051
		2.459	2.45	2 424	1	7.381	2.339	2.298	2 250	200	2.221	2.185	2.45	277	2.110	2.084	2.052	2002	1000	1.893	1.985	1.937
1 (my)	AA (CIII) AIIIII	0.017	0.00	8000	0.020	0.034	0.039	0.045	900	3	0.058	0.082	780 O	20.0	0.0/3	0.078	0.084	080	0.00	0.095	0.1	0.108
l	WEIL	3.637	0 442	200	o.uga	0.081	0.096	0.083	1000	10.0	0.075	0.079	7770	0.07	0.074	0.074	0 073	4200	0.0	0.061	0.057	0.051
	>	0.073	000	0.002	0.002	0.002	0.001	1000	3	100.0	0.002	0 000	200	0.002	0.00	0.001	000	1000	0.001	0.001	0.001	1000
	× G	0.492	100	0.48	0.484	0.478	0.468	a v	24.0	0.452	0.444	0.437		0.43	0.423	0.417	77.0	2 .	0.404	0.398	0.393	1000
	ζ <u>ς</u>	2 4 50	4.430	2.45	2.421	2.381	2330	200.0	7.280	2.259	2 221	2 405	2.100	2.15	2 118	2084	4.004	2:032	2.022	1.993	1 985	
	Time (sec) Vc	100	ō	81	101	121	177	100	101	181	201	200	777	241	282	200	107	302	322	342	282	3 3

20 cm. Control 5wat point $X_c = 1.084$ $W_{lin} = 4.932$

0.0095 0.0491





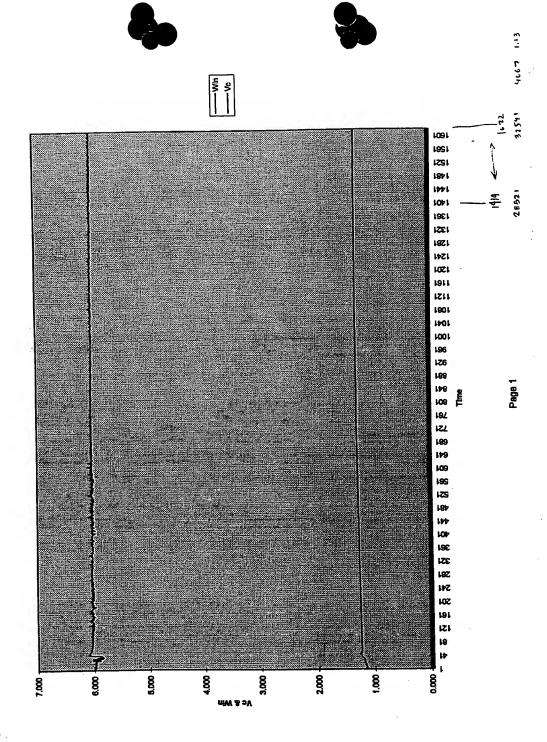






										_					_
		Max	1.301	6.033											
	hrsj	Min	1.297	5.987											
	1,135 Statistics from 1419-1622 [1.13 hrs]	Std Dev	0.001	8000								4	T.		
	rom 1419-	Average	1 299 0.001	and a	0.00										
	Statistics !		3		AAIII										
2	1.135	1 137	1 130 Ve	1.100	1.14 I WIII	1.144	1.148	1.148	4 4 80	1.130	1.152	1.154	1.156	1.158	1.161
Win	5.980	000	9.00	000	2.882	5.895	6.002	5.974	2003	3.8/4	5.972	5.982	6.009	5.980	5.980
	0.119	000	0.120	0.120	0.120	0.120	0.120	0 119		9119	0.119	0.120	0.120	0.120	0.120
×	0 227	2000	0.227	0.220	0.228	0.228	0.229	0 229		0.230	0.231	0.231	0.231	0.232	0.232
, JAC	1 135	2011	1.13/	1.138	1.141	1.144	1.148	4148	2	1.150	1.152	1.154	1.158	1.158	1.181
Time feer!	7		131	151	171	181	211	100	107	251	271	291	311	331	351

20 cm control
6 wath point
V_C 1,299 0.008
Wie 6.009 0.008

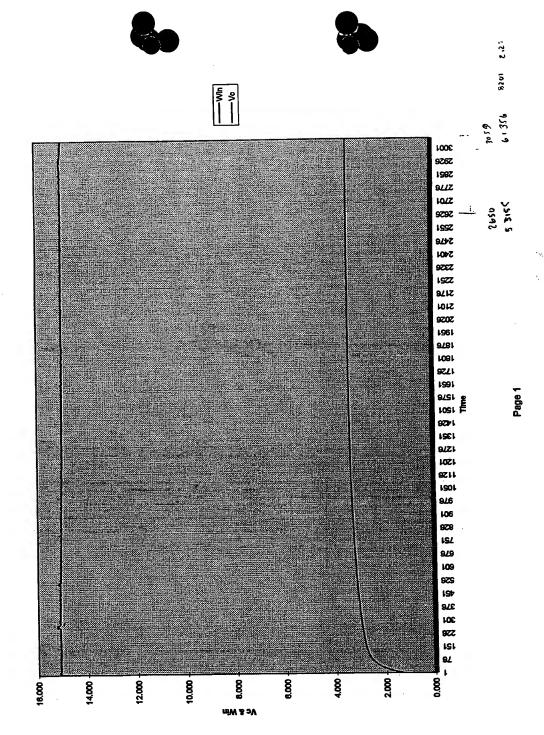






-								_					_			_		_			_
			Max	3.461	100 37	10.034			_												
	Hrs	1		1 441	ľ	14.937											L				
	2004 Occasion from 2000-2000 2 278 Hrs	2000	Std Dev	8000		0.018	-						y	ļ							
	from SARO.	110111 4000	Average	9 464	0.4.0	14.982															
	04444	STRIBUCE) VC	Min			Ĺ							_					_
۲	ľ	1.301	ľ			1.397 Win		1.43/					1.548			1.616	1		4 A70		1709
Win		14.686	14 890		14.938	14.951		15.071	45 404	10.10	48 448	١	15.128	١		15 145	1	15.145	١	١	15.13
		0.294	90C U	0.400	0.299	0 200	2071	0.30	000	0.302	0000	U.30K	0 303		0.303	0 303	3	0.303	6000	0.303	D 303
1	2	0.260	1000	0.404	0.271	0.270	0.210	0.287		0.295	000	0.302	0 240	2123	0.317	0 222	0,020	0.330	0000	0.338	CPEU
		1 301	200	1.322	1.358	4 207	1.00.	1 437	-	1,475		1.512	4 540	0+0.	1.583	1010	010.1	1.649		1.678	4 700
- 1	ime (sec) Vc	84	5	2	105		124	4/4	2	184		185	100	COZ	225		242	285	2	282	200

20 cm Contel 15 wat point 16 3.451 0.006 Win 14.982 0.018

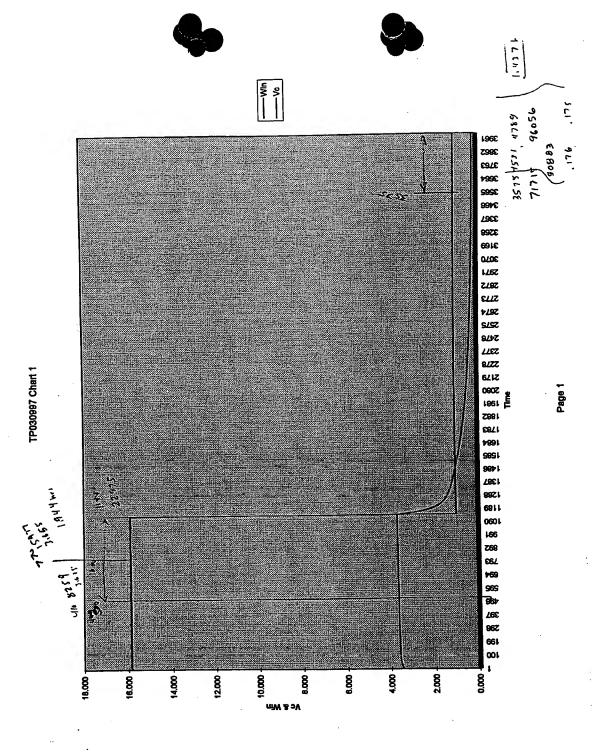






		T																				
			olnt								-				1				1			
	tuint moint	watt pour	and from 4531-4789 [1.437 hrs] for 1 watt point	Max	X B	3.671	15 93	2		0.178	4 070			A 17R		1.078						
	Land 600 48	3,453 Statistics from 770-1144 [1.944 nrs] for 16 walk point	[1.437 hrs]	-		3.853	1 4E 857			0.173		1.U38		0 479		1.039		\ \ \			L	
	770 73 777	-1144 [1.944	4531-4789		Sta	0.005	0 043			74 0.001		0.007	_		0.00	54 0.007						-
-	-	cs from 770	and from	Ī	Average	3.664	1	15.865		0 174		1.054		į	0.1/4	1.054					-	
 -		53 Statistic	2	3	3.459 16-watt	2 483 Ve	2	3.466 Win	3.47 1 watt	2 472 Me	3 0	3.476 Win	9 A70	0	82	3 485		3,488	3.49	3 493		3.485
5	3	_													1 3.482							
18/20	AAIII	15.791	١		15.809			15.835	15.832		13.04	15.865	45 979		15.871	18 ARS		15.855	15.875	15 872		15.885
	×	0.316	950	0.310	0.318			0.317	0.317		0.31/	0.317	l		0.317			0.317	0.318	0 247		0.318
	2	0 691	1	LRQ.O	+ 0 892	1000	0.083	0.693	A ROS		0.685	0.698		0.090	0 897		180'0	0.698	0.698			0.699
		2 453	0.10	3.455	2 450	30.430	3.403	3.468	217		3.473	3.478		3.478	2 482	101.0	3.400	3.488	3.49	000	3.483	3.495
	Time [sec] Vc	70	0	66	110		139	159	470	2	188	240		239	250	800	8/2	288	310		255	360

20 cm Control
16 wat X Or 3.664 0.005
Wir 15.885 0.012
1 wat 0.174 0.001
Wir 1.059 6.007







control	
20 cm	

P. 00.0 Ve oseo

TP031097

0.001

0.000

Average Std Dev N 0.000 0.000 0.050 0.001

0.188 Win 0.189 Vc

0.183 0.181

0.001 0.001 0.001 0.001 0.001

0.034

0.174 0.168

107 127 147

0.148 0.143

0.001 0.001 0.001 0.001

0.029 0.029 0.028 0.028

0.139

0.139 0.141

.

0.148

0.151

0.001 0.001 0.001

0.163 0.158 0.158 0.158 0.151 0.148 0.148

167 168 207 228 247 288 288 308 328 348 368

0.158

0.053 0.053 0.053 0.053 0.053 0.054 0.054 0.055 0.055

0.158

0.032 0.031 0.030

0.032 0.031

Max

Σ

0.174 Statistics from 502-3147 [16.67 hrs]

0.048 Ν

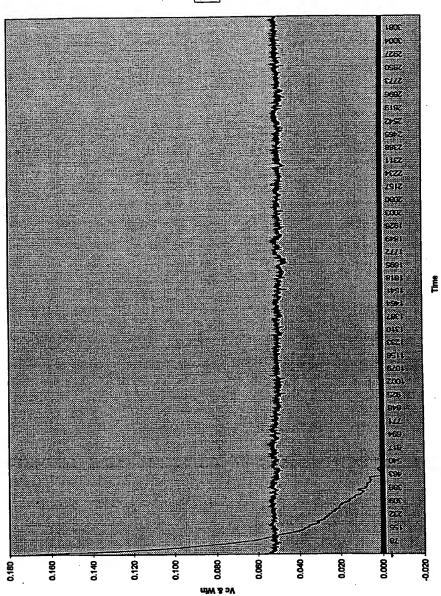
Λ¢

[380]









Page 1





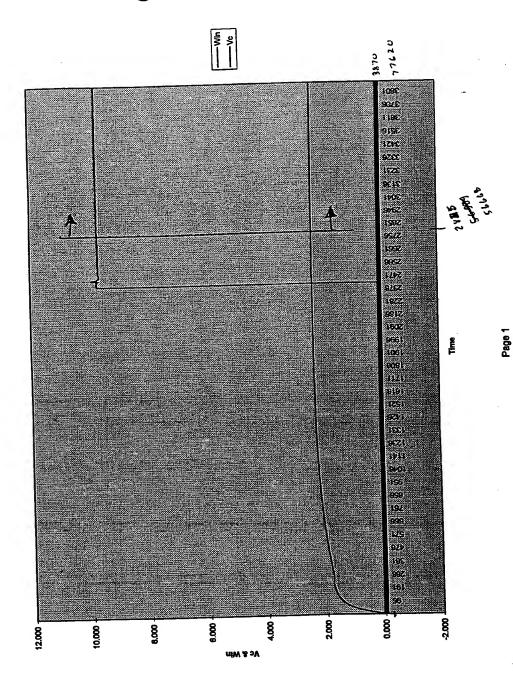
T	T					1																				
		1100	Pressure Additional RZC	S.	Yes	3	2	Yes	Yes	Yes	Yes	Yes	Yes	Yes	Yes	Yes	Yes		Yes	Yes	Yes					
			Pressure	253.7	CAT Charle	Disdot-100	253	0.15T-1.7atm	253-265T	0.1-576T	0.075T	0.068-0.075T	0.068T	0.068T	0.0675-0.069T	0.0875T	0.04-813T		0.8-813T	0.04-0.06T	0.040T		Average of Points	Minimum	Мехатит	Std Devlation
	ental Results		Excess Power [watts]	0.577						0.592	1.184		0.879	0.537	0.404		0.172		605.0-	0.396	0.412		0,640	0.172	1.231	0.308
	cm Experin		Hours [ss]	000	3.00	5.5/5	4.272	2.899	13.635	7.484	14.439	31.194		3.578	6.870	14.698	4.836	.836 Hour Peri	0.752	1.198	0.515					
	Summary of 20 cm Experimental Results		Date[s] of Run	101101	IDIAL-71	13-Mar	15-Mar	16-Mar	16-Mar	17-Mar	17-Mar	18-Mar	19-Mar	19-Mar	20-Mar	20-Mar	21-Mar	Subsets of Data in 4.836 Hour Period Above	21-Mar	21-Mar	21-Mar					



_		\neg	_	_	_	_	_	$\overline{}$	-	1	_		Т	1	7	T	٦
1	-	1	1	1	1			1		1	1		1		1		
	4	-	60	9	\downarrow	4		$\frac{1}{1}$	_	-	-	\dashv	\downarrow	4		+	4
		Max		9.718													
	្ន		2.328	9.847													
	0.000 Statistics from 2825-3870 [5.82 hrs]	Std Dev Min	0.002	0.012			-										
	rom 2825-3	Average 8	2.333	9.683													
	Statistics f			Win													
۸c	0.000	0.000	0.008 Vc	0.032 Win	0.059	0.088	0.118	0.149	0.180	0.212	0.244	0.277	0.309	0.341	0.372	0.403	0.433
Win	0000	0.000	0.00	0.000	0.000	0.000	0.000	0.000	0.000	0.000	0.00	0.00	0.000	0.000	0.000	0.000	0.000
5	0.190	0.190	0.192	0.194	0.195	0.196	0.197	0.199	0.189	0.199	0.199	0.199	0.199	0.200	0.199	0.188	0.188
Vc.	0.000	0.000	0.002	0.00	0.012	0.017	0.023	0.030	0.038	0.042	0.049	0.055	0.082	0.088	0.074	0.080	980.0
	0000	0000	0.008	0.032	0.059	0.088	0.118	0.149	0.180	0.212	0.244	0.277	0.309	0.341	0.372	0.403	0.433
Time [sec] Vc	88	68	109	129	149	169	189	209	229	249	269	289	308	330	348	370	390

From Calibration Line Ve : 2,333 = 10,260 wath expressed.

excess walts = 0577



TP031297 Chart 1

the property of the party of th

passed were and the second

		9)
	T	T	

Т	1	7	T	T		Ţ	T	T	1	Т	Т	7	Т	Т	1	-	7
												-					
		Max	2.378	9.888													
		ii.	2.309	9.657													
	[5.575 hrs]	Std Dev	00'0	0.080													
	2.333 Statistics from 2-2004 [5.575 hrs]	Average 8	2.323	9.880													
	Statistics		۲ç	Win													
۸c	2.333	2.333	2.333 Vc	2.333 Win	2.334	2.334	2.334	2.334	2.334	2.334	2.334	2.334	2.334	2.334	2,333	2.333	2.334
M	9696	9.694	9.890	9.686	9.714	9.693	9.695	9.692	869'6	9.678	9.657	9.684	9.705	9.694	9.723	9.708	9.682
_	0.194	0.194	0.194	0.194	0.194	0.194	0.194	0.194	0.194	0.194	0.193	0.194	0.194	0.194	0.194	0.194	0.194
<u>^</u>	0.486	0.487	0.487	0.467	0.467	0.467	0.487	0.487	0.467	0.487	0.467	0.467	0.487	0.467	0.467	0.487	0.487
<u>ح</u>	2 333	2 333	2 333	2.333	2.334	2.334	2.334	2,334	2.334	2,334	2.334	2.334	2.334	2.334	2.333	2.333	2 334
Ime fseci	45	55	85	78	85	98	108	118	128	138	147	158	188	178	186	198	208

From Calibration Line. Ve = 2,323 = 10,217 wetts expreshed

exacr wats (0,337 wetts

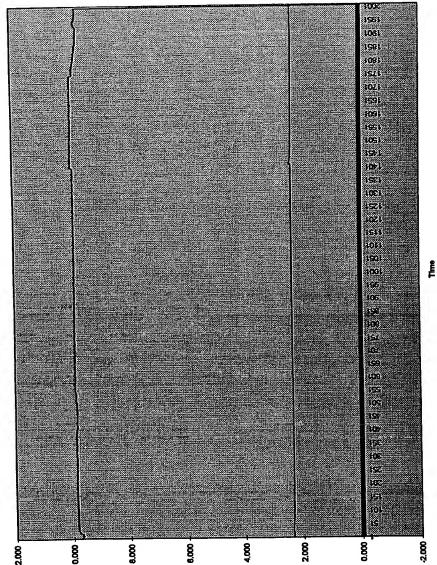




TPO31397 Chart 1







1 908

8

							T		T									
		Max		2.437	9.845													
	72 hrs]				9.671													
	0.000 Statistics from 5555 to 7089 [4.272 hrs]		Std Dev	0.010	0.058													
	rom 5555 t		Average	2.419	0 R24	0.021												
	Statistics	Charles		γ	Miles													
Ņ	1	3	0.00	0000	000	0.000	0.004	0.023	0.044	0.067	680'0	0.111			0.171			0.224
Win	200	0.00	0000	0000	000	0.000	3.962	3.951	3.957	9.828	9.797	9.818	9.817	9.815	9.801	8.809	9.798	9.724
	777	110.0	0.159	0 198	9	0.198	0.198	0.198	0.198	0.197	0.198	0.198	0.198	0.198	0.198	0.198	0.198	0.194
1/01	- 1	0.000]	0000	000	30.0	0.000	0.001	0.004	0.00	0.013	0.018	0.022	0.028	0.030	0.034	0.038	0.041	0.045
	0000	0.00	0000	000	0.000	0.00	0.004	0.023	0.044	0.067	0.089	0.111	0.132	0.152	0.171	0.189	0.207	0.224
The Passes West	I IIII Sec	48	ខ្	8	â	79	68	8	109	118	129	139	149	159	189	479	189	199

From Calibration Line

Vc = 2.419

= 10.628 walls expected

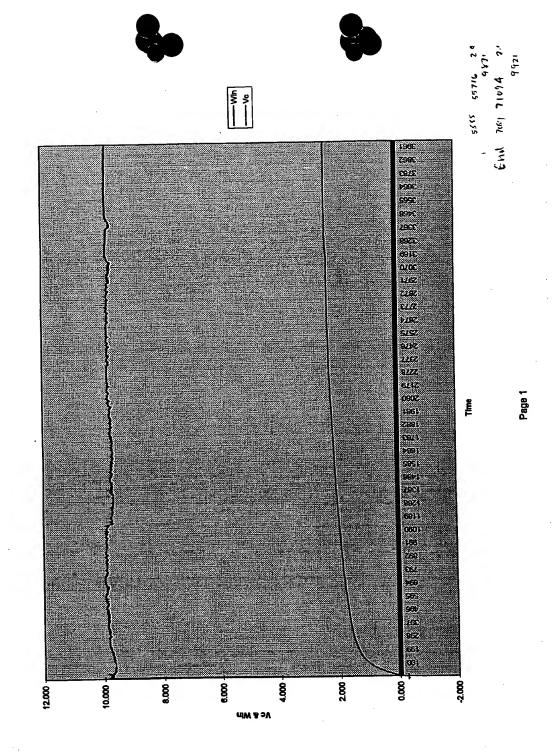
Exers Watts = 0.804







	•			<u> </u>				
	Win	Predicted \	Vc	1				
	0	-0.0605		Given Vc=	2.419			
	1	0.1728		Estimated				
		0.4061		Watts Out	10.628	watts of po	wer	
+		0.6394		Actual =	9.824	watts of in	put power	ļ
		0.8727			0.804	excess wa	tts of power	produce
	5		1					
	6							ļ
	7	1.5726					· · · · · ·	
	- 8	1.8059					 	
		2.0392						
	10	2.2725				 		
	11					ļ	 	
	12					<u> </u>	 -	
	13						 	
	14					+		+
	1:						· · · · · ·	
	16	3.6723					+	
						 		+







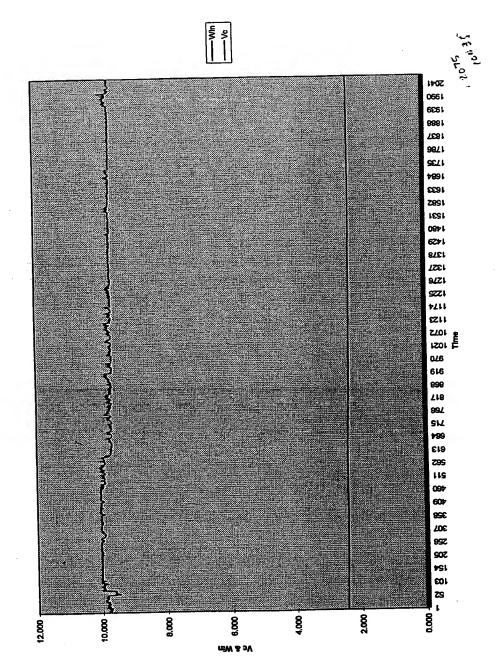




Win	Predicted Vc				ł
	-0.0605	Given Vc=	2.350		
	0.1728	Estimated			
2	0.4061	Watts Out	10.333	watts of power	
- 3	0.6394	Actual =	9.765	watts of input power	
4	0.8727		0.568	excess watts of power	produced
5	1,106				
6	1.3393				ļ
7	1.5726			· ·	<u> </u>
8	1.8059				
9	2.0392				ļ
10	2.2725				
11	2.5058				
12					
13					
14				<u> </u>	
15				 	
16	3.6723				







ide 1

4



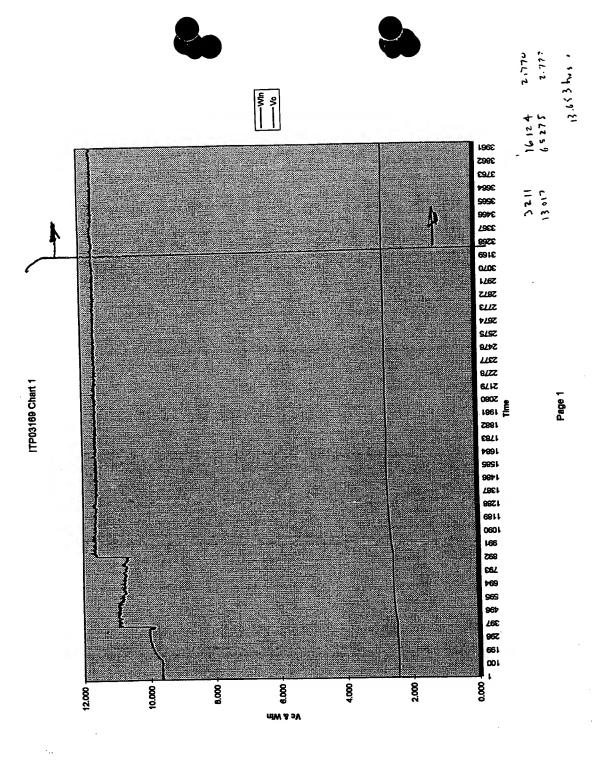


T																	
		ă X X		11.787													
		E	2.767														
	2.434 Statistics from 3211 to 13017 [13.635 hrs]	Std Dev		0.035													
	rom 3211	Average	2.78	11.6													
	Statistics f		2	Win													
Š	2.434	2.434	2.434	2.435	2.435	2.435	2.435	2.435	2.435		2.435		2.435	2.435	2.435	2.435	
Win	9.847	9.658	9.660	9.660	9.650	9.665	9.657	9.684	9.683	9.628	9.635	9.643	9.641	9.652	9.660	9.680	9.678
	0.193	0.193	0.193	0.193	0.193	0.193	0.193	0.194	0.193	0.193	0.193	0.193	0,193	0.193	0.193	0.194	0.194
۸c.	0.487	0.487	0.487	0.487	0.487				0.487						0.487	0.487	0.487
	2.434	2 434	2 434	2.435	2.435	2.435	2.435	2.435	2.435	2.435	2.435	2.435	2.435	2.435	2.435	2.435	2 425
me [sec] Vc	39	44	40	54	82	8	68	72	62	88	89	8	8	5	109	114	440





						
 Win	Predicted \	<u>Vc</u>				
0	-0.0605		Given Vc=	2.793		
 1	0.1728		Estimated			
 2	0.4061		Watts Out		watts of power	<u> </u>
 3	0.6394		Actual =		watts of input power	1
 4	0.8727			0.607	excess watts of power	r produced
 5	1.106					
6	1.3393					
 7	1.5726					
 8	1.8059					
9	2.0392					
10	2.2725					
 11	2.5058					
 12						
13	2.9724					
14	3.2057					
 15						
16	3.6723				ļ	+
 1						







			600	2.883	11.945															
_	_	Max			11.523 11	-	-	1			1						-		$\frac{1}{1}$	
	64hrs]	Min		ı		-				-	_	_		-	-		+		$\frac{1}{1}$	
	5363 [7.4]	Std Day			0.054				.						_					٠.
	from 2 to	Average			າ 11.652															
	2 773 Statistics from 2 to 5363 [7.464hrs]			۲ ۲	Win										_		_			_
Λc	2773	27.5	7.7.13	2.773	2.773	2.773	2.773	2.773	2.773	2.773		2.773	2.773							2 773
W.	11 827	10.0	010.TT	11.64	11.641	11.819	11.603	11.624	11.614	11.607	11.843	11.625	11.804	11.643	11.649	11,678	11.68	11.668		44 24
	0 223	0.50	0.232	0.233	0.233	0.232	0.232	0.232	0.232	0.232	0.233	0.233			0.233	0.234	0.234	0.233	0.233	0000
Vc.	OFFE	0.00	0.555	10.555	0.555	0.555	0.555	0.555	0.555	0.555	0.555	0.555	0.555	0.555	0.555	0.555	0.555	0.555	0.555	200
	0 773	۲.//۵	2.773	2773	2.773	2773	2773	2.773	2.773	2.773	2773	2773	2773	2.773	2.773	2.773	2.773	2.773	2.773	4
Time feer IVe	A COOL OF THE	/7	32	38	42	48	52	57	62	87	72	14	2	87	92	26	102	101	112	

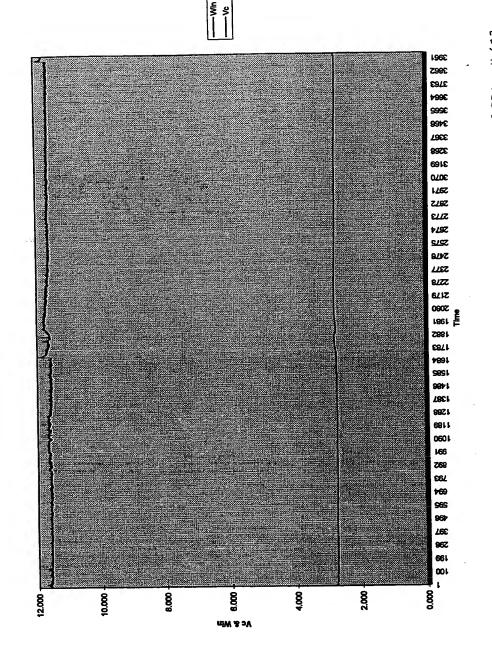
Contact Street





Win		Predicted \	VC.					
VVIII	0			Given Vc=	2.796			
	- 1	0.1728		Estimated				
	- 1/2	0.4061		Watts Out	12.244	watts of power	er	
	_ 3			Actual =	11.652	watts of input	power	
					0.592	excess watts		
	5							
	<u></u>							
	$-\frac{3}{7}$							<u> </u>
	8	1.8059						
	9							
	10	2.2725				ļi-		
	11					 -		
	12					 		
	13							
	14							
	15					 		
	16	3.6723	·			 		
		 	+-		· · · · · ·	 		—
		 	┼			 		
			+					







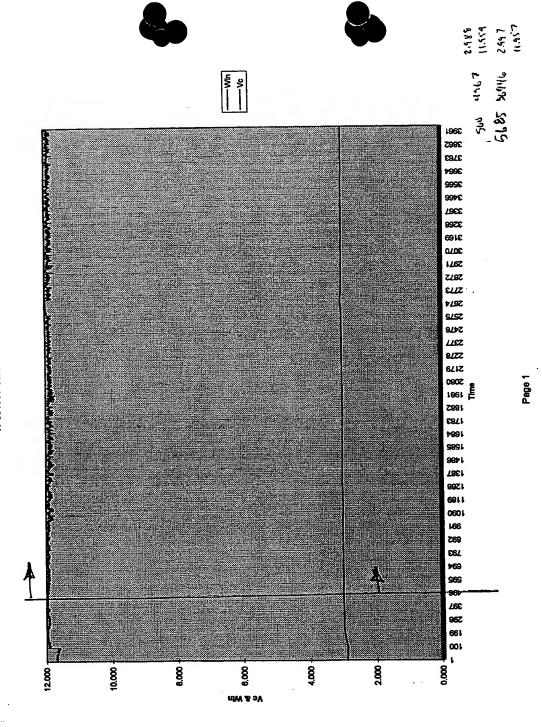


			5	2			+								1							
		Max		١	11.998									-								
	39 hrs	Min		2.908	11 700																	
	5685 [14.4	Otal Day		0.008	0.082	0.002																
	Statistics from 500 to 5685 [14.439 hrs]		Average	2.985	44 800	11.080																
	Statistics f			Vc	1000	MIN																
Vc	0 000	2.002	2.882	2 882		2.882	2.882	2.882	000	7.007	2.882	2 882	4.004	2.883	2.883	2 883	i	2.003	2.883	2 002	2.003	2.883
Win	44 000	000.1	11.670	11 RR0		11.684	11.679	11.680	000	789.11	11.703	44 897	200	11.686	11.691	44 AR4	I		11.690	1		11.887
	100	0.234	0.233	0 223	203.0	0.234	0.234	D 234		0.234	0.234	7600	0.634	0.234	0.234	1200	0.234	0.234	0 234		0.234	0.233
×	-1	0.5//	0.577	677	1,5,0	0.577	0.577	0.577	200	0.577	0.577	-	0.577	0.577	0.577	1	0.07	0.577	0.577		0.577	0.577
۸۵.		2.882	2 882		7.007	2.882	2 882	0000	7.007	2.882	2 882		2.882	2.883	2 883	2000	2.883	2.883	2 882	4.000	2.883	2 883
We feer! Vr	and BI	32	25		74	47	52	1	67	35	AK	?	22	85	76	2	8	95	36,	20	115	426





	Predicted	Vc				l	
Win			Given Vc=	2.985			
			Estimated				
	1 0.1728		Watts Out	13 054	watts of po	wer	
	2 0.4061			11 80	watts of in	nut power	
	3 0.6394		Actual =	4 464	excess wa	tte	
	4 0.8727			1,164	EXCESS WE	1	1
	5 1.106						
	6 1.3393	3]				10 Ye	
	7 1.5726	3					-
	8 1.8059	9			 	 	+
	9 2.039	2			ļ	 	┼
	10 2.272	5				 	
	11 2.505	В					+
	12 2.739	1					
	13 2.972	4			<u> </u>	+	+
	14 3.205						┼
	15 3.43						+
	16 3.672				<u> </u>	 	+
		+			1		





_		1	_	1	_	T	1	- T	_	_	Т	_	T	Т	Т	Т	Т	٦
		1100		1	12.024													
	4 hrs	1	CIN.		11.558													
	2 000 Statistics from 2 to 11198 [31,194 hrs]		Std Dev	0.070	0.160													
	from 2 to 1	2 4 110 11	Average	2.999	11.883									2.2				
	Chatletine	Otationica		ΛC	Win													
Ve		3.008	3.009	3.008	3.008	3.008	3.007	3.008	3.005	3.005	3.004	3.004	3.003	3.003	3.002	3.001		3.001
Win	1 000	040'11	11.876	11.866	11.878	11.820	11.888	11.862	11.787	11.882	11.807	11.757	11.752	11.909	11.931	11.904	11.893	11.895
ĺ.	000	0.235	0.238	0 237	0.238	0.238	0.237	0.237	0.238	0.238	0.238	0.235	0.235	0.238	0,239	0.238	0.238	0.238
, , , ,	- 1	0.602	0.802	0 802	0.802	0.602	0.602	0.602	0.602	0.601	0.601	0.601	0.601	0.601	0.801	0.601	0.601	0.601
279		3.008	3 000	3008	800.5	3.008	3.007	3.008	3.005	3,005	3.004	3.004	3.003	3.003	3.002	3.001	3.001	3.001
1	I I Bec	9	2	2 6	38	9	110	120	131	140	150	180	170	180	180	200	210	220

Page 1



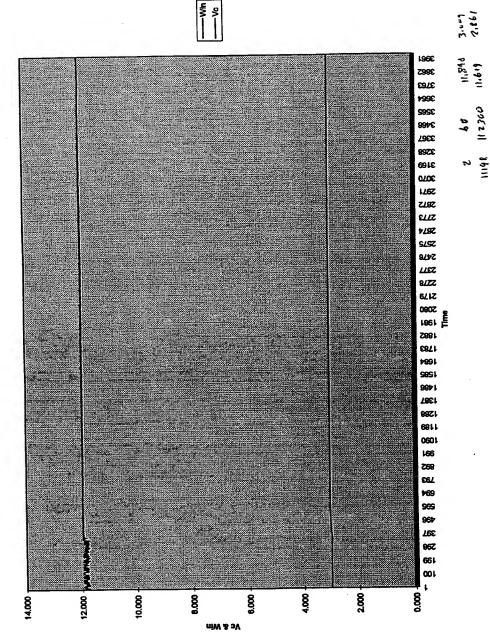


March 5 - March 10, 1997

1							├ ─
							┼
Wi	n	Predicted \	/c				┼
	0	-0.0605		Given Vc=	2.999		
	1	0.1728		Estimated			——
	2	0.4061		Watts Out		watts of power	
	3	0.6394		Actual =		watts of input power	
	4	0.8727	-		1,231	excess watts	
-	5	1.106					
	6						┼──
	7						
	8	1.8059					
	9	2.0392					┼
$\neg \neg \neg$	10	2.2725					
	11	2.5058					
	12	2.7391					
	13	2.9724					
	14	3.2057					┿
	15	3.439				L	+
	16	3.6723					







Page 1





		Max	2.847 2.882	11.533 11.779			\neg	Max		11.874 11.982							
	5310 [14.781 hrs]	Std Dev Min	0.004	0.024			to 6594 [3.576 hr	Std Dev Min	0.001	0.011							
	2.861 Statistics from 2 to 5310 [14.781 hrs]	Average	Vc 2.857	Win 11.827			2.861 Statistics from 5311 to 6594 [3.576 hrs]	Average	Vc 2.843	Win 11.909							
Vc	2,861 St	2.881	2.861	2.881	2.881	2.861	2.881 8	2.861	2.861	2.861	2.861	2.861	2.861	2.861	2.860	2.861	
WIn	11.583	11.608	11.624		11.597	11.629	11.632	11.831	11.830	11.628	11.845	11.835	11.854	11.641	11.642	11.645	
J	0.232	0.232	0.232	0.232	0.232	0.233	0.233	0.233	0.233	0.233	0.233	0.233	0.233	0.233	0.233	0.233	
۲ ۷۶.	0.573	0.573	0.573	0.573	0.573	0.573	0.573	0.573	0.573	0.573	0.573	0.573	0.573	0.573	0.573	0.573	
	2.861	2 861	2 881	2.881	2.881	2.861	2.881	2.861	2.881	2.881	2.861	2.861	2.861	2.881	2.880	2.881	
me [sec] Vc	35	45	55	92	75	85	85	105	115	125	135	145	155	165	175	186	

10e 1





March 5 - March 10, 1997

Win	Predicted	<u>Vc</u>				
0			Given Vc=	2.857		
1	0.1728		Estimated			
2	0.4061		Watts Out		watts of power	
3	0.6394		Actual =		watts of input power	•
4	0.8727			0.879	excess watts	_
5	1.106					
6						
7						
8						_
9						-
10						
11						
12						
13					<u> </u>	
14						
15						
10	3.6723	1				





March 5 - March 10, 1997

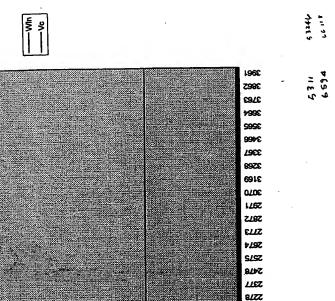
 Win	Predicted Vc				
 - 1	-0.0605	Given Vc=	2.843		
 	0.1728	Estimated			
 - 	0.4061	Watts Out	12,446	watts of po	wer ,
 3	0.6394	Actual =		watts of ing	
 	0.8727			excess wat	
 5	1,106				
 - 6					
 $-\frac{3}{7}$	1.5726				
 - 1 8					
 		— 			
 10					
 11					
 12					
 13					
 14					
 15					
 16					

6.000

10.000

4.000





TP031997 Chart 1

Sage 1

supplemental participation and the state of

- Acceptance





me feec! Vc		Vc.	×	Win	Vc				100		
	2 844	0.589	0.238	11.905		2.844 Statistics from 600 to 3067 [6.8/0 nrs]	from 600 to	3067 6.8	u nrsj		
- 1	2 844			11.908	2.844		Average Std Dev Min	Std Dev	Min	ğ	
70	2 844			11.918	2.844	Λc	3.078	١	- 1		
1 6	2 844			12.711	2.844	Win	13.040	0.024	12.961	13.080	
87	2 844		0.260	13.012							
5 6	2 845	١		13.023							
10	2.846			13.045							
117	2.848	0.570	0.281	13.056							
127	2.851		0.261	13.051	1						
137	2854	0.571	0.261	13.045							
147	2 858	1	ł	13.054							
157	2.859			13.048							
167	2.861										
177	2.883	0.573	0.281			5					
187	2.886		0.281	13.053							
197	2.868	0.574				8					
202	2 870	0.574	0.281	13.048	2.870	0					





Final report for period October-December 1996 In fulfillment of Service Contract with HydroCatalysis Power Corp. (now BlackLight Power, Inc.)

REPORT ON CALORIMETRIC INVESTIGATIONS OF GAS-PHASE CATALYZED HYDRINO FORMATION

Submitted by Prof. Jonathan Phillips* and Julian Smith Department of Chemical Engineering Penn State University University Park, PA 16802

Ph: (814) 863-4809 Fax: (814) 865-7846

Jonathan Phillips

Jalian Smith

Stewart Kurtz

Professor Stewart Kurtz Department of Electrical Engineering Penn State University University Park, PA 16802

Ph: (814) 863-8407 Fax: (814) 863-8561









SUMMARY

Tests for heat production associated with hydrino formation were carried out with two types of calorimeters during the period October-December 1996. Experiments carried out in a modified Calvet system yielded extremely exciting results. Specifically, initial results are apparently completely consistent with the Mill's Hydrino formation hypothesis. In three separate trials between 10 and 20 K Joules were generated at a rate of 0.5 Watts, upon the admission of approximately 10^{-3} moles of hydrogen to the 20 cm 3 Calvet cell containing a heated platinum filament and KNO3 powder. This is equivalent to the generation of $1*10^7$ J/mole of hydrogen, as compared to $2.5*10^5$ J/mole of hydrogen anticipated from standard hydrogen combustion. Thus, the total heats generated appear to be two orders of magnitude too large to be explained by conventional chemistry, but the results are completely consistent with the Mill's model. It must be noted that although the results presented in this report are very exciting, they require further verification. Moreover, it should be noted that some control studies are not yet complete.

Also included is a brief report on an attempt to replicate the Calvet cell results on a larger scale using the water bath calorimeter (described in some detail in an earlier report). Unfortunately, no evidence of 'excess heat production' was found. This can be linked to a failure to maintain the catalyst ions (K +) in the vapor phase. Specifically, it is hypothesized that the KNO3 catalyst evaporated from the containing pot at the reactor center, where the temperature is high, and deposited on the reactor walls, which are cold due to immediate contact with the calorimeter water bath. (That is, the catalytic material is 'cryo-pumped' by the cold walls.) Indeed, at the conclusion of the experiment, when the reactor was removed from the water bath, the walls of the quartz reactor were observed to be white in the general vicinity of the pot which contained the KNO3.





INTRODUCTION

Experiments were conducted to test the hypothesis that in the gas phase potassium ions will catalyze the conversion of hydrogen atoms to hydrino atoms. These experiments were initially carried out in a Calvet cell as this type of calorimeter is highly sensitive and accurate. Moreover, the conditions of the calorimeter are controlled.

RM's theory of hydrino formation requires that both K+ ions and H-atoms are present in the gas phase. In order to generate gaseous K+ ions, KNO3 is placed in a small (2cc) quartz 'boat' inside the calorimeter cell. The boat is heated, to increase the vapor concentration of KNO3, with a platinum filament, which is wound around the boat. A second function of the platinum filament is to generate H-atoms. It is well known that hydrogen molecules in contact with a heated filament will decompose, yielding a relatively high H-atom concentration in the boundary layer around the filament. Thus, according to RM's model, in a cell containing KNO3 in the boat and vapor phase hydrogen, there is a small region in the boundary layer around the heated metal filament which should contain sufficient concentrations of both H-atoms and K+ ions for hydrino formation to occur.

Calorimetric considerations require that a stable baseline exists before the heat generating process is initiated. Thus, signal change away from the baseline can be correlated to the onset of the process under investigation. In the present experiments the cell was run with KNO3 in the boat and the filament fully 'powered'. The calorimeter was allowed to equilibrate until a steady baseline existed. The 'hydrino formation' process was initiated by then adding gaseous hydrogen. Good calorimetric practice also requires that adequate control studies be carried out. Also required are repeated electric calibrations.

In the present work, data is presented which indicates that significant heat evolved upon the introduction of hydrogen to the Calvet calorimeter cell. In contrast, no heat was evolved upon the admission of helium. Repeated calibrations were also conducted. Thus, it appears that The RM





hypothesis is supported by the present results. A more definitive statement must await repeats of these experiments, and the results of a few additional control experiments.

An attempt was also made to employ the water bath calorimeter (see previous report to HPC) to detect excess heat. Indeed, the positive results of the Calvet study present a staggering challenge to conventional physics. Challenges of this magnitude require enormous experimental support. Thus, evidence of excess heat production from a second type of calorimeter would be useful. Unfortunately, the experiment failed to yield any evidence of excess heat. However, there is reason to believe that catalyst concentration was low and thus the failure to observe excess heat does not disprove the Mill's hypothesis.

EXPERIMENTAL SYSTEM

Calvet Calorimeter. The Calvet-type calorimeter employed in this study is similar to one described in the literature (attached) and is also described in earlier reports to HPC (now BLP). In essence a stainless steel cup of almost exactly 20 cm³ volume is placed in a calorimeter well such that the cup is surrounded by thermopiles on its sides and bottom. The cup and calorimeter are surrounded by a thick layer of insulation, and the entire device is placed inside a commercial convection oven. In all cases experiments were conducted with the oven temperature set to 250 C.

Reaction cell. For these experiments the top of the calorimeter cup/reactor cell was fitted with a Conflat knife edge flange. The top element of the flange is connected to a gas supply system outside the convection oven with a 0.5 cm OD ss tube, and with two welded vacuum high current copper feedthroughs. The feedthroughs were connected on the cup side of the flange to a coiled section of 0.25 mm platinum wire approximately 18 cm in length. Fitted inside the coiled platinum was a small quartz boat into which 200 mg of powdered KNO3 were placed.

<u>Plumbing.</u> On the outside of the oven the gas feed through is connected to a line leading to hydrogen and helium tanks, a pressure gauge, and a standard vacuum roughing pump. It is notable that the gas lines were all well insulated, both inside the oven, and for about 50 cm outside the oven.





The plumbing system was so arranged that the cell could be evacuated, and then isolated from the pump in such a way that hydrogen or helium could be added directly from high purity gas tanks. Great care was taken before the experiments were initiated to evacuate and flush the gas lines several times. It was also determined that the lines held gas pressure, with no loss in pressure, for several days. That is, there were no leaks.

Water Bath Calorimeter. This instrument is described in detail in the previous report to HPC. Two minor modifications were made for the present experiment. First, to facilitate the decomposition of hydrogen, the center section of the mandrel was wrapped with a 60 cm length (about 8 cm of mandrel) of 0.25 mm diameter platinum wire. Second, in the center of this section the same quartz boat (again filled with about 200 mg of catalyst) used in the Calvet system, wrapped with the same coil of platinum wire, was inserted into the circuit. (The experiment described was carried out after the completion of the Calvet system experiments.)

RESULTS

<u>Calvet Calorimeter.</u> The Calvet studies suggest large amounts of heat are generated upon the admission of hydrogen to the cell. In contrast, virtually no heat is observed upon admission of helium to the cell.

Calibration. The first tests performed on the Calvet system were electrical calibration experiments. The system was set-up for full experimentation: KNO3 was in the boat, the system was evacuated, and 10 watts of steady power were supplied to the platinum coil. After a steady baseline was achieved (approximately 10 hours after the oven was adjusted to 250 C), the cell was isolated from the pump and the pressure allowed to equilibrate (approximately 100 Torr). This did not appear to impact the baseline in any fashion. The power supply was then adjusted to deliver an additional 1 watt (11 watt rather than 10) for a specified time period. The power was then returned to the original 10 watt setting. A typical response curve is shown in Figure 1. The area under the response curve can be used to obtain a calibration constant which relates signal area increase to the number of extra Joules delivered. This was done in four cases (Table I). As can be seen, there is some error (+/- 15%) in the calculated calibration constant.





Control Studies. Helium was admitted, approximately 10 psig, to the cell to test the impact of a change in pressure, and heat transfer characteristics on the response of the cell. The helium was admitted after the cell had been isolated from the pump for a considerable time and a steady pressure (approximately 100 Torr) achieved. As can be seen in Figure 2a, the response was a short-lived small increase in output signal, followed by a relatively short time period during which the signal gradually returns to the original baseline. Within an hour the signal returned to the original baseline, with some drift evident.

The response of the system is expected. The helium increases the rate of heat transfer away from the platinum filament, and heated boat. Thus, the initial addition of helium to the system results in a temporary increase in the amount of heat reaching the thermopiles. That is, the boat and the filament cool off, until such time as the boat and filament have reached their new steady state temperatures. The steady state temperature of boat and filament are a function of heat transfer mechanism. After the admission of helium most heat transfer is occurring by convection to the walls. Before the admission of helium a considerable fraction is by radiation. Radiative transfer of 10 watts requires a higher filament/boat temperature than does convective heat transfer.

Figure 2b illustrates again the impact of adding pressure, or removing gas, from the system. Upon the addition of helium there is a very short lived increase in heat reaching the thermopiles. Upon pumping there is a period of time, perhaps an hour, during which the heat signal goes below the baseline. This is consistent with the model in that pumping makes convective and diffusive heat transfer minimal. Virtually all heat transfer is by radiation, which requires that the filament/boat temperature increase. It takes some time for this new steady-state temperature to be reached.

Hydrogen Admission. Hydrogen admission was carried out in much the same fashion as helium admission. The cell reached an equilibrium pressure, approximately 100 Torr, and then hydrogen at 10 psig was admitted to the cell. The valve to the hydrogen source, which was a steel line 4 meters by 0.6 cm OD, was closed off by a valve in front of the regulator during admission. Moreover, it was open for only a couple of seconds in each case. This was done on three separate





occasions, and the signal that evolved in response to these three processes is recorded in Figures 3, 4 and 5. One other observation recorded was that the pressure decreased gradually over time, such that after about an hour the pressure returned to the original equilibrium pressure of the cell. It must also be noted that the heat production was ended deliberately in all three cases by pumping the system to 5*10⁻³ Torr. It is clear 'excess heat' evolution would have continued in all cases if the system had not been evacuated.

It is expected that in the absence of reaction that the response of the cell to the addition of hydrogen would be similar to that observed for helium. Indeed, given that pressure measurements suggest that most hydrogen is adsorbed, or in some other fashion removed from the cell after an hour, even heat transfer effects should be totally transitory. Even in the event of reaction no more than a small heat signal is expected. Indeed, a high end estimate is that 25 cm³ of hydrogen at a temperature of 300 K and a pressure of 2 atmospheres entered the cell. This is equivalent to 2*10⁻³ moles of hydrogen. If all of that hydrogen interacted with oxygen to form water only 510 J would be generated. It is possible to imagine that the hydrogen could interact with nitrogen in KNO3 to form ammonia. Even less energy would evolve from this process. Thus, the largest heat peak might be expected to be 0.5 watts for 1000 seconds (approx. 17 minutes). A block of this size is marked on Figure 3.

It is clear from figures 3, 4 and 5 that hydrogen admission to the cell apparently leads to far more energy evolution than can be explained by any conventional chemical process. It is interesting in this regard to graphically contrast the response of the system to helium admission to the response to that for hydrogen admission. This is done on Figure 6 in which Figure 3 and Figure 2a are superimposed.

Water Bath Calorimeter. Studies conducted with the water bath calorimeter do not indicate the evolution of any excess heat. As shown in Figure 7 the increase in temperature almost exactly parallels the increase predicted on the basis of the amount of energy added to the system and the known heat capacity of water.





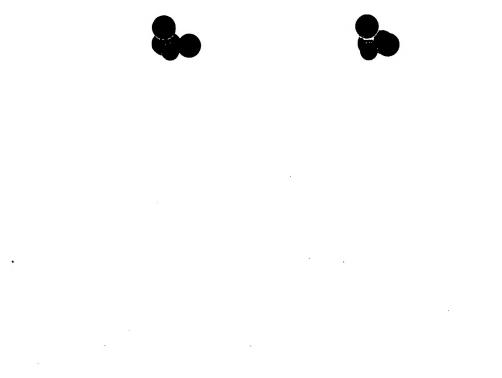
Do the results of the experiment refute the RM hypothesis? No. At the conclusion of the experiment the large cell was removed from the water bath and a white coating was seen on the walls in the vicinity of the pot which contained the KNO3. This suggests that the KNO3 was rapidly cryopumped by the walls, and that the gas phase concentration of catalyst was too low to be effective.

DISCUSSION

The evidence presented in this report clearly suggests that an extraordinary phenomenon takes place upon the admission of hydrogen to a cell containing a heated platinum filament and KNO3. This phenomenon appears to generate a tremendous amount of 'excess' heat. Still, the author of this report urges that a cautious approach be taken at present. Additional experimental work is required. A partial list of proposed additional experiments is given below:

- A control experiment consisting of admission of hydrogen to a cell in which 10 watts of power is applied to a platinum filament, but no KNO3 is present.
- 2) Hydrogen is admitted to a cell containing a platinum filament and KNO3 in a boat, but no power is applied to the filament.
- 3) The experiments are run as described in the present report, but the boat containing KNO3 is at the bottom of the cell, rather than in the center of the platinum coil.
- 4) The hydrogen admission experiments described above are repeated BUT continued for times sufficient to return the signal to the original baseline.

In addition, modifications in the apparatus should be made. First, insulation should be added to improve the stability of the baseline. Second, a quality pressure gauge should be attached to a known volume outside the oven such that all uncertainty regarding the number of moles of hydrogen admitted to the cell can be eliminated. Third, the plumbing should be re-arranged to facilitate 'capture' of gas for analysis using gas chromatography. Fourth, provision should be made to permit pressure to be recorded as a function of time.

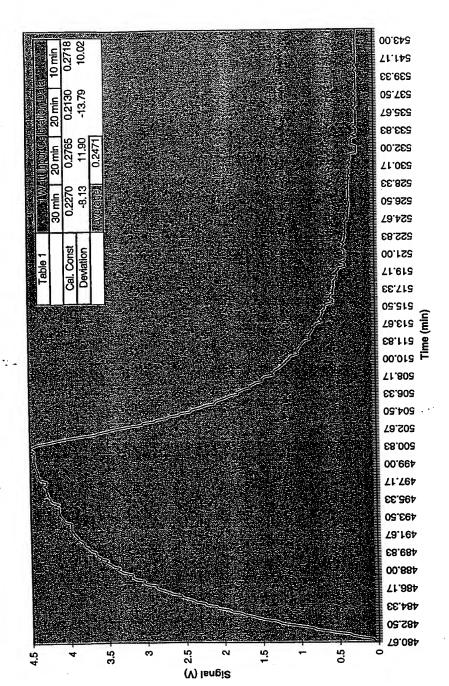


 $\cdot_{\scriptscriptstyle >}$





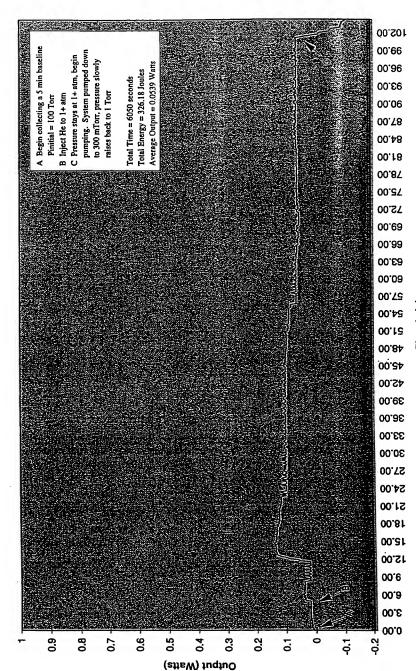
Typical Calibration Experiment: 1 W Input, 20 Mins







Heat Production, KNO3 w/ Helium Injection (BL1220A)

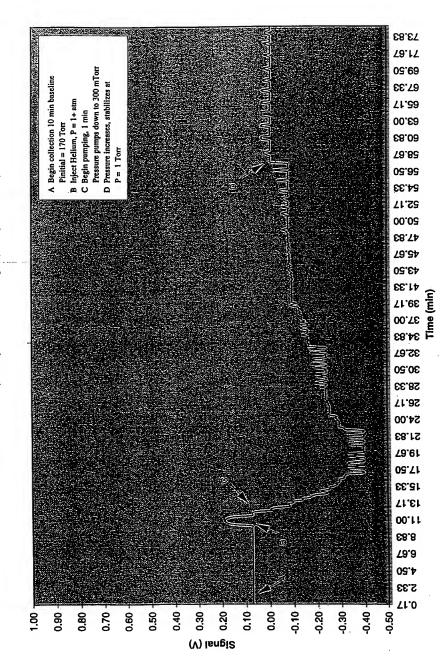


me (min)





Heat Production, KNO3 w/ Helium Injection (BL1219B)





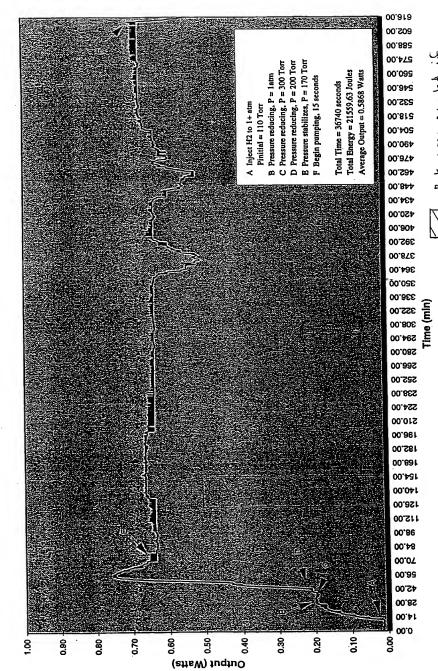


Sorm H20.

Figure 3

all admitted Hz reacts

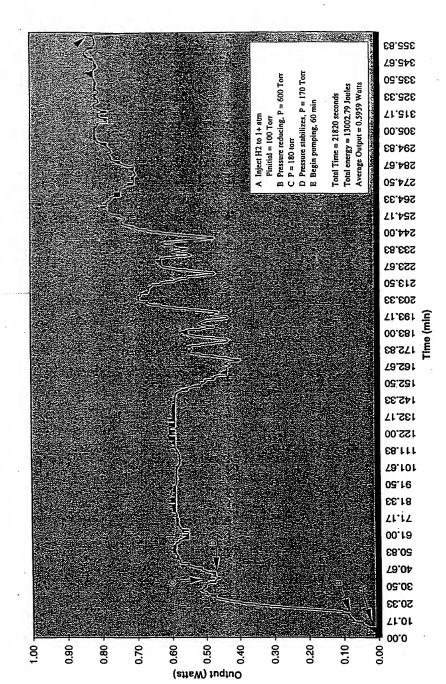
Heat Production, KNO3 w/ H2 Injection (BL1218CD)







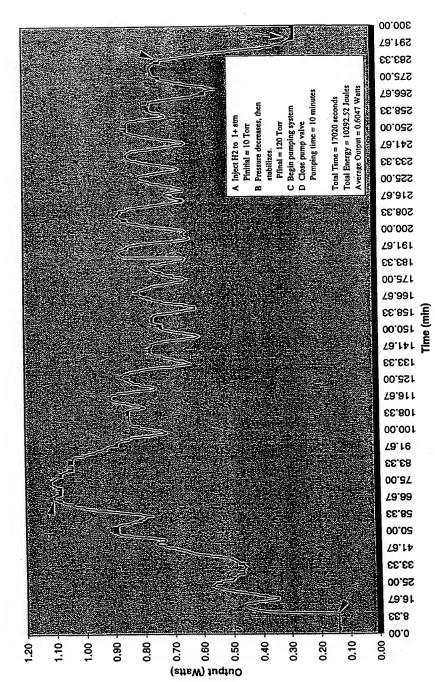
Heat Production, KNO3 w/ H2 Injection (BL1220BC)







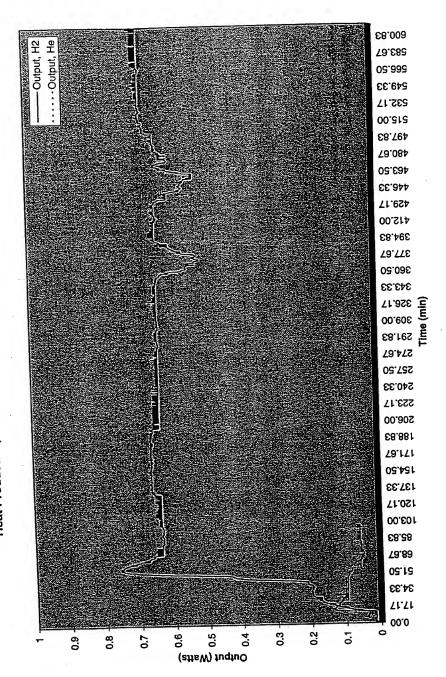
Heat Production, KNO3 w/ H2 Injection (BL1221AB)







Heat Production, KNO3 w/ H2 and He Injection (BL1218CD,BL1219B)



aure 6





THIS PAGE BLANK (USPTO)





CONSULTING REPORT

January 1, 1996

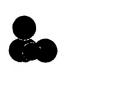
ADDITIONAL CALORIMETRIC EXAMPLES OF ANOMALOUS HEAT FROM PHYSICAL MIXTURE OF K/CARBON AND PD/CARBON

By Jonathan Phillips and Hyunsip Shim Department of Chemical Engineering Penn State University 133 Fenske Lab University Park, PA 16802 Ph: (814) 863-4809

Jonathan Phillips

Ph: (814) 863-4809 e-mail: PWA@PSU.EDU

CONFIDENTIAL





.

•

į.

,

,

.





INTRODUCTION

Repeatedly during the period from June to October 1995 apparent 'anomalous' heat was observed using one class of catalytic materials supplied by HCP corporation. Specifically, heats were observed, calorimetrically, of a magnitude not readily explained by conventional chemistry when pure hydrogen streams of about two atmosphere pressure were passed over the catalytic materials. The successful catalysts in all cases were physical mixtures of two materials: carbon supported potassium nitrate and carbon supported platinum.

The current report regards efforts to test four hypotheses. First, that HCP has mastered procedures which insure anomalous heat can be repeatedly obtained. Second, to illustrate that the choice of the carbon employed as a support has a small, but measurable, impact on the procedure for generating anomalous heat. Third, to demonstrate that the choice of noble metal can also marginally impact the process.

The fourth hypothesis is more complex. It is that the model of potassium transformation postulated in earlier reports is correct. That model consists of three parts. (i) Potassium nitrate is gradually reduced to potassium metal in the cell during the time that anomalous heat is observed. (ii) Once the potassium is fully reduced, heat evolution ceases. (iii) Potassium oxide (KO2 or KOH) only forms upon air exposure. Tests were designed to allow the testing of this model using weight loss, calorimetric measurement of heat evolution from oxygen exposure after catalyst deactivation, and x-ray studies.

Three samples were studied. The first sample discussed in this report was different than those studied previously for two reasons: (i)the support was changed to a commercial 'charcoal', (ii) the noble metal in the mix was palladium rather than platinum. The other two samples were prepared on the 'standard' support material, Grade GTA Grafoil (Trademark, Union Carbide), a moderate surface area, high purity, graphitic material. However, changes were made in the composition of these catalytic mixtures as well. Carbon supported palladium, rather than carbon supported platinum, was mixed with these samples.





All three samples produced 'anomalous' heat. On the basis of these results it is clear that HCP has developed procedures which allow the repeated observation of 'anomalous' heat, which can be observed in different laboratories. Yet, it was found that the identity of the support material does impact the result. In order to obtain anomalous heat from a charcoal supported sample it was necessary to operate at a higher temperature. The use of palladium rather than platinum also appears to have some impact. The two graphite supported samples contained palladium almost immediately produced heat upon the introduction of hydrogen at 125 C. Generally with platinum containing mixtures there was a lengthy 'induction' period, and in most cases a temperature higher than 125 C was required to insure the observation of anomalous heat.

Some NOVEL tests were carried out with the two Grafoil supported samples to test the model of potassium transformation. Specifically, careful measures of weight loss and careful calorimetric measures of heat evolution (only one sample) during oxygen exposure of the deactivated catalyst were carried out. The values obtained were in close agreement with the postulated transformations. Specifically the weight loss and the heat observed during oxygen exposure of the deactivated catalyst were near values anticipated on the basis of the model and the x-ray results.

In sum, the present results contain two important findings. First, HCP can produce catalysts which repeatedly yield anomalous heat, and second, the model of potassium transformation is consistent with all measures. The latter finding has particular significance as it gives additional credence to the claim that anomalous heat is observed. Indeed, the heat anticipated for the over-all conversion of KNO3 to KO2 or KOH, even accompanied by the creation of water and ammonia, is only weakly exothermic. The actual heat observed was significantly more than that anticipated from conventional chemistry. If these findings can be repeated (twice) and if DIRECT evidence of the conversion of the potassium to a zero valent state during hydrogen flow can be obtained (e.g. in situ x-ray) these findings can be made the basis of an article for the peer-reviewed scientific literature.





It must be emphasized that calorimetric measures alone are somewhat ambiguous and that in situ x-ray studies are strongly advised before sending the material for publication. It is also recommended that 'control studies' be carried out. In the absence of a noble metal it is likely that potassium nitrate will follow the same decomposition course, but the process should yield an endotherm, rather than a strong exotherm.

Finally, it must be noted the results of even the most careful calorimetric, x-ray and weight change experiments will not serve as a proof of the existence of hydrinos. Results from our lab will only provide strong evidence that heats higher than predicted by conventional chemistry are observed in the dry HCP cells.

EXPERIMENTAL

All experimental procedures and equipment was identical to that described in earlier reports with two exceptions: (i) a new BLUE M furnace was employed, (ii) a gas sampling system on the exit line was employed. Neither change should have any impact on the calorimetric studies.

RESULTS

SAMPLE 111395A - The sample contains 5.9567 gms of total material, and was nominally 43 percent by weight potassium nitrate (2.56 gms or 0.0253 moles KNO3). The support in this case was an activated charcoal obtained from Alpha Chemical. Charcoal loaded potassium made up 97% of the material, and the remaining 3% of the material was carbon supported palladium.

Previous experience with these samples at HCP indicated that heat is only observed at 200 C. Thus, after testing the calorimeter (Fig. 21-1) and baseline stabilization at 200 C in flowing helium (Fig. 21-2) hydrogen was introduced at 200 C. Almost immediately, a peak characteristic of hydride formation was detected (Fig. 21-3).

The signal decayed more gradually than usual for 'hydride' formation, and in fact, before reaching the original baseline the signal strength began a sharp climb in value. As shown in Figure





21-4 about 18 K seconds after hydrogen was first admitted the signal strength increased. In fact, about 24 K seconds after the increase began the signal saturated the amplifier (Figure 21-4). In fact, for almost 28 K sec. (approx. 7.5 hrs), the signal strength was higher than that computed for complete hydrogen conversion to water (0.24 Watts at a total flow rate of 2.16 ml/min at 300 K and I atmosphere of pressure). As usual, the signal gradually decayed to zero (Figs. 21-5,6,7).

The total heat produced before the signal decayed to zero was at least 23.4 kJ, or equivalently a minimum of 925 kJ was generated per mole of potassium. The actual heat generation was clearly higher as the amplifier saturated for about 6 K sec (Figure 21-4). Weight loss was also carefully determined. It was found to be 1.032 gms. Computations of the heat which would be generated by conventional chemistry were made. Only models consistent with the measured weight loss, and the x-ray analyses were considered. As discussed later the most likely set of reactions (Reaction Sequence I) is as follows:

 $\Delta H=+118.08 \text{ kcal/mole}$

 $\Delta H = -57.08 \text{ kcal/mole}$

 $\Delta H = -10.96 \text{ kcal/mole}$

For a sum reaction:

$$5/2 H_2 + KNO_3 --> K + H_2O + NH_3 + O_2 \Delta H = +49.32 \text{ kcal/mole}$$

This 'most likely' chemistry indicates that the reduction of the nitrate to the metallic state is an ENDOTHERMIC process. Rather than observing heat evolution, heat should have been absorbed during the reduction process:





Thus, there is a difference of more than 28 kJ between the observed process and the heat anticipated on the basis of the 'most likely' chemistry.

Not all of the data fully supported the Reaction Sequence I (RS I) model. First, the weight change was greater than predicted, and second the x-ray work showed that KO₂ (not potassium metal) was present after the reaction was completed and the sample exposed to air. Both findings can be partially explained by the fact that air exposure of fully reduced and well dispersed potassium should lead to a rapid exothermic process in which potassium metal is converted to KO₂ and concomitantly heat is generated. That is, following the formation of potassium metal it is likely two additional reactions (RS II) took place upon air exposure:

$$\Delta H = -68.1 \text{ kcal/mole}$$

$$\Delta H = -94.05 \text{ kcal/mole}$$

If both RS I and II took place the mass loss associated with the net process would be that of one N atom and one O atom for each molecule of KNO3 initially present. On this basis, and given the fact that 0.0253 mole of nitrate were initially present, the anticipated weight loss is: 0.76 gms. The measured weight change was -1.033 gms. (In fact, the above measure probably slightly overstates the weight loss as some sample is invariably lost during the two transfer processes between measurements: transfer to the calorimeter at the beginning, and transfer from the calorimeter at the end.) On this basis it is postulated that 0.273 gms were lost via the formation of carbon dioxide. The process of carbon dioxide formation that would use up 0.273 gms of carbon would yield a heat of 8.95 kJ.

In order to explain observed heats it is always reasonable to postulate chemistry different from the 'most likely' scenario (RS I). For example, if RS I and II both took place in the cell prior to air exposure (potassium oxide and carbon dioxide being the final products) a total of 10.94 kJ of heat would be generated. This is considerably less than that observed experimentally (23.4 kJ),





but not enough less that one could comfortably claim anomalous heat production. Moreover, this proposed sequence (I + II) is consistent with the x-ray data, as well as with the observed weight loss.

Other reaction processes are also consistent with the x-ray data. It appears that these other reactions ALL yield heats LESS THAN that for RS I plus RS II.. For example:

 $\Delta H = -7.82 \text{ kcal/mole}$

This reaction only yields 0.83 kJ for the number of moles of nitrate initially present. If this reaction occurred and carbon dioxide formation in the cell accounted for the remaining mass loss than a total of 9.78 kJ would be observed. Again, the computed total heat evolution is within a factor of 3 of that measured experimentally.

Given the composition of the catalyst, it is clear the greatest heat generation per gram would occur via the direct combustion of carbon. Indeed, if all the weight loss were associated with CO2 formation the heat evolved would be 33.04 kJ for a weight loss of 1.03 gms. This would clearly account for all the observed heat, as well as the weight change. It is not consistent with the x-ray results, or gas phase chemical analysis reported by HCP.

As shown in the x-ray results the sample prior to treatment consists primarily of carbon and potassium nitrate. The 'Before' results do indicate the limitations of X-ray analysis. For example, even lines from palladium, an element known to be present, cannot be found. Still, the comment that carbon and potassium nitrate are the predominant species initially present is undoubtedly correct (21-8, 21-9, 21-10). It is also clear that following the deactivation of the catalyst and is subsequent exposure to air the predominant potassium phase is KO2.

In sum, the above analysis indicates that additional data must be collected which limits the number of reasonable reaction sequences. The gas phase analysis conducted by HCP for example, tends to support the 'most likely' scenario above. That is, the discovery of NH3 and no reports of





CO or CO₂ support this analysis. The discovery of some NO supports the suggestion that the process may even be more endothermic than that suggested by the 'most likely' scenario.

In the next couple of experiments efforts were made to eliminate CO₂ formation during air exposure, and to insure that the heat released during the reaction of oxygen with reduced metal was determined calorimetrically.

SAMPLE 113095A - The sample contains 8.3276 gms of total material, and was nominally 37 percent by weight potassium nitrate (3.08 gms or 0.0305 moles KNO3). Grafoil loaded potassium made up 97% of the material, and the remaining 3% of the material was carbon supported palladium.

After the initial touch test (Fig. 22-1) the calorimeter temperature was raised to 125 C and held at that temperature in flowing helium for about 12 hours at which time it was determined the baseline was reasonably stable (Fig. 22-2). Hydrogen was introduced into the cell and almost immediately a moderate sized heat peak, generally considered to result from the formation of hydride, was observed (Fig. 22-3). About two hours after the 'hydride peak' reached its apex the signal began to rise significantly (Fig. 22-3). In fact, after about six hours the signal reached a value equivalent to the production of about 0.50 watts. Given a net input flow rate of 2.1 ml/min, and assuming a perfect stoichiometry of 2 hydrogen molecules per oxygen molecule, water formation would yield 0.24 watts. Assuming that all of the oxygen was 'free' and already present in the sample chamber (air leaks flowing inward against two atmosphere of hydrogen pressure assumed to be minimal), this flow rate of hydrogen completely converted to water would yield 0.35 watts. (In fact, there is no reason to believe there is any 'free' oxygen in the system. Any oxygen associated with a potassium oxide would yield scant heat upon potassium reduction and hydrogen oxidation. Reduction of carbon oxides would in fact be endothermic in most cases.) On the basis of the first calculation, it can be seen (22-4,5,6) that the rate of heat production exceeded that anticipated from the formation of water for 66 ksec (more than 18 hours). The catalyst clearly deactivated over the next 20 ksec (Figs. 22-6,7) until no heat at all was being produced. During





the period of heat production a total of more than 31 kJ of energy was evolved, or equivalently more than 1016 kJ/mole potassium initially present.

According to the model proposed by Phillips in earlier reports, the state of the fully deactivated catalyst should be metallic potassium. This suggestion was tested by exposing the deactivated sample to dry air (20% oxygen) slowly (approx. 20 cm³/min). A slow exposure to oxygen should prevent the type of rapid heating which conceivably can lead very high heating and concomitantly a limited amount of combustion of the carbon support. Unfortunately, due to a communication breakdown, no attempt was made to measure the amount of heat evolved.

A final measure of the weight loss of a sample which was handled in a fashion designed to eliminate post-deactivation combustion was quite revealing. The sample was found to lose 0.856 gms of weight. A net loss of one nitrogen and one oxygen per mole of nitrate initially present would lead to a weight loss of 0.915 gms. This suggests 'good' agreement between the model of potassium nitrate decomposition (RS I) and then potassium oxide (KO₂) formation during air exposure as outlined in the discussion of the previous sample above. According to that model at most 2.4 kJ could have been generated. This assumes there is no carbon dioxide formation. Indeed, given the weight loss there is no reason to believe carbon dioxide was formed.

If a worse case scenario is assumed, and all weight loss is attributed to the formation of carbon dioxide, we find that 28 kJ of total heat would be generated. This is close to the total amount of heat actually observed. Clearly it is important to unambiguously demonstrate that carbon monoxide and carbon dioxide are not generated to any extent during the 'reduction' cycle.

A 'best case' scenario may also be envisaged. Imagine that the decomposition process only produced potassium metal, oxygen and nitrogen (see first line in RSI). How many electron volts would be produced per atom of potassium initially present? That is, we assume that the 31 kJ observed is the net AFTER the heat required for the endothermic decomposition process is subtracted. This scenario requires that a total of 46 kJ were generated in an 'anomalous' fashion in order to account for the observed 31 kJ. Given the number of moles of





potassium initially present, this is equivalent to the generation of 15.7 eV/atom of potassium initially present.

Finally, it must be noted that analysis of this sample is not complete. X-ray study of the post treatment state of the potassium has not yet been carried out. The assumption that KO₂ is the final state of the potassium has not yet been demonstrated. As discussed with reference to sample 120495A (below), this is not always the case.

SAMPLE 120495A - The sample contains 8.82 gms of total material, and was nominally 37 percent by weight potassium nitrate (3.26 gms or 0.0323 moles KNO3). Grafoil loaded potassium made up 97% of the material, and the remaining 3% of the material was carbon supported palladium.

After the initial touch test (Fig. 23-1) the calorimeter temperature was raised to 125 C and held at that temperature in flowing helium for about 12 hours at which time it was determined the baseline was reasonably stable (Fig. 23-2). Hydrogen was introduced into the cell and almost immediately a moderate sized heat peak, generally considered to result from the formation of hydride, was observed ((Fig. 23-3). About four hours after the 'hydride peak' reached its apex the signal began to rise significantly (Fig. 23-4). In fact, after about seven hours the signal reached a value equivalent to the production of about 0.50 watts. Given a net input flow rate of 3.3 ml/min, and assuming a perfect stoichiometry of 2 hydrogen molecules per oxygen molecule, water formation would yield 0.37 watts. Assuming that all of the oxygen was 'free' and already present in the sample chamber, this flow rate of hydrogen completely converted to water would yield 0.55 watts. (In fact, as explained with reference to sample 113095a there is no reason to believe there is any 'free' oxygen in the system.) On the basis of the first calculation, it can be seen (23-4,5,6) that the rate of heat production exceeded that anticipated from the formation of water for 55 ksec (more than 15 hours). The catalyst clearly deactivated over the next 40 ksec (Figs. 23-6,7) until no heat at all was being produced. During the period of heat production a total of more than 33 kJ of energy was evolved.





According to the model proposed by Phillips in earlier reports, the state of the fully deactivated catalyst should be metallic potassium. This suggestion was tested by exposing the deactivated sample to dry air (20% oxygen) slowly. The air was mixed with helium to insure the rate of heat evolution during the oxidation process could be measured. Also, a slow exposure to oxygen should prevent the type of rapid heating which conceivably can lead very high heating and concomitantly a limited amount of combustion of the carbon support. The composition of the oxygen containing mix was nominally that shown on Figure 23-8; however, there is reason to believe that the mix ratio was not precisely controlled. In any event, it is clear that heat did evolve upon the slow exposure of the sample to an oxygen containing mix for several days (Fig. 23-9 through 23-17). The total heat evolved during this period of time was about 10.5 kJ.

X-ray studies revealed that the primary product of the slow oxidation process was potassium hydroxide. There was evidence that KO₂ was present in limited amounts. In previous studies conducted in this laboratory the Grafoil supported deactivated samples were found to be primarily KO₂ with some KO₃ present. The reason that KOH formed in the present case probably relates to difference in the rate of oxidation. In previous studies oxygen exposure was rapid, probably leading to great increases n temperature, which probably favored more complete oxidation.

Weight loss can be used as a check on the x-ray analysis. The weight 'loss' anticipated for the net conversion of 0.0323 moles of KNO₃ to KOH is 1.45 gms. The observed weight loss was 1.20 gms. In contrast if 50% of the potassium nitrate converted to KOH and 50 % to KO₂ the expected weight loss would be 1.21 gms. This suggests that the later estimate is more reasonable. In any event, there is no reason to believe that any weight loss should be attributed to carbon combustion.

Given x-ray analysis showing KOH as the final product rather than KO2, an effort to convert KOH to KO2 was undertaken. The sample was heated in air for four hours at 200°C. This caused the sample to gain weight, such that the NET weight loss was 1.02 gms (and not 1.20 gms). Given the number of moles initially present, the predicted weight loss for complete





conversion of KNO3 to KO2 is 0.97 gms. The measured weight loss is consistent with this model. X-ray studies to determine the final state of potassium are planned.

Given the assumption that potassium metal was present at the start of the oxidation process and the final composition of the potassium is a 50/50 mixture of KOH and KO2 the heat evolved should be 11.3 kJ. This compares very well with the actual heat evolved of 10.5 kJ.

An alternative hypothesis is suggested by the x-ray revelation that the final state of the potassium was KOH (Figs 23 18-26). This suggests that a model must account for the presence of hydrogen in the final structure. One explanation is that the potassium state prior to oxygen exposure was KH and not K-metal. This would increase the expected heat to some extent. That is, we assume the following reactions take place in parallel during oxygen exposure:

 $\Delta H = -87.7$ kcal/mole of potassium

 $2KH + 5/2 O_2 --> 2KO_2 + H_2O$ $\Delta H = -83.3 \text{ Kcal/mole of potassium}$

Next, we assume the same final disposition of the potassium (accounts for measured weight change) was a 1/1 mix of oxide and hydroxide. This would lead to the generation of 11.5 kJ. This is almost the same as that computed for the system assuming the final state of potassium was metallic.

It's revealing to compare the total heat evolved with the total heat anticipated simply from conventional chemistry. The conversion of 0.0323 moles of KNO3 per the reaction below:

$$KNO_3 + 4H_2 --> KOH + NH_3 + 2H_2O$$
 $\Delta H = -52 \text{ kcal/mole potassium}$

yields only 7 kJ for the amount of potassium originally present. Other scenarios yield even less heat. For example, if all the potassium were converted to oxide:





 $5/2 H_2 + KNO_3 --> KO_2 + H_2O + NH_3$ $\Delta H =-19$ kcal/mole potassium

less heat would be produced. In fact only 2.6 kJ would be produced via this route. Thus, the MAXIMUM heat that can be accounted for by conventional routes for potassium nitrate conversion is 7 kJ. Other factors, for example the need to account for weight change, suggest even less heat should have been observed.

Even this maximum value for heat production from conventional chemistry is more than a factor of six less heat than observed experimentally. The observed experimental heat, greater than 43 kJ, is the sum of that released during hydrogen flow (>33kJ) and that measured during oxygen flow (>10kJ). In fact, the predicted heat is less than that observed during the oxidation process alone.

Finally, it is worth considering a worse case scenario. How much heat would be released if all the weight loss were due to carbon combustion? Given the weigh loss of 1.02 gms, equivalent to less than 0.1 moles of carbon, we find 34 kJ would have been evolved to form CO2. This value is uncomfortably close to the value actually measured. Yet this scenario is extremely unlikely. Indeed, where would 'free' oxygen come from during the hydrogen flow process? Why would it react to form carbon dioxide and not water? Moreover, carbon doesn't combust well at only 125 C. How do we explain the clear change in the crystal structure of the potassium without concomitant weight loss associated with that process?

SUMMARY/RECOMMENDATIONS

It is now clear that heat can be produced repeatedly from mixtures of potassium nitrate loaded carbon and noble metal carbon samples provided by HCP. It is also clear that there is a regular pattern: hydrogen flow leads to heat production, initially at a very high rate, but gradually decaying to yield a 'deactivated' catalyst. This deactivated catalyst releases additional heat during subsequent exposure to oxygen. Moreover, a final x-ray analysis indicates the crystal structure of





the potassium changes from a nitrate to an oxide during the process. Weight change can be attributed to changes in potassium crystal structure alone, if oxygen is admitted slowly.

It is also clear that there are many conventional chemical scenarios which lead from the initial nitrate structure to the final oxide structure. None of these can account for the observed heats.

It is clear that the model of potassium transformation accompanied by anomalous heat needs to be strengthened before this model is submitted to the scientific community. Specifically, three recommendations for further study are made. First, it is recommended that tests to confirm directly the postulated change in the potassium from nitrate to metal in flowing hydrogen be undertaken. If it can be verified that heat is released during a process which converts potassium nitrate to potassium metal, then the claim that anomalous heat has been observed is greatly strengthened. The change from nitrate to metal is ENDOTHERMIC. The best method for carrying out the proposed work is to employ *in situ* x-ray analysis.

Second, it is recommended that the heat release and crystal structure transformations of potassium nitrate on carbon in the absence of any noble metal be studied. In the absence of hydrogen atoms it is postulated that the same decomposition of the nitrate will take place. However, there should be no anomalous heat production. In fact, the overall transformation of the nitrate to a metallic state in flowing hydrogen at elevated temperature should be endothermic. Following the complete decomposition of the nitrate oxygen exposure should lead to significant heat release. The behavior of these samples should also be studied using both calorimetry and *in situ* x-ray diffraction.

One change in procedure is urged. Every effort should be made to study the composition of the off-gas during anomalous heat production. A clear certification that carbon oxides are not detected strengthens the argument that weight changes are related to changes in the structure of the potassium nitrate and not to the combustion of the support material.









Fig. 21-1 Touch Test (111395a)

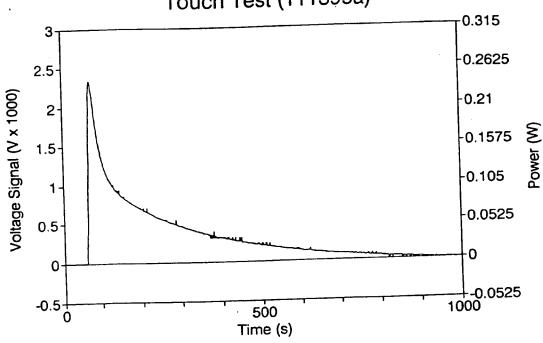






Fig. 21-2 Base Line 1 at 200 C (111395a)

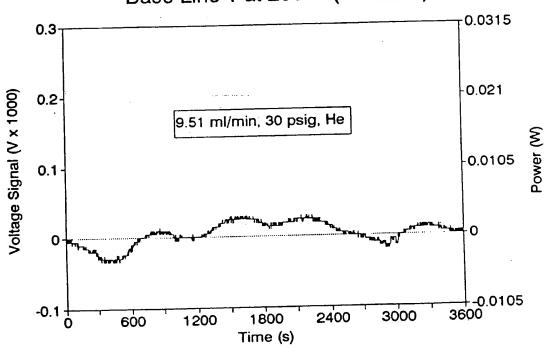






Fig. 21-3 Switch from He to H2 at 200 C (111395a)

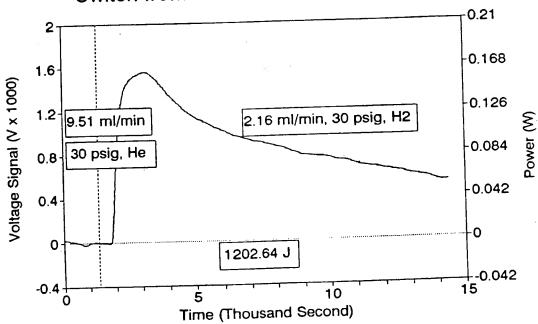






Fig. 21-4 H2 reaction 1 at 200 C (111395a)

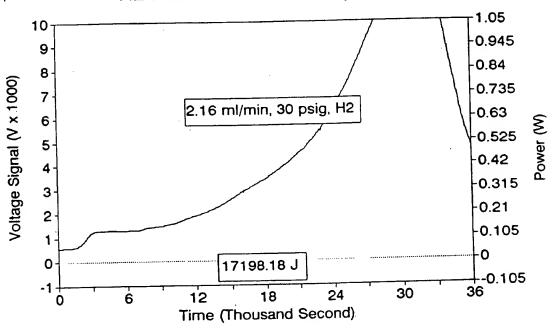






Fig. 21-5 H2 reaction 2 at 200 C (111395a)

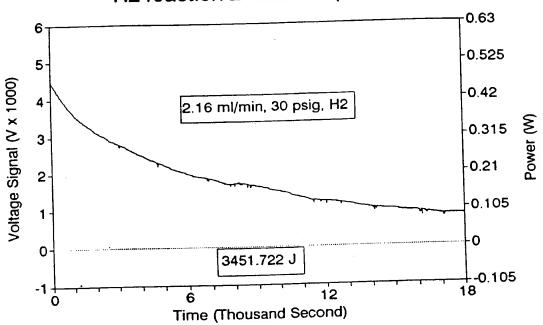






Fig. 21-6 H2 reaction 3 at 200 C (111395a)

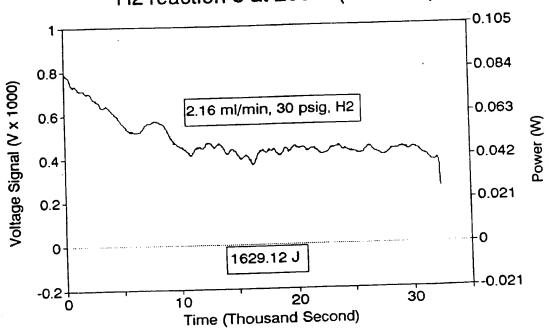
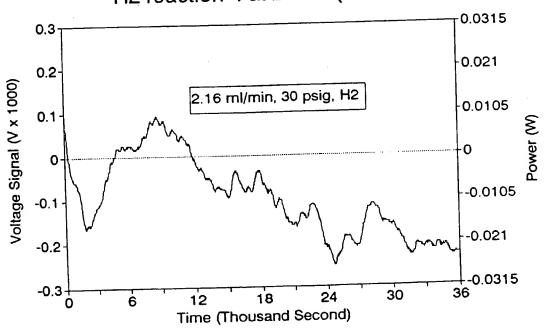






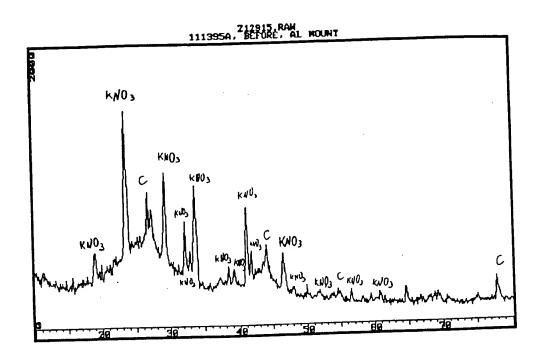
Fig. 21-7 H2 reaction 4 at 200 C (111395a)







111 395 A. Before

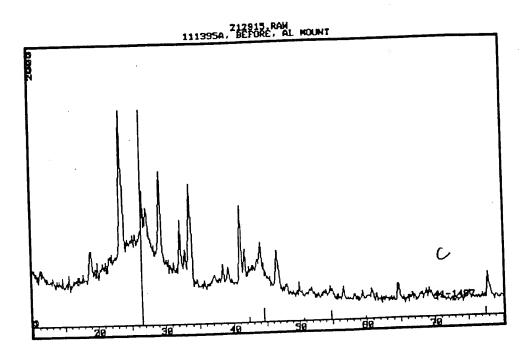






21-4

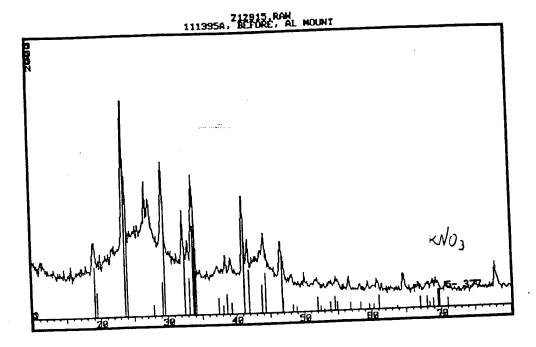
111 395 A, Before







21-10



:





Fig. 22-1 Touch Test (113095a)

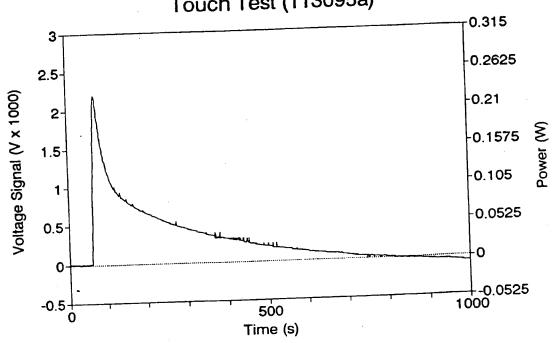






Fig. 22-2 Base Line 1 at 125 C (113095a)

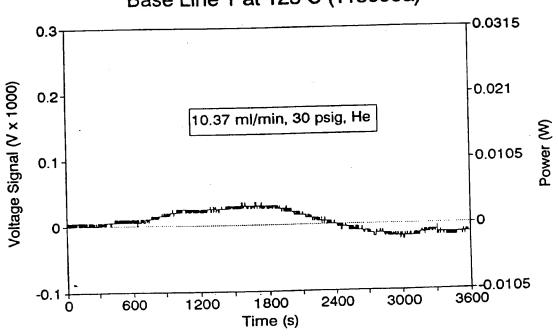






Fig. 22-3 Switch from He to H2 at 125 C (113095a)

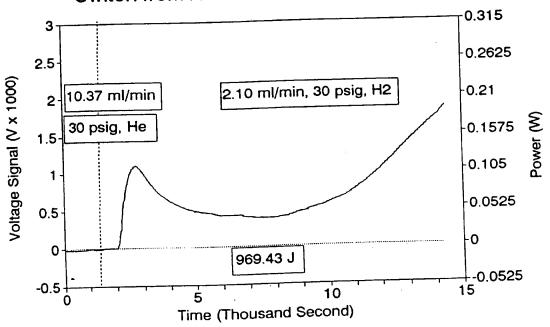






Fig. 22-4 H2 reaction 1 at 125 C (113095a)

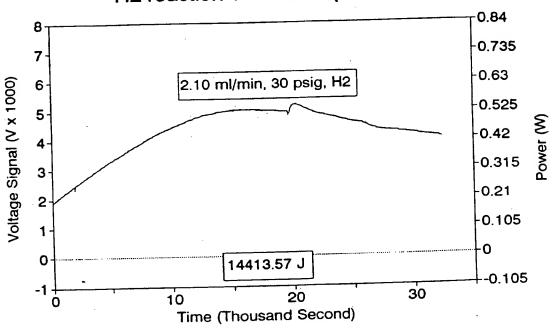






Fig. 22-5 H2 reaction 2 at 125 C (113095a)

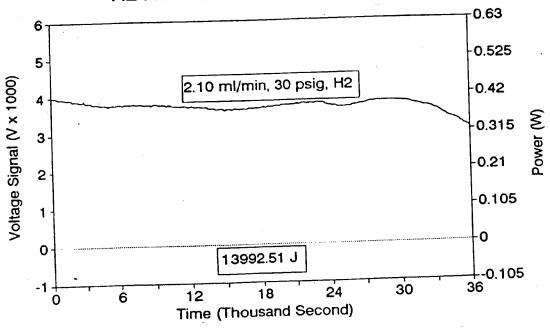






Fig. 22-6 H2 reaction 3 at 125 C (113095a)

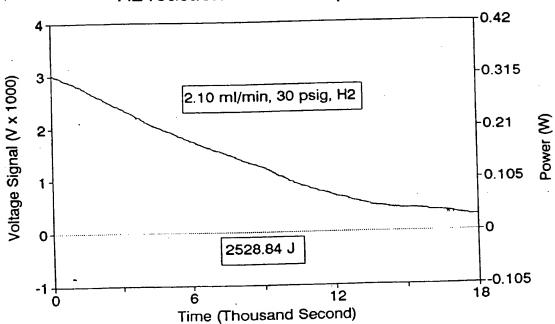






Fig. 22-7 H2 reaction 4 at 125 C (113095a)

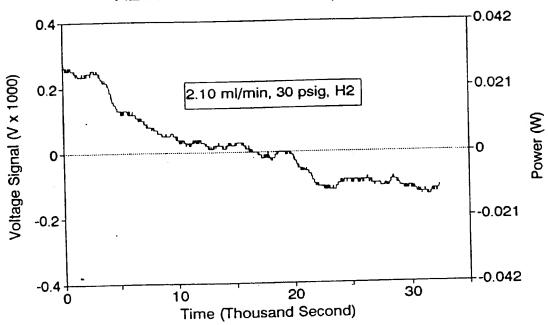






Fig. 23-1 Touch Test (120495a)

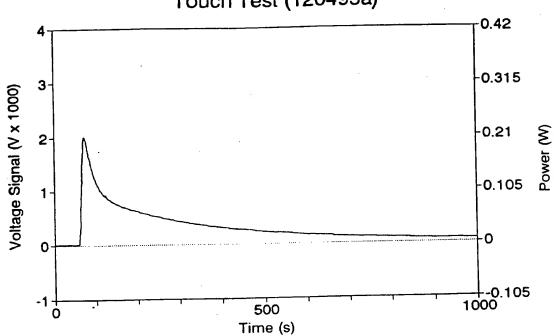






Fig. 23-2 Base Line 1 at 125 C (120495a)

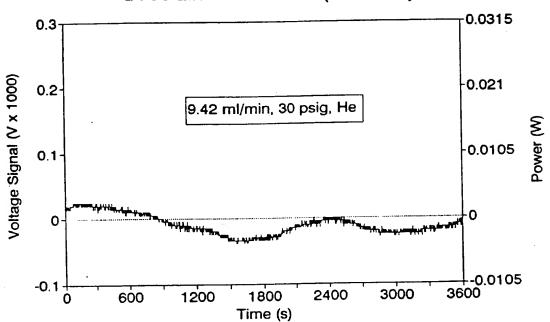






Fig. 23-3 Switch from He to H2 at 125C (120495a)

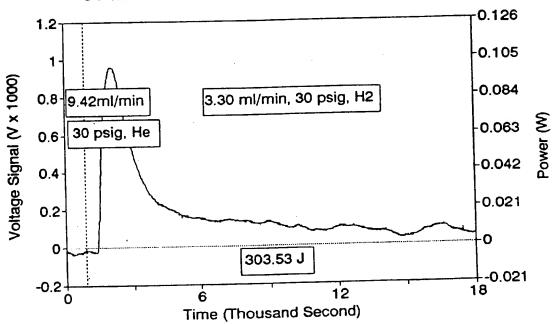






Fig. 23-4 H2 reaction 1 at 125 C (120495a)

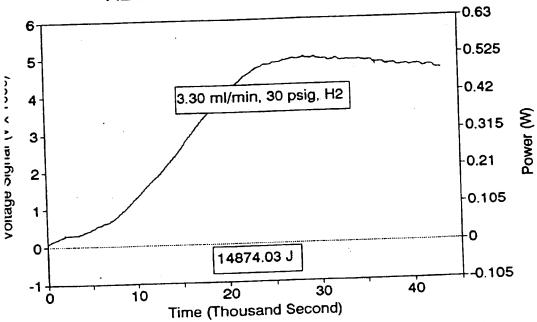






Fig. 23-5 H2 reaction 2 at 125 C (120495a)

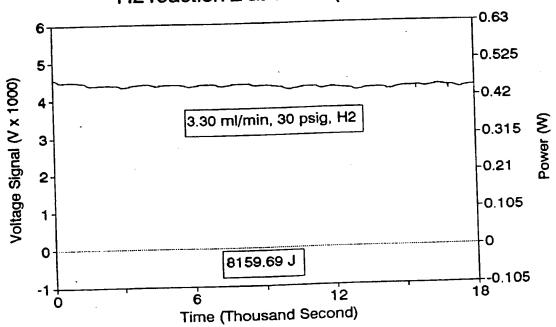






Fig. 23-6 H2 reaction 3 at 125 C (120495a)

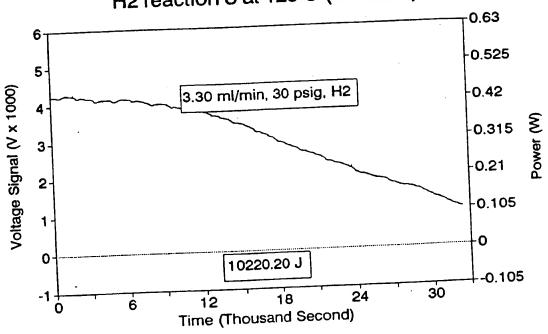






Fig. 23-7 H2 reaction 4 at 125 C (120495a)

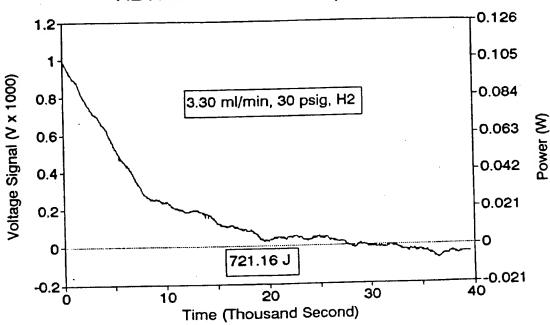






Fig. 23-8 Switch to (He+Air) at 125 C (120495a)

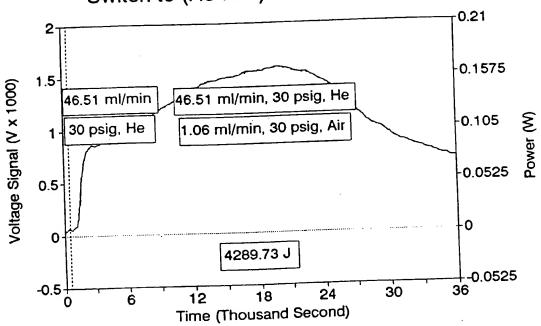






Fig. 23-9 Air reaction 1 at 125 C (120495a)

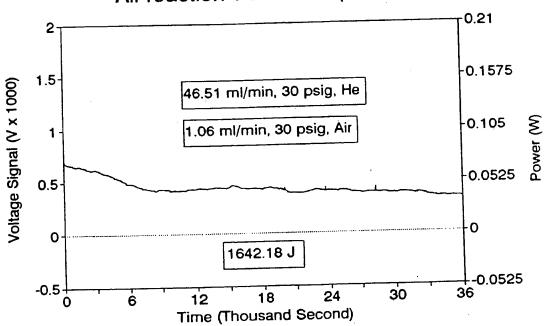
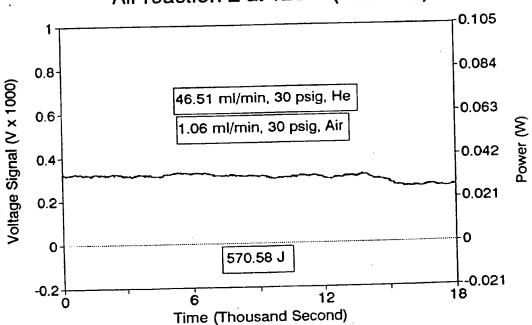






Fig. 23-10 Air reaction 2 at 125 C (120495a)



:





Fig. 23-11 Air reaction 3 at 125 C (120495a)

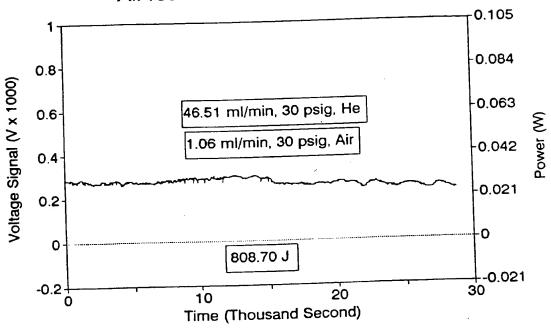






Fig. 23-12 Air reaction 4 at 125 C (120495a)

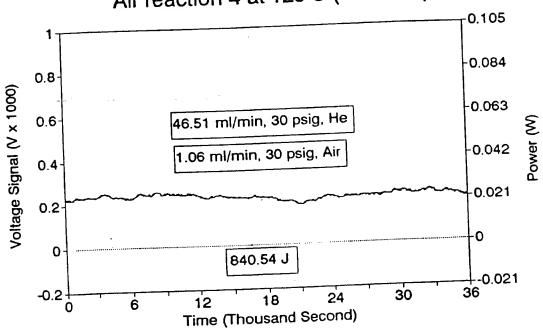






Fig. 23-13 Air reaction 5 at 125 C (120495a)

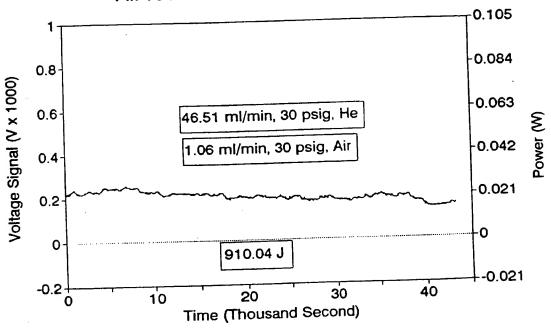






Fig. 23-14 Air reaction 6 at 125 C (120495a)

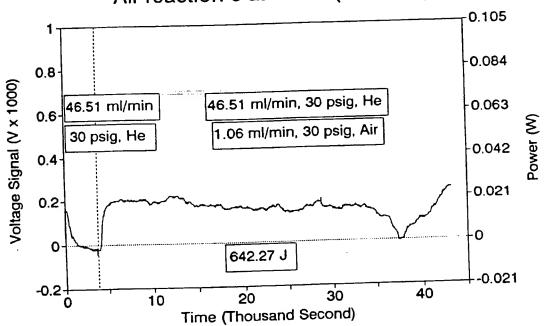






Fig. 23-15 Air reaction 7 at 125 C (120495a)

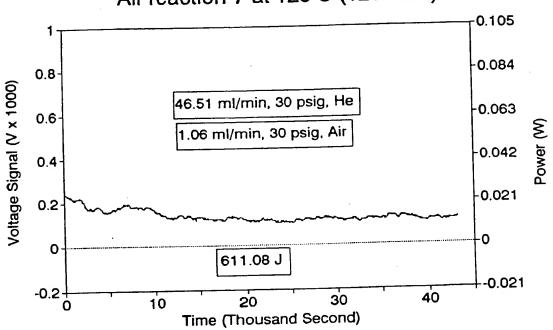






Fig. 23-16 Air reaction 8 at 125 C (120495a)

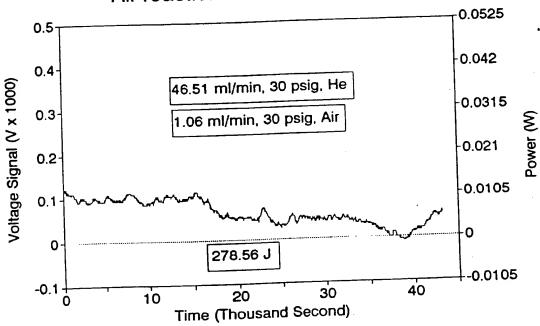
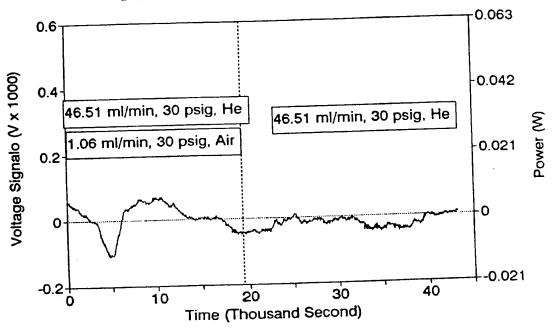






Fig. 23-17 Switch to He at 125 C (120495a)



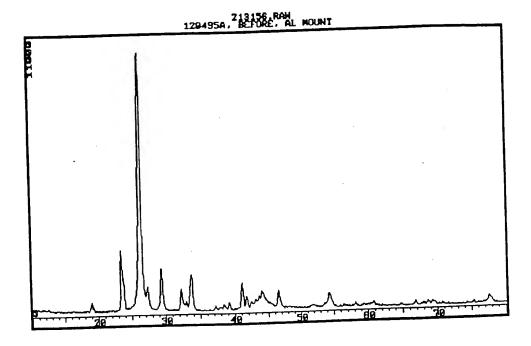




120 495 A

Before





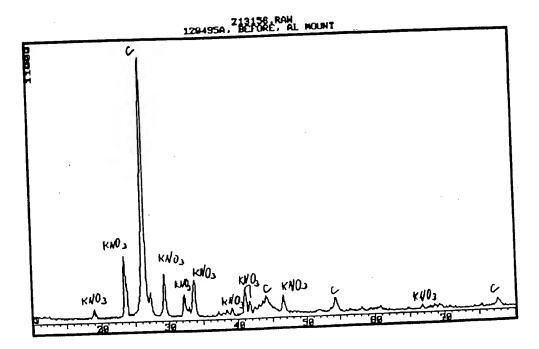
į





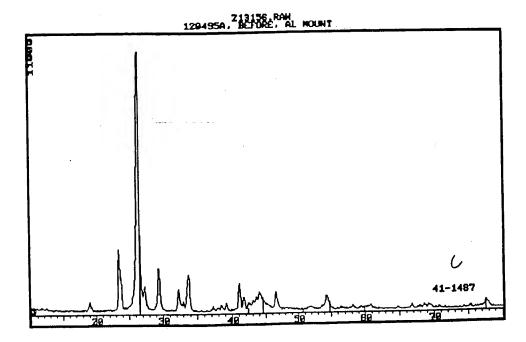
1204984

Before



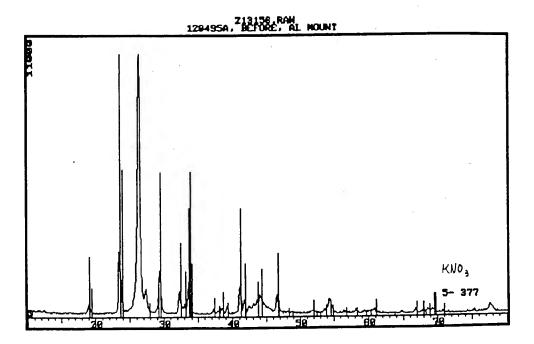














1421 /25



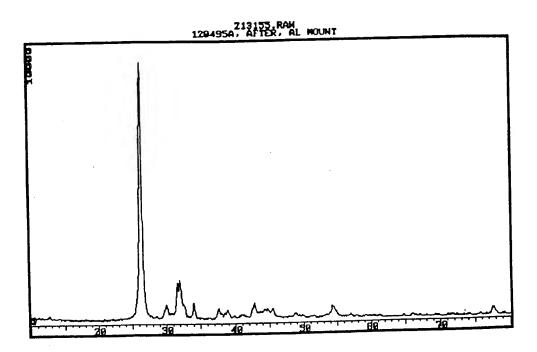
KO 2





120 49\$ A

Alter



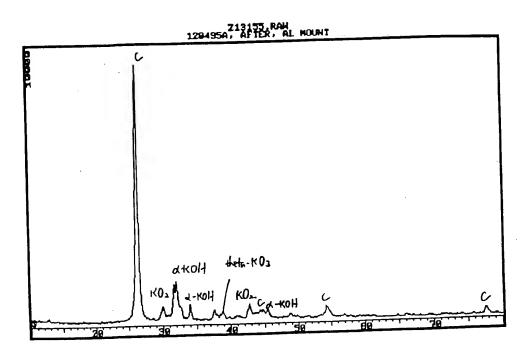






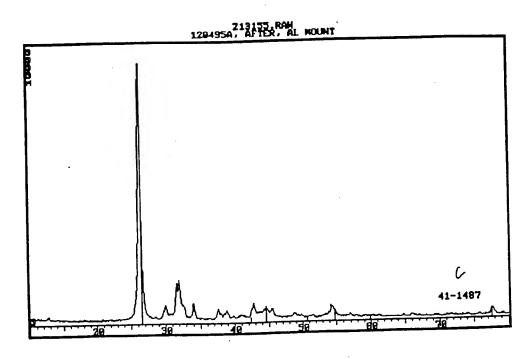
120 K95 A

Affer





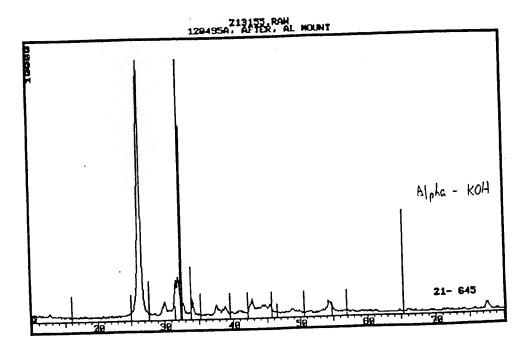








23.25







THIS PAGE BLANK (USPTO)

TO ESERGIA (UST TO)





CONFIDENTIAL

A Calorimetric Investigation
of the
Reaction of Hydrogen
with
Sample PSU#1

A
Confidential Report
submitted to
Hydrocatalysis Power Corporation

by

Michael C. Bradford, MS

11 September 1994



•





I. Experimental Methodology and Theory of Operation

Enclosed at the end of this technical report is a majority of Chapter III from my, Michael C. Bradford, Master of Science thesis at the Pennsylvania State University, entitled, "A Calorimetric Investigation of the Lithium-Water and Lithium Hydride-Water Reaction Systems at Elevated Temperatures." Within this chapter is contained a schematic of the experimental apparatus, the theory by which it can be used to obtain thermodynamic data, and calibration data for the instrument. It also describes the capability of the system for quantifying pulses of gases, hydrogen and water, in an inert carrier gas stream.

II. Site Preparation and Installation of Equipment, 9 September 1994.

Ultra high purity (99.999%) helium and hydrogen were obtained from Matheson for use in the experiment. The schematic of the experimental apparatus, Figure III.2 in Chapter III, should be modified slightly to take the gas changes into consideration. The argon supply was removed and replaced by the hydrogen and helium supplies, connected to a common line through a three-way valve, which permitted instantaneous switching between hydrogen and helium. It should also be noted that the gases were further purified prior to entering the reactor by passing them though an oxygen trap (Alltech).

After installation of the equipment, a quick touch test of the calonimeter was performed at 298 K. Simply, the inner wall of the calonimeter was touched for a period of roughly 10 seconds. The resulting exotherm (Figure 1) was integrated, and the total amount of heat input into the calonimeter by my hand, roughly 21.5 Joules, was determined. This quick test verified the functionality and high sensitivity of the calonimeter.

The sample prepared by Hydrocatalysis Power Corporation, herein referred to as #1, was loaded into the reactor cell under a 40 psig UHP helium blanket to minimize any ambient contamination. The remainder of PSU#1 not loaded into the reactor cell was stored in a desicator within the dry box under a helium blanket. The reactor cell was loaded into the experimental apparatus at 298 K under 1.5 ml/s helium purge, and the piping was leak tested with Snoop. After insulation was placed around the calorimeter, the oven was ramped to 523 K and allowed to thermally equilibrate for 24 hours prior to experimentation.



III. Experimental Data for the Reaction of Hydrogen with

On 10 September, the first data set at 523 K was obtained (Figure 2). This data is contained on a 1.44 M IBM diskette in ASCII format, DATA1.OUT, and as a Quattro Pro spreadsheet, DATA1.WQ1. After sampling the baseline (1 Hz) for 1 hr, the helium was switched to hydrogen at a constant flow rate of 1.5 ml/s. As Figure 1 indicates, there was essentially no indication of any exothermic processes taking place. The slight deviation in the baseline can be attributed to small thermal fluctuations, \pm 0.5 K in the oven.

The second data set at 523 K was then obtained (Figure 3). This data is contained on a 1.44 M IBM diskette in ASCII format, DATA2.OUT, and as a Quattro Pro spreadsheet, DATA2.WQ1. At about t=0 s, the hydrogen flow rate was increased to 4.5 ml/s. A new steady state, roughly at 0.03 W, was then obtained within about 1 hr. At this time, the hydrogen flow rate was then increased to 7.5 ml/s, during which a more substantial exotherm resulted. The new steady state, roughly 0.2 W, was reached in roughly 3 hr.

The third data set at 523 K was then obtained (Figure 4). This data is contained on a 1.44 M IBM diskette in ASCII format, DATA3.OUT, and as a Quattro Pro spreadsheet, DATA3.WQ1. At about t=0 s, the hydrogen flow rate was increased to 13.5 ml/s. The heat output reached roughly 0.5 W after about 1 hr on stream. Before steady state was obtained, the hydrogen flow was switched back to helium. It is clear that a switch to helium resulted in an immediate cessation of heat production, as indicated by the exponential decay of the calorimetric signal. However, note that the new steady state for no reaction was now at roughly 0.25 W. This is a flow induced phenomena and is not yet fully understood. However, it has been documented clearly during past research (Michael C. Bradford, 26 March 1993, Notebook#1, page #80.).

The fourth data set at 523 K was then obtained (Figure 5). This data is contained on a 1.44 M IBM diskette in ASCII format, DATA4.OUT. The helium flow was reduced back to 1.5 ml/s to try to re-establish the original baseline. As the figure indicated, a decrease in helium flow resulted in an abrupt decay of the calorimetric signal toward the original baseline. The original baseline. O.O W was not reached in the figure because sufficient time was not allowed for equilibrium to be reached.





IV. Correction of Data for Baseline Drift and Flow Variation

Using the data in Figure 2 and Figure 4, it is clear that changing the helium flow from 1.5 ml/s to 13.5 ml/s resulted in a baseline shift from roughly 0.0 W to 0.25 W. This phenomenon corresponds to a flow correction factor of 0.0021 W/(ml/s). This correction factor permits a correction to be made to the obtained data.

Table I. Experimental Data.

v (H2) ml/s	P (W), raw	P(W), corrected
1.5	0.00	0.00
4.5	0.03	0.02
7.5	0.20	0.18
13.5	≈0.50	≈0.47
13.5		

The values reported at 13.5 ml/s hydrogen are approximate because steady state had not been reached. Thus, the true heat production values at this flow condition must certainly be higher.

V. Conclusions

PSU#1 does substantially react with flowing hydrogen with considerable activity for extended periods of time. This reactivity was found to be dependent upon hydrogen flow rate. Thus, it is speculated that either the total pressure of hydrogen in the gas phase, or the diffusion of hydrogen through #1, strongly influences the sample reactivity.



Calorimeter Signal Response (V x 1000)

1.5

0.5

0.7%

-0.5 ---

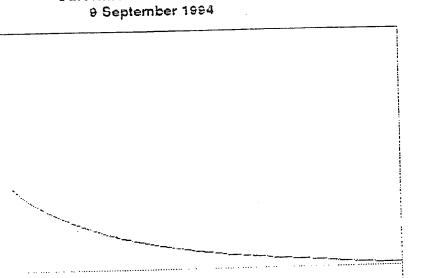
100

200



Figure 1

Calorimeter Test at 298 K



Michael C. Bradford, MS

700

600

500

400

Time (sec)

300

900

800





Figure 2

First Data Set at 523 K - DATA1.OUT 10 September 1994

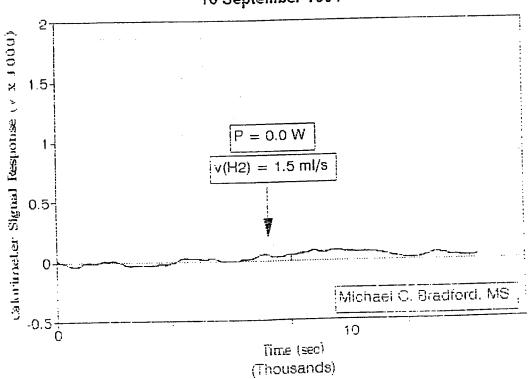
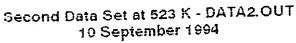






Figure 3



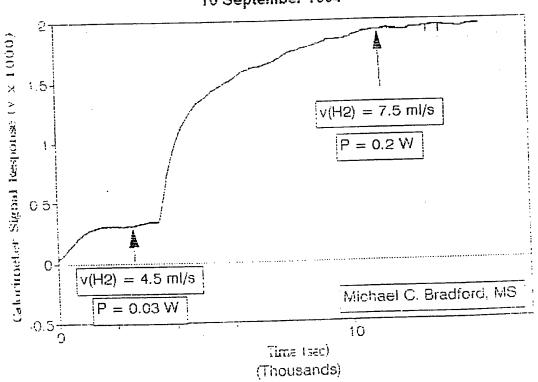






Figure 4

Third Data Set at 523 K - DATA3.OUT 10-11 September 1994

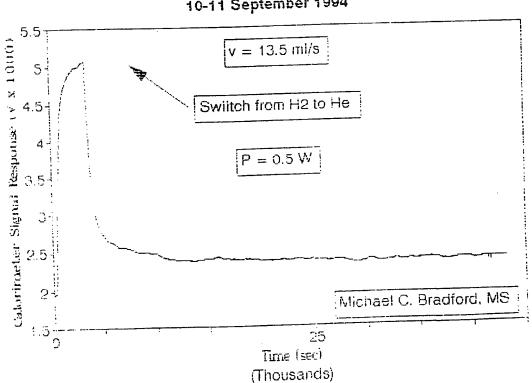






Figure 5

Fourth Data Set at 523 K - DATA4.OUT 11 September 1994

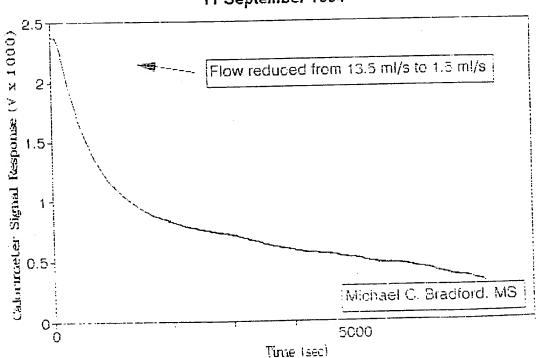
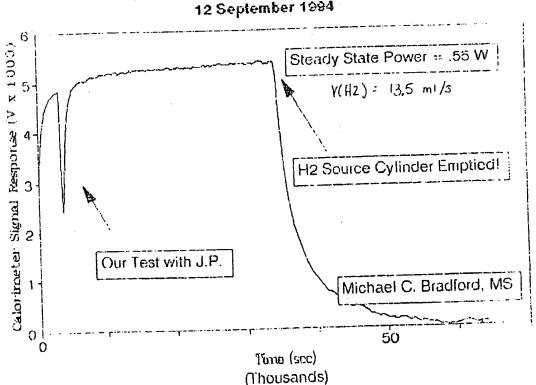






Figure 6

Fifth Data Set at 523 K - DATA5.OUT 12 September 1994







Chapter III Methodology

The initial step in the course of this investigation was to design an experimental apparatus which would adequately resemble a HYDROX fuel reactor (Chapter III.1). After this apparatus was constructed and the theory of the experimental measurement was understood (Chapter III.2), a calibration of the components of the apparatus was performed (Chapter III.3). A general experimental procedure (Chapter III.4) was then used to conduct two test experiments of known elementary reaction systems to validate the utility of the experimental apparatus (Chapter III.5).

III.1 Design

The main objective of the experimental design was to maximize the similarity of the experiment to an actual HYDROX fuel reactor. Thus the experimental apparatus had to be designed to operate at elevated temperatures, ca 588 K, and required the use of a cylindrical reactor, an open flow system, and an excess of fuel (lithium, lithium hydride, or lithium oxide).

There were several difficulties associated with the design of flow, Calvet reaction calorimeter for investigations at elevated temperatures.

- (1) Acceptable materials of construction had to be found. Today, most commercial thermopile insulating materials are not stable at temperatures above 530°K (32). Also, at high temperatures, lithium reacts with many materials, including silica and aluminum (14,44,77), which might ordinarily be used to construct the calorimeter shell.
- (2) A stable high temperature baseline had to be produced. Although some versions of the Calvet-type calorimeter have been constructed to operate at temperatures in excess of 1000°K, the baseline stability and inherent precision of these instruments has been reported as poor (78).
- (3) The calorimeter had to provide accurate heat of reaction data when operated with a constant gas flow, rather than when operated in the batch mode generally associated with Calvet-type calorimeters. Ketchen and Wallace (79) claim that in a flow calorimetric system, reaction heat is inevitably lost, thus necessitating





batch operation for the Calvet-type calorimeter.

- (4) A method of injecting constant, quantified doses of water vapor into the calorimeter had to be devised. It was also necessary to insure that the water enter the calorimeter at the calorimeter temperature.
- (5) The apparatus had to insure adequate mass transfer of the reacting species to minimize, or eliminate, bypass of water out of the reactor.
- (6) A method to analyze the reactor effluent stream for unreacted water and hydrogen had to be developed.

One of the large material concerns was overcome when recently, high temperature, high sensitivity thermopiles became available at reasonable prices, thus making the use of a Calvet-type calorimeter practical at elevated temperatures. A cylindrical heat flux microcalorimeter (International Thermal Instrument Co., Model CA-100-1) was used to measure the heat of reaction during this investigation. To avoid the complication of corrosion, a cylindrical reactor, machined from 304 stainless steel to fit inside of the calorimeter, was used to contain the fuel (Figure III.1).

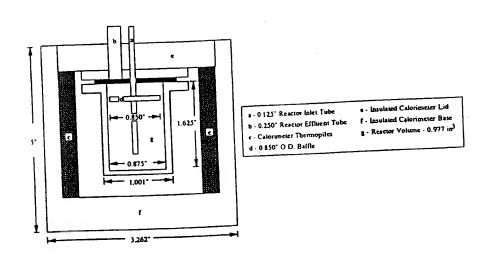


Figure III.1: A schematic diagram of the reactor and the calorimeter.





Although the stainless steel does create an additional heat transfer resistance, it was needed to prevent corrosion of the calorimeter by the fuel. Lithium corrosion of stainless steels and ferritic alloys is negligible at temperatures below 723 K (14), and thus, stainless steel is frequently used and recommended for containment of lithium compounds (14,58,76,77). The additional heat transfer resistance created by the reactor to the calorimeter thermopiles was minimized by the use of thin reactor walls (0.16 cm). Although the maximum operating temperature of this calorimeter is 588 K, gradual sublimation of the thermopile insulating materials limited use of the calorimeter to approximately 2000 hours (31). Although this sublimation process did not affect the sensitivity of the calorimeter, it did require periodic manufacturer maintenance.

A schematic diagram of the entire experimental apparatus is outlined in Figure III.2. To address the operational issues mentioned previously, important support systems were installed (a) to maintain temperature control, (b) to introduce the water into the reactor, (c) to analyze the effluent gas, (d) and to enhance the reaction mass transfer.

To maintain an isothermal reaction system and improve baseline stability, the calorimeter was placed inside of a commercial convection oven (Despatch, Model LND 1-42-3), that could be operated from room temperature to 616 K. Also, the calorimeter and reactor were enclosed within a cubic insulated box, constructed of Durok (United States Gypsum Co.) and fiberglass, to further dampen thermal oscillations in the oven. The use of multiple *insulating* layers to dampen thermal perturbations in the infinite heat sink was demonstrated by Tian as early as 1923 (78), and can be easily illustrated using a basic heat transport model (Appendix B).

As mentioned previously, a flow, rather than a batch reaction process, was required for the experiment to resemble the HYDROX operating environment. Flow calorimeters have been used by other investigators to measure the heats of adsorption of liquids on porous solids temperatures up to $523^{\circ}K$ (80,81,82). However, the use of a continuous gas flow can lead to a loss of heat, and thus a loss in accuracy of the experimental measurement. Barton (80) noticed during the calibration of his flow calorimeter that slight changes in flow rate altered the calibration constant by up to 20%. It was thus desirable to illustrate that gas flow rate would not significantly influence the experimental results of this investigation. Calibration experiments (Chapter III.3.4) conducted with an 18Ω resistor (Mills Resistor Co.) and a fixed current (40-165 mA) source showed that the calibration constant of the calorimeter was not sensitive to the flow rate of gas, over the range of conditions which experiments were conducted. The argon





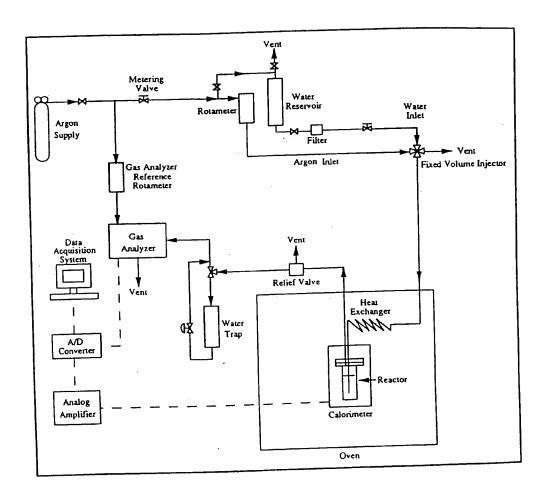


Figure UI.2: A schematic diagram of the experimental apparatus.





purge stream also served as a carrier gas, by providing a method for introduction of the limiting reagents (water or hydrogen) into the reactor.

The accurate step input of trace quantities of limiting reagent into the argon stream was accomplished using a four port fixed volume injector (Valco Instruments Co. Inc., Model No. Cl4UWP) for water, and a six port fixed volume injector (Valco Instruments Co. Inc., Model No. C6WP) for hydrogen. The argon (MG Industries, 99.999% purity) purge stream was passed through an oxygen trap (Alltech, Catalog No. 4004), to remove any oxygen impurities, prior to entering the fixed volume injector. After sampling the limiting reagent, this stream then passed into the oven, and into a 300 cm x 0.241 cm ID teflon lined, stainless steel tubing coil, prior to entering the reactor. This tubing coil primarily functioned as a heat exchanger. Standard heat transfer calculations showed that it was of sufficient size to both vaporize the injected liquid water and bring the entire sample stream to the oven temperature (Appendix C).

During experiments, the reaction cell was loaded with the solid reagent as a packed bed of particles of less than 4 mm O.D. (Chapter III.4). To insure good mass transfer between the gaseous limiting reagent and the fuel, the gas was injected into the bottom of the packed bed, and forced to circumvent a horizontal baffle before exiting the reactor (Figure III.1). Experiments conducted with alternate reactor configurations did not sufficiently reduce channeling of the limiting reagent out of the reactor.

In this investigation, a method of gas analysis was required to quantify step inputs of hydrogen, produced during some reactions, and water vapor, channeled out of the reactor. The utility of in-situ gas chromatography (GC) to separate water and hydrogen mixtures has been demonstrated by Mindrup (83). However, because GC typically uses intermittent, periodic sampling to measure relative gas concentrations, it was not feasible to use in-situ GC in this investigation. Although there are many ex-situ GC methods for the quantification of trace quantities of water, including Karl Fischer Titration (84), the use of organic solvents (85,86), the use of calcium carbide (87,88), and the use of a Helium Ionization Detector (89), ex-situ methods for measuring water and hydrogen were not desirable in this investigation. A commercially available instrument, the hygrometer, is capable of accurate in-situ quantification of water in gas streams (90,91). Also, hydrogen adsorption on palladium films has been demonstrated as a viable candidate for in-situ hydrogen detection and quantification (92,93,94,95). However, budget constraints demanded the use of a single, economical instrument for both water and hydrogen analysis.





For this reason, an in-situ thermal conductivity-type gas analyzer (MSA, Model T-3 Type TC) was used to quantify hydrogen and water vapor in the reactor effluent stream. After the reactor effluent left the oven, it was passed through a 1.0 µm Nupro filter, to remove any entrained solid particulates, prior to entering the gas analyzer. Coincidentally, the optimal carrier gas for hydrogen detection using a thermal conductivity detector is argon (96), and fortunately, the gas analyzer is also sensitive to water vapor. In some experiments, to separate any unreacted water from hydrogen in the effluent stream, the reactor effluent was passed through a 13x molecular sieve (Alltech, Catalog No. 5269).

After the calorimeter signal was amplified, at 1000x magnification, the analog signals from the gas analyzer and the calorimeter were digitized with an Analog to Digital Converter (Real Time Devices, Model ADA1100) and sampled at a 5 Hertz frequency using standard data acquisition software (Real Time Devices, Atlantis) on a Swan 486 PC. All experimental data was converted to an ASCII format so that it could be imported into QBASIC for data analysis (see Appendix D for a listing of the data manipulation software).

III.2 Theory of Measurement

In this investigation, two in-situ measurements were made to quantify both the energy and material balances of the reacting systems. The heat of reaction was measured using a heat flux calorimeter, and both water bypass and hydrogen gas production were measured with a gas analyzer. The combination of the quantification of energy and material balances with basic reaction stoichiometry permitted determination of the overall reaction mechanism without the use of ex-situ analysis of solid reaction products.

III.2.1 Heat Flux Calorimetry

The cylindrical calorimeter walls contain a thermopile structure composed of two sets of thermoelectric junctions. One set of junctions is in thermal contact with the internal calorimeter wall, at temperature T_i , and the second set of thermal junctions is in thermal contact with the external calorimeter wall, at temperature T_e . Unless utilizing a twin calorimeter system, it is imperative for meaningful experimental results that T_e maintain constant throughout the duration of the experiment⁴.

⁴ Although, in this investigation, the oven maintained the infinite heat sink temperature to within \pm 0.30K, the calorimeter was sensitive to these slight thermal fluctuations. The insulating box surrounding





When heat is generated within a calorimetric cell, the calorimeter radially transfers a constant fraction of this heat, γ , into the surrounding heat sink⁵. As heat flows through the calorimeter walls, a temperature gradient, (T_i-T_e) , is established between the two sets of thermoelectric junctions. As stated by O'Neil et al. (97) this temperature gradient generates a voltage which can be mathematically represented by a series expansion.

$$\Delta V = C_I(T_i - T_e) + (C_2/2)(T_i - T_e)^2 + \dots$$
 (111.1)

If (Ti-Te) is negligibly small, then the series is adequately represented by the first term.

$$\Delta V = C_I \left(T_i - T_e \right) \tag{III.2}$$

The heat flux, (dQ/dt), through the calorimeter walls is also directly proportional to this temperature gradient. Thus, the integrated value of the generated voltage, ΔV , produced in the thermopile over time is also directly proportional to the total heat produced, Q, by the reaction process (97).

$$Q = C \int_{0}^{\infty} \Delta V dt \tag{III.3}$$

The proportionality constant, C, is typically determined experimentally during a calibration procedure (Chapter III.3.4). At a fixed temperature, if C is independent of the quantity of heat input, the calorimeter response is said to be *linear*. Typically however, the proportionality constant is a function of temperature. Failure to account for this temperature dependence has previously caused errors in data interpretation (97). The integral quantity, $\int \Delta V dt$, is the area of the experimental thermogram and was obtained, in this investigation, by direct numerical integration of the experimental data (Appendix D).

the calorimeter was added to dampen the oscillating thermal fluctuations of the infinite heat sink and to maintain a constant T_e (see Appendix B for a mathematical proof of this postulate). The insulation did not make the system adiabatic.

⁵ Typical thermal losses include axial conduction (which is minimized by internal calorimeter insulation), conduction losses through the calorimeter signal cable, radiation, and convection. Although it is safe to assume that radiation and conduction losses are negligible, it is not so easy to dismiss the possibility of convective heat loss in a flow system. However, a statistical analysis of the calibration constant data revealed that convective heat losses were indeed negligible in this experimental system (Chapter III.3.4).





Equation (III.3) is identical in form to the well known integrated Tian Equation (78,98,99).

$$Q = \frac{nk}{g\gamma} \int_{0}^{\infty} \Delta V dt \tag{III.4}$$

Equation (III.4) provides a better intuitive look into the temperature dependence of the proportionality constant than equation (III.3) by providing a mathematical form for the proportionality constant.

$$C = \frac{nk}{g\gamma} \tag{III.5}$$

where n is the number of thermoelectric junctions in the thermopile, k is the thermal conductivity of the thermopile, and g is an unknown function of n, the power of the thermoelectric junctions, and the amplification of the signal. Due to the unknown nature of g, the proportionality constant in Tian's equation must also be determined experimentally by a calibration.

However, during the course of this investigation, an improved theoretical form of equations (III.3) and (III.4) was rigorously derived using a straight forward heat transport model (Appendix A). The simplified result is

$$Q = \frac{Vk\pi^3}{3.88nSL^2} \int_0^\infty \Delta V dt \tag{111.6}$$

The Seebeck Coefficient, S, is a thermal property of the thermoelectric junctions and is available for most known thermoelectric junctions over an extremely wide range of temperatures (100). The volume in which heat is generated, V, and the characteristic dimension of the calorimeter, L, are easily determined physical quantities. The thermal conductivity of the calorimeter, k, if not known, can be either measured or estimated with a suitable correlation (101-103).

Equation (III.6) predicts that the calorimeter response is independent of heat generation rate within the calorimeter, as observed experimentally (Chapter III.3.4), and permits the direct theoretical calculation of the calorimeter proportionality constant, provided that the physical and thermal properties of the calorimeter are well known.

34





A simplified form of the proportionality constant, obtained from the model in Appendix A for steady state heat generation within the calorimeter, defines the *intrinsic* sensitivity of a heat flux calorimeter.

$$C = \frac{P}{(\Delta V)_{ss}} \tag{III.7}$$

P is the rate of heat generation, and $(\Delta V)_{SS}$ is the steady state voltage response to P. "The intrinsic sensitivity ... ", numerically equivalent to the inverse of the calibration constant, "... is defined as the value of the steady emf that is produced by the thermoelectric elements when a unit of thermal power is dissipated continuously in the active cell of the calorimeter" (78). Equation (III.7) is established in the field of calorimetry as an experimental means of determining C, and can be derived by less rigorous mathematical treatment (104). Although the aforementioned mathematically derived results, equations (III.6) and (III.7), offer two significant theoretical improvements in heat flux calorimetry, determination of the proportionality constant is restricted to experimental calibration unless reliable thermal conductivity data for the complex structure of calorimeters becomes available.

The successful experimental applicability of equation (III.3)⁶ requires constant external wall temperature, T_e, and uniform radial symmetry of the thermal perturbations. It should also be noted that equation (III.3) is independent of the physical properties of the material inside of the calorimeter. Thus, all heat produced within the calorimeter must eventually flow into the infinite heat sink, regardless of the calorimeter contents. Although Gravelle (78) has suggested that equation (III.3) is not suitable for the analysis of thermograms produced by rapid heat input, due to the inherent thermal lag of the heat flow calorimeter, Evans (99) is convinced that this is not the case. Nonetheless, the proper method of determining the validity of equation (III.3) for the study of rapid reactions is through experimental determination of the range of linearity of the calorimeter response. The range of linearity is the range of heat quantity and input rate, at a fixed temperature, for which C is a constant, and is determined by an experimental calibration.

⁶ Equation (III.3) is herein considered to be equivalent to the general experimental forms of equations (III.4) and (III.6).





III.2.2 The Gas Analyzer

The gas analyzer was primarily used for the in-situ quantification of hydrogen production, and occasionally used for unreacted water quantification. The gas analyzer essentially consists of four electrically heated metal filaments suspended in a reference gas stream. These filaments are designed to maintain heat losses due to convection and radiation constant, and therefore are sensitive only to the difference in thermal conductivity of the sample stream and the reference stream (105). The change in thermal conductivity of the sample stream causes a change in the resistance of the filaments, thereby inducing a change in the output electrical signal. This transient signal is then sampled with the data acquisition software for analysis.

Because this instrument was designed to measure the *concentration* of a sample gas (S) in a flowing reference gas stream (R), the electrical output signal, ΔV dt, is directly proportional to the concentration of S in R.

$$\Delta V dt \quad \alpha \quad [S]$$
 (III.8)

Using the following definition of concentration

$$[S] = \frac{\eta_S}{v_R} \tag{111.9}$$

where v_R is the volumetric flow rate of R and η_S is the molar quantity of S, equation (III.8) may be written as

$$\eta_S = C_S v_R \int_{t_i}^{t_f} \Delta V dt \tag{III.10}$$

where CS is merely a proportionality constant dependent only on S, and t_i and t_f are the initial and final integration times, respectively. The validity of equation (III.10) was established experimentally for hydrogen and water vapor (Chapter III.3.3). The interesting result from equation (III.10) is that for constant η_S , the integral signal area increases for decreasing v_R . This empirical phenomenon influenced the choice of low reference flow rates in this investigation.





III.2.3 The Governing Experimental Equations

The governing equations used in this investigation for quantification of heat of reaction

$$Q = C \int_{0}^{\infty} \Delta V dt$$
 (III.3)

and quantification of gas in the effluent stream

$$\eta_S = C_S v_R \int_{t_i}^{t_f} \Delta V dt \tag{III.10}$$

have identical mathematical forms and can be derived quasi-theoretically. The proper use of these two equations in this investigation required a statistically relevant calibration procedure to determine the calibration constants, C and CS.

III.3 Apparatus Calibration

In this investigation, the accurate measurements of the heat of reaction, the amount of water bypass, and the quantity of hydrogen produced required the accurate determination of the limiting reagent volumes, the argon purge gas flow rate v_R , the calorimeter calibration constant, C, and the gas analyzer calibration constants, C_S . The numerical values of all calibration constants are reported with 95% confidence limits.

III.3.1 Limiting Reagent Volumes

A four port fixed volume injector was utilized for the introduction of liquid water into the argon purge stream. Because this injector was manufactured only to deliver reproducible fixed volumes ca 2 μ l (106), it was necessary to calibrate the fixed volume injector. An HP5890 gas chromatograph with a six foot Chromosorb 102 packed column was utilized for this calibration procedure. Using 1.0 μ l (SGE, Model 1BR-7) and 5.0 μ l (SGE, Model 5BR-7) precision syringes, fixed volumes of n-hexane (Aldrich) were manually introduced into the chromatograph to calculate an n-hexane calibration constant,





 $C_n = 2.00 \pm 0.05 \times 10^{-7} \, \mu l$ / area unit. The four port fixed volume injector was then utilized to inject an *unknown* volume of n-hexane into the chromatograph. The mean integral area of the fixed volume injector areas, $A_m = 1.34 \pm 0.02 \times 10^7$ area units, was simply multiplied by C_n to determine the water sampling volume of the four port injector, $V_{\rm H2O} = 2.68 \pm 0.11 \, \mu l$.

A six port fixed volume injector with a nominal 2 ml sample loop was utilized for the introduction of hydrogen into the argon purge stream during the gas analyzer calibration. Because the manufacturer reported the volume range as V = 2.0 ± 0.2 ml (106), the volume of the nominal 2 ml sample loop also needed to be calibrated. Using the experimental apparatus (Figure III.2), the sample loop was filled with liquid water at 298°K, and then emptied into a graduated cylinder of known mass. Using a Mettler AE100 balance, the mass of the water contained within the cylinder was then obtained. After five identical measurements, the mean mass of the water sample was determined to be m = 2.195 ± 0.005 g. The volume of the six port injector sample loop was obtained by dividing the measured mass by the density of water at 298°K, p = 0.9974 g/cm³ (100). From this procedure, the volume of this sample loop, and thus the volume of hydrogen used during calibration of the gas analyzer, was determined to be VH2 = 2.201 ± 0.005 cm³.

III.3.2 Volumetric Flow Rate of the Argon Purge

The flow rate of the argon purge to the reactor was regulated with a rotameter and a metering valve (Figure III.2) and was determined from a standard bubble-meter calibration procedure. A schematic of this simple apparatus is provided in Figure III.3. Using the bubble-meter, a soap bubble was introduced into the reactor effluent. The volume, V, traveled by the soap bubble in the effluent was measured directly from the graduated markings on the pipette wall of the bubble meter. The duration of time, t, required for the soap bubble to travel V was measured with a single event stopwatch (Cole Parmer, Model 8668). The volumetric flow rate of argon, v_R , was then easily calculated. The measurement of v_R was performed at random, multiple times during an experiment to obtain a statistically relevant mean value and to monitor any possible abnormal deviations in flow rate. A typical value for v_R used in this investigation was 1.52 ± 0.01 cm³/sec.





III.3.3 The Gas Analyzer

Accurate knowledge of the limiting reagent volumes and the argon flow rate permitted the calibration of the gas analyzer over a wide range of v_R for hydrogen(g) and water(g). The entire experimental apparatus (Figure III.2) was used during this calibration procedure. At constant v_R , a known volume of limiting reagent was input into the argon stream using the appropriate fixed port injector. The limiting reagent then passed into the oven, through the empty reactor, and directly into the gas analyzer. The response of the gas analyzer to both hydrogen and water is illustrated in Figure III.4. The integral area of the gas analyzer signal response to the limiting reagent was then calculated numerically (Appendix D). To calculate the proportionality constants, C_S , from the experimental data using equation (III.10), the volume of limiting reagents had to be converted to absolute molar quantities. The molar amount of water, η_{H2O} , was calculated directly from the known calibration volume.

$$\eta_{H_2O} = \frac{\rho V_{H_2O}}{MW} \tag{III.11}$$

where ρ is the density of water at 298°K, and MW is the molecular weight of water. The molar amount of hydrogen, η_{H2} , was calculated directly from the ideal gas law at 298°K.

$$\eta_{H_2} = \frac{PV_{H_2}}{RT} \tag{III.12}$$

The static hydrogen pressure, P, in the fixed volume injector was measured using the pressure gauge on the hydrogen source cylinder. The calibration constant for each limiting reagent is listed Table III.1 along with a range of v_R to which CS is restricted.

Table III.1

Gas analyzer calibration constants for the limiting reactants.

S	$v_R (\text{cm}^3 / \text{s})$	CS (µmol/V cm ³)
hydrogen (g)	1.5 - 4.45	0.970 ± 0.006
water (g)	1.5 - 4.45	4.86 ± 0.23





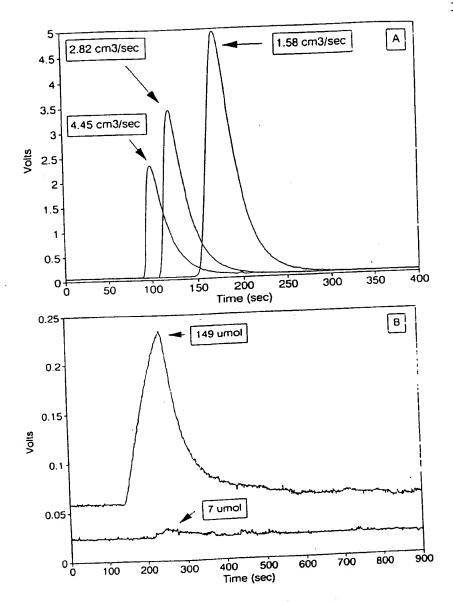


Figure III.3: The gas analyzer signal response to (a) 274 μ mol hydrogen gas at various gas flow rates, and (b) various amounts of water vapor at a flow rate of 1.58 cm³/sec.





Because the thermal conductivity of hydrogen is much greater than that of water vapor (101), the gas analyzer is more sensitive to hydrogen. The sensitivity of the gas analyzer is the inverse of CS and is a relative measure of the size of the integral signal response. The relatively larger deviation in CH2O can be attributed to possible partial condensation of the water on the gas analyzer thermal filaments. The manufacturer of the gas analyzer has acknowledged that condensation of vapor can slightly alter the gas analyzer signal response (105).

III.3.4 The Heat-Flux Calorimeter

Quantitative experimental measurement of the heat of reaction with the calorimeter required a determination of the proportionality constant, C, in equation (III.3). Experimental determination of C was accomplished through a standard electrical calibration technique (78,107,108). A high precision beryllium core 18Ω resistor (Mills Resistor Co.) was placed within the reactor, inside of the calorimeter. The resistor, as part of a simple circuit, was connected to a constant current (40-165 mA) output source. A known quantity of current, I, flowing through a known resistance, R, for a known duration of time, I, produces a total amount of heat, Q, simply given by the expression

$$Q = I^2 R t = I V t \tag{111.13}$$

where V is the voltage. Both I and V were measured in-situ during all calibration experiments for an accurate determination of Q. Numerical integration of the calorimeter signal response curve corresponding to a known quantity of heat input, Q, permits calculation of the proportionality constant, C, of the calorimeter using the expression

$$C = \frac{IVt}{if}$$

$$\int_{t_i} \Delta V dt$$
(111.14)

The infinite integration limits have been replaced by t_i and t_f , the experimental initial and final integration times, respectively. For proper experimental use of equation (III.3), it was crucial to demonstrate that C, as calculated from equation (III.14), was independent of rate of heat generation, P, the total quantity of heat input, Q, and the flow rate of the argon





purge, v_R . The influence of infinite heat sink temperature, T, on C also needed to be determined. Thus, an appropriate test was devised to statistically ascertain the influence of P, Q, v_R and T on C.

For the calibration and statistical analysis it was necessary to write C as Cijk, where i, j, and k are the numerical indices 1 or 2, referring to specific numeric values of P, ν_R , and T, respectively (Table III.2).

Table III.2
Numerical values for Cijk indices.

Indice #	· i (W)	j (cm ³ /sec)	k (*K)		
1	0.24	0	505		
2	0.60	4.448	588		

The combined indices ijk refer to the environmental conditions at which Cijk was determined. A total of eight combinations of i, j, and k were used in this investigation.

During the electrical calibration procedure, a graph of $]\Delta Vdt$ vs Q was constructed at each temperature to demonstrate the linearity of the calorimeter response (Figure III.4). Although there is scatter in the data, the linearity of the curve indicated that the calorimeter signal response was independent of Q over the range of 10 to 75 Joules (This was also the range of heat observed in the actual reaction experiments). To determine the effect of rate of heat generation, P, and gas flow rate, v_R , on the calorimeter signal response, a standard statistical analysis was used.

Using each data point in Figure III.5, the individual Cijk values were calculated directly from equation (III.14), and an average of the multiple observations of Cijk was obtained (Table III.3). All reported Cijk values include the calorimeter signal amplification of 1000x magnification.

An F-Test (109), at the α =0.05 level of significance, was performed at each temperature to determine the effect of P and v_R on Cijk. The first step was to postulate the Null Hypothesis, H_O , at constant temperature (k).

$$H_0: C_{11k} = C_{12k} = C_{21k} = C_{22k}$$
 (III.15)





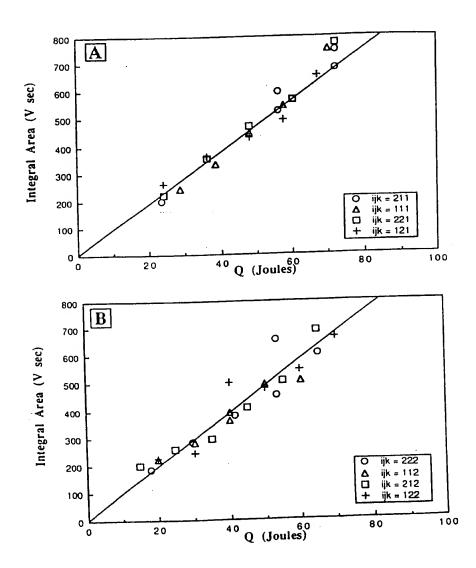


Figure III.4: A plot of the integral calorimeter signal response, $\int \Delta V dt$, versus total heat input, Q, during the electrical calibration procedure at (a) 505°K and (b) 588°K.





Table III.3

Experimental values of Cijk at 1000x magnification.

Ciii (J / V sec)	Cij2 (J / V sec)
	0.105 ± 0.010
	0.102 ± 0.017
	0.100 ± 0.017
	0.103 ± 0.013
	Cij1 (J / V sec) 0.108 ± 0.012 0.109 ± 0.007 0.104 ± 0.012 0.103 ± 0.008

The null hypothesis is merely a postulate that no statistical difference will be found between the inclusive means. Although "researchers rarely desire to prove the null hypothesis" (110), the validity of H_0 needed to be established for the purposes of this investigation. When validating H_0 it is important to minimize a *Type II error*, which is the probability of failing to reject H_0 when in fact there is a difference. The *Alternate Hypothesis*, H_0 , at constant temperature (k)

$$H_a: C_{11k} \neq C_{12k} \neq C_{21k} \neq C_{22k}$$
 (III.16)

is a postulate that there is a statistical difference between the inclusive means. Although some researchers feel that the F-test is inadequate to test the validity of the *null hypothesis*, this procedure is outlined in Mickley et al. (111) and was recommended by *The Statistical Consulting Center* at The Pennsylvania State University. An L-test (111), at the α =0.05 level of significance, was also performed to validate the implicit assumption in the F-test that the variance of each Cijk is the same (109). Because the results of the F-test indicated that H₀ was valid at 505 K (k=1) and 588 K (k=2), a grand mean was calculated at each temperature from all the independent observations for Cijk (Table III.4).

The preceding analysis, through verification of H_0 , permitted the conclusion that at a fixed temperature, the calorimeter signal response was independent of P and u_R . To determine the effect of temperature on the calorimeter signal response, an F-test was designed with the following hypothesis:

$$H_0: C505 = C588$$
 (III.17)





Table III.4

The grand means, Ck, of the calorimeter calibration constants, Cijk.

Temperature (*K)	Ck (J / V sec)				
505	0.106 ± 0.004				
588	0.103 ± 0.006				

$$H_a: C_{505} \neq C_{588}$$
 (III.18)

Because the results clearly showed that H_0 was valid, it was reasonable to conclude that the calorimeter signal response was also independent of temperature, over the narrow range used in this investigation.

The preceding analysis of the calorimeter calibration constant, C, indicated that it was independent of rate of heat input, quantity of heat input, flow rate of argon gas, and temperature, with the limits of this investigation. However, because the manufacturer of the calorimeter indicated that C was slightly temperature dependent, it was decided to use the values for C determined at each temperature during reaction experiments, and not to lump them into another grand mean. The most important result of this analysis was that the flow rate of the argon gas, v_R , did not significantly after C. This phenomenon required a physical interpretation.

During heat generation, heat is removed from the reactor within the calorimeter by either conduction through the thermopiles or by bulk transport with the exiting gas. Alternate avenues of heat loss are assumed to be constant and negligible (Chapter III.2.1). The conduction through the thermopiles is limited by the heat flux through the argon stream and the reactor wall. It was thus desirable to show that the rate of bulk heat removal by the flowing argon stream was negligible compared to the rate of heat removal to the thermopiles. Both of these processes are dependent upon the temperature difference, ΔT , which exists between the reactor within the calorimeter and the infinite heat sink.

The rate of bulk heat transfer, \dot{Q}_c , to the carrier gas can be written as

$$Q_c = \rho v_R C_p \Delta T \tag{III.19}$$





where C_p is the heat capacity and ρ is the density of the carrier gas. The overall heat transfer coefficient, U, for the rate of heat removal to the thermopiles, Q_h , can be defined as

$$Q_h = UA\Delta T \tag{III.20}$$

where A is the total internal surface area of the reactor. Note that the ratio of Q_c/Q_h

$$\frac{Q_{c}}{Q_{h}} = \frac{\rho v_{R} C_{p}}{UA} \tag{111.21}$$

is only indirectly dependent on ΔT , through the possible dependence of U on ΔT . Using the data in Table III.5, the ratio of $Q_c/Q_h=4.6\%$ was calculated from equation (III.21).

Table III.5

Data for the calculation of Q_c/Q_h

Parameter	Value ⁷
U(W/cm ² *K)	0.00116
A (cm ²)	36.55
ρ (g/cm ³)	8.51 x 10 ⁻⁴
Cp (J/g*K)	0.5207
v_R (cm ³ /sec)	4.45

A minimum estimate of U, 0.00116 W/cm²·K, was obtained directly from the literature as a mean value for free convection (103). The use of a minimum estimate of U maximizes the ratio of Q_c/Q_h , which can thus be taken as the upper limit to experimental error introduced by the argon purge. Including other avenues of heat transfer, such as radiation and forced convection, into the analysis would only increase the value of U.

⁷ The physical property data for argon was obtained from Lienhard (102).





Thus, because the rate of heat loss due to the argon purge, 4.6%, is essentially the same magnitude as the 95% confidence limit on the calorimeter calibration constant (Table III.4), heat loss due to the argon flow is within experimental measurement error. Thus, as determined experimentally using a statistical analysis of the calorimeter calibration data (Chapter III.3.4), the bulk rate of heat removal by the argon purge stream is negligible for the range of argon flow rates used in this study.

This preceding analysis introduces a general guideline to the design of flow calorimeters. It indicates that the error in measurement introduced by the carrier stream is negligible (< 5%) if the carrier stream has a small heat capacity. Although Barton (80) used extremely small carrier flow rates (ca 0.06 cm³/sec) in his flow calorimeter, he observed that the adjustment of carrier flow rate altered the calorimeter calibration constant by up to 20%. This phenomenon was most likely due to the large heat capacity of water (relative to argon), which he used as a carrier fluid.

It was not possible to ascertain the validity of the previous analysis for the presence of a solid reactant in the reactor. Calibration tests were not conducted with solid reagent present in the reactor because the calibrating resistor occupies a considerable fraction of the reactor volume, and would not fit within the reactor with a load of reactant present. However, the preceding physical interpretation suggests that the overall heat transfer coefficient should increase when solid reactant is present in the reactor, due to the improved conduction properties of metallic compounds over gases. Therefore, it is reasonable to conclude that with solid present in the reactor, the bulk rate of heat removal by the argon purge is also negligible.

III.4 Experimental Procedure

A general experimental procedure was followed for the two reactions used to test the apparatus (Chapter III.5), and the two fuel reactions of primary interest to this investigation (Chapter IV).

(1) The dry, solid reagent was loosely poured into the reactor in a dry box (Terra Universal, Model 1689-00) under a continuos blanket of argon at 298 K. A copper gasket was then placed on top of the test cell, and the reactor lid was fastened to the reactor with eight .375" stainless steel bolts. The bolts were coated with a small layer of high temperature anti-seize to minimize strain due to repeated thermal cycling. The inlet and



outlet pipes to the reactor were then sealed with swagelock fittings so that the reactor could serve as a temporary, batch, inert environment.

- (2) The reactor was removed from the dry box and placed within the calorimeter. During this time, argon was continuously purged through the system and into the oven. The heat exchanger was then connected to the reactor inlet pipe, and the reactor outlet was connected to the effluent pipe. After securing the insulation around the calorimeter, the oven temperature was gradually ramped to the desired experimental temperature, either 505°K or 588°K. After thermal equilibrium was established, typically within 16 hours as indicated by a steady calorimeter baseline, the system was ready for experiment initiation.
- (3) At time zero, the data acquisition system was activated for sampling data at 5 Hertz. The baseline was sampled for exactly 120 seconds, synchronized with a digital stopwatch, prior to the injection of limiting reagent into the argon stream to accurately determine the initial baseline voltage. Data acquisition was continued for approximately 3600 seconds after the injection of limiting reagent into the reactor. After the reaction terminated and thermal equilibrium was established, the data was saved in ASCII format for later analysis. Up to ten injections of liming reagent into the reactor were performed during the course of one reaction investigation in order to obtain a statistically relevant sample size.
- (4) At the completion of the reaction investigation, the system was cooled down to room temperature, the reactor was removed from the system, and then placed in the dry box. The solid contents of the reactor were removed under an argon blanket and saved in a calcium sulfate dessicator to minimize atmospheric contamination. The reactor was then removed from the dry box and submerged in a water bath to cleanse it of any lithium containing materials. After drying the reactor with acetone, it was ready for use in a new experiment.

III.5 Test Experiments

Prior to using the experimental apparatus to investigate the lithium-water and lithium hydride-water reaction systems, two test experiments were conducted to determine the extent of reliability of the experimental apparatus. Chemical reaction calibration is commonly used in microcalorimetry to independently verify the calibration constant of the calorimeter (107,108). Although the most common reaction in use is the reaction of sodium hydroxide with hydrochloric acid (107), the two following reactions





THE PACE MEDIC CO. CO.

THIS PAGE BLANK (USPTO)





DECLARATION OF MICHAEL G. JACOX

- I, Michael G. Jacox do hereby declare and say as follows:
- 1. I received a Bachelor of Science Degree in Nuclear Engineering from the Georgia Institute of Technology in 1985. I received a Masters of Science Degree in Nuclear Engineering from the University of Idaho in 1992.
- 2. From 1998 to the present, I have been employed as an Assistant Director for the Commercial Space Center for Engineering (CSCE), Texas A & M University, where I have developed a strategic plan for a newly created NASA commercial space center which resulted in an increase of NASA funding from \$500K to \$1M annually. I planned and executed the campaign for industry input and support of the CSCE. I led the development of the first integrated payload design center at Texas A & M University.
- 3. From 1996-1998, I was employed as a Program Manager at the Space Dynamics Lab, Utah State University, where I defined, promoted and managed the \$50M Solar Orbit Transfer Vehicle (SOTV) space experiment and technology development program. I also completed the first ever system-level ground test of the Integrated Solar Upper State (ISUS) on time and within the \$15M budget.
- 4. From 1994-1996, I was employed as a Systems Engineer at Lockeed-Martin Idaho Technologies, where I managed a team of more than 30 engineers and scientists from NASA, the Naval Research Lab, Air Force Research Lab and industry in a highly successful \$1M system definition study of the ISUS space power and propulsion concept. I also managed a joint DOD-DOE nuclear biomodal systems engineering team that evaluated concepts and developed preliminary designs of combined power and propulsion reactors.
- 5. From 1989-1994, I was employed as a Senior Scientist at EG&G Idaho, where I conceived the design and managed the development and testing of the first integrated thermionic/heat-pipe module for nuclear bimodal applications. The multi-million dollar effort resulted in successful prototype testing. I also managed the design and installation of a unique multi-million dollar hot hydrogen test facility at the Idaho National Engineering Lab. I further originated the design of the Small-Ex-core Heat Pipe Thermionic Reactor (SEHPTR), led the SEHPTR conceptual design team, and received a patent covering the SEHPTR. I also developed and benchmarked the first three-dimensional neutronics model of the Advanced Test Reactor.
- 6. From 1985-1989, I was empolyed as a Nuclear Research Officer at USAF Weapons Lab, where I led the Air Force's space nuclear power application studies resulting in significant national program modifications and the development of the Military Space Reactor Initiatives. I also installed advanced nuclear reactor analysis codes on inhouse computers.

Declaration of Michael G. Jacox Page 2 of 2

- 7. While employed at EG&G, I contracted for the Idaho National Engineering Laboratory (INEL) under a DOE contract. At INEL, I conducted three experiments in which hydrogen was reacted with a catalyst, (K+, K+), generated from aqueous K_2CO_3 , in an electrolytic cell containing nickel and platinum electrodes. The test conditions and results are shown in the attached report. As can be seen from the test results, 20 to 30 watts of excess heat was observed and in one instance the ratio of excess power to input electrolysis joule heating power was 850%.
- 8. The evidence presented in the attached report clearly demonstrates that a phenomenon takes place upon the admission of hydrogen to an electrolytic cell containing aqueous KCO₃. This phenomenon generates heat in excess of that expected from any known chemical process, given the content of the reactants in the cell. A detailed analysis of all constituents was conducted to ensure that no chemical reactions were occurring which could be generating the excess heat observed.
- 9. I declare further that all statements made herein of my own knowledge are true and that all statements made on information and belief are believed to be true; and further that these statements were made with the knowledge that willful false statements and the like so made are punishable by fine or imprisonment, or both, under Section 1001 of Title 18 of the United States Code and that such willful false statements may jeopardize the validity of the application or any patent issuing thereon.

Michael G. Jacox

Date: __*Z*

Experimental Verification by Idaho National Engineering Laboratory

Methods

A search for excess heat during the electrolysis of aqueous potassium carbonate (K*/K* electrocatalytic couple) was investigated using cells supplied by HydroCatalysis Power Corporation and a cell fabricated by Idaho National Engineering Laboratory (INEL). To simplify the calibration of these cells, they were constructed to have primarily conductive and forced convective heat losses. Thus, a linear calibration curve was obtained. Differential calorimetry was used to determine the cell constant which, was used to calculate the excess enthalpy. The cell constant was calculated during the experiment (on-the-fly-calibration) by turning an internal resistance heater off and on, and inferring the cell constant from the difference between the losses with and without the heater.

The general form of the energy balance equation for the cell in steady state is:

$$O = P_{appl} + Q_{htr} + Q_{xs} - P_{gas} - Q_{loss}$$
 (III.I)

where P_{appl} is the electrolysis power; Q_{hlr} is the power input to the heater; Q_{xs} is the excess heat power generated by the hydrogen "shrinkage" process; P_{gas} is the power removed as a result of evolution of H_2 and Q_2 gases; and Q_{loss} is the thermal power loss from the cell. When an aqueous solution is electrolyzed to liberate hydrogen and oxygen gasses, the electrolysis power P_{appl} (= E_{appl} I) can be partitioned into two terms:

$$P_{appl} = E_{appl}I = P_{cell} + P_{gas}$$
 (111.2)

An expression for $P_{gas}(=E_{gas}I)$ is readily obtained from the known enthalpy of formation of water from its elements:

$$E_{gas} = \frac{-\Delta H_{form}}{\alpha F}$$
 (111.3)

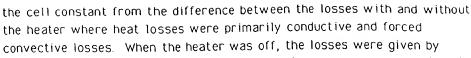
(F is Faraday's constant), which yields E_{gas} = 1.48 V for the reaction

$$H_2O \rightarrow H_2 + \frac{1}{2}O_2$$
 (111.4)

The net faradaic efficiency of gas evolution is assumed to be unity; thus, Eq. (III.2) becomes

$$P_{cell} = (E_{appl} - 1.48V)I$$
 (111.5)

The cell was calibrated for heat losses by turning an internal resistance heater off and on while maintaining constant electrolysis and by inferring



$$c(T_C - T_D) = P_{appl} + 0 + Q_{xs} - P_{gas}$$
 (III.6)

where c is the heat loss coefficient; T_b is ambient temperature and T_c is the cell temperature. When a new steady state is established with the heater on, the losses change to:

$$c(T_{C'} - T_{D}) = P'_{appl} + Q_{hlr} + Q'_{xs} - P'_{gas}$$
 (III.7)

where a prime superscript indicates a changed value when the heater was on. When the following assumptions apply

$$Q_{xs} = Q_{xs}, P_{appl} = P_{appl}, P_{gas} = P_{gas}$$
 (111.8)

the cell constant or heating coefficient a, the reciprocal of the heat loss coefficient(c), is given by the result

$$a = \frac{T_C - T_C}{Q_{\text{blc}}} \tag{111.9}$$

In all heater power calculations, the following equation was used $O_{htr} = E_{htr}I_{htr} \tag{III.10}$

LIGHT WATER CALORIMETRY EXPERIMENTS

INEL EXPERIMENT I (DC Operation)

The present experiments were carried out by observing and comparing the temperature difference, ΔT_1 =T(electrolysis only) – T(blank) and ΔT_2 = T(electrolysis plus resistor heating) –T(blank) referred to unit input power.

The cell comprised a 10 gallon (33 in. x 15 in.) Nalgene tank (Model # 54100-0010). Two 4 inch long by 1/2 inch diameter terminal bolts were secured in the lid, and a cord for a heater was inserted through the lid.

The cathode comprised 1.) a 5 gallon polyethylene bucket which served as a perforated (mesh) support structure where 0.5 inch holes were drilled over all surfaces at 0.75 inch spacings of the hole centers and 2.) 5000 meters of 0.5 mm diameter clean, cold drawn nickel wire (NI 200 0.0197", HTN36NOAG1, A1 Wire Tech, Inc.). The wire was wound uniformly around the outside of the mesh support as 150 sections of 33 meter length. The ends of each of the 150 sections were spun to form three cables of 50 sections per cable. The cables were pressed in a terminal connector which was bolted to the cathode terminal post. The connection was covered with epoxy to prevent corrosion.

The anode comprised an array of 15 platinized titanium anodes (15 - Engelhard Pt/Ti mesh 1.6" x 8" with one 3/4" by 7" stem attached to the 1.6" side plated with 100 U series 3000). A 3/4" wide tab was made at the end of the stem of each anode by bending it at a right angle to the anode. A 1/4" hole was drilled in the center of each tab. The tabs were bolted to a 12.25" diameter polyethylene disk (Rubbermaid Model #2666) equidistantly around the circumference. Thus, an array was fabricated having the 15 anodes suspended from the disk. The anodes were bolted with 1/4" polyethylene bolts. Sandwiched between each anode tab and the disk was a flattened nickel cylinder also bolted to the tab and the disk. The cylinder was made from a 7.5 cm by 9 cm long x 0.125 mm thick nickel foil. The cylinder traversed the disk and the other end of each was pressed about a 10 A /600 V copper wire. The connection was sealed with



Teflon tubing and epoxy. The wires were pressed into two terminal connectors and bolted to the anode terminal. The connection was covered with epoxy to prevent corrosion.

Before assembly, the anode array was cleaned in 3 M HCl for 5 minutes and rinsed with distilled water. The cathode was cleaned in 3% $H_2O_2/$ 0.57 M K_2CO_3 and rinsed with distilled water. The anode was placed in the cathode support and the electrode assembly was placed in the tank containing electrolyte. The power supply was connected to the terminals with large cables.

The electrolyte solution comprised 28 liters of 0.57 M K₂CO₃ (Alfa K₂CO₃ 99%) in the case of the MC 3 cell or 28 liters of 0.57 M Na₂CO₃ (Alfa Na₂CO₃ 99%) in the case of the MC 2 cell.

The heater comprised a 57 ohm 1500 watt Incoloy coated cartridge heater which was suspended from the polyethylene disk of the anode array. It was powered by a regulated power supply. The voltage was measured with a digital meter, and the current was measured as a voltage across a precision resistor with a digital meter.

The stirrer comprised a 1 cm diameter by 43 cm long glass rod to which an 8 cm by 2.5 cm Teflon half moon paddle was fastened at one end. The rod passed through a bearing hole in the tank lid and through a bearing hole in the center of the anode array disk. The other end of the stirrer rod was connected to a variable speed stirring motor. The stirrer shaft was rotated at 4 Hz. With the stirrer connected, the stirrer motor drew 4.7 W. With the stirrer disconnected, the stirrer drew 4.4 W; thus, 0.3 W was the stirrer power.

Electrolysis was performed at 39.5 amps constant current with a constant current power supply. The cells were operated in the environmental chamber in the INEL Battery test Laboratory. The chamber maintained the average temperature of the cell surroundings within 1 $^{\rm O}$ C. The bottom of the cell rested on a 1/2 inch thick sheet of Styrofoam.

The temperature was recorded with a series of Teflon-coated Type E thermocouples inserted in several places. The ambient temperature reference was a closed one-liter container of water



with a thermocouple nominally in the center of the water volume.

Data from thermocouples, voltages, and currents were logged by one of the Battery Lab's computer based data systems and recorded at 5 minute intervals. The delta temperature ($\Delta T = T(\text{electrolysis only}) - T(\text{blank})$) and electrolysis power were plotted. The heating coefficient was determined "on the fly" by the addition of heater power. The delta temperature $\Delta T_2 = T(\text{electrolysis} + \text{heater}) - T(\text{blank})$) and the electrolysis power and heater power were plotted.

Mass spectroscopy of the gasses evolving from the MC 3 (K2CO3) cell was performed using a VG Instruments model SXP-50 high -precision mass spectrometer with 0.01-amu mass resolution and 6 decade sensitivity.

A 100 ml sample of the 0.57 M K₂CO₃ electrolyte of the MC 3 (K₂CO₃) cell was removed after 20 days of cell operation, and a chemical analysis was performed on the electrolyte using an Inductively Coupled Plasma-Atomic Emission Spectrometer.

RESULTS Light Water Calorimetry

The results of the electrolysis for INEL cell runs MC 2 and MC 3 at 39.5 A constant current appear in Figure 1 (hand plot of data by INEL scientists). As shown in Figure 1, the MC 3 (K_2CO_3) cell intercepts the Total Input Power axis at 35 W; whereas, the MC 2 (Na_2CO_3) cell intercepts the Total Input Power axis at 59 W. The input power to electrolysis gases given by Eqs. (III.2–III.5) is (39.5)(1.48) = 58.5 W. The production of excess enthalpy of 25 W is observed with the MC 3 (K_2CO_3) cell, and energy balance is observed with the MC 2 (Na_2CO_3) cell.

Mass spectroscopic analysis of the gasses evolved by the MC 3 (K2CO3) cell showed that a significant fraction of the sample was air with standard constituents. When the spectrum associated with air was removed, the residue showed a majority of diatomic hydrogen and oxygen gases in approximately the 2-1 proportion expected from the electrolysis and residual water vapor. There were no hydrocarbons, no metallic constituents or other anomalies except that a slightly higher than expected hydrogen to oxygen ratio was observed. No

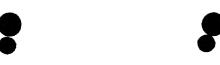
tritium or deuterium measurements above normal background were observed.

Chemical analysis of an electrolyte sample from the MC ${\tt 3}$ (K2CO3) cell after 20 days of operation found the following components at levels above the background levels in the water used to fill and replenish the cell: 1.7 ppm silicon, 1.1 ppm sulfur, and 46.5 ppm sodium in addition to the K2CO3 salt. Small quantities of silicon are known impurities in the nickel wire and may have also come from the glassware used in various processes. Sulfur is a common impurity in the salt, and it may have come from the resin beds used for water deionization. Sodium is a probable salt impurity, and it may also have come from hand contact with the system. The potassium was measured at 43,000 μg/ml corresponding to a salt molarity of 0.55 M (within measurement error of the initial 0.57 molarity determined by weighing the salt and measuring the water for the initial charge). The electrolyte retained its molarity. The cell potential characteristics were essentially unchanged over the duration of operation. There were no nickel or other metallic compounds present in the electrolyte. A visual inspection of the cell showed that all of the structural components were intact. The cell comprised about 155 moles of nickel in the cathode, about 6.5 moles of titanium in the anodes, and about 13.7 moles of K_2CO_3 . The only material consumed in the cell was nano-pure deionized water.

INEL EXPERIMENT II (Pulsed Power Operation)

The MC 3 (K_2CO_3) cell was wrapped in a one-inch layer of urethane foam insulation about the cylindrical surface. The top was not insulated. The bottom of the cell rested on a 1/2 inch thick sheet of Styrofoam.

The cell was operated in a pulsed power mode. A current of 10 amperes was passed through the cell for 0.2 seconds followed by 0.8 seconds of zero current for the current cycle. The cell voltage was about 2.4 volts, for an average input power of 4.8 W. The electrolysis power average (Eq. (III.5)) was 1.84 W, and the stirrer power was measured to be 0.3 W. Thus, the total average net input power was 2.14 W. The cell was operated at various resistance heater settings, and the temperature



difference between the cell and the ambient as well as the heater power were measured.

RESULTS

Light Water Calorimetry

The results of the excess power as a function of cell temperature with the MC 3 cell operating in the pulsed power mode at 1 Hz with a cell voltage of 2.4 volts, a peak current of 10 amperes, and a duty cycle of 20 % appears in Figure 2.

Figure 2 shows that the excess power is temperature dependent for pulsed power operation, and the maximum excess power shown in Figure 2 is 18 W for an input electrolysis joule heating power of 2.14 W. Thus, the ratio of excess power to input electrolysis joule heating power is 850 %.

INEL EXPERIMENT III (Forced Convection Calorimetry Of INEL Cell)

INEL scientists constructed an electrolytic cell comprising a nickel cathode, a platinized titanium anode, and a 0.57 M K₂CO₃ electrolyte. The cell design appears in Appendix I. The cell was operated in the environmental chamber in the INEL Battery test Laboratory at constant current, and the heat was removed by forced air convection in two cases. In the first case, the air was circulated by the environmental chamber circulatory system alone. In the second case, an additional forced air fan was directed onto the cell.

The cell was equipped with a water condensor, and the water addition to the cell due to electrolysis losses was measured.

RESULTS

Light Water Calorimetry

The data of the forced convection heat loss calorimetry experiments during the electrolysis of a 0.57 M K2CO3 electrolyte with the $^{\circ}$ cell appears in Table I and Figure 3. The comparison of the calculated and measure water balance of the INEL cell appears in Table 2 and Figure 4.

The intercept of the Net Input Power (calculated using Eq. (HL5)) axis of Figure 3 for both cases of forced convection is $13\ \%$. Thus, $13\ \%$ of excess power was produced by the INEL cell. This excess power can not be attributed to recombination of the hydrogen and oxygen as indicated by the





equivalence of the calculated and measured water balance as shown in Figure 4.

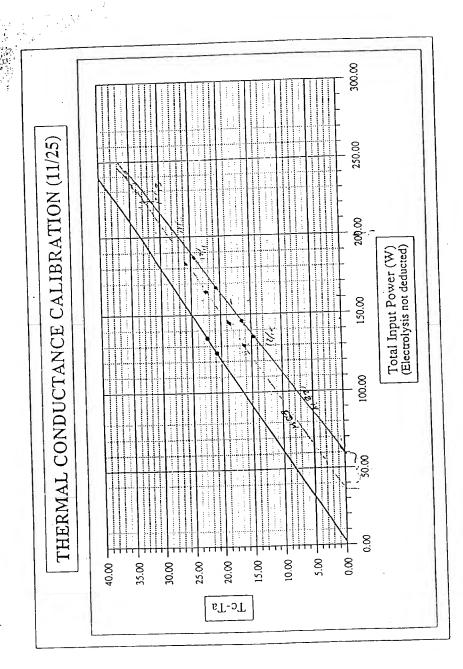
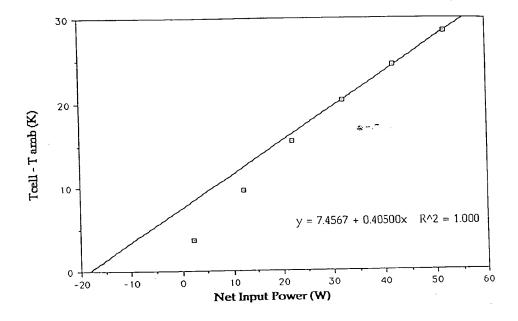
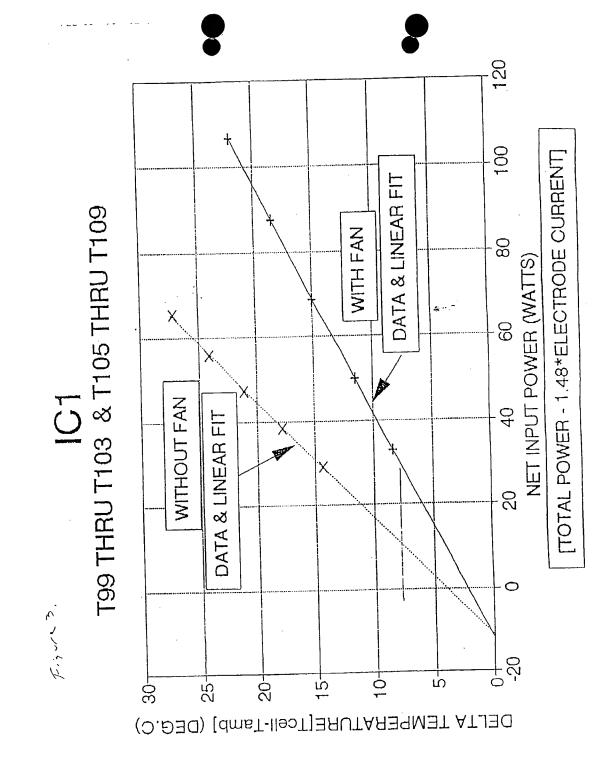
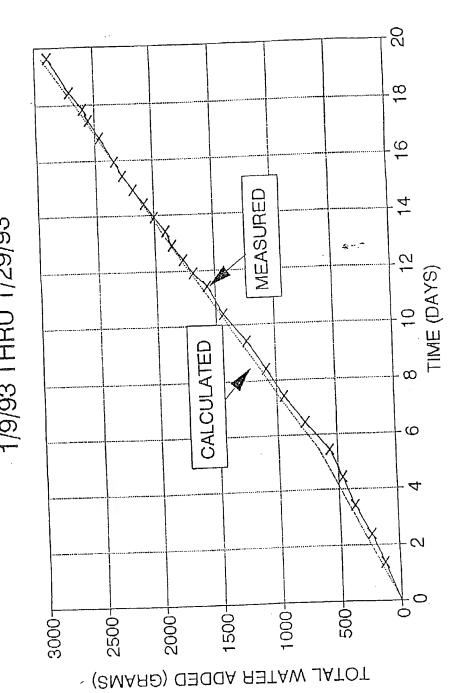


Figure >.







FEB Ø.

Table 1. FILE IC1





	TOTAL	DELTA	LF .	DELTA	LF	PWR-A*1.48
TEST NO	POWER	TEMP	DT	TEMP	DT	
T99	94.8	27.2	27.36265			65.2962
T100	85.2	24.05	23,93155			55.6962
T101	76.8	21.05	20.92933			47.2962
T102	67.8	17.75	17.71267			38.2962
T103	68.57	14.3	14,4138			29,0662
1100	18.24	, ,,,	-0.00042			-11.2638
T105	136.07		*****	21.95	21.94573	106.6662
T108	117.05			18.42	18.42674	87.5462
T107	98.25			14.95	14.94844	68.7462
T107	79.45			11.47	11.47015	49.9462
	62.58			8.35	8.348937	33.0762
T109	17.45			0.01	-0.00082	-12.0538

. .. -

		TIME		QPRO	QPRO .	DATE-START	ELECTRO	MATER	WATER	RSTAW	TOTAL	ADDEO/CALC
DATE	HOURS	MINUTES	SECONDS	TIME	DATE+TIM	DAYS	AMPB	GRAMS	TOTAL	CALO	CALC	
01/09/93	21	30	0	0.895633	33978.9	-0.00416667	16	0	0	0	0	
	,	15	0	0.302063	33980.3	1.402083333	15	131	131	169.9935		0.77061781
01/11/93	7	10	0	0.298511	33981.3	2.398611111	15	108	239	120,4645		0.82963844
01/12/03	7		0	0.311808	33982.31	3.411806658	14.84	131	310	121.9693	412,4473	0.69106475
01/13/93	7		0	0.330556		4,430558556	14.94	89	469	192.6582	838,1088	0.8677747
01/14/93		. 50	0	0.326389		5.428388869	14.93	102	661	119.8168	654,9243	0.8586875
01/15/93			0	0.351369		6.461388889	18.93	205	766	164,6302	810.564B	0.03465404
01/16/93			ő	0.546828		7.448527778	10.93	168	934	169.8341	979.3867	0.9536891
01/17/93	8 7		-	0.320833		8.420833333		160	1084	158.5665		0.95428301
01/18/93	•			0.313889		0.413888889		154	1238	150.4005		0.96864903
01/19/93	7			0.309028		10,40902778		184	1432	159.9143	1455.369	0.98394292
01/20/93	,		_			11.42083333		133	1666	182.511		0.96751620
01/21/03	19					11.01111111		110.5	1875.	78.7489		0.057\$4829
01/21/93	7					12.41368888		63	1758.0	80,76369		0.96937791
01/22/93						12.91736111		6:	1860.			
01/22/83		-				13.4136686		4	1896.			0.97856882
01/23/93			•					10	1998.	78.86744		0.09086111
01/23/93		7 2				14,4111111	19.93	8	4 2082.	5 81.31126		0.99251593
01/24/93						1 14.90888564			3 2175.	5 79.41813		0.0002727
01/24/03		7 3		0,31803		2 16.4180656			4 2269.	6 BZ.31512		1.00423316
01/26/03			-	0.83402		3 15.9340277		6	5 2334.	5 62.67261	2342.800	0.09645461
01/25/93				0.68819		0 16.7681044		12	2 2450	9_ 437,1911	2479.996	0.99052498
01/26/03				0.32291		2 17.4229156		, 6	6 2552.	5 101.946	8 2681.94	0.98859824
01/27/93	•	7 4	_	-		3 17.8326388		(5	5 2508	85.840	8 9847.78	0.98516331
01/27/93		נ ז.		0.73253		2 18.4243055	-		7 2715	6 95.0304	7 2742.81	5 0.99004131
01/28/93	•	-	•	0 0.32430			-			5 194.508	5 2937.32	3 0.95269741
01/55/6:	3 1	2 (0	0 0.63473	33998.5	19.6347222						

Appendix I.

: ETAG

December 15, 1992

:OT

Richard Deaton MS 4139, Ext. 6-2016, FAX 6-2681

FROM:

R. L. Drexler MB 3123, Ext. 6-1789

SUBJECT:

INEL CELL CATHODE ESTIMATE

Attached are the following sketches and revised sketches:

12/15/92 Cathode Assembly for INEL CELL 12/15/92 Narrow Cathode Strap for INEL CELL 12/2/92 Cathode C-1 INEL CELL 12/8/92 Mandrel - Cathode Winding 12/15/92

INEL CELL Electrode Bus Ring

Would you please give us a firm estimate for fabrication of two "identical" cathode assemblies per the 12/16/92 sketch, and two Electrode Bus Rings per the 12/15/92 sketch.

The cathode windings could be made on a mandrel per the sketch 12/8/92 or similar suitable arrangement.

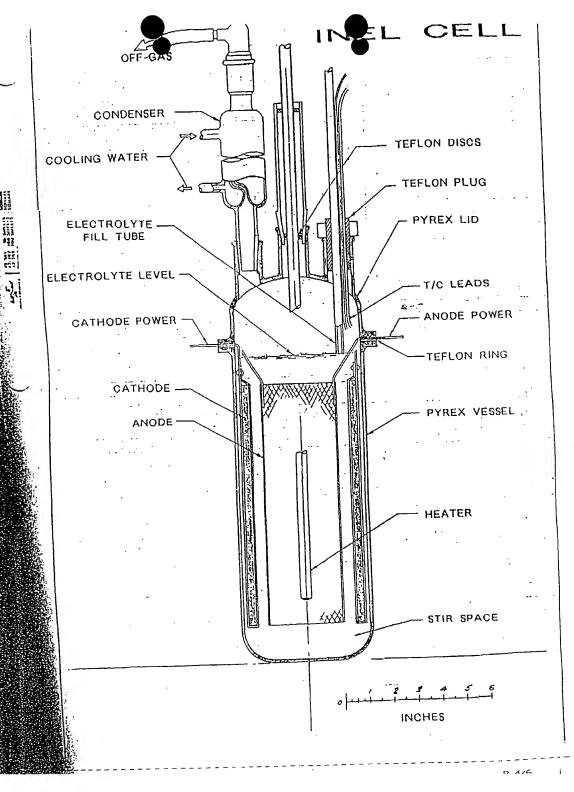
These cathodes and bus rings are similar to those previously fabricated except:

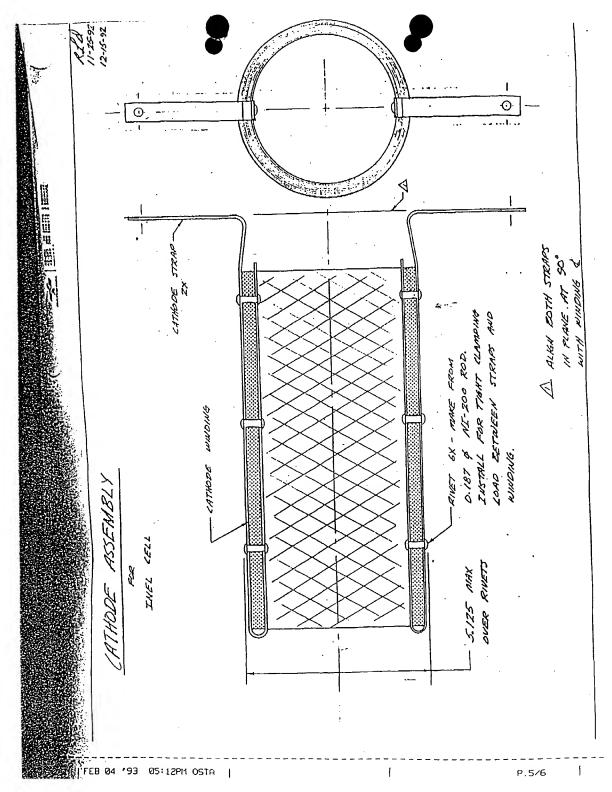
- 1. The straps are 0.5 in. wide rather than 1.0 in. wide. These narrower straps would be flat rather than arched to fit the winding curvature.
- 2. There are no secondary straps as were added to the windings of the first cathode assembly.
- 3. Windings would be less dense than the first winding. A much steeper pitch is probably necessary to achieve the more open wind.
- 4. Weight of the NI-200 wire of each winding should be very close to 3.33 pounds, and both windings should have the same weight as closely as possible.
- 5. Slots in the Teflon Buss Ring for the cathode straps would be 0.50 wide rather than the 1.0 width of the first ring.

FEB 04 '93 05:11PH OSTA

P.3/6







U CATHODE STRAF 12-15-92 018×45° INEL CELL 0.25 \$ 25 -1.0<u>A</u> 0.25 R -30 * MATL. - AD65 STOCK NI - 200 \oplus 6.0 NUMBER READ. - 2 PARTHORE **(** REMORE BURRS & SHARP EDGES 8. 2.188 8074 3 3× TOL. X £ 0.10 1 0.03 \oplus .xx £ 0.010 .xxx OR AS NOTED IN THE LO LONG ZONE DESIGNATED o, UIEW A-A 20000 FLAT WITHIN 0.005 SCALE - FULL

CATHODE INEL CELL NI- 200 CATHOPE STRAP -TWO AT 1800 To the state a state of 123 (Z WINDING N1-200 WIRE 0.010 DIAM 3.33 18 0.2 SOLID WRAP 0 0 NUMBER REDD. - ONE PER CELL THIS PAGE BLANK (USPTO)





HPC
Confidential
Information

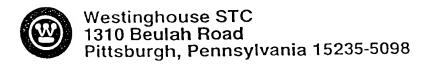
EVALUATION OF HEAT PRODUCTION FROM LIGHT WATER ELECTROLYSIS CELLS OF HYDROCATALYSIS POWER CORPORATION

S. H. Peterson Technology Development

February 25, 1994

APPROVED:

Dale L. Keairns, Manager Environmental Technologies



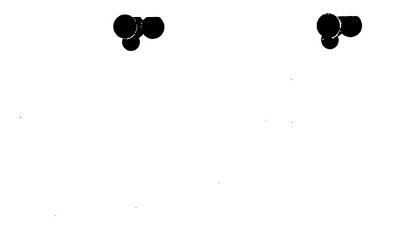






ABSTRACT

An experimental study was undertaken to evaluate heat production in electrolysis cells designed and set up by Hydrocatalysis Power Corporation (HPC). Results show 50% more heat production in cells with an "active electrolyte" of 0.57 molar K₂CO₃, compared to a cell with a control electrolyte of 0.57 molar Na₂CO₃. Other calorimetric data are presented. Evidence for the mechanism proposed by HPC is discussed, along with an alternative mechanism proposed by Arnold Isenberg. Critical experiments to resolve the question of heat production are proposed.









1. Introduction

Hydrocatalysis Power Corporation (HPC) has developed electrolysis cells that are reported to produce excess power, as heat, during electrolysis of a potassium carbonate electrolyte with a nickel cathode. This may be loosely associated with "Cold Fusion" although HPC claims an advanced quantum theory that provides a purely chemical explanation for the heat production. The effect occurs in cells containing only normal water, arguing against any nuclear phenomenon. An investigation of this heat production was undertaken to determine if there is an effect that could be the basis of advanced power generation, or if the claimed effects can be attributed to poor calorimetry or other experimental artifacts.







Following an exchange of information about requirements and facilities, Mr. William Good, of HPC, came to STC on December 7, 1993 to set up four cells for our evaluation. Experiments were conducted until December 23. This letter report is a brief summary of experiments conducted and their results.







2. Conclusions

- Electrolysis cells provided by Hydrocatalysis Power Corporation demonstrated 50% excess heat with K₂CO₃ electrolyte, compared to a control cell containing Na₂CO₃ electrolyte.
- 2. Comparison of heating due to resistance of electrolysis current to heating from an immersed auxiliary heater was consistent, in some instances, with the excess heat observed with electrolyte comparison. However, design problems with the HPC cell make power balance comparisons uncertain. The design problems include the high operating temperature of the cells, and the variation of operating temperature with operating conditions.
- Evidence for the mechanism leading to the observed anomalous heat is sparse.
 Data provided by HPC were unconvincing when reviewed by STC experts. In an independent experiment, Arnold Isenberg demonstrated an alternative, chemical mechanism that would not provide a basis for power production.
- A basis for improved cell design and more significant experimental characterization of the HPC thermal effects was established by these experiments. Critical experiments were identified.







3. Recommendations

- 1. It is essential to determine if the anomalous heat observed in the HPC cells was due to the difference in Faraday efficiency of electrolytic gas generation between the K₂CO₃ and Na₂CO₃ electrolytes, as Isenberg observed with a different cell geometry. If the anomalous heat is only due to difference in Faraday efficiency, there is no effect worth further investigation.
- If the heat anomaly survives the determination of Faraday efficiency, further studies should be directed at determination of scaling effects. Improved cell design features have been identified for such studies. These are described in the discussion.
- HPC has developed a gas phase cell that does not require an electrolyte or electrolysis. These cells merit further attention.







1

4. Experimental:

4.1 HIGH TEMPERATURE CELLS

Initially, three cells were set up identically in 2 liter dewars. Each had a cathode made up of 500 m of 0.38 mm diameter Ni wire (ALFA, .99999 pure), giving 0.6 M² surface area. The cathodes were wound loosely on porous teflon forms. The anode of each cell was Pt deposited on a Ti mesh, approximately 14 cm long by 4 cm wide, folded back on itself about 6 cm. Two such pieces were used for each cell, for an approximate area of 200 cm².

The cells were constructed by placing the cathode in the dewar, placing the anode down the center of the teflon form, and also placing an auxiliary heater and a thermocouple in a glass tube down the center of the tefion form. All three cells were connected in series with a common power supply. This was to ensure that equal electrolysis was done in each cell.

The components of each electrolysis cell were prepared by following a protocol established by HPC, appendix 1. Each of these first three cells was set up by Bill Good.

The cells were polarized and electrolyte, 0.57 M K₂CO₃, was added to permit electrolysis current to flow. This step was done as quickly as possible to ensure that no cathode was exposed to the highly basic, corrosive electrolyte without undergoing electrolysis, for more than the minimum time necessary. Initially, 1.5 I of electrolyte was added to each cell, to bring the electrolyte level to the top of the electrode assembly. Later, after the electrolyte had heated up and expanded, it was necessary to remove 100 ml of solution, leaving a charge of 1.4 l of electrolyte in each cell. The power supply was adjusted to provide a nominal electrolysis current of 3 amperes. This initial set up was somewhat rushed because Bill Good had only 3 days available at STC.

A plastic foam lid was made for each cell. The lids had some thermal insulation value, but were definitely not gas tight. Lead wires penetrated for the electrodes and for the auxiliary heater. Additional penetrations permitted insertion of the thermocouple and a small funnel that allowed for addition of water to compensate for the water lost to electrolysis, calculated to be 25 mVday for electrolysis at 3 A.

A data collection system was set up, based on a Molytek data recorder acquired for this purpose. It was set up to measure the following parameters:







Series current

Room Temperature (measured in a dummy dewar cell containing distilled water).

For each cell:

Voltage drop

Cell temperature

Heater voltage

Heater current, measured as voltage drop across a 0.01 ohm, 1% precision resistor.

The Molytek allows channels to be used for calculations based on the information in other channels. So, for instance, the heater power was calculated for each cell. By the time the fourth cell was on line, all 32 channels of the data logger were in use.

Initial experiments were performed with 0.57 M K₂CO₃ in all 3 cells. They were run at 3 A until they reached thermal equilibrium. At these equilibrated conditions the three cells were at the following temperatures: Cell A, 68.1 °C; Cell B, 68.8 °C; and Cell C, 69.4 °C. Since the room temperature was 23.7 °C, that meant the three cells were showing very similar response, about 45 °C above ambient temperature.

The power being delivered to each cell was determined by measuring the voltage drop across each cell. The total power is then the product I_{series}V_{cell} into each cell, but the power available for heating the cell is less due to the loss of heat from evolution of electrolysis gases. HPC assumes 100% Faraday efficiency for electrolysis gas evolution, so the power available for cell heating is reduced by the enthalpy of formation of the gases from water, which corresponds to 1.48 volts. Then the heating power into the cell, assuming 100% Faraday efficiency of gas formation, is

$$W_{el} = I_{series}(V_{cell}-1.48)$$

Auxiliary heaters were placed in each cell, to permit "on-the-fly" calibration of the power balance in the cells at conditions close to any given set of operating conditions. A series of experiments were performed in which combinations of electrolysis power and heater power were applied, and the equilibrium temperatures of the cells determined. These experiments are summarized in figures 1 to 3, which show the conditions of operation summarized as the







electrolysis heating power, W_{el} , auxiliary heater power, W_{hlr} , $W_{total} = W_{el} + W_{hlr}$, and the heating coefficient for those conditions. Figures 4 to 6 show the temperature rise for each cell at the same conditions.

On December 20, cell A was switched from the K₂CO₃ electrolyte to Na₂CO₃ to provide a control experiment. Na₂CO₃ is not expected to be catalytic for extracting energy from H atoms, and HPC routinely use it as a control. Prior to the electrolyte switch, all three cells were again equilibrated at 3 A electrolysis current with no auxiliary heat, and were still showing similar behavior with temperatures ranging from 66.4 to 73.8 °C. After the electrolyte switch, Cell A equilibrated at 49.9 °C, while Cells B and C were at 69.2 and 74.9 °C.

4.2 LOW TEMPERATURE CELL

The high operating temperatures of the first three cells caused several problems, such as

- At such high temperature, the vapor pressure of water is approximately 0.5 atm, and the variation with temperature is significant. The gases lost through electrolysis will thus carry off an approximately equal volume of water vapor, and this loss is temperature dependent. This makes it difficult to interpret thermal effects associated with changes in power to the cell which result in operation at various temperatures.
- The resistance of the electrolyte to current flow is temperature dependent.
 When the heat loss coefficient of a cell is as low as that for these dewar cells, resulting in a heating coefficient of >10° C/watt, each change in cell conditions produces a different heating effect due to operation at a different temperature.
- Water was added to each cell periodically to make up for the gases lost through electrolysis. However, the additional loss due to evaporation was significant and more difficult to compensate. When this effect became evident, one cell (B) was put on a balance to provide daily weight information. However, since this effect is temperature dependent, the same correction did not apply to all cells. Furthermore, periodic addition of cold water is equivalent to a power loss that is not considered in the power balance calculation. Adding the same amount of water to each cell balanced the





power effect, but did not adequately compensate to maintain constant electrolyte composition.

Because of the high cell temperature, addition of auxiliary heat required the heater to run at even higher temperature. Heat conduction through the lead wires was probably significant, reducing heat into the solution and causing the heating coefficient for auxiliary heat to be low.

A fourth cell was set up, using another set of electrodes provided by HPC. Instead of a dewar, the cell was made with a 2 gallon high density polyethylene pail with a tight fitting lid. The cell setup was essentially the same as the three smaller volume dewar cells, except that the pail had enough room on the bottom to use a magnetic stirrer off to one side to provide additional stirring to supplement the mixing due to bubbles from the electrolysis. A larger (but unfiltered) power supply permitted running this cell at a higher current, up to 7 amps. This cell was filled with 7 liters of 0.57 M K₂CO₃. Initial heating with only the auxiliary heater, at power up to 6.1 W heated this cell up to only about 1 °C above ambient. When electrolysis was begun, it was set at 7 amps, with a voltage drop across the cell of 4.2 volts, giving net electrolysis heat of about 19 W. The cell equilibrated at about 32 °C, 9.5 °C above ambient, giving a heating coefficient of 0.5 deg/W. An attempt was made to reduce the electrolysis power to 10 W and replace that power with auxiliary heat, but under these conditions the daily variation in room temperature was larger than any other observed effect.

4.3 Results

4.3.1 Experiments with K2CO3 electrolyte

Initial results showed approximately 11-13 degrees/watt of heating when the cells were run with only electrolysis. When the auxiliary heaters were used in addition to the electrolysis heat, the additional heat rise was equivalent to about 8 deg/watt. Thus, the "excess heat" from electrolysis seemed to be about 50%, based on the assumption of 100% Faraday efficiency of electrolytic gas production. Other tests were designed to further check this initial observation. These consisted of various settings of electrolysis and auxiliary heater powers, illustrated by figures 1 to 3, which show the various power







levels and the observed heating coefficients for cells A, B, and C, respectively. Figures 4 to 6 show the same power data, along with the observed temperature rise for these cells. In all these figures, each point represents equilibrated behavior at the indicated conditions, based on at least several hours of stable traces observed on the chart recording of the data logger. In most cases, multiple points were recorded and plotted at constant conditions, to illustrate the reproducibility and stability of the experiments.

In figure 1, the heating coefficient for cell A is shown for electrolysis at 3 amps, with three levels of auxiliary heating of 0, 0.54 and 1.2 W. Each time the heater power is increased, the heating coefficient decreases. However, as figure 4 shows, the temperature of the cell does increase as the power is increased. Some more subtle effects are also apparent. The electrolysis power decreases a little each time the auxiliary heat is increased. This is because the conductivity of the electrolyte increases with temperature, so at constant current the voltage drops and the power decreases slightly.

Following the experiments at 1.2 W of auxiliary heat, an attempt was made to provide the same total power with electrolysis alone. The heating coefficient did increase a little, as would be expected if there is an anomalous heat source associated with electrolysis. However, as mentioned above, loss of heat from the heater through the electrical leads would also cause the same effect.

Finally, the electrolysis current was set at 3 amps again to establish the equilibrium behavior before changing the electrolyte in cell A to Na₂CO₃. The temperature rise and heating coefficient were very close to those observed in the initial 3 A electrolysis with no auxiliary heating.

Cells B and C showed effects similar to those observed for cell A, except that their auxiliary heater levels were set at other values to get more information on the effects of auxiliary heat. However, cell C consistently had the highest temperature of the three cells, and thus was susceptible to the largest loss of water from evaporation. This became apparent when the temperature was observed to continue a slow increase under steady operating conditions, illustrated by data from Dec. 14 and 15 in figure 6. Cell resistance kept dropping and the temperature kept rising as the salt concentration increased.

25 ml of water was being added daily to each cell to replace the calculated loss due to electrolysis. However, it became clear that this was inadequate due to the likely







evaporative loss. A high capacity balance was then obtained and placed under cell B (chosen because it was intermediate in temperature). The weight change over 24 hours was about 50 g, consistent with the expectation of 25 g for electrolysis and an equal amount of evaporation if the vapor pressure of water is 0.5 atm. Accordingly, the daily water addition was changed to 50 ml per cell. This would still be expected to slightly overcompensate in cell A, the coolest cell, and undercompensate in cell C, the hottest cell. In the end, when the cells were shut down and dismantled, the volume of electrolyte in each cell was measured. Cell C was down to 1000 ml, showing a net loss of about 400 ml of water over the duration of the experiments. Cell B contained 1300 ml of electrolyte, showing that it had been fairly well replenished once the weight change information was available. Cell A had 1350 ml, but it had been changed over to Na₂CO₃ electrolyte only a few days earlier.

The electrolyte stability was a matter of concern once the evaporative loss problem was recognized. Accordingly, samples were extracted from each cell for Total Inorganic Carbon (TIC) analysis. For these electrolytes, TIC should be a direct measurement of CO₃⁼ concentration. On 12/20, the three cells showed the following values of TIC:

	TIC
Cell	<u>molar</u>
A	0.46
В	0.47
С	0 .44

Thus there seems to be some loss or destruction of carbonate under the cell operating conditions.

4.3.2 Control Experiment with Na₂CO₃ Electrolyte

Because Cell C was more erratic than the other two, and because Cells A and B were very similar, it was decided to change the electrolyte in cell A to 0.57 molar Na₂CO₃ for a control, since Na₂CO₃ is not expected to be catalytically active for hydrogen shrinking. An objective of this test was to adjust the electrolyte concentration to match the resistance of cells A and B, and thus to run them at the same input power. Since the concentration of CO₃⁼ had changed,







according to the TIC measurement, the resistances were expected to be different. However, when the cells approached equilibrium and the resistance stopped changing with temperature, they turned out to be very close, so no adjustment was needed. This meant that the cells were running with nearly identical electrical input power, 3.42 W for Cell A and 3.79 W for Cell B. With a heating coefficient of 12 deg/W, one would expect cell A to be about 5 degrees cooler than cell B under these conditions. However, the equilibrated cell temperatures were A: 50°C, and B: 69°C. Cell C was at 75°C. Thus it seems that there is anomalous heat in cell B that causes >15° additional heating. If cell A is a true control, and its temperature represents the effect of resistance heating, then the true heat coefficient is about 8 deg/W, and the anomalous heat in cell B is about 50% greater. The effect of switching electrolytes is illustrated in figure 7.

Considering that the time for these experiments allowed only a few characterization tests, and no real optimization, the 50% excess heat with K₂CO₃ compared to Na₂CO₃ electrolyte seems to be the effect predicted by HPC. The actual temperature difference of 15°C is large enough to give confidence that trivial measurement errors are not the cause of the effect. However, two additional sources of information have added doubt about the HPC mechanism and to the question of whether such cells represent a source of useful heat.

4.3.3 Isenberg's Check of Faraday Efficiency

Arnold Isenberg was an interested and very helpful observer of these experiments. When I had the opportunity to describe the final results, especially the difference between the K₂CO₃ and Na₂CO₃ electrolytes, he raised a potential alternative mechanism based on the formation of percarbonates due to the reaction of dissolved oxygen with the carbonate in the electrolyte. He requested, and received, permission to conduct a brief experiment experiment, described in attachment 2, to see if this might indeed cause the observed difference in temperature rise for the two electrolytes. As he describes, the Faraday efficiency of electrolysis gas evolution in the two electrolytes was different, and the presence of peroxy species was demonstrated.

4.3.4 Byers' Review of ESCA Data

HPC has conducted a search for the "shrunken hydrogen" product of the electrode reaction that produces excess energy in these reactions. If the existence of shrunken hydrogen, at the energy levels of the Mills theory, could be proven, a promising new energy source could be assured and further development would be clearly warranted. Unfortunately, Art Byers'







evaluation of the Electron Spectroscopy for Chemical Analysis (ESCA) data presented by HPC is that the evidence is not convincing (see attachment 3).

4.3.5 Other Factors for Consideration

As will be discussed below, the cells presented for evaluation by HPC performed as expected, showing excess energy when K₂CO₃ was used for the electrolyte, compared to a control cell filled with Na₂CO₃ electrolyte. However, the time available did not allow for much parametric investigation. The data represent certain experimental conditions, but no optimization studies were performed.

Other factors should be examined before final decisions are made about this technology. In particular, the following seem worthy of consideration:

- HPC claims observation of cells that produce more heat than the total input electrolysis power. If such claims can be substantiated, alternative mechanisms involving chemicals such as percarbonates would not explain the observations.
- After a discussion of cathode preparation between Bill Good and John Jackovitz.

 John provided a sample of Ni felt, annealed under hydrogen at 1100°C. Initial response from HPC was that with this cathode material, a cell drawing 80 amp, with voltage drop of 2.2V, for total electric power input of 0.176W, produced 0.250W of heat. They requested 7 additional sheets of the Ni felt, to produce a cell that would develop 120W of excess heat. The effect of this cathode material could be evaluated at STC. The results of HPC tests are not known at this time.
- HPC has also described energy production in cells that use gaseous hydrogen, and which do not involve electrolysis. In these cells, high pressure H₂ is applied to a cell prepared with a coating of the catalytic K₂CO₃, and high rates of heat production are observed. In fact, it is reported that excess energy production continues after input energy is terminated, for significant periods of time.







5. Discussion

In general, the cells provided by HPC performed as they were expected to. The heat generated by resistance to electrolysis current, assuming 100% Faraday efficiency of electrolysis gas generation, was greater than the heat generated by the pure resistance heating of the auxiliary heaters. Furthermore, the heat production was greater with K₂CO₃ than with Na₂CO₃ electrolyte, by about 50%. On the basis of these results, HPC feels that this demonstration was successful.

Unfortunately, several factors reduce one's confidence that these cells have identified an attractive heat source that could be developed for power generation purposes. These will be discussed below.

The first factor to be considered in discussion of these experiments is problems with the heat measurements. Part of the problem was that these cells operated at quite a high temperature; higher than was anticipated. The operating temperature was difficult to predict because the heat loss coefficient for this size and design of cell was unknown. When these cells turned out to equilibrate around 70°C, it caused at least three problems:

- At this temperature, the vapor pressure of water is about 0.5 atm, and it varies
 significantly with temperature. Thus, changing operating conditions in a way that
 changed temperature changed the heat loss due to evaporation of water.
 Furthermore, there was uncertainty about how much water to add to a cell each day
 for replacement of water loss due to electrolysis.
- The effect of the auxiliary heaters was difficult to interpret. The heater had to get quite hot to generate significant heating at the cell conditions. Power loss through the heater wires could be significant, and difficult to estimate. This could explain the low heating coefficient for the auxiliary heaters relative to the heating due to electrolysis.
- Finally, there was loss of inorganic carbon during the experiments, perhaps from thermal breakdown of carbonate ion, or perhaps due to aerosol formation and transport. This is evidence for chemical reactions that are not accounted for in the HPC model; how the power balances of the cells are affected is unknown.







Another feature of the heat effects was that the heating coefficient decreased any time a change was made that increased the cell temperature. This includes changes such as increasing the electrolysis current, as well as changes such as adding auxiliary heating at constant electrolysis current. This effect is probably due to increased evaporation loss, but it makes interpretation of the heat measurements more difficult.

An altempt was made minimize the effect of temperature change by operating the cells at the same total input power by varying both heater and electrolysis powers. The equilibrated results are shown in the figures for data of 12/18 to 12/19. These results are not very conclusive; the cell temperature and heating coeficient are determined mostly by the total input power, and not on how the power is partitioned between electrolysis current and auxiliary heater. This was also the case when the same thing was tried with cell D, operating at much lower temperature.

If the temperature measurements do not show a clear heating anomaly, the effect of changing electrolyte from K₂CO₃ to Na₂CO₃ was remarkable. The intent was to change electrolyte in one cell, and to match the power input for the two cells (A and B) connected in series. This worked out quite well, and the Na₂CO₃ cell equilibrated at a temperature 20°C lower than the cell containing the K₂CO₃ electrolyte. At first, this looked like clear confirmation of the HPC effect.

Isenberg's measurement of the difference of Faraday efficiency for the two electrolytes raises quite a different possibility for the difference in temperature between the K and Na electrolytes. He observed Faraday efficiency of 57% for K₂CO₃ in the temperature range of 55-65°C, and 69% for Na₂CO₃ at 50-55°C. This 12% difference, scaled to the 3A electrolysis current, would account for about half of the observed temperature anomaly. Given the difference in geometries of the experiments, it is not clear how to compare them. Isenberg's setup had the anode and cathode concentric with a thin insulator between them, giving maximum opportunity for the recombination reaction. In the cells described in this report, the electrode separation was much greater, but there was sufficient agitation of the electrolyte solution that when the cells were opened on 12/23, the electrolyte was very uniformly filled with tiny bubbles. This was good in terms of providing sufficient agitation to provide uniform temperature in the cell, but possibly also of promoting recombination.

In contrast to Isenberg's experiment, the daily weight loss in Cell B indicated loss of 50 g of water/day. This is fully consistent with 100% Faraday efficiency plus loss of an equal







amount of water due to evaporation at the 0.5 atm vapor pressure of water at the cell temperature. Alternatively, the 50 g/day loss could result from lower Faraday efficiency and evaporative loss if there is significant formation and transport of aerosol from the cells.

5.1 Additional Studies

Some additional experiments, based on these preliminary observations, should be able to resolve the issues raised here. The following approach is suggested:

- 1. It is essential to determine if the depolarization observed by Isenberg, attributed to chemical reactions leading to the formation of percarbonates, caused the difference in temperature between cells when Na was substituted for K in the electrolyte. The principle change in our setup required would be to use a sealed lid on the cell with a vent for gas release, which would permit the evolved gases to be measured and characterized. Hard plastic lids that would meet this need were machined, but there was not time to use them.
- 2. The sealed cell configuration of test 1 would also permit examination of the effect of increased agitation to assure uniform temperature distribution in the cell, and a test of a mechanism proposed by Gene Struhl (Baltimore, retired). He has proposed that the heat observed results from chemical reaction of the hydrogen formed at the cathode, and that the effect could be enhanced by sparging with oxygen, or diminished by sparging with nitrogen. Sparging would provide a way of varying the agitation in the cell, as well as a way to investigate the effect of the sparging gas on cell heat production.

The results of these tests 1 and 2 would determine the Faraday efficiency of electrolytic gas production in our cells. If it is shown that the observed temperature anomaly is a result of differing Faraday efficiencies for the two electrolytes, there would be no reason to pursue further experiments at this time. However, it would be desirable to continue to monitor developments that might indicate true anomalous heat production, particularly in gas phase cells in which the problems associated with electrolysis do not arise.







If the observed heat anomaly survives the Faraday efficiency test, there are a number of additional tests that should be considered as a sound development program. These include the following:

- It will be very valuable to establish a mode of operation that will permit separation of the cell temperature from the cell power. This can be done by operating a flow cell in which flowing electrolyte is introduced into the cell at a preset (variable) temperature, and the temperature rise in the cell is determined. In such a flow cell, the temperature rise can be controlled by controlling the flow rate. Shorter residence time in the cell should also minimize electrolyte destruction, and permit determination of electrolyte stability. Experimental parameter variations will be under much better, controlled conditions. Jim Bauerle has considered the design of a flow calorimeter for such experiments, and his input will be invaluable in designing and carrying out these tests.
- The cooperation between John Jackovitz and Bill Good has identified Ni mesh, annealed under H₂ at 1100°C as a cathode material with the potential to produce true excess energy greater than the product of cell voltage times current. This electrode material should be employed in our well designed flow cell.
- HPC recommends understanding electrolysis cells before trying experiments with gas cells. However, the gas cells provide a possible route to the high temperature operation needed for power generation, without the problems associated with carrying out electrolysis in aqueous solution at temperatures above the boiling point of water. An objective of advanced testing should be to test and characterize gas cells, including use of the 1100°C, H₂ annealed Ni telt as the catalytic surface.





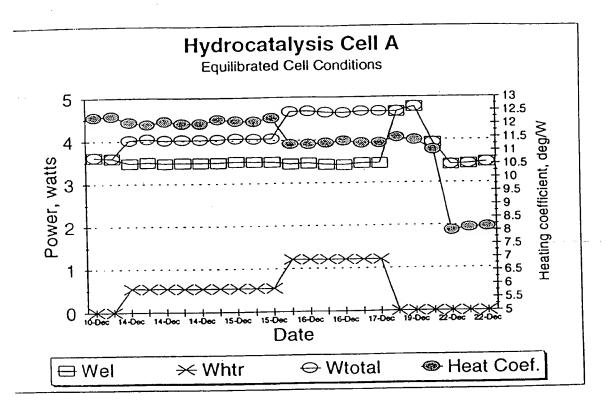


Figure 1. Equilibrated values for heating coefficient of cell A at various conditions of input power. Points before 12/22 are with \(\cdot 2CO_3 \) electrolyte; last three points are with \(\cdot 2CO_3 \) electrolyte.





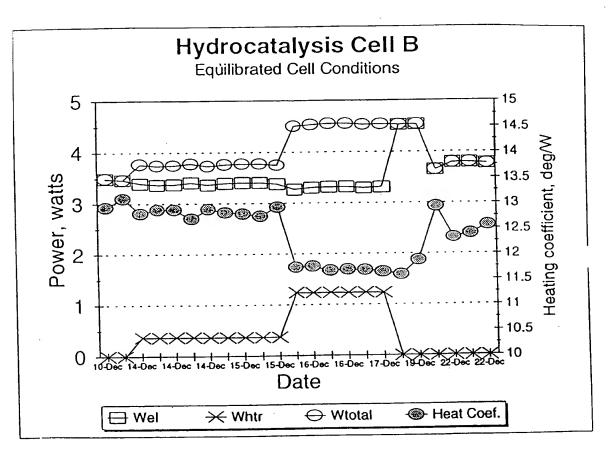


Figure 2. Equilibrated values for heating coefficient of cell B at various conditions of input power. All points are with K₂CO₃ el xtrolyte.





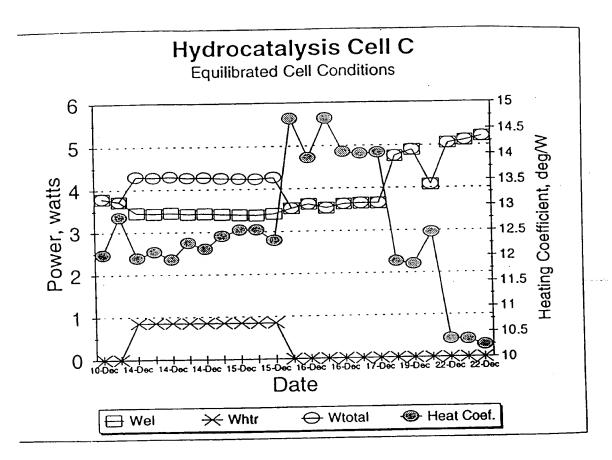


Figure 3. Equilibrated values for heating coefficient of cell C at various conditions of input power. All points are with K2CO3 electrolyte.





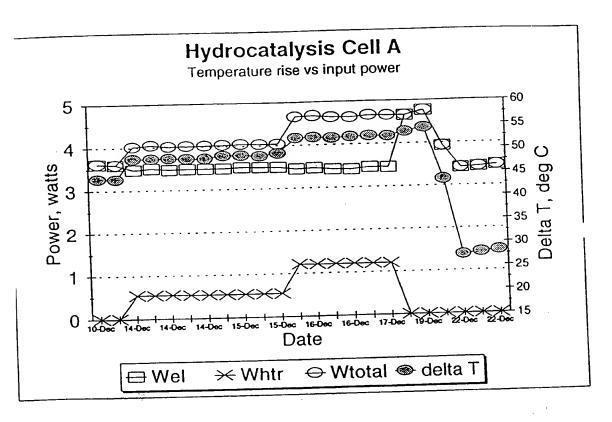


Figure 4. Equilibrated values for temperature rise (ΔT) of cell A at various conditions of input power. Points before 12/22 are with K₂CO₃ electrolyte; last three points are with Na₂CO₃ electrolyte.







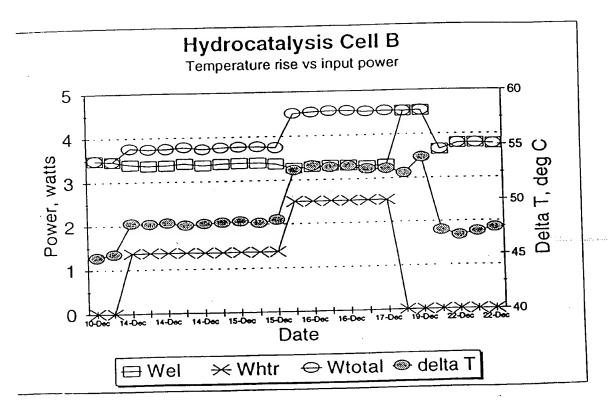


Figure 5. Equilibrated values for temperature rise (ΔT) of cell B at various conditions of input power. All points are with K_2CO_3 electrolyte.





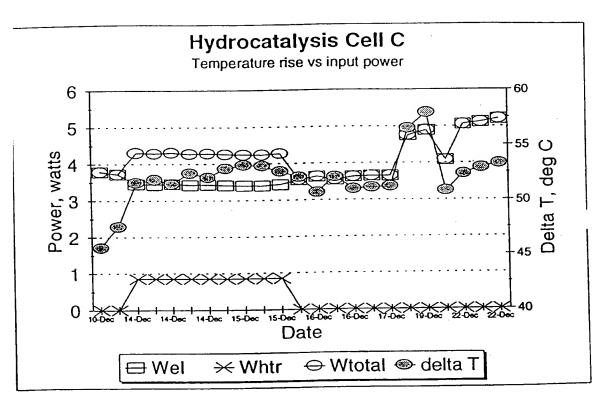


Figure 6. Equilibrated values for temperature rise (ΔT) of cell C at various conditions of input power. All points are with K₂Ch₃ electrolyte.





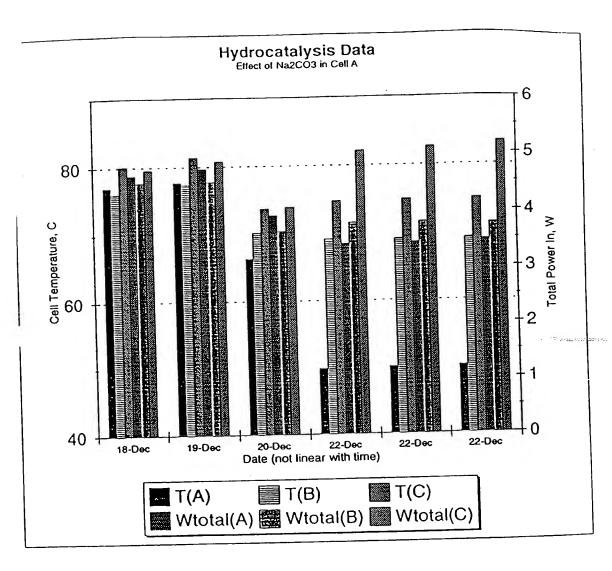
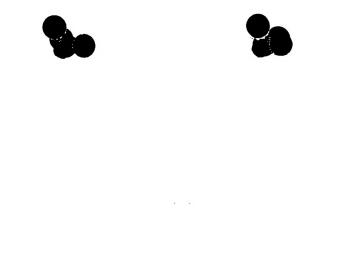


Figure 7. Effect of changing electrolyte in cell A from K₂CO₃ (before 12/22) to Na₂CO₃. Bars show equilibrated temperature for various input power conditions.



.





Attachment 1 HPC Experimental Protocol





•

•

Attachment 2 Isenberg's Determination of Faraday Efficiency









From:

Science & Technology Center

WIN: 236-2157

MIN: 200 210.

Date: January 14, 1994

Date: January 14, 1994 Subject: Thermal Effects in Electrolysis of Aqueous K₂CO₃-Solutions

To:

S. H. Peterson

501-3E17

œ:

W. J. Dollard

501-2W59

S. D. Harkness J. A. Spitznagel 801-3C54C 801-3C54D

P. R. Emtage

501-2B32

Recently you conducted some nice calorimetric measurements on electrochemical cells during the electrolysis of potassium- and sodium-carbonate solutions, in order to verify data that had been obtained by R. L. Mills and W. R. Good of HydroCatalysis Power Corporation using anode/cathode hardware; that they provided to you. As you informed me, you confirmed that the thermal effects during the electrolysis of K_2CO_3 solutions were significantly more exothermic than in Na_2CO_3 solution as electrolyte.

Mills and Good have observed this effect and explained it through a rather bizarre theory involving new energy states of hydrogen. The thermal effects, in my view, needed an immediate rational explanation. Therefore, I conducted several electrochemical measurements that can explain higher exothermal reactions during the electrolysis of aqueous K2CO3-solutions as compared to Na2CO3-solutions. In the interpretation of enthalpy measurements as proposed by Mills and Good, the assumptions are made that the faradaic efficiency with respect to gas evolution is 100%. This assumption enters into the computation as a loss of energy from the calorimetric system. However, when electrochemical side reactions take place, gas evolution rates may be reduced and the side reactions can contribute to exothermic effects within the calorimeter. Computations, therefore, must take such thermal effects into account.

I electrolyzed aqueous solutions of K₂CO₃ and Na₂CO₃ within the confines of a 500 ml gas burette, in order to measure the total volume of gas evolving from anode and cathode. The rate of gas evolution was measured and pressure, temperature, and humidity corrections were made. No special pretreatment (purification) of electrodes or electrolyte were made. I suspected anodic side reactions could involve the formation of percarbonates (adducts of hydrogen peroxide and carbonates). These compounds would depolarize (be reduced at) the cathode and lead to a lower than theoretical rate of gas evolution (<10.45 ml gas per ampere minute).







The presence of percarbonales can be detected by acidifying the electrolyte and by subsequent reaction of the solution with potassium iodide. The presence of $\rm H_2O_2$ (from percarbonate) will lead to the formation of free iodine which is colorimetrically detected with a starch indicator. Both electrolyte solutions did show a strong iodine reaction after electrolysis had been performed, thus, explaining the low efficiency in observed gas evolution.

The essential experimental data are summarized in Table 1 and the simple electrolysis apparatus is shown in Figure 1.

Following observations have been made:

- Gas evolution in both electrolytes is significantly below 100%.
- Higher efficiency of gas evolution is observed in the Na₂CO₃-electrolyte, which explains higher enthalpy values in an otherwise "mirror" K₂CO₃ system.
- Increased electrolyte temperature decreases gas evolution efficiency in both electrolyte solutions significantly.

The last observation was not expected because H_2O_2 is less stable at higher temperature. This would indicate that the cathode depolarization reaction rate determines the gas evolution efficiency. This rate would be expected to go up with temperature.

Condusions:

- Comparison of thermal effects in the electrolysis of K₂CO₃ and Na₂CO₃ can only be made if careful gas evolution and gas composition analysis is conducted in addition to the calorimetric measurements.
- Anodic/cathodic side reactions in the two electrolysis systems are expected
 to depend very much on the geometry of the electrochemical cell, current
 density, temperature, electrolyte volume, and power supply current profiles.
- The experimental apparatus of this study <u>underestimates</u> gas evolution inefficiencies because of a relative low current (as compared to 3A in your calonmetric experiment), higher dilution of anodic by-products (2 liter electrolyte), and partial removal of anodic by-products from the electrolysis cell active region by the increasing gas column in the gas burette/electrolysis cell envelope.

The latter point is demonstrated by comparison of experiment 1 and 2 in Table 1. Before the start of the second experiment, the electrolyte had been enriched with anodic by-products from the first experiment. Then, the electrolyte column in the





burette was raised to the top and during the second experiment the electrodes operated in an environment of accumulated anode by-products. This explains the lower gas evolution rate under otherwise similar conditions.

Please feel free to use this information in the interpretation of your carefully executed calorimetric measurements.

Amold O. Isenberg Consulting Scientist

Advanced Energy Conversion Division

Arweld O. Furkey

dk

Attachments

P.S.: One could tell the "hydrino theoreticians" to use sodium or potassium borate solutions as electrolyte. The expected anodic by-product concentrations would be even higher (perborates) and the expected "unexplainable" thermal effects would be even more exothermic (if one conveniently assumes 100% gas evolution efficiency). Sorry, there is a little bit of a nasty streak to mel





**

•





Table 1

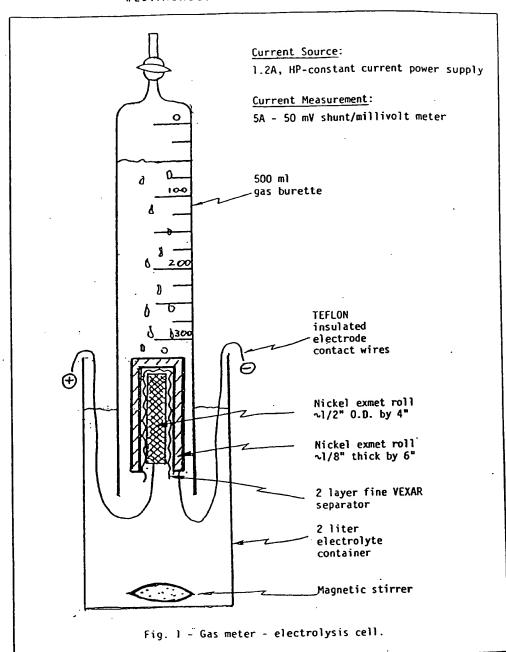
Efficiency of Gas Evolution in
Alkaline Carbonate Electrolysis Cells

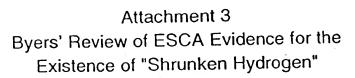
Experiment	Electrolyte Type	Electrolyte Temperature OC	Current A	Collected Gas Volume ml, S.T.P	Gas Evolution Rate ml/min	Gas Evolution Efficiency
1	0.57m K ₂ CO ₂	19	1.00	216.7.	7.01	67.1
	_	19	1.00	260.9	6.74	64.5
· 2	0.57m K ₂ CO ₃	•	-	200 3	7.92	75.8
3	0.57m Na ₂ CO ₃	22	1.00	256.3	1.52	.5.0
. 4	0.57m Na ₂ CO ₃	50-55	1.00	250.3	7.18	68.8
5	0.57m K ₂ CO ₃	55-65	1.00	252.0	5.98	57.2
6	0.57m K ₂ CO ₃	65-70	1.00	251.5	5.89	56.4





WESTINGHOUSE ELECTRIC CORPORATION











From:

SCIENCE & TECHNOLOGY CENTER

WIN:

236-1678

Date: Subject: January 18, 1994

Review of ESCA Evidence for Fractional Quantum Energy Levels of

Hydrogen

To:

STC

John Spitznagel

œ:

S. H. Peterson

A. Isenberg

R. J. Jacko.

W. G. Clark, Jr.

I have reviewed the paper by Randell L. Mills and William R. Good on the evidence for fractional quantum energy levels of hydrogen. This paper proposes the creation "hydrino" atoms on nickel electrodes during the electrolysis of aqueous potassium carbonate. The proposed hydrino atoms are hydrogen atoms which have dropped into a new electronic ground state where n=1/2. The existence of this fractional quantum level is used to explain the production of heat in electrolysis experiments which was previously attributed to cold fusion. ESCA characterization of the nickel electrodes was used to support the hydrino theory.

The ESCA evidence consisted of a broad peak at 55 eV binding energy in a spectrum from an electrode in which excess heat was observed. This is the binding energy which was predicted for an electron in a hydrino atom. The authors state that "There is no known atom which has an electron with a binding energy in this region that was present in the electrolytic cell." While it is true that none of the elements which were intentionally added to the cell have electrons with binding energies in this area, the possibility of the presence of trace impurity elements must be considered. A cathodic electrode will concentrate even ultratrace elements to levels detectable by ESCA.

A search of the NIST XPS database identified a number of compounds which had elements with photoelectron transitions in this area. The most common are compounds of iron. The binding energy for Fe 3p electrons ranges between 52.8 and 57.95 eV depending on the oxidation state of the iron. The broad peak which was observed is common for iron compounds of mixed valence state or for iron





oxide mixtures. The presence of iron could be confirmed by looking at the more intense 2p photoelectron peak which have a binding energy near 710 eV. The ESCA scan in the Mills paper went no higher than 310 eV. Compounds of lithium and osmium could also have produced peaks in the 55 eV region. The authors would have built a more convincing argument for a new quantum state had they addressed the impurity issue.

Another consideration which sheds doubt on the authors interpretation of the ESCA results is that the lightest elements are very difficult to detect. The minimum detection limit for lithium is typically near 10 atomic %, and hydrogen cannot be detected at all under normal conditions. The expected poor detection limit for the hydrino atom requires that it be present at high concentration at the nickel electrode surface. This is unlikely because of the high vacuum required for ESCA.

In summary, the ESCA data presented by Mills and Good does not provide strong evidence for fractional quantum states of hydrogen.

W. A. Byers

Cit Byers

Corrosion Technology





HYDROCATALYSIS POWER CORPORATION

Comments to Confidential Draft Report from Westinghouse STC, "Evaluation of Heat Production From Light Water Electrolysis Cells of HydroCatalysis Power Corporation", February 25, 1994

Light Water Calorimetry Experiments

Westinghouse scientists report that excess heat was observed during the electrolysis of aqueous potassium carbonate (K^+/K^+) electrocatalytic couple); whereas, no excess heat was observed during the electrolysis of aqueous sodium carbonate.

The data of the temperature of the cell minus the ambient temperature shows that when potassium carbonate replaced sodium carbonate in the same cell with the same input electrolysis power, the potassium experiment was twice as hot as the sodium carbonate experiment for the duration of the experiment, one month. The present experimental results are consistent with the release of heat energy from hydrogen atoms where pairs of potassium ions (K+/K+ electrocatalytic couple) induce the electrons of hydrogen atoms to relax to quantized energy levels below that of the "ground state" by providing a net enthalpy equal to an integer multiple of 27.2 eV which stimulate these transitions. The balanced reaction is given by Eqs. (1-3) below. Excess heat was observed only when Na₂CO₃ was replaced by K₂CO₃. For two sodium ions, no comparable reaction with a net enthalpy equal to an integer multiple of 27.2 eV is possible. (see Eq.(4) below). The excess energy could not be explained by recombination or known chemistry.

Theoretical Explanation An efficient catalytic system that hinges on the coupling of three resonator cavities involves potassium. For example, the second ionization energy of potassium is 31.63 eV. This energy hole is obviously too high for resonant absorption. However, K(I) releases 4.34 eV when it is reduced to K. The combination of K(I) to K(II) and K(I) to K, then, has a net energy change of 27.28 eV.

$$27.28 \ eV + K^{+} + K^{+} + H \left[\frac{a_{H}}{p} \right] \rightarrow K + K^{2+} + H \left[\frac{a_{H}}{(p+1)} \right] + [(p+1)^{2} - p^{2}]X13.6 \ eV$$
 (1)

$$K + K^{2+} \rightarrow K^{+} + K^{+} + 27.28 \ eV$$
 (2)

And, the overall reaction is

$$H\left[\frac{a_H}{p}\right] \to H\left[\frac{a_H}{(p+1)}\right] + \left[(p+1)^2 - p^2\right] X 13.6 \text{ eV}$$
(3)

For two sodium ions, no comparable reaction with a net enthalpy equal to an integer multiple of 27.2 eV is possible. For example, 42.15 eV of energy is absorbed by the reverse of the reaction given in Eq. (2.14), where Na⁺ replaces K⁺:

$$Na^+ + Na^+ + 42.15 \ eV \rightarrow Na + Na^{2+}$$
 (4)





Faraday Efficiency

A Westinghouse research scientist proposes that the excess energy may be due to recombination (burning of the evolving hydrogen and oxygen) or some exotic chemical reaction of the counterion of the electrolyte which consumes some of the current that otherwise would electrolyze water.

The general form of the energy balance equation for the cell in steady state is:

$$0 = P_{in} + P_{xs} - P_{loss}$$
 (5)

where P_{in} is the input power; P_{xs} is the excess power generated (the source of this power is given by Eqs. (1)-(3) above); and P_{loss} is the thermal power loss from the cell. In these experiments, the applied voltage, V_{appl} , and the current, I, were constant. Thus, the input power is given by

$$P_{in} = V_{appl} I \tag{6}$$

When an aqueous solution is electrolyzed to liberate hydrogen and oxygen gases, the input power can be partitioned into two terms:

$$P_{in} = P_{ohm} + P_{gas} \tag{7}$$

where P_{ohm} is the ohmic power that heats the cell and P_{gas} is the power needed to produce the H_2 and O_2 gases.

$$H_2O(l) \to H_2(g) + \frac{1}{2}O_2(g)$$
 (8)

An expression for $P_{gas}(=V_{gas}I)$ is readily obtained from the known enthalpy of formation of water ($\Delta H_f = -286$ kJ/mole):

$$V_{gas} = -\frac{\Delta H_f}{\alpha F} = -\frac{-286 \times 10^3 \text{ J / mole}}{2 \times 96484 \text{ C / mole}} = 1.48 \text{ volts}$$
(9)

where α is the number of moles of electrons involved in the reaction and F is the Faraday constant. The net Faraday efficiency of gas evolution is assumed to be unity. Thus, the ohmic power is given by

$$P_{ohm} = (V_{appl} - 1.48) I$$
 (10)

The experimentally observed rise in temperature of the potassium experiment was twice that of the sodium experiment. The temperature rise cannot be attributed to a hypothesis that the net faraday efficiency of gas evolution is not unity, because it was experimentally measured to be unity by weighing the experiment to determine that the expected rate of water consumption was observed, and the output power exceeded the total input power. This further overcomes the hypothesis of Isenberg that an extremely unusual chemical reaction of the carbonate ion was responsible for consuming the current. Furthermore, the hypothesis of Isenberg is highly improbable, for the following reasons:





- The chemical reactions proposed by Isenberg would be expected to occur to the same extent
 in the sodium control experiment, which showed no excess, heat because they both
 potassium and sodium cells contained equivalent amounts of carbonate and were operated
 under identical conditions.
- Production of percarbonate from carbonate consumes energy, as opposed to producing energy.
- The carbonate concentrations of all of the experiments was analyzed following their completion, and the final carbonate concentration in all cases was about the same as the starting concentration. The slight decrease in carbonate over the length of the experiments is attributed to the very slow conversion of carbonate to carbon dioxide and hydroxide at the anode at elevated temperature as given by Itskovich ["Electrolysis of aqueous potassium carbonate solutions in a model electrolytic cell", Itskovich, A. R.; Merenkov, P. T., (Inst. Khim., Tashkent, USSR). Dokl. Akad. Nauk Uzb. SSR 1968, 25(7)].
- Electrochemical reactions which consume the electrolyte can be ruled out because any
 proposed electrochemical reactant would be completely consumed over the duration of these
 experiments.

In the case of the last point above, the current of each experiment was 3 A, and each experiment contained 1.5 liters of 0.57 molar electrolyte. Thus, the total number of moles of electrolyte was

$$0.57 \text{ moles/liter X } 1.5 \text{ liters} = 0.85 \text{ moles}$$
 (11)

According to Faraday's Law, a current of 3 amperes consumes one mole equivalent in 8.9 hours.

$$\frac{96484 \text{ coulombs / mole equivalent}}{3 \text{ coulombs / second}} = 32,161 \text{ seconds} = 8.9 \text{ hours}$$
 (12)

The duration of the experiment was one month, and the excess energy was constant over the duration of the experiment.

<u>Summary</u>

The data clearly indicate that excess heat was generated in each electrolytic cell experiment using potassium carbonate. The experiments were permitted to operate for weeks, and the excess heat remained relatively constant. What is the source of this excess enthalpy? Electrochemical reactions which consume the electrolyte can be ruled out, because any proposed electrochemical reactant would be completely consumed over the duration of these experiments. The Faraday efficiency was measured to be 100% for both electrolytes. The results are consistent with the release of heat energy from hydrogen atoms where the K^+/K^+ electrocatalytic couple induces the electrons of hydrogen atoms to relax to a quantized potential energy level below that of the "ground" state, by providing a redox energy-energy hole (27.28 eV) resonant with this transition. The balanced reaction is given by Eqs. (1-3).

No excess heat was observed until K₂CO₃ replaced by Na₂CO₃. For two sodium ions, no comparable reaction with a net enthalpy equal to an integer multiple of 27.2 eV is possible as given by Eq. (4).





THIS PAGE BLANK (USPTO)





EXCESS ENERGY CELL FINAL REPORT 25 APRIL 1995

C. W. HALDEMAN, E. D. SAVOYE, G. W. ISELER, H. R. CLARK

OUTLINE

REVIEW

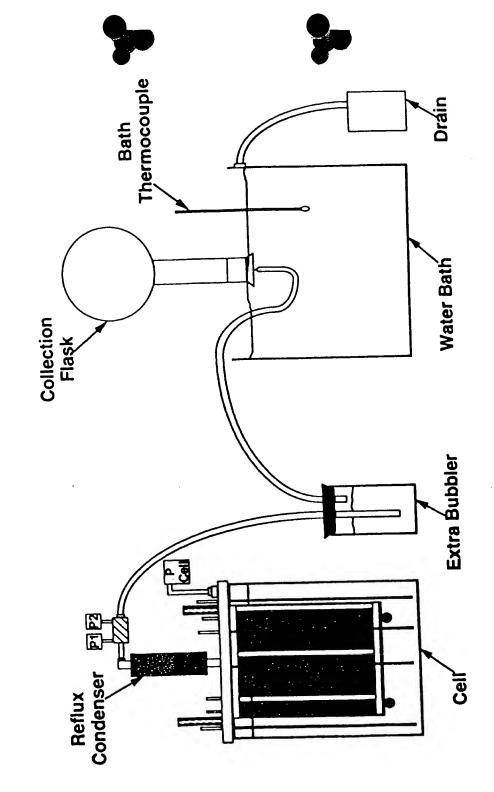
- RETURN TO ROOM THERMAL ENVIRONMENT CHANGES SINCE LAST REPORT
 - RE-WOUND CELL
- RESIDUAL GAS ANALYSIS

• ENERGY MEASUREMENTS

• GAS MEASUREMENTS

• CONCLUSIONS





Mass Spectrometer Power Supply **Glow Wire** Platimum Water Bath Gas Collection With Combustion Tube Teflon Tube Extra Bubbler Flame Suppressor

SUMMARY OF CELLS ASSEMBLED

			7		
RESULTS NO EXCESS ENERGY	NO EXCESS ENERGY	5——10% EXCESS ENERGY	5—►30% EXCESS ENERGY	20 —► 50% EXCESS ENERGY	20 — 1400% EXCESS ENERGY 4 x VI INPUT (S)
C/A RATIO 520: 1	17:1	<u>τ</u> .	5:1	61: 1	75: 1
ANODE PLATINIZED Ti 100 cm ²	SOFT NICKEL SHEET 3000 cm ² PLATINIZED TI 100 cm ²	SAME	PLATINIZED Ti SHEET 3100 cm ²	SAME	SAME
# CATHODE ANNEALED #41 NICKEL 1.8 lbs 52000 cm ²	SAME WIRE HEAT TREATED IN H ₂ 770°C	HARD DRAWN 0.5 mm NICKEL 16,000 cm ²	NEW WINDING HARD DRAWN 0.5 cm ² NICKEL 15,000 cm ²	HARD DRAWN - SCRATCHED #44 NICKEL 190,000 cm ² (0.002 in.) 0.05 cm dia.	#46 HARD DRAWN SMOOTH NICKEL WIRE 240,000 cm ²
CELL #	4	а	2A	ო	4

OCTOBER 1994 PLANS

- USE SEALED SYSTEM RECOMBINER / CONDENSER TO COLLECT GAS
- 2. REWIND CELL WITH SMOOTH #46 WIRE
- 3. USE WET CHEMICAL GAS ANALYZER
- CONTINUE TO LOOK FOR HIGHER EXCESS ENERGY AND CHARACTER OF RESIDUAL GAS





RE-WOUND CELL

• CATHODE - 4.7 lbs #46 NICKEL WIRE Dia. (0.00157 inch) 0.00399 cm

SURFACE AREA 240,000 cm² CURRENT DENSITY 41 μ a/cm² @ 10a

• ANODE - 5 FOLDED SHEETS Pt PLATED Ti 15.2 x 20.3 cm

SURFACE AREA 3200 cm² CURRENT DENSITY 32 ma/cm² 75:1 CATHODE: ANODE RATIO

@ 10a

• ELECTROLYTE - 161 0.6 M K₂ CO₃ IN LAB DI WATER





GAS FLOW ABSOLUTE MEASUREMENT

- DIRECT WATER DISPLACEMENT - 2000 ± 0.5 cc VOLUMETRIC FLASK
- ullet WATER BATH TEMPERATURE $\pm\,0.1^{\circ}\mathrm{C}$
- TIME MEASUREMENT ± 0.02 sec
- NATIONAL WEATHER SERVICE BAROMETER CORRECTED FOR TEMPERATURE AND LATITUDE $\pm\,0.1$ mm • BAROMETRIC PRESSURE
- MEASURED VOLUME CORRECTED FOR
 - TEMPERATURE
 - PRESSURE
- WATER VAPOR CONTENT









30 Electrolytic Cell Data Results 25 Net Input Power (Watts) **Pulsed Runs** Calibration DC Runs 00 S 0 0 S 5

Cell - Ambient Temperature (C)

Color Colo	Flectrokific	ų				ä	Lemostatutes								
Color Colo			Duty	Eng Pask			Thier		20 Porest	Chen Inent	Corent (watte)	A Power (watte)	Quinnill.	Culbuill' (F=1)	(sme)
Column C	X I (Volte) (Ampe			(Hz) (Volt		5	<u></u>	<u>©</u>	(**)						0 73
Column	- 1						907 95	2 753	0.0796	7.776	10.379	2.603	133.5%	161.94	0 78
\$1.51 1.125 1.00% 0.0% 0.00% 0	4.00			0	κ è	100	10.658	4,113	0.1125	7 992	11.365	7 A	•	4/1	
\$\begin{array}{cccccccccccccccccccccccccccccccccccc	2,893 5.01			۰ ۰	4 6	8 9 13	20.202	6.711	0.1761	7,994	5 to 10	Z Z	4/N	4 i	
1,1,1,1,1,1,1,1,1,1,1,1,1,1,1,1,1,1,1,	2,758 5,12			- (1.453	20.648	10.605	0.3006	7.658		W/W	4 / N	4/2	;
6.751 1.5.75 </td <td></td> <td>14.2</td> <td></td> <td></td> <td>· ·</td> <td>34.92</td> <td>20.73</td> <td>14,10</td> <td>0.2325</td> <td>9.401</td> <td>11.666</td> <td>3.607</td> <td>145.3%</td> <td>166.0%</td> <td>2.0</td>		14.2			· ·	34.92	20.73	14,10	0.2325	9.401	11.666	3.607	145.3%	166.0%	2.0
0.000 53.75 10.00 0.025 0.02					7	3.862	19.507	4.205	0.1331	90.474	25.06	4,386	121.2%	134.1%	
10,000 33,000 30,452 20,837 20,837 20,835 20,835 20,835 20,845 2				•	8	8.662	19.75	6.912	0.1700	20.67	al-5 W heaters adde	4/1	۲\ ک	¥/# :	0 20
1,500 0.0112 0.004 0.0445 20.52 4.052 4.052 4.052 4.052 4.052 4.054 4.044 4.						30.62	20.837	0.003	0.2418	24 681	26.043	3.362	113.6%	40.221	900
1,000 0.11 0.00 0.12 0.00					•	10.455	20.52	0.035	0.363		12.2	4.032	140.4	6.07	; -
4,555 12.555 100%				. 0	~	14.184	19.78	4.404	10.0		12,206 W heaters at	4	¥ :		
4,478 1,479 100% 0 2,472 10.54 4.35 0.116 1.40 1.40 1.40 1.40 1.40 1.40 1.40 1.40					~	16.013	19.852	9.161	0000		1,718 W heaters ad	4/1	4 ×	ž Š	08.0
2.576 6.257 (100% C) 22.589 (10.57) (1.10) (1.10) (1.2.52 Windows and MIA MIA MIA MIA MIA MIA MIA MIA MIA MIA					•	14,726	20.36	4.366	0.2800		89.6	3.179	193.5%	5	
2.575 6.257 100% 0 22.659 10.677 2.662 0.172 0.120 Windows as NIA NIA NIA NIA NIA NIA NIA NIA NIA NIA		_			•	21.9	19.516	2.384	0.1158	9.50	O 272 W healers ad		¥ iz	4/2	
2.579 6.250 100% 2.300 (8.571 4.335 1.300 4.824 147.7%					**	22 820	19.054	2.875	0.1212	3.250	On W health?		¥/¥	4 :	
2.878 8.825 100% 22.467 10.25% 4.324 132.4% 142.2%						21 008	10.671	4.336	0.0993	3.299	Of the bearing and		K X	¥/¥	
Column C						22.487	10.625	2.862	0.1172	3.33)	2001				92.0
7.901 26.467 10.64 7.89 0.0700 10.110 10.47 4.476 11.24 <		•									20 119	4.024	132.4%		::
7.000 2.2.7.0 1.0.6.6 0.056	Nudmoo or	r fallure		•	,	26.803	19.604	7.100	0.0700			4.476	129.9%	142.0%	
7,803 2,644 100% 0.00 1,42 0.0036 -1,135 3,47 3,47 MAA 1,84	26 7.9						19.545	8.972	0.114			3.259	587.3%	ď	
2.250 2.000 20% 6 2.2150 10.042 1.503 0.0031 0.735 6.185 3.300 221.3% NVA 0.0000 2.00000 2.0000 2.00000 2.0000 2.0000 2.0000 2.0000 2.0000 2.0000 2.0000 2.0000 2.0		5		۰ ۰		21.080	19.660	1.42			3.05	3,417	563.1%	4 1	2.08
2.226 2.600 20% 0 2.27.004 2.221 0.00751 2.234 0.00751 2.354 0.110 2.702 2.509 % N/A 124.5% N/A 2.0094 2.509 2.509 0.0094 2.254 0.110 2.702 2.509 % N/A 2.0094 2.207 100% 0 2.7004 1.457 0.0004 1.200 2.709 2.709 2.209 0.0091 1.200 2.207 2.009 2.7094 2.009 1.200 2.207 2.009 2.7094 2.0094 1.207 2.009 2.207 2.009 2.209 2.209 2.709 2.209 2.709 2.209 2.709 2.209 2.709 2.209 2.709 2.209 2.709 2.209 2.709 2.209 2.709 2.209 2.709 2.209 2.709 2.209 2.		~				21.185	19.662	1,503			4 185	3.390	221.3%	4 2	
2.21 4.000 100% 0 2.000 2.000 1.457 2.216 0.0004 1.457 0.0005 1.200 2.8118 2.200 2.881 1.890 1.590 M.A. M.A. M.A. M.A. M.A. M.A. M.A. M.A						22 150	19.917	2.241			100 41	3,663	124.5%	136.4%	7.7
2.226 2.207 10% 6 2.8 21.206 1.375 2.216 0.0004 1.320 3.96 2.730 311.5% NIA 2.226 2.207 10% 6 2.8 21.206 1.3004 1.437 0.0001 1.320 3.96 2.861 2.90.6% NIA 2.2226 2.207 10% 6 2.8 21.206 2.0504 1.437 0.0001 0.064 3.30 2.641 1.907 NIA 1.908 NIA 1.907 10% 6 2.8 21.206 2.0504 1.202 0.0001 0.064 3.308 2.481 1.907 10% 6 2.8 21.206 2.0508 0.0001						27.004	20,336	0.608				3.762	250.6%	4 / I	
2.256 2.07 10% 6 2.6 21.461 20.004 1.457 0.0050 1.279 5.86 2.661 200.6% M/A 2.226 2.070 10.6% 1.280 1.480 1.		9		•	•	21.991	10,775	2.210	0		4 029	2.736	311.5%	4/2	
2.626 2.207 10% 6.26 2.126 16.49 1.439 0.0061 1.374 0.03 2.848 407.0% M/A M/A <td></td> <td>₹</td> <td></td> <td>,</td> <td></td> <td>21.461</td> <td>20.004</td> <td>1,457</td> <td>0</td> <td></td> <td>40 c</td> <td>2.861</td> <td>209.6%</td> <td>ď Ž</td> <td>70</td>		₹		,		21.461	20.004	1,457	0		40 c	2.861	209.6%	ď Ž	70
2.226 2.462 20% 2.6 2.170 0.0036 0.011 1.000 Wheelers and MIA MIA <t< td=""><td></td><td>N</td><td></td><td>• •</td><td></td><td>21 288</td><td>10.840</td><td>1.438</td><td></td><td></td><td></td><td>2 8 4 6</td><td>467.0%</td><td>4/2</td><td>7</td></t<>		N		• •		21 288	10.840	1.438				2 8 4 6	467.0%	4/2	7
1.806 1.373 10% 6 2.8 22.365 20.182 2.213 0.0036 0.811 1.000 W.M. M. M. M. M. M. M. M. M. M. M. M. M.		~				70	20.584	1.202			3.33		4/1	4/1	4 X
1.656 1.142 1094 6 2.8 5.4.09		_		•	2.6 2.6	20.75	20 182				1.086 W Neemen and		452.0%	M/M	2.10
1,826 1,137 10% 6 2 1503 2,0000 10.000 0.134 2.000 2.000 0.134 2.000 2.000 0.134 2.000 0.1		_		•	5. 8.	22.305			۰		2.401		*****	625.3%	_
0.276 0.476 100% 0 20.69 19.63 10.27 0.134 20.06 16.71 0.134 10.20 10.2				.	5 .6	21.503					2.023	2.216		1382 6%	_
0.276 0.477 100% 0 21.151 10.206 1.753 0.0015 0.168 1.1000 W/hasters and M/A W/A W/A W/A W/A W/A W/A W/A W/A W/A W				,		20.6					2.005	1.871	# D D 3 T	4/1	4/1
0.276 0.467 100% 0 21.151 10.388 1.733 0.0014 0.202 3.008 W.hawwe and M.A. M.A. 200.2% 20.278 0.465 100% 0 21.353 20.247 1.005 0.0014 1.559 0.0088 1.479 100.9% 177.8% 20.002 4.304 100% 0 22.00 1.465 10.00% 0 22.00 1.405 10.00% 10.00% 0 22.00 1.405 10.00% 10.00% 0 22.00 1.405 10.00% 10.00% 10.00% 0 22.00 1.405 10.00% 10.00% 0 22.00 1.400 10.00% 0 22.00 1.400 10.00% 0 22.00 1.400 10.00% 0 22.00 1.400 10.00% 0 22.00 1.400 10.00% 0 22.00 1.400 10.00% 0 22.00 1.400 10.00% 0 22.00 1.400 10.00% 0 22.00 1.400 10.00% 0 22.00 1.400 10.00% 0 22.00 1.400 10.00% 0 22.00 1.400 10.00% 0 22.00 1.400 10.00% 0 22.00 1.400 10.00% 0 22.00 1.400 10.00% 0 22.00 1.40						18.834		_			1,960 W hesters ad		4 /R		¥ ×
0.276 0.046 100% 0 21.785 16.30 2.485 0.046 1,476 133.1% 177.8% 2.002 4.304 100% 0 21.353 20.247 1,106 0.0146 1.026 6.689 2.407 10.09% 177.8% 2.002 4.304 100% 0 22.049 18.48 0.3847 6.500 6.500 1.014 10.0%				0		21.151					3,998 W heaters ad		4	1 5	
0.022 0.000		, ,				21,785							103.1%	230.2	_
2,000 2,000 10% 0 22.06 19,666 2.381 0.0420 10.04 101.9% 110.5% 110.5% 20.00 10% 0 28,07 20.40 10.0% 0 28,07 20.40 10.0% 0 28,07 20.40 10.0% 0 28,07 20.40 10.0% 0 28,07 20.40 10.0% 0 28,07 20.00 10.0% 0 28,07 20.00 10.0% 0 28,07 20.00 10.0% 0 28,07 20.00 10.0% 0 28,07 20.00 10.0% 0 28,07 20.00 10.0% 0 28,07 20.00 10.0% 0 28,07 20.00 10.0% 0 28,07 20.00 10.0% 0 28,07 20.00 10.0% 0 28,07 20.00 10.0% 0 28,07 20.00 10.0% 0 28,07 20.00 10.0% 0 28,07 20.00 10.0% 0 28,07 20.00 10.00 10.0% 0 28,07 20.00 10.						21.353			•			2.407	160.0%	20.771	
2,000 Pilot 100% 0 20,049 18,48 0.1344 12,500 1,449 12,5% 13,5% 13,5% 13,5% 13,5% 13,5% 13,5% 13,5% 13,5% 13,5% 13,5% 13,5% 141,7% 141,7% 2,389 11,097 100% 0 21,643 18,574 2,389 0.0136 4,109 2,324 2,093 14,109 2,324 40,6% W/A 2,089 11,097 100% 0 2,6 2,134 18,635 1,449 0.0036 0.166 2,109 2,269 2,269 319,7% W/A 2,149 1,763 10% 4 2,8 2,109 1,175 0.0035 1,019 2,749 2,899 2,749 2,899 2,109 2,109 1,009 2,899 2,109 2,109 1,009 2,109 1,009 2,109 1,009 2,109 1,009 1,009 2,109 1,009 1,009 2,109 1,009 1,009 2,109 1,009 1,			-			22.08		•				1.014	101.0%	110.9	
20.000 79.14 1007 100% 0 21.943 19.574 2.388 0.000% 5.531 8.324 2.803 143.9% N/A 3.909 11.007 100% 0 2.386 2.001 3.014 0.0048 0.0048 0.0048 0.0056 4.100 3.264 40.00% N/A 2.004 1.607 100% 0 2.00 2.139 10.409 1.176 0.0046 0.0048 0.0048 2.209		• ;				36.079						1,440	128.5%	4.5.4	
3.167 8.084 100% 0 23.816 20.801 3.014 0.0309 3.054 40.05% 4.109 3.264 40.05% N/A 1.00 3.264 40.05% N/A 1.00 3.264 40.05% N/A 1.00 11.00% 0 2.0 21.321 18.835 1.486 0.0046 0.056 3.266 2.236 319.7% N/A 2.064 1.807 10% 6 2.0 2.067 1.016 3.266 2.266 2.206 4.27% N/A 2.016 1.807 10% 6 2.0 2.105 10.004 0.074 2.066 2.061 2.001 2.004 2.001 10% 6 2.0 2.105 10.004 1.077 2.006 1.077 2.006 1.077 2.006 1.077 2.006 1.077 1.001 1.00		-				21,943						2.603	147.8%		_
3,896 11,087 100% 8 2.6 21,321 19,835 1,486 0,0046 0,000 3,266 2,236 319,7% M/A 2,004 1,007 10% 4 2.8 20,873 19,486 1,175 0,0035 1,016 3,266 2,265 4,270 M/A 3,216 1,763 10% 4 2.8 21,143 19,486 1,387 0,0040 0,874 3,865 2,261 2,681 442,1% M/A 3,015 1,004 0,874 3,865 2,261 2,681 2,681 M/A 3,015 1,004 0,874 3,882 1,677 4,286 2,681 2,681 2,681 M/A 3,017 2,675 10% 6 3,0 2,120 19,75 1,044 0,0163 1,677 4,286 2,681 4,111 175,7% M/A 3,017 10% 6 4,6 24,801 18,81 4,991 0,0163 18,316 1,081 1,08		•				23.616		0				3.264	40.004	d i	-
2.084 1.887 1074 2 2.6 20.673 10.488 1.175 0.0035 1.078 2.086 2.886 4.22.04 N/A 2.082 1.078 2.082 1.078 2.082 1.000 4.22.14 N/A 2.082 1.000 1.084 2.082 1.000 4.22.14 N/A 2.082 1.000 1.087 4.288 2.881 4.171 175.74 N/A 3.087 2.875 1074 6 4.0 23.383 18.031 3.482 0.0115 8.430 8.541 4.11 175.74 N/A 3.082 1.000 1.084 0.000 1.000		_	-	, . , .		21.321		_				2,238		4 A	
2.186 1,783 10% 12 2.0 21.06 10.866 1.386 0.0046 0.744 3.865 2.881 442.1% N/A 2.00 1.004 1.386 0.0046 0.744 3.865 2.881 2.881 N/A 2.00 1.004 0.874 4.288 2.881 1.78.7% N/A 2.004 1.007 4.288 2.881 1.78.7% N/A 2.004 1.007 4.288 1.004 0.004 0.874 4.288 2.881 1.78.7% N/A 3.067 2.878 10% 6 4.0 23.383 18.031 3.462 0.015 5.430 0.844 4.111 1.78.7% N/A 3.004 0.0				• !		20.473		-	0			2.065		M/M	× 2
2.016 1.601 10% 4 2.6 21.13 10.746 1.397 0.0040 0.874 2.26 2.681 2646% NVA 2.126 1.007 0.0040 0.877 4.286 2.681 2.644 NVA 2.126 1.007 0.0040 0				ž ·	•	20 00		-	•			2.001	442.1%	¥ Ì	7.7
2.120 1700 10% 0 2.120 10.75 1.644 0.0006 1.677 2.420 4.11 175.7% N/A 1.5.007 2.875 10% 0 3.0 21.200 10.75 10.015				*				-	0			2.601	254.6%	4 Ì	-
3,067 2.875 10% 6 4.0 23,383 19,831 3.452 0.0115 5,430 9,541 10.01 10% 6 4.0 23,383 19,831 0.0163 9,866 13,849 3,963 140,1% W/A 6,89 13,416 10% 6 4.8 24,601 18,81 4,901 0.0163 9,866 13,89 1,629 33,6% W/A 6,89 13,416 10% 6 2.6 2,27,320,336 0.042 0.0091 17,236 18,316 1.061 106,3% 112,7%				*	•	200		-	•			-	175.7%	W/W	. Z
6.216 7.001 10% 6 4.0 23.352 140.1% M/A mally adopted 2.510 1.520 3316% M/A mally adopted 2.510 1.520 3316% M/A 5.510 1.520 3316% M/A 5.510 1.520 3316% M/A 5.510 1.520 3316% M/A 5.510 1.500 10% 6 2.6 21.27% M/A 5.510 1.500 10% 6 2.6 21.27% M/A 5.510 1.500 10% 6 2.6 21.27% M/A 5.510 1.500 10% 6 2.6 21.27% M/A 5.510 1.500 10% 6 2.6 21.27% M/A 5.510 1.500 10% 6 2.6 21.27% M/A 5.510 1.500 10% 6 2.6 21.27% M/A 5.510 1.500 10% 6 2.6 21.27% M/A 5.510 1.500 10% 6 2.6 21.27% M/A 5.510 1.500 10% 6 2.6 21.27% M/A 5.510 1.500 10% 6 2.6 21.27% M/A 5.510 1.500 10% 6 2.6 21.27% M/A 5.510 1.500 1.					9			•	•	<u>~</u>	•	; ;			
8.689 13.410 10% 6 4.6 24.601 18.61 4.991 0.0163 8.686 (2.840 2.840 33.6% M/A 3.6% 1.6.2 33.6% 1.2.7% 1.2.7% 1.2.7% 1.2.7% 1.6.0 10% 6 2.8 21.27 20.329 0.044 0.054 1.7.230 1.8.19 1.0.61 1.0.6.3% 1.2.7%				• *	9	23.38		,	!				* 071	Ž	.03
8.609 13.418 10% 6 2.8 21.27 20.326 0.842 0.0041 0.790 2.819 1.081 108.3% 112.7% 10.00 10% 6 2.8 21.27 20.326 0.0391 17.236 18.319 1.081 10.08.3%												3.000	***		:
200 10% 6 2.6 21.27 C. 15 0.0391 17.236 18.319 1.00.5				• *	•	24.60	٠					1.020	1 2 2 2 2		_
				94.	5 .0	21.2						.00.	£	į	•

			The Following Runs are the Stant of Experiments with the new Smooth Nicke wire Calmood on 1911	are are the St	an of Expert	ments with th	e nest Smo						
										Flourate a	Fereday	Date Taken Over	
				5	5	Z	ឆ	P adlice	ជ	(ce/min)	Efficiency	Time Rappe	
	(Torr)	(Torr)	(belg)	1 6) [_	=	(beled)	(<u>)</u>	(nony com.)			
ĺ	man Berocell	(celibrated)					1		117	47.20	64.29%	1250-1350	
		75.0 AA	0.6032	0.6013	15.27	0.4896		71110	10.747	11.94	65.60%	3200-3600	
Pun285	787.20	759.30	0.7183	0.7202	15.37	0.6555	19.91	7190	20.031	44.81	77.08%	2000-2200	
Run288	745.81	739.31	0.7753	0.7777	15.05	0.7161		0.0691	20.522	47.58	81.36%	1650-1700	
Renzel	766.63	750.33	0.0375	0.0405	15.60	0.0		0.0648	20.443	53,68	83.27%	1050-1100	
	767.68	760.32	0.7066	0.7003	5.00	0.01		0.0586	19,740	47.31	94.42%	3800-3700	
HUNZER	758.43	751.43	0.7775	0.7604	15.28	0.7210	15.20	0.0639	19.725	06'90	85.46%	7200-7500	
Purificial a	771.05	763.56	0.5429	0.5451	15.20	4805		0.1267	20.656	6.63	96.30	1360.1350	•
Pinc 202	765.75	758.48	0.6049	2/09/0	5 5	5830		0.1379	20.577	111.08	90.00	2000-2100	
9,000	778.78	766.16	0.7184	0.7208	19.3	0.3757	15.10	0.0836	18,962	47.05	90.00	2500-3000	
Run 284	774.00	767.26	0.4375	0.4388	15.48	0.5951	15.40	0.0766	10.866	45.20	7.7.60	950-1030	
Runzos	774.80	767.25		0.000	15.59	1.0383	15.51	0.0777	20.500	28.00	91.43%	\$000-6000	
Purzee	156.79	749.85	05.00	1.0260	15.92	0.9491	15.85	0.0769	19.680	24.55	04.024	1230-1315	
Run297	779.70	79.77	0000	1.0720	16.65	0.0843	15.57	0.0777	20.201	23.58	91.66%	1800-2200	
Run 200	782.46	2007	0.0820	0.9650	19.67	0.6646	15.50	0.0613	0.00	23.64	61.00%	3500.4000	
Aun 200	769.11	39.187	1.0940	1,0970	15.03	1.0263	15.75	0.0707					
Rundoo	770.62						;	37.00.0	10 413	78.57	96.40%	1900-2200	
Auton - Date Lost due	Local due to computer revord	757.83	1.3066	1,3110	15.94	1.2235	15.83	0.00.0	000.01	77.38	87.34%	1150-1250	
Run302	775.04	767.39	.2.5190	.2.5200	12.29	.2.5824	12.25	0.0424	090 01	9.77	37.75%	5000-5150	
Pursos	179.04	772.02	.8.2970	.0.2870	9.6	6.4183		7 7 7	20 08 5	07.0	37,48%	2400.2800	
A 100 A 100 A		740.66	0006.9	7.0210	21 40	6.8746		0 1200	20,183	14.07	35.74%	1900-2000	
The state of the s		771.53	-5.7390	-5.7340		9.63e	3	0.0371	20.661	79.90	98.46%	1272-1325	
Har508	73.07	765.50	0.0063	0.0071	15.66	0.670		0.0031	20.110	12.52	34.75%	1800-2000	
HUNCO	773.04	765.47	0.3967	0.4207	2	0.4.0	74.97	0.0020	20.270	6.79	23.98%	2800-2800	
HUND!	755.01	749.01	0.4164	0.4155	14.0	2 4 5 5	15.18	0.0020	20.184	9.47	33.04%	3260:3660	
Harmo	771.98	784.45	0,4091	0.4081			15.06	0.00	21,043	6.15	26.41	000-009	
900	765.66	756.38	0.4140	0.4144	0.00		14.89	0.0012	20.422	9.7	22.15%	900.000	
2000	757.22	750.27	0.4143	0.4146		9140	15.23	0.000	20.964	3.00	23.32%	3300.3600	
- 6164.0	775.36	767.70	0.4157	0.4163	10.60	0.4144	14.02	0.00.0	19.936	9.12	45000		
0.411	758.38	751.36	0.4156	0.4.03	15.00	0.4219	15.09	0.0005	10.422	7.97	*86.50		
2000	767.17	759.83	0.4218	0.4224	15.28	0.3943	15.28	0.0003	19.535	2.08	41314	800-1000	
1000	779.08	771.27	0.3937	97.70	15.22	0.4115	15.22	0.0001	19.405	39 65	41.74		
B.m316	175.02	767.37	0.4106		15.12	0.4123	15.11	0.0045	20.453	06.95	85 47%	•	
Run317	769.10	761.66	0.4156	9000	15.19	0.5991	15.18	0.010	19.767	00.00	A00.70	2450-2750	
Runs 18	762.60	755.44	0.00	0.2115	14.76	0.0479	14.60	0.1636	20.205	22.18	62.48%	3600-3600	
Run318	760.92	793.62	7814	0.7829	16.22	0.6605	15.12	0.1024	10.77	17.54	63.74%	1200-1500	
Runszo	766.02	748.18	60.6.0	0.6116	15.11	0.4812	14.98	0.1306	20.748	6.28	26.08%	1600-2200	
Purist?	750.18	76.63	.0.2201	0.2211	14.79	0.2186	14.78	6200.0	107.01	5.47	22.33%	3000-3500	
Aur.322	761.75	761.28	0.8840	0.6660	15.58	0.0037	15.58	0.0023	010 01	6.02	26.60%		
Aur323	766.66	746.83	0.2617	0.8860	15.28	0.6636	15.20	0.0022	19.927	9, 16	25.01%		
Awitz	707.00	787.44	1.2460	1.2470	16.07	1.244	9 4	0 0023	10.078	9.80	25.04%	400-800	
Aun 325	164.48	751.10	0.3652	0.3664	14.86	0.3641		1600 0	20 149	18.04	25.68%	2000-2200	
Purcise	7.57.00	750.00	2.5690	2.6660	17.08	2.5649	2						
Punda?	8			,		11212	17.71	0.0040	19.700	25.46	26.514		
Purkey . I'm	é §	766.73	3.1290	3.1260	7.7	0.000	18.70	0.0023	20 687	90.0	26.63%	3000.3200	
HUNSTE	774.31	766.68	0.0030	0.000		7 1356	21.77	0.0054	19 946	62.27	4/6/16		
Rightson Disconstituted lid		788.00	7,1170	7.1410									



3,233 8,001 25,667 100%

Aun348



Oscibil a M	0.62	0.87	0.92	0.63	0.87	2 63	0.92	10.4	0.73
Sutaul/E (F=1)	121.1%	345.3%	4 4	K / W	4 4 2 2	< <	2 2	4	155.7%
Outsull?.	114.9%	362.0%	211.3%	124.6%	126.3%	498.2%	134.6%	1010.6%	127.24
A Power (watte)	2.084	1.217	2.303	2.301	1.303	3.367	3.407	1,702	4.027
Output Power (wette)	16.049	15,486	4,372	6.583	9.26	4,213	12,458	27.037	16.652
net_inest)	13.965	13.631						25.335	
H2Q Power Correction (watte)	1	0.0355						0.0732	
46	1	5.571		2.38	4.23	7.29	4.	9.591	9.756
Ambleof. (c)	400	19.687	•					20.065	
19		25.716		21.336	23.96	27.271	21,325	24.827	21.208
Prog Prok. V	(ug) (ug)	00	•	5.0			6 2.6 3.6		e o
Duty Stelle		100%	¥00	20%	źź	4 04 4 04	10 X	200	20%
a .	(Wette)	25.146	1.932	3.847	7.188	7.211	1.589	14.370	0.700
_	Ampa)	7.032	0.001	3.182	7,969	5.819	2.027	6.103	0.839
- -	(Volts)	3.678	1.950	2.051	2.220	2.139	1.799	2.484	1.711
50	lun Na.)	un332/wei lid	Un335bwei IId	un328 - This run f un337/wet 11d	un308/wef lid	lungatoren lid	tun341 1un342	TUNDAD 2.470 0.110	3un348

9-

Deta Takan Over Ilma Bacos (min)	3300-3800 2000-2500 8600-7200	3200-3400 3200-3500 2500-2400 3400-3600 1400-2000	3400-3600 2500-2600 4150-4250 2600-2600	8000.8500
Foradoy Efficiency	92.75% 90.86% 97.67%	30.28% 40.36% 30.84% 25.31% 52.86%	26.75 26.70 26.70 36.87 35.87 4.80 5.80 5.80 5.80 5.80 5.80 5.80 5.80 5	M1.47%
Plowrate {cc/min} {hully cor.}	73.11 71.51 10.85	14.01 22.20 34.52 16.51 66.78	5.62 35.60 33.34 81.69	92.04
1 6	20,186 19,633 20,443		20,088 20,102 20,341 20,468 20 509	20 714
P artition (peled)	0.0200	0.0938 0.0974 0.0120 0.0031	0.0306 0.0076 0.0072 0.0199	0 0322
23 (g	16.20	15.53	76.23 76.23 44.23 76.23	15.06
2 <u>§</u>	3.6900	0.6300	0.5645	0.4001
ដ 🗟	16.22	15.63	15.20	90.91
រ ទឹ	3.7100 6.8710	1.8200 0.7238 0.6416 0.0548 2.2320	0,4415 0,6151 0,2458 0,9482	0.3381
1 (1)	5.0730	1,8190 0,7219 0,6398 0,0534 2,2250	0.4369 0.6167 0.2436 0.6456	0.3366
Ber, Erseauth	믝		757.31 756.72 761.04 756.22 765.36	
Par Property	(Torr) (hom Berocell) 768.66	AutoSobwer ins AutoSobwer ins AutoSobwer ind AutoSobwer ind AutoSobwer ind AutoSobwer ind AutoSobwer ind AutoSobwer ind AutoSobwer ind AutoSobwer ind AutoSobwer ind AutoSobwer ind AutoSobwer ind AutoSobwer ind AutoSobwer ind AutoSobwer ind AutoSobwer ind AutoSobwer ind AutoSobwer ind	766.41 764.56 762.60 763.43	776.32 just a temp run-no data 766.38
***************************************	Run Na.) Run332/wed Hd	Autosomenties Rucoso This run Rucoso This run Rucoso The run Rucosomenties	Rundadbroot lid Rundat Rundas Rundas	Rundas Rundas Rundas This run Rundas

0.278 Ampere Data 2 3 Input Power (Watts) Electrolytic + Heaters Electrolytic Only Calibration 0.5 0 2.5 Cell - Ambient Temperature (C)





MASSACHUSETTS INSTITUTE OF TECHNOLOGY

2 May 1995

TO:

Ad Hoc Committee Distribution

FROM:

C. W. Haldeman Cul

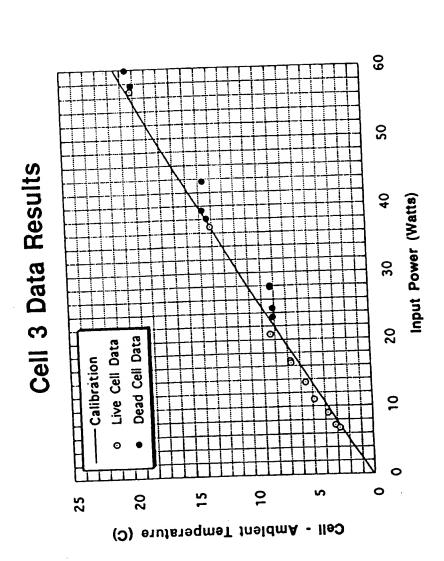
SUBJECT:

Additional Material

You should have all received my viewgraphs from the 25 April meeting. At that meeting Mary and Ron requested that I replot the data from the new cell (Cell 4) in terms of excess power vs. net input power. This has been done and is attached. The large scatter seems to indicate that the excess power is not a function of net input or at least has a stronger dependence on some the excess power is not a function of net input or at least has a stronger dependence on some the excess power is not a function of net input or at least has a stronger dependence on some the excess power is not a function of net input or at least has a stronger dependence on some the excess power is not a function of net input or at least has a stronger dependence on some the excess power is not a function of net input or at least has a stronger dependence on some the excess power is not a function of net input or at least has a stronger dependence on some the excess power is not a function of net input or at least has a stronger dependence on some the excess power is not a function of net input or at least has a stronger dependence on some the excess power is not a function of net input or at least has a stronger dependence on some the excess power is not a function of net input or at least has a stronger dependence on some the excess power is not a function of net input or at least has a stronger dependence on some the excess power is not a function of net input or at least has a stronger dependence on some the excess power is not a function of net input or at least has a stronger dependence on some the excess power is not a function of net input or at least has a stronger dependence on some the excess power is not a function of net input or at least has a stronger dependence on some the excess power is not a function of net input or at least has a stronger dependence on some the excess power is not a function of net input or at least has a stronger dependence on some the excess power is not a function of net input or at least has a strong

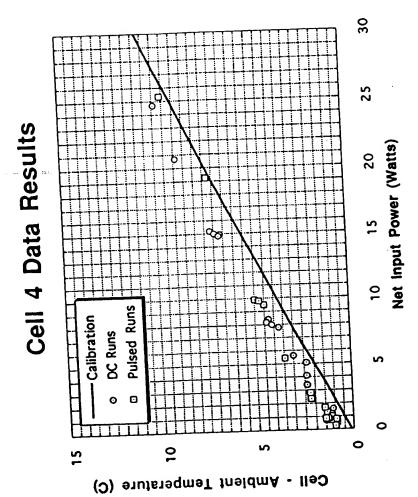
Since the data now includes both Cell 3 and 4, I replotted the Cell 4 results to avoid confusion. This is the same plot in the presentation which was entitled "Electrolytic Cell Data Results." Please add these figures to the package.

CWH:jf Attachments

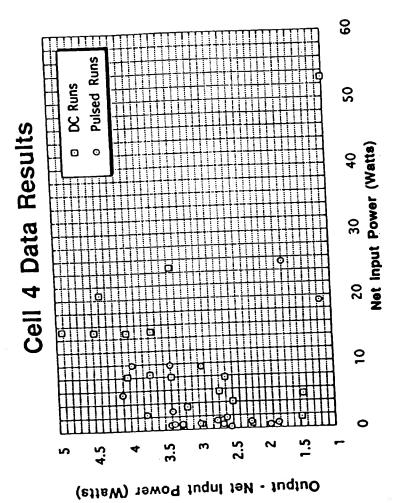














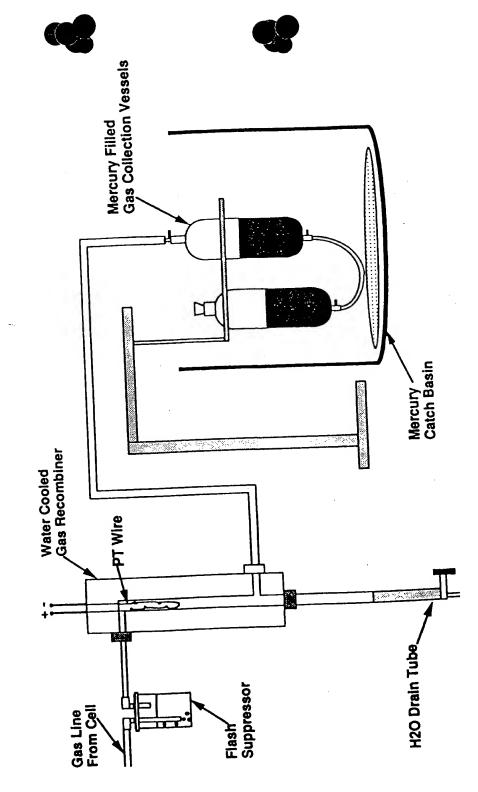




- CHEMICAL ABSORPTION
 BURRELL WET ANALYZER
- INFICON QUADRAPOLE 102 VOLT ENERGY MASS SPECTROMETER
- CRYO CONDENSATION

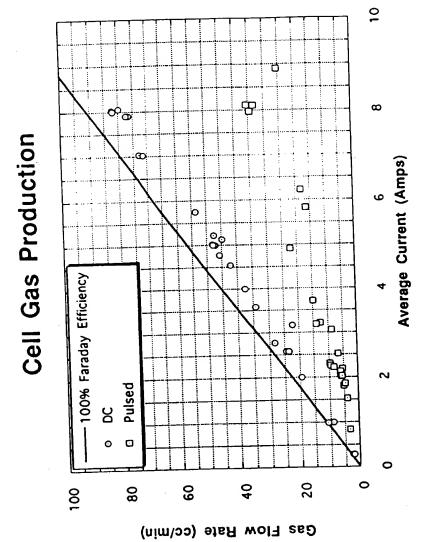


Electrolytic Cell Current Gas Collection System









BURRELL ABSORPTION TUBE ANALYZER GAS WET ANALYSIS

RELL ABSORPTION 1
GAS TESTED FOR

ABSORBENT

c0₂

KOH sol

CrCl2 sol

0

HOT (300°C) C_uO





WET ANALYSIS RESULTS

PERCENT

SAMPLE	CO ₂ O ₂		Н2	RESIDUE
AIR	0	21	0	79
RAW CELL GAS	0	32	29	01
RECOMBINED CELL GAS MANY SAMPLES	0	1822 00.2	00.2	BALANCE 78——82 CALLED PROCESSED CELL GAS

MASS SPEC ANALYSIS OF PROCESSED CELL GAS SHOWS N₂, A, H₂O

HYDRO-CATALYSIS CLAIMS TO HAVE FOUND 1-2% H_2





RECOMBINER RESULTS

• GAS GENERATION

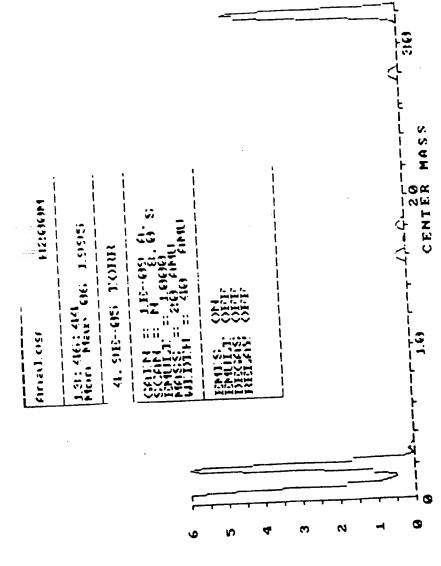
2 TO 100 cc/minute 2.8 TO 144 l/day RECOMBINED WATER CHECKS OUT GAS MEASUREMENT

• RESIDUAL GAS FROM RECOMBINER - 50 — 100 cc/day - 1.8% TO 0.1% OF TOTAL GAS FLOW - NEARLY 100% CONDENSED OVER LN2





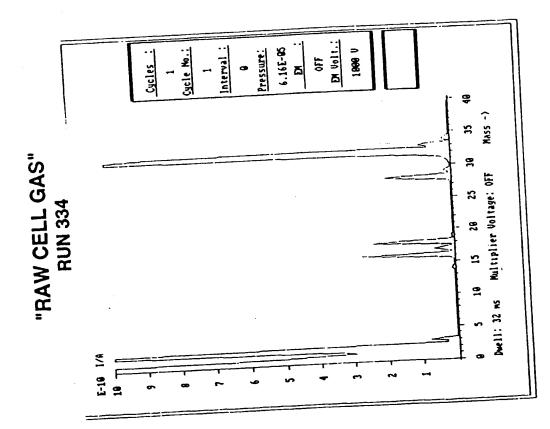
"RAW CELL GAS"



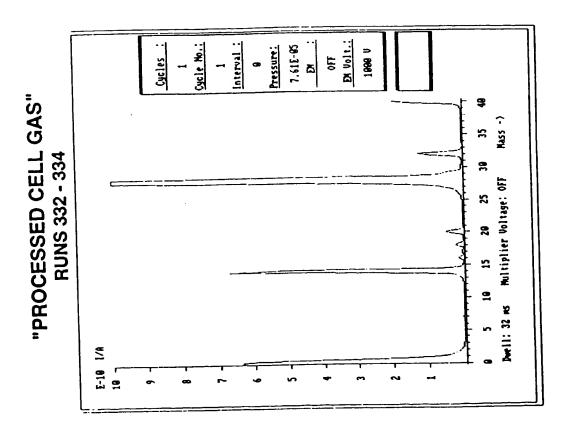
AMPL1TUOE





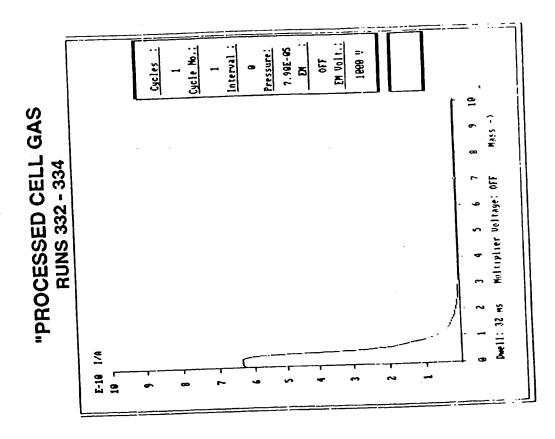












ISOTOPIC RATIOS - HD/H2

SAMPLE

3/2 RATIO TEST PRESSURE TORR

BOTTLE HYDROGEN

 1.3×10^{-4}

0.052

LAB DI WATER

 9.7×10^{-5}

0.025

0.035

 9.8×10^{-5}

 8.9×10^{-5}

RECOMBINER WATER

CELL GAS

CELL ELECTROLYTE

0.031

0.044

 9.9×10^{-5}





WHAT TO DO NEXT FOR HIGHER ENERGY

- STUDY GAS CELL WHICH HAS MUCH HIGHER ENERGY DENSITY - HYDROCATALYSIS WILL PAY -- CRDA?
- ullet TEST PALLADIUM SILVER COATED NICKEL WIRE WITH D $_2$ O SYSTEM ACC CONTINUATION?
- •INVESTIGATE TUBULAR REACTOR USING PALLADIUM SILVER





CONCLUSIONS

• EXCESS ENERGY IS PRESENT AT 0.5 TO 5 W LEVEL 0.5 TO 2.5° ABOVE CALIBRATION

TEMPERATURE CALIBRATIONS ± .02°C

• GAINS ARE HIGH 5 TO 14 x NET INPUT 1.5 TO 4 x GROSS VI INPUT

BUT ONLY AT 1-4 W EXCESS

- SOURCE IS NOT DETERMINED
- LOWER STATE HYDROGEN WAS NOT FOUND WHY? CHEMICALLY MORE REACTIVE THAN REPORTED EASILY ABSORBED IN METAL NOT THERE
- ISOTOPIC RATIOS CONSISTENT WITH ELECTROLYTIC CELL **DECOMPOSITION OF WATER**
- CANNOT PROVE OR DISPROVE POSSIBLE EXPLANATIONS **FOR EXCESS HEAT**



